Charles University in Prague
Faculty of Science

Developmental and Cell Biology

Mgr. Monika Baxa

The Generation of Transgenic Huntington´s Disease Miniature Pig

Doctoral Thesis

Supervisor: prof. MUDr. Jan Motlík, DrSc.
Consultant: Ing. Zdenka Ellederová, PhD.

Prague, 2019

Declaration of the Author/Prohlášení autorky

I declare that this PhD. thesis has been composed by myself under the supervision of prof. Jan Motlik and Dr. Zdenka Ellederova. Next, I declare, that all the literary sources were cited properly and that the work has not been submitted to reach the same or any other academic degree or professional qualification.

Prohlašuji, že jsem předkládanou dizertační práci vypracovala samostatně pod vedením prof. MVDr. Jana Motlika, DrSc., a Ing. Zdenky Ellederové, PhD. Dále prohlašuji, že všechny použité literární zdroje jsou řádně uvedeny a, že tato práce ani její podstatná část nebyla předložena k získání stejného či jiného akademického titulu.

Prague/Praha, 31.08.2019

_____

Monika Baxa

Declaration of the Supervisor/Prohlášení školitele

I declare that Monika Baxa has contributed significantly to the publications presented in this thesis. Monika contributed importantly to the conduction of experiments, conceptual ideas, experimental design, statistical analyses, writing and revisioning the publications. Specific Monika´s contribution is declared in the summaries of her papers or in publications themselves.

.

Prohlašuji, že Monika Baxa významně přispěla k získání výsledků prezentovaných v předkládané práci. Monika přispěla svou experimentální prací, nápady, návrhem experimentů, statistickými analýzami, psaním a revizemi jednotlivých publikací. Konkrétní přínos Mgr. Moniky Baxa je uveden v souhrnech jednotlivých publikací, popř. přímo v jejich textu.

Prague/Praha, 31.08.2019

_____

Prof. MVDr. Jan Motlík, DrSc.

ACKNOWLEDGEMENT

I would warmly like to thank my supervisor Jan, who showed me the beauty of the research and power of the scientific community. His words of encouragement have helped me in research and his moral principles were a source of inspiration in my personal life. Similarly, my sincere thanks belong to Zdenka, always full of enthusiasm and great ideas. Her motivation and insightful guidance have enhanced my scientific spirit. I am very grateful to my colleagues for their kindness, support, and friendship. I especially thank my family for their endless support, patience and help. From the bottom of my heart I thank my beloved and unique kids, who have given me the most important and the most valuable lessons in my life.

.

.

This study was supported by

CHDI Foundation (RA-1035, A-5378, A-8248, RA A-11609); the project EXAM from the European Regional Development Fund (CZ.1.05/2.1.00/03.0124); The Technical Agency of the Czech Republic (TA01011466), Czech-Norwegian research programme (7F14308); the Norwegian Financial Mechanism 2009–2014, the Ministry of Education, Youth and Sports (MSMT-28477/2014); National Sustainability Programme, Czech Ministry of Education, Youth and Sports (MSMT-LO1609); COST (LD15099), RVO 67985904; Charles University Grant Agency, (GAUK589412); and Internal Grants of Institute of Animal Physiology and Genetics (IGA UZFG 11/09, IGA UZFG 10/10, IGA UZFG 09/08, IGA UZFG 08/10).

ABSTRACT

Huntingtons´s disease (HD) is devastating neurodegenerative disorder manifesting by motor disturbances, cognitive decline and personal changes. The huge effort to find a cure for HD has brought several promising therapeutic treatments on the scene. Each of the prospective approaches needs to be investigated for safety, tolerability and efficacy. Mouse and rat models were a lot helpful in examination of pathological mechanisms of HD, but they are not sufficient for completion of pre-clinical testing.

Therefore, we aimed to generate transgenic HD minipig to overcome the gap between rodents and humans. Minipig transgenic for the first 548 aminoacids of human mutant huntingtin gene (TgHD) under the control of human HD promotor was manipulated by lentiviral transduction of porcine one-cell stage embryos. Currently, six generations of minipigs expressing single copy of N-truncated human mutant huntingtin protein (mtHtt) with a repetition of 124 glutamines are at disposal.

The more the model simulates the disease symptoms the better it is for translational research as the efficacy of the cure can be finer evaluated. Hence, the second aim was to demonstrate HD-like phenotype in our model. Testicular degeneration that preceded the clinical symptoms onset was observed as a consequence of expression of mtHtt. Continuous age-dependent accumulation of mtHtt fragments was detected in TgHD brains. Moreover, further age-related molecular alterations discriminative for HD brain were revealed in TgHD brain tissues, including neuronal loss, activated microglia and demyelination. Newly developed tests for examination of cognitive abilities and stress-induced behavior showed decline in their performance. Furthermore, impaired gait and increased physical activity were observed in TgHD minipigs. Manifestation of clinical symptoms at the age of 6-7.9 years is a result of mild but ongoing brain degeneration.

Slow progression of the disease makes TgHD minipig a suitable model for investigation of pre-clinical stage of the disease and long-term HD therapy research. The methods and results obtained in this study will be used for longitudinal evaluation of efficacy of the gene-lowering therapy for HD.

ABSTRAKT

Huntingtonova choroba (HCH) je devastující neurodegenerativní onemocnění, projevující se poruchami motorických i kognitivních funkcí, a také osobnostními změnami. Obrovské úsilí najít léčbu této nemoci přineslo na scénu několik slibných léčebných procedur. Každý z perspektivních terapeutických přístupů však musí být prozkoumán z hlediska bezpečnosti, snášenlivosti a účinnosti. Myší a potkaní modely byly velmi užitečné při zkoumání patologických mechanismů HCH, ale v předklinickém testování nejsou dostačující.

Proto, aby se překlenula biologická vdzálenost mezi hlodavci a lidmi, zaměřili jsme se na vytvoření transgenního miniaturního prasete s HCH. Transgenní miniaturní prase kódující prvních 548 aminokyselin lidského mutovaného huntingtinu (TgHD) pod kontrolou lidského promotoru pro huntingtin vzniklo po lentivirové transdukci prasečích jednobuněčných embryí. V současné době je k dispozici šest generací miniprasat exprimujících jednu kopii N-terminální části lidského mutovaného proteinu huntingtin (mtHtt) s prodlouženou repeticí 124 glutaminů.

Čím více model simuluje příznaky nemoci, tím lepší je pro translační výzkum, protože účinnost léčby lze vyhodnotit přesněji. Druhým cílem proto bylo demonstrovat v našem modelu fenotyp HCH. V důsledku exprese mtHtt byla pozorována testikulární degenerace, která předcházela nástupu klinických příznaků. V mozcích transgenních zvířat byla detekována kontinuální akumulace fragmentů mtHtt závislá na věku. Kromě toho, v mozkových tkáních transgenních prasat byly odhaleny další molekulární změny, které jsou charakteristické pro mozek pacientů s HCH, včetně ztráty neuronů, aktivované mikroglie a demyelinizace. Nově vyvinuté testy pro zkoumání kognitivních schopností a chování v stresových situacích prokázaly pokles v jejich provedení. Navíc byla pozorována porucha chůze a zvýšená fyzická aktivita transgenních prasat. Projevování klinických příznaků ve věku 6-7.9 let je výsledkem mírné, ale věkem postupující degenerace mozku.

Díky pomalému rozvoji onemocnění je TgHD miniprase vhodným modelem pro zkoumání preklinického stadia nemoci, a také pro dlouhodobý výzkum zaměřený na nalezení terapie pro HCH. Metody a výsledky získané v této studii budou použity pro dlouhodobé experimenty hodnotící účinnost genové terapie pro snížení hladiny exprese mutovaného huntingtinu.

ABBREVIATIONS

ABMI	animal body mass index
ACBD3	Acyl-coenzyme A binding domain containing 3 protein
CAG	cytosine - adenine - guanine
DARPP32	dopamine- and cAMP- regulated neuronal phosphoprotein
GFAP	glial fibrillary acidic protein
HD	Huntington's disease
HD KI	HD knock-in
HCH	Huntingtonova choroba
HTT	huntingtin gene
Htt	endogenous huntingtin protein
Iba1	ionized calcium-binding adapter molecule 1
mRNA	messenger RNA
miRNA	micro RNA
MRI	magnetic resonance imaging
mtHTT	mutant huntingtin gene
mtHtt	mutant huntingtin protein
mtDNA	mitochondrial DNA
PBMC	peripheral blood mononuclear cells
PCR	polymerase chain reaction
polyQ	polyglutamine tract
qPCR	quantitative polymerase chain reaction
Qs	glutamines
SCNT	somatic cell nuclear transfer
SDH	succinate dehydrogenase
SDHA/SHDB	succinate dehydrogenase A/ succinate dehydrogenase B
TgHD	transgenic for N-truncated mutant human huntingtin gene
WB	Western blot
WT	wild-type
8-oxo-G	8-oxoguanine

TABLE OF CONTENT

INTRODUCTION 9

AIMS 12

RESULTS 13

Paper I *A Transgenic Minipig Model of Huntington's Disease* 15

Paper II *Mutated Huntingtin Causes Testicular Pathology in Transgenic Minipig Boars.* 50

Paper III *Gradual Phenotype Development in Huntington Disease Transgenic Minipig Model at 24 Months of Age.* 70

Paper IV *A transgenic minipig model of Huntington's disease shows early signs of behavioral and molecular pathologies.* 85

Paper V *Transgenic minipig model of Huntington's disease exhibiting gradually progressing neurodegeneration.* 105

Paper VI *Longitudinal study revealed motor, cognitive, and behavioral decline in transgenic minipig model of Huntington's disease.* 131

Paper VII *Grunting in a Genetically Modified Minipig Animal Model for Huntington's Disease – a Pilot Experiments* 153

DISCUSSION 160

Generation of germline transgenic large animals with human mutant huntingtin gene 160

Sperm and testicular degeneration 162

Alterations in mitochondrial metabolism 163

Brain pathology 164

Clinical symptoms manifestation 167

CONCLUSIONS 170

FUTURE PROSPECTS 172

REFERNECES 173

INTRODUCTION

Huntington's disease (HD) is rare neurodegenerative disorder with a prevalence of 3-10 affected persons per 100.000 individuals in Western Europe and North America [1], [2]. This disorder is caused by the prolonged glutamine (polyQ) repetition in exon 1 of the huntingtin gene (HTT) encoding mutant huntingtin protein (mtHtt) [3]. The polyQ repeat size inversely correlates with the age of onset and severity of the disease [4].

Clinical symptoms manifested by personal changes together with motor and cognitive decline are typically discerned between thirty and fifty years of age [5], [6]. HD patients suffer from chorea, impaired gait, lack of balance coordination, and disturbed fine motor skills like tongue persistence protrusion and phonatory dysfunction [7]–[11]. Among prominent cognitive symptoms belong impaired judgment, the inability to complete a task, and also difficulty with tasks requiring flexibility or speed [12], [13]. The behavioral disturbances include anxiety, and impulsive and aggressive behavior interchanging with apathy [14]. In addition, disruption in circadian rhythm was demonstrated in HD gene carriers [15].

Clinical symptoms are a consequence of progressive degeneration of the brain. Even if the brain pathology is a result of harmful effect of mtHtt, reduction of endogenous huntingtin protein (Htt) or combination of both, a hallmark of HD is a loss of medium-sized spiny neurons [1] and formation of mtHtt aggregates tightly corresponding to the disease progression [16]. Numerous studies indicated that aggregation is a successive process when aggregates are assembled from N-terminal mtHtt fragments and mtHtt oligomers that trigger cellular dysfunctions in affected tissues [17], [18]. N-terminal fragments of mtHtt accumulate with the disease progression, and their abundance varies among tissues, which may be consistent with cell susceptibility to HD [19]–[21]. Nuclear localization of mtHtt fragments is connected to more severe manifestation of the disease [22]. In addition, white matter atrophy, reduced myelination and activated microglia were observed in HD individuals [23], [24]. Various studies showed increased oxidative stress in HD [25], [26] that was suggested to cause an inhibition of mitochondrial functions [27] since reduced activity of complexes II, III and IV were detected in brains of HD patients [28], [29].

Even though HD is considered to be a disorder of the brain, the whole body is affected. Severe cachexia manifesting by obvious skeletal muscle wasting and weight loss was recognized in HD patients [30]–[33]. Furthermore, testicular abnormalities, decrease

in numbers of germ cells as well as abnormal morphology of seminiferous tubules were found in HD men [34].

HD is inherited in an autosomal-dominant manner thus possessing a devastating impact on several family generations since there is no cure available up to date. Huntingtin protein plays a role in diverse cellular processes including transcription, RNA splicing, vesicular trafficking, anti-apoptotic processes, endocytosis, and cellular homeostasis [35], hence the complexity of the disease has made the HD treatment research very challenging.

Animal models constitute an important tools for appreciation of therapies for neurodegenerative disorders. Unfortunately, a number of promising therapies with very auspicious results in HD rodent models, failed to be beneficial in humans [22], [36]–[38]. Small brain size and differences in neuro-architecture to humans limit rodent models for assessment of drug doses, design of the therapy, the same as for usage of medical equipment applicable for human patients [39]. Therefore, large animal models heve been generated with an expectation to provide better pre-clinical outcomes including safety, tolerability, biodistribution, longitudinal investigation, and efficacy of novel therapeutic approaches [40]. Among large animals, minipigs represent a good economical and ethical choice [41]. Vigorous advantages of minipigs are their rather large brain that is similarly structured as in humans, resemblance in body size, physiology, longevity of 15-20 years [42] and not least a 96% homology between porcine and human huntingtin genes and proteins [43].

Several different approaches can be used for transgenesis in large animal models. Somatic cell nuclear transfer (SCNT) allowed the first genetic manipulations in large animals [44]. However, efficacy of SCNT is very low. Therefore, transduction with lentiviral vectors [45] was developed as an alternative to SCNT. Both approaches have their advantages and disadvantages. The SCNT enables to transfer only genetically modified embryos into a surrogate sow. On the other side, prenatal and neostnatal death is not such frequent when lentiviral transduction is manipulated [46]. Recently, the CRISPR/Cas9 system has become the most widespread approach for genetic modifications since it enables sequence-specific targeting of genome and editting in the endogenous locuses. All of these approaches were used for generation of HD large animal models with various impacts on created transgenic animals and their progeny. SCNT was applied for generation of HD pigs [47], lentiviral transgenesis was employed in generation of HD non-human primates [48], [49], HD sheep [50] and HD minipigs [51], and lately CRISPR/Cas9 technique succeeded in generation of HD knock-in (HD KI) pigs [52].

This study introduces the generation of minipig transgenic for N-truncated part of human mutant huntingtin (TgHD) achieved by lentiviral transduction. Next, manifestation of HD-like phenotype is demonstrated in both pre-clinical and clinical stages of the disease. Thus, TgHD minipig could serve as a useful model for testing of therapeutic treatments for HD.

AIMS

All of the potential therapeutic approaches for HD need to be tested for their safety, tolerability and efficacy. TgHD minipig could bridge the gap between rodents and humans.

AIM 1) Generation of transgenic minipig with mutant human huntingtin gene

To confirm transgenesis, determine the transgene copy number and its localization in porcine genome. To validate the number of glutamines in polyQ repetition. To prove the expression of transgenic mtHtt protein in porcine brain and peripheral tissues. To produce transgenic progeny.

However, the generation of transgenic animal does not mean that the disease model was generated. The phenotype observed in transgenic animals needs to correlate with the disease manifestation in patients.

AIM 2) Demonstration of both pre-clinical and clinical manifestation of the disease in transgenic minipigs

Autosomally dominant inheritance of HD enabled the production of transgenic offspring. However, considering the periods for reaching sexual maturity and gestation time, at least one year is needed for achieving the next generation of the progeny. Taking into account the number 4-6 piglets in the litter, an optimal strategy for phenotype monitoring needed to be designed, in order some of the animals could be used for observation of brain pathologies and simultaneously, some of the animals could reach the age when clinical symptoms of the disease are demonstrable. Therefore, we decided to assess the disease using:

AIM 2A) invasive methods

To investigate formation of mtHtt aggregates. To confirm neuronal loss in brain. To analyze brain pathologies caused by the expression of mtHtt.

AIM 2B) non-invasive methods

To identify potential biomarkers of the disease progression in peripheral tissues. To develop a battery of tests for monitoring of behavioral, motor, and cognitive changes. To evaluate behavior together with motor and cognitive performances.

RESULTS

Publications included in the thesis

Baxa, M., *Hruska-Plochan, M., Juhas, S., Vodicka, P., Pavlok, A., Juhasova, J., Miyanohara, A., Nejime, T., Klima, J., Macakova, M., Marsala, S., Weiss, A., Kubickova, S., Musilova, P., Vrtel, R., Sontag, E.M., Thompson, L.M., Schier, J., Hansikova, H., Howland, D.S., Cattaneo, E., DiFiglia, M., Marsala, M, and Motlik, J.* (2013). **A Transgenic Minipig Model of Huntington's Disease**. Journal of Huntington's Disease 2, 47–68.

Macakova, M., Bohuslavova, B., Vochozkova, P., Pavlok, A., Sedlackova, M., Vidinska, D., Vochyanova, K., Liskova, I., Valekova, I., ***Baxa, M.,*** *Ellederova, Z., Klima, J., Juhas, S., Juhasova, J., Klouckova, J., Haluzik, M., Klempir, J., Hansikova, H., Spacilova, J., Collins, R., Blumenthal, I., Talkowski, M., Gusella, J., Howland, D.S., DiFiglia, M., and Motlik, J.* (2016). **Mutated Huntingtin Causes Testicular Pathology in Transgenic Minipig Boars.** Neurodegenerative diseases 16, 245–59.
IF 2.842

Vidinská, D., Vochozková, P., Šmatlíková, P., Ardan, T., Klíma, J., Juhás, Š., Juhásová, J., Bohuslavová, B., ***Baxa, M.,*** *Valeková, I., Motlík, J., and Ellederová, Z.* (2018). **Gradual Phenotype Development in Huntington Disease Transgenic Minipig Model at 24 Months of Age**. Neurodegenerative diseases 18, 107–119.
IF 2.785

Askeland, G., Rodinova, M., Štufková, H., Dosoudilova, Z., ***Baxa, M.,*** *Smatlikova, P., Bohuslavova, B., Klempir, J., Nguyen, T. D., Kuśnierczyk, A., Bjoras. M., Klungland, A., Hansikova, H., Ellederova, Z., and Eide, L.* (2018). **A transgenic minipig model of Huntington's disease shows early signs of behavioral and molecular pathologies.** Disease Models & Mechanisms 11, dmm035949.
IF 4.398

Ardan, T., ***Baxa, M.,*** *Levinska, B., Sedlackova, M., Nguyen, T.D., Klima, J., Juhas, S., Juhasova, J., Smatlikova, P., Vochozkova, P., Motlik, J., and Ellederova, Z. (2019).* **Transgenic minipig model of Huntington's disease exhibiting gradually progressing neurodegeneration.** Disease Models & Mechanisms, **submitted**; MS ID#: DMM/2019/041319.
IF 4.398

Baxa, M., Levinska, B., Skrivankova, M., Pokorny, M., Juhasova, J., Klima, J., Klempir, J., Motlik, J., Juhas, S., and Ellederova, Z**.** (2019). **Longitudinal study revealed motor, cognitive, and behavioral decline in transgenic minipig model of Huntington's disease.** Disease Models & Mechanisms, **submitted***;* MS ID#: DMM/2019/041293.
IF = 4.398

Tykalova, T., Hlavnicka, J., Macakova, M., ***Baxa, M.,*** *Cmejla, R., Motlik, J., Klempir, J., and Rusz, J.* (2015). **Grunting in a Genetically Modified Minipig Animal Model for Huntington's Disease – a Pilot Experiments.** Ces a Slov Neurol a Neurochir, 78/111(Suppl 2):61-65.
IF 0.209

Paper I

A Transgenic Minipig Model of Huntington's Disease

Baxa, M., *Hruska-Plochan, M., Juhas, S., Vodicka, P., Pavlok, A., Juhasova, J., Miyanohara, A., Nejime, T., Klima, J., Macakova, M., Marsala, S., Weiss, A., Kubickova, S., Musilova, P., Vrtel, R., Sontag, E.M., Thompson, L.M., Schier, J., Hansikova, H., Howland, D.S., Cattaneo, E., DiFiglia, M., Marsala, M, and Motlik, J. (2013).*

.

Journal of Huntington's disease 2, 47–68.

IF: Journal of Huntington's Disease was launched in June 2012 and thus did not have an IF

Motivation of the study

All of the HD families crave for a cure that would not only help manage the symptoms but also treat the disease itself. Hunting for potential therapies brought a question of evaluation of their safety and efficacy since the results gained from rodent studies could not be sufficiently translated to humans. There was no large animal model for HD in 2007 when we have started with our study. Thus, we decided to generate transgenic minipig with human mutated huntingtin. The main reasons were not only long lifespan, similar physiology of minipigs to humans and large gyrencephalic porcine brain allowing detailed identification of brain structures by imaging techniques, but also very large similarity between the porcine and human huntingtin genes and proteins. The number of cytosine-adenine-guanine (CAG) repeats in huntingtin gene varies from 6 to 37 triplets in unaffected individuals and from 37 to 180 repeats in mutated allele of HD patients. The longer is CAG tract the earlier is HD onset. With the strategy to observe a clicical phenotype in minipig within estimated 2-4 years of age, we decided to use a sequence of 145 glutamines (Qs) in human huntingtin gene.

Summary

Lentiviral vectors carrying the sequence of the first 548 amino acids of human huntingtin gene including a tract of 145 glutamines under the control of human HD promoter (HIV1-HD-548aaHTT-145Q) were created. Their transduction potential both with the expression of the transgene were tested in porcine differentiated neural stem cells. Next, embryos at pronuclear stage were microinjected with the vector constructs into the perivitelline space, cultured into the blastocyst stage *in vitro* and then laparoscopically transferred into the fallopian tubes of recipients sows. After standard duration of gravidity, the first HIV1-HD-548aaHTT-145Q manipulated piglets were born. One gilt was transgenic in a litter of 6 live newborns. Since HD is autosomally dominant inherited disorder, we produced F1 and F2 generations of TgHD minipigs by mating of TgHD and wild-type (WT) animals.

The first of all, we needed to confirm incorporation of the transgene into the porcine genome, its presence at RNA level and its protein expresssion in the brain and peripheral tissues. We were interested where the transgene was inserted, in how many copies and what was the length of polyQ tract in transgene.

Transgenesis was confirmed by genotyping in genomic DNA from porcine skin biopsies or skin fibroblasts. One copy of the transgene integrated to the genome was detected by relative comparison of quantitative DNA amplification between the endogenous porcine

HTT and the transgenic human HTT genes. Localization of transgene with 124 glutamines was proved on q arm of chromosome 1 (1q24-q25).

Eight minipigs at the age of 4-16 months were sacrificed and their brains and tissues were used in biochemical and immunohistochemical examinations.

We confirmed expression of mutant Htt protein in different regions of the brain and spinal cord the same as in peripheral tissues. No nuclear inclusions were detected in the TgHD brain up to the age of 16 months.

One of the hallmarks of HD is a loss of medium sized spiny neurons which express high levels of dopamine- and cAMP- regulated neuronal phosphoprotein (DARPP32). We showed expression of DARPP32 in neostriatal neurons and neuropil. However, only slight non-significant decrease in median number of DARPP32+ neurons per mm^3 was revealed in caudate and putamen of the TgHD minipigs.

Since the the testicular pathology in humans was related to the presence of mutant Htt we decided to examine also semen and testicular tissues of TgHD boars. We showed a significant decline in the median number of spermatozoa in TgHD boars and significantly reduced number of intact WT minipig oocytes penetrated by TgHD spermatozoa what indicated impaired penetration activity of spermatozoa in TgHD boars. Removal of the zona pellucida markedly increased penetration rate in the WT and TgHD groups to 100% level.

We did not observe the differences in the development and behavior of the TgHD minipigs from F0-F3 generations and no motor deficits specific for HD were evident in the TgHD animals up to 40 months of age.

This study demonstrated successful establishment of a transgenic model of HD in minipig. Transgenesis did not influence survival or normal development of animals through multiple generations. Both female and male transmissions of the HD transgene were confirmed. The lentiviral delivery did not cause mosaicism, since the expression of mutant Htt was confirmed in both brain and peripheral tissues in F1 and F2 TgHD minipigs and maintained the same number of glutamines. We detected slight reduction in the number of DARPP32+ neurons in caudate and putamen of 16-month-old brain. We observed a decline in fertility in 13-month-old boars caused by reduced sperm number and penetration rate. No changes in behavior or motor functions were observed up to the age of 40 months. The study was limited by the low number of animals in experimental groups as minipigs become sexually mature at the age of 5 months, the gestation time is almost 4 months and not all of the transgenes could be sacrificed in young ages in order to have a chance to produce transgenic offspring and study their phenotype in older ages.

My contribution

I isolated, cultured and characterizated the porcine neural differentiated stem cells derived from brains of porcine 40-day-old fetuses. I transducted differentiated stem cells by lentiviral constructs and immunocytologically tested the transduction potential of lentiviral vectors. I designed all of the primers for genotyping, detection of mRNA and validation of copy number variation of inserts in porcine genome. I isolated DNA, RNA and conducted all of the PCR and qPCR reactions including those determined for the validation of glutamine number in mtHTT polyQ tract. I prepared protein lysates and participated on western blot (WB) analyses. I participated on modifying the protocols for processing of porcine brains for immunohistochemical analyses. I observed the development and behavior of TgHD animals and evaluated the rates of trangenesis and mutant huntingtin gene transmission to next generations. I wrote a draft of the manuscript.

Journal of Huntington's Disease 2 (2013) 47–68
DOI 10.3233/JHD-130001
IOS Press

Research Report

A Transgenic Minipig Model of Huntington's Disease

Monika Baxa[a,b,1], Marian Hruska-Plochan[a,b,c,d,1], Stefan Juhas[a], Petr Vodicka[a,p], Antonin Pavlok[a], Jana Juhasova[a], Atsushi Miyanohara[e], Tetsuya Nejime[c], Jiri Klima[a], Monika Macakova[a,b], Silvia Marsala[c,d], Andreas Weiss[f,r], Svatava Kubickova[g], Petra Musilova[g], Radek Vrtel[h], Emily M. Sontag[i,j], Leslie M. Thompson[i,j,k], Jan Schier[l], Hana Hansikova[m], David S. Howland[n], Elena Cattaneo[o], Marian DiFiglia[p], Martin Marsala[c,d,q] and Jan Motlik[a,*]

[a]*Laboratory of Cell Regeneration and Plasticity, Institute of Animal Physiology and Genetics, v.v.i., AS CR, Libechov, Czech Republic*
[b]*Faculty of Science, Department of Cell Biology, Charles University in Prague, Prague, Czech Republic*
[c]*Neuroregeneration Laboratory, Department of Anesthesiology, University of California, San Diego, La Jolla, CA, USA*
[d]*Sanford Consortium for Regenerative Medicine, San Diego, La Jolla, CA, USA*
[e]*Vector Development Laboratory, Human Gene Therapy Program, Department of Pediatrics, University of California, San Diego, La Jolla, CA, USA*
[f]*Novartis Institutes for Biomedical Research, Neuroscience Discovery, Basel, Switzerland*
[g]*Department of Genetics and Reproduction, Veterinary Research Institute, Brno, Czech Republic*
[h]*Department of Clinical Genetics and Fetal Medicine, Palacky University, University Hospital Olomouc, Olomouc, Czech Republic*
[i]*Department of Biological Chemistry, University of California, Irvine, CA, USA*
[j]*Department of Psychiatry and Human Behavior, University of California, Irvine, CA, USA*
[k]*Department of Neurobiology and Behavior University of California, Irvine, CA, USA*
[l]*Institute of Information Theory and Automation v.v.i., AS CR, Prague, Czech Republic*
[m]*Laboratory for Study of Mitochondrial Disorders, First Faculty of Medicine, Department of Pediatrics and Adolescent Medicine, Charles University and General University Hospital in Prague, Prague, Czech Republic*
[n]*CHDI Foundation, Princeton, NY, USA*
[o]*Department of Pharmacological Sciences and Centre for Stem Cell Research, Università degli Studi di Milano, Milan, Italy*
[p]*Department of Neurology, Massachusetts General Hospital, Boston, MA, USA*
[q]*Institute of Neurobiology, Slovak Academy of Sciences, Kosice, Slovak Republic*
[r]*IRBM Promidis, Pomezia, Italy*

[1]The first two authors contributed equally to this work.

*Correspondence to: Jan Motlik, Institute of Animal Physiology and Genetics, v.v.i, Laboratory of Cell Regeneration and Plasticity, Rumburska 89, 27721 Libechov, Czech Republic. Tel: +420 315639560; Fax: +420 315639510; E-mail: motlik@iapg.cas.cz.

ISSN 1879-6397/13/$27.50

Abstract.

Background: Some promising treatments for Huntington's disease (HD) may require pre-clinical testing in large animals. Minipig is a suitable species because of its large gyrencephalic brain and long lifespan.

Objective: To generate HD transgenic (TgHD) minipigs encoding huntingtin (HTT)1–548 under the control of human HTT promoter.

Methods: Transgenesis was achieved by lentiviral infection of porcine embryos. PCR assessment of gene transfer, observations of behavior, and postmortem biochemical and immunohistochemical studies were conducted.

Results: One copy of the human HTT transgene encoding 124 glutamines integrated into chromosome 1 q24-q25 and successful germ line transmission occurred through successive generations (F0, F1, F2 and F3 generations). No developmental or gross motor deficits were noted up to 40 months of age. Mutant HTT mRNA and protein fragment were detected in brain and peripheral tissues. No aggregate formation in brain up to 16 months was seen by AGERA and filter retardation or by immunostaining. DARPP32 labeling in WT and TgHD minipig neostriatum was patchy. Analysis of 16 month old siblings showed reduced intensity of DARPP32 immunoreactivity in neostriatal TgHD neurons compared to those of WT. Compared to WT, TgHD boars by one year had reduced fertility and fewer spermatozoa per ejaculate. *In vitro* analysis revealed a significant decline in the number of WT minipig oocytes penetrated by TgHD spermatozoa.

Conclusions: The findings demonstrate successful establishment of a transgenic model of HD in minipig that should be valuable for testing long term safety of HD therapeutics. The emergence of HD-like phenotypes in the TgHD minipigs will require more study.

Keywords: Huntington's disease, mutant huntingtin, minipigs, large animal model, lentiviral transgenesis, FISH analysis, mRNA and protein expression, immunohistochemistry, DARPP32, AGERA assay, TR-FRET assay, spermatozoa

ABBREVIATIONS

AGERA	Agarose gel electrophoresis for resolving aggregates
HD	Huntington's disease
HTT	Huntingtin
TgHD	Transgenic HD
TR-FRET	Time-Resolved Förster Resonance Energy Transfer

INTRODUCTION

Huntington's disease (HD) is an inherited autosomal dominant neurodegenerative disorder with a worldwide prevalence of 3–10 affected individuals per 100,000 persons in Western Europe and North America [1, 2]. Progressive impairment of motor, emotional and cognitive functions [3, 4] is a consequence of the expansion of the CAG repeat stretch in exon 1 of the gene encoding huntingtin (HTT) protein [5]. The onset and the severity of HD correlates inversely with CAG repeat number [6]. The current pharmacotherapy of HD provides improvement of symptoms but no treatment is available to stop disease progression [7, 8].

Animal models are important tools to evaluate therapies for neurodegenerative disorders. Models of HD in rodent, Drosophila, C. elegans, and non-human primate have been generated. In general, each of these models shows some biochemical and neuronal features similar to HD in humans [2, 3]. Rodent and fly models of HD have been very useful for understanding the molecular basis for behavioral and neuronal abnormalities [2]. Although rodent models of HD that express either truncated [9–11] or full-length [12, 13] human mutant HTT display differences in onset and severity of phenotypes, these models collectively have provided valuable information related to target validation and drug therapy. However, the rodent's small brain size and differences in neuroarchitecture to humans limits their use for detailed neuroanatomic characterization associated with HD [14–17] and for adapting methods such as non-invasive imaging that are used in human clinics [18–20]. Large HD genetic models such as sheep [21] and the non-human primate [22] have been generated to help address these problems.

Pigs, and mainly minipigs, represent an optimal model for preclinical drug trials and long-term safety studies [20, 23–26]. This species has a physiology resembling in several aspects that of humans [27–29]. The large size of the pig brain permits detailed identification of brain structures by imaging techniques such as PET [30–32] and MRI [33–39]. There has been recent progress in defining the porcine genome [40–43], porcine single nucleotide polymorphisms [44], microRNAome [45–47], and improved techniques for genetic modification of pigs [48–51]. The porcine homologue of the huntingtin gene has a large ORF of 9417 nucleotides encoding 3139 amino acids with a predicted size of 345 kDa (GenBank, Accession No. AB016793). There is a 96% similarity between

the porcine and human huntingtin genes (GenBank, Accession No. AB016794). The number of CAG repeats in the porcine HTT gene is polymorphic, ranging from 8 to 14 units, and falls within the range of the normal human huntingtin gene [52]. Similar to humans, miniature pig possesses two HTT transcripts of approximately 11 and 13 kb [52, 53]. The similarities between porcine and human huntingtin genes and proteins have provided further impetus to use the pig as a model of HD [20, 54].

Recently, a cloning strategy was used to generate a transgenic HD minipig. Unfortunately, this porcine model suffered frequent perinatal mortality for reasons that are unclear [55]. Here we used a strategy based on lentiviral infection of porcine embryos and report the successful germ line transmission through successive generations (F0, F1, F2 and F3 generations) of a HD transgene encoding the first 548 aa of HTT with 124 glutamines under the control of human HTT promoter. Mutant protein expression is detected in both CNS and non-CNS tissues and in brain is comparable to the endogenous huntingtin. DARPP32 immunoreactivity in a 16 month old TgHD minipig was reduced compared to a WT sibling. At about one year of age, sperm number and oocyte penetration were severely affected in TgHD minipigs. These findings suggest that we have in hand a suitable large animal model for evaluating potential HD therapeutics.

MATHERIALS AND METHODS

Supplementary data

Supplementary Data (S1 –S8) are placed on the website of The Institute of Animal Physiology and Genetics, v.v.i.: www.iapg.cas.cz/CentrumPIGMOD/JHD

Minipigs

The Institute of Animal Physiology and Genetics in Libechov imported the first miniature pigs in 1967 from the Hormel Institute, University of Minnesota (two boars and three sows) and from the Institute for Animal Breeding and Genetics, University of Göttingen, Germany (two boars and four sows). Since then breeding, animal health and body shape have been thoroughly controlled and outbreeding conditions maintained by import of several additional boars from Göttingen [29]. Through continuous selection there has been an increase in the average litter size (now about 6–8 piglets) and maintenance of a white color, which has enabled the study of epidermal stem cells [56]. The animals were bred beginning at about 5 months of age when they reach sexual maturity. At this stage they weigh about 12–15 kg. In our minipig colony longevity is unknown because animals are housed for a maximum of about 8 years. However, the survival of parental minipig breeds (Hormel and Göttingen) has been reported to be 12 to 20 years. In this study, as is standard practice, the gilts (sexually mature, regularly estrous cycling minipig females) and weaned sows were housed in groups of 3–4 minipigs, and boars were kept individually. The regular estrous cycle (20 days) facilitated reproductive experiments.

All components of this study were carried out in accordance with the Institutional Animal Care and Use Committee of Institute of Animal Physiology and Genetics, v.v.i. and conducted according to current Czech regulations and guidelines for animal welfare and with approval by the State Veterinary Administration of the Czech Republic. The ample body size of the minipigs made feasible all surgical and laparoscopic approaches and their execution in a timely way. General anesthesia of minipigs was induced by TKX mixture (Tiletaminum 250 mg, Zolazepamum 250 mg, Ketamine 10% 3 ml, Xylazine 2% 3 ml) in a dose of 1 ml per 10 kg of body weight for experimental procedures including embryo transfer and oocyte collection. All surgery was conducted under sterile conditions in a standard surgical room. Postoperative care included treatment with analgesics and antibiotics. Animals were housed separately during recovery from anesthesia and then returned to the animal colony. Profound barbiturate anesthesia (Thiopental Valeant, 1g, i.v.) was used for transcardial perfusions.

Construction and production of the HIV1-HD-548aaHTT-145Q vector and verification of vectors in vitro

N-terminal truncated form of human huntingtin was created from the plasmid pFLmixQ145 comprising human full-length HTT cDNA with 145 CAG/CAA repeats (obtained from Coriell Cell Repositories, Camden, NJ). The first 548 aa of huntingtin (ending with residues AVPSDPAM) and including 145 Q was ligated with the HD promoter and inserted into the backbone plasmid pHIV7, which contained cPPT and WPRE cis-enhancing elements. Lentiviral vectors were produced by transient co-transfection of HEK293T cells. HIV1-CMV-EGFP vector (1×10^9 IU/ml) was used as the standard (See Supplementary Data S1 for details). Transgene expression was tested on porcine differentiated neural stem

cells. Subsequently, transduction potential of lentiviral vectors was evaluated using porcine zygotes. Matured porcine oocytes were laparoscopically aspirated from pre-ovulatory follicles. After IVF, embryos at pronuclear stage were microinjected with 10–20 pl of HIV1-CMV-EGFP construct into the perivitelline space and cultured into the blastocyst stage *in vitro* (See Supplementary Data S2 for details).

Transgenesis

Gilts were synchronized by Regumate (Jenssen Pharmaceuticals) (5 donors and 3 recipients per experiment). Donor females were superovulated by administration of pregnant mare's serum gonadotropin (PMSG) (Intervet International B.V.) and ovulation was induced by GnRH (Intervet International B.V.). After mating with the boars, pronuclear stage embryos were flushed from oviducts and microinjected into the perivitelline space with HIV1-HD-548aaHTT-145Q lentiviral vector (50–100 viral particles per zygote). The injected embryos were laparoscopically transferred into the fallopian tubes of recipients (See Supplementary Data S3 and S4 for details).

Genotyping

Biopsies of porcine skin were used to obtain DNA which was purified using DNeasy Blood & Tissue kit (Qiagen). The presence of the transgene was determined by PCR amplification of the region containing the WPRE coding sequence within the transgene (254 bp amplicon). Each PCR reaction contained 0.75 ng/μl of purified gDNA in 20 μl of reaction mixture and underwent 32 cycles of amplification (94°C for 30 s, 56°C for 40 s, 72°C for 40 s) following an initial 3 min denaturation period. SELK gene (360 bp amplicon) was used as an endogenous control. Primer sequences:

WPRE Fwd: 5′ GAGGAGTTGTGGCCCGTTG TCAGGCAACG 3′
WPRE Rev: 5′ AGGCGAGCAGCCAAGGAAA GGACGATG 3′
SELK Fwd: 5′ ACAGGCCCAAACTAATAAGAG 3′
SELK Rev: 5′ CAAATTTGGAGCCTTTTGT 3′

Fluorescent in situ hybridization

The localization of transgenes within the porcine genome was detected by Fluorescence *in situ* hybridization (FISH) analysis [57]. Mutant HTT sequence from the recombinant plasmid (HIV1-HD-548aaHTT-145Q) was labeled with biotin-16-dUTP (Roche Diagnostics GmbH) using a nick transcription kit (Abbott). The resulting probe did not detect the endogenous porcine HTT gene. Immunodetection and amplification were performed using avidin-FITC and anti-avidin-biotin. Chromosomes were counterstained with propidium iodide and DAPI. Karyotyping was determined using image analysis of reverse DAPI banding.

Microdissection of chromosomes and analysis of copy number variation

The incorporation of transgenic HTT into the q arm of chromosome 1 was confirmed by microdissection of q arms of both chromosomes 1 followed with a non-specific degenerate oligonucleotide-primed (DOP) PCR. 2 μl of DOP PCR amplification product were used as a template to carry out PCR amplification of the transgene.

Primer sequences:

MDS Fwd: 5′ TTCATAGCGAACCTGAAGTC 3′
MDS Rev: 5′ TTGTGTCCTTGACCTGCTGC 3′

The number of copies of the transgenes integrated into the porcine genome was determined using relative comparison of quantitative DNA amplification between the endogenous porcine HTT and the transgenic human HTT. HTT primers and probe 6-carboxyfluorescein, (6-FAM, TaqMan Probe, Applied Biosystems) were designed to detect HTT of both species. ACTB (VIC, TaqMan Probe, Applied Biosystems) was used as a reference gene. Each multiplex qPCR reaction was performed in a reaction volume of 20 μl using TaqMan Gene Expression chemistry (ROX passive reference, Applied Biosystems) using 75 cycles of amplification (30 s at 94°C, 30 s at 51.1°C, 30 s at 72°C) following an initial 3 min denaturation period. The qPCR data were analyzed using LinRegPCR software [58].

The sequences of the oligonucleotides:

HTT TaqMan MGB Probe: 6-FAM-TCTGCGTC ATCACTGC-MGBNFQ
HTT Primer Fwd: 5′ CTTCTGGGCATCGCTATG 3′
HTT Primer Rev: 5′ CATTCGTCAGCCACCATC 3′
ACTB TaqMan MGB Probe: VIC-AGTCCCTG CCTTCCCAAA-MGBNFQ

ACTB Primer Fwd: 5′ GTCATTCCAAGTATCAT GAGATG 3′
ACTB Primer Rev: 5′ TGGAGTACATAATTTA CACTAAAGC 3′

Determination of glutamine number in human mutant huntingtin

The number of glutamines in human mutant HTT was determined by PCR using primer pairs that flanked the region of the CAG/CAA repeat. The length of the PCR fluorescently labeled product was detected using Fragment analysis on an Applied Biosystems 3130 Genetic Analyzer. Samples were separated in gel polymer POP-7 gel at 60°C using LIZ 600 size standard. Data analysis was performed by GeneMapper® software.

Primer sequences:

HD1: 5′ ATGAAGGCCTTCGAGTCCCTCAAGT CCTTC 3′ (6-FAM)
HD3pig: 5′ CGGCGGCGGTGGCGGTTGCTGT TGCTGCTG 3′

PCR protocol: 95°C for 5 min, followed by 40 cycles of denaturation at 94°C for 30 s, annealing at 70°C for 30 s and elongation at 72°C for 30 s with a final extension of 3 min.

Detection of mRNA expression of mutant human HTT

Purified RNA was obtained from cultured porcine skin fibroblasts using RNeasy Plus minikit (Qiagen). RT PCR amplification was performed in a reaction mixture containing 2.0 ng/μl of total RNA with reaction volume of 20 μl. The primer set for RNA huntingtin insert (1446 bp amplicon) was designed using Beacon Designer. ACTB (~100 bp amplicon, PrimerDesign Ltd) was used as a reference gene. The HTT amplification was performed in one step starting with reverse transcription at 50°C for 30 min and denaturation at 95°C for 15 min, followed by 50 cycles of denaturation at 94°C for 45 s, annealing at 56°C for 45 s and elongation at 72°C for 95 s with the final extension of 2 min. The amplification of ACTB reference gene was performed in a one-step reaction (50°C for 30 min, 95°C for 15 min, followed by 35 cycles of amplification at 94°C for 45 s, 61°C for 30 s and 72°C for 30 s with the final extension of 3 min. Reaction mixtures missing reverse transcriptase were included for each animal sample to exclude the possibility of contamination with genomic DNA.

Primer sequences:

HTT RNA Fwd: 5′ GAAACTTCTGGGCATCGC TATG 3′
HTT RNA Rev: 5′ GAAAGCCATACGGGAAG CAATAG 3′

Biochemical assays

Eight minipigs at the age of 4 ($N=4$), 10 ($N=2$) and 16 months ($N=2$) from F2 generation (4 TgHD + 4 WT) were perfused under deep anesthesia with ice-cold PBS. The left hemisphere of each perfused brain was dissected and used in biochemical assays (SDS-PAGE and Western blot and TR-FRET). Brain and tissue biopsies were stored at –80°C.

15 μg of total protein from crude homogenates of TgHD minipig and WT littermates samples were diluted by NuPage 4× LDS sample buffer (LifeTech #NP0007) and 0.1 M DTT. Samples were loaded onto 3–8% Tris-acetate (LifeTech #EA03755) gel and run at 125 V in Tris-Acetate SDS Running Buffer (LifeTech #LA0041) until the 30 kDa band of Novex Sharp protein standard (LifeTech #LC5800) had migrated to the end of the gel. Gels were then immersed in transfer buffer containing 1% SDS and 20% MetOH for 8 minutes and then transferred onto nitrocellulose membrane (LifeTech #IB301001) using an iBlot gel transfer device (LifeTech #IB1001) P3 for 8 minutes. Membranes were blocked with 5% milk for 30 min at RT (BioRad #170-6404) and probed with anti-HTT antibody (Ab1, 1:1,000; [59]) overnight at 4°C. Membranes were then incubated for 1 h at RT in a 1:5,000 dilution of Peroxidase-conjugated Donkey Anti-Rabbit secondary antibody (Jackson ImmunoResearch #711-035-152); followed by 5 min incubation in Supersignal West Pico (Pierce #3408). Signal was detected on autoradiographic film (GE Healthcare #28906839). Membranes were stripped by Re-Blot Plus Strong Solution (10×) (Millipore #92590) for 15 minutes at RT, blocked by 5% milk and re-probed with anti-actin antibody in a 1:500 dilution (Sigma #A4700). After 1 h incubation at RT in secondary Donkey anti-Mouse antibody (Jackson ImmunoResearch #715-0350150), detection was performed as described above.

SDS-agarose gel electrophoresis for resolving aggregates (AGERA) and Western blot analysis

The analysis of mutant HTT oligomers by SDS-AGE and Western analysis was performed as described previously [60–63]. 50 μg of total protein from

crude homogenates of TgHD minipig samples were diluted 1:1 into non-reducing Laemmli sample buffer (150 mmol/l Tris-HCl pH 6.8, 33% glycerol, 1.2% SDS and bromophenol blue). Purified ferritin (440 kDa) was used as a high molecular weight size marker and positive indicator of migration and transfer of protein (Sigma). Eight week old R6/2 mouse striatal tissue was used as a positive control for mutant HTT oligomers [63]. Samples were loaded onto 1% agarose gel containing 0.1% SDS and run at 100 V in running buffer (192 mM glycine, 25 mM Tris-base, 0.1% SDS) until the bromophenol blue dye front had migrated 12 cm. The gel was transferred onto PDVF membrane (Millipore) at 200 mA for 1 h in transfer buffer (192 mM glycine, 25 mM Tris-base, 0.1% SDS, 15% MetOH) using Semi-dry electroblotter model HEP-1 (OWL Scientific). The thickness of the 1% gels decreased substantially during transfer, so the electroblotter was tightened periodically to ensure constant and even contact between the gel sandwich and the electroblotter. After transfer, the membrane was blocked for 1 h in StartingBlock™ T20 (TBS) Blocking Buffer (Pierce) at room temperature and incubated in a 1:500 dilution of anti-HTT antibody (Millipore MAB5374, EM48) overnight at 4°C. The membrane was then incubated for 1 h in a 1:10,000 dilution of Horseradish peroxidase-conjugated anti-mouse secondary (Jackson ImmunoResearch Laboratories) at room temperature and signal was detected using Supersignal West Pico (Pierce).

Filter retardation assay

The same homogenates used in the AGERA assays were also analyzed for SDS-insoluble mutant HTT by filter-retardation assay as previously described [62–64]. 50 μg of homogenate were diluted in 0.1% SDS and filtered through cellulose acetate membrane (Schleicher & Schuell, 0.2 μm pore size) using a dot blot filtration apparatus (Bio-Rad) and washed using 0.1% SDS. The blot was then blocked for 1 h in 5% non-fat milk at room temperature and probed with primary and secondary antibodies and developed as described above.

TR-FRET quantitative analysis

TR-FRET (Time-Resolved Förster Resonance Energy Transfer) quantification of soluble mutant huntingtin was performed as previously described [65]. In short, 5 μl tissue sample homogenates and 1 μl detection buffer (50 mM NaH_2PO_4, 400 mM NaF, 0.1% BSA and 0.05% Tween + detection reagents) were added per well of a low-volume 384-well plate. The labeled antibodies used for detection of soluble mutant HTT were 2B7 bound to terbium cryptate (TB) and MW1 bound to D2 fluorochrome. The final amounts of antibodies were 1 ng 2B7-Tb and 10 ng MW1-D2. After incubation for 1 h at room temperature, samples were analyzed by excitation of the Terbium donor at 320 nm. After a time-delay of 100 μs, TB and D2 emission signals were detected at 620 and 665 nm with an Envision reader (PerkinElmer, Switzerland). TR-FRET signals are presented as the total protein normalized ratio of 665 nm signal divided by 620 nm signal. This calculation benefits from the internal signal intensity reference of the TB donor fluorescence, thereby providing a mutant HTT protein signal corrected for potential assay-interfering artifacts such as turbidity, light scattering or quenching capability of the sample, differences in sample volume due to slight pipetting variability, and day-to-day assay fluctuation caused by differences in excitation lamp energy.

Immunohistochemistry

The right hemisphere of each perfused brain was immersed in a fixative solution composed of 4% paraformaldehyde (PFA) in phosphate buffer saline (PBS, pH 7.4) for 5–6 days and then embedded in HistOmere [66, 67] for 2–4 minutes in dorso-ventral direction, so that the optic chiasm and mammillary bodies were in horizontal position, and cut into 6 slabs. Brain slab no. 2 contained the majority of the neostriatum. The brain slabs were post-fixed in 4% PFA for another 7–10 days and then placed into 30% sucrose containing 0.01% sodium azide. 40 μm thick coronal brain sections were cut using a clinical cryostat (Leica Biosystems, CM1950). The endogenous peroxidase activity was blocked with a solution of 0.3% of hydrogen peroxide in MetOH for 20 min and the free-floating sections were immunostained using the following primary antibodies listed with dilutions and sources: Ab1 (1:1,000, [59]), AB585 (1:500, [59]), MW8 (supernatant, Hybridoma Bank, University of Iowa, USA), mEM48 (1:50, MAB5374, Millipore) and DARPP32 (1:15,000, ab40801, Abcam). Secondary goat fluorescent antibodies (Alexa Fluor® 488, Alexa Fluor® 555, Alexa Fluor® 647 from Invitrogen, Life Technologies) were used for visualization of some primary antibodies. Some sections were treated with biotinylated secondary antibodies (1:400, Amersham, Buckinghamshire, UK) followed by avidin-peroxidase complex (1:400, A3151; Sigma-Aldrich). The avidin-peroxidase complex was visualized by incubation with DAB tablet (#4170, Kementec Diagnostics). The sec-

tions were finally mounted with DePeX (Sigma). Analysis was performed using a confocal microscope equipped with 4 lasers (405, Argon, 561 and 633 nm lasers) (SP5, Leica Microsystems), virtual microscopy scanners (VS110®-5, Olympus, NanoZoomer 2.0-HT, Hamamatsu) and a light microscope (Primo Star, Zeiss).

Determination of the number and intensity of DARPP32 + neurons

Images of regions of caudate and putamen were obtained using the confocal microscope and a HCX PL APO lambda blue 63.0 × 1.40 OIL UV objective to detect DAPI staining. PMT setup, pinhole sizes (1 Airy) and contrast values were kept constant across different sessions. The number of coronal sections analyzed per caudate nucleus and putamen ranged from 3–5 and 25 areas were scanned in each section. Areas of analysis were sectioned in the *z plane* in 1-micron optical sections (13–20 μm) using FiJi software (http://fiji.sc) and only cells confirmed to include the entire DAPI stained nucleus were included in the analysis. This sampling method is an optical dissector technique and minimizes sampling errors (due to partial cells) and stereological concerns, as minor variations in cell volumes do not influence sampling frequencies [68, 69]. The DAPI staining in DARPP32 labeled cells revealed nuclei of two distinct morphologies-large grainy nuclei mainly in the caudate nucleus and smaller compact nuclei mainly in putamen. Only cells with DARPP32 labeling and these nuclear features were included in the analysis. A total of 5,256 neurons in TgHD minipig and 3,644 neurons in WT minipig were counted. All values were reported as the number of neurons positive for immunoreactive DARPP32 per mm^3 tissue. In the same scanned areas used for the cell based analysis the overall intensity of DARPP32 signal was also measured. The average signal intensity was determined for all images in a stack and expressed as the mean intensity.

Semen collection and penetration test

Semen samples from 2 transgenic boars of F1 generation (G117 and G118) and 3 wild type boars (F808, F630, F719) were collected starting at age 12 months and periodically over 14 months. Five and 18 samples were taken for the WT and 16 and 18 for the TgHD minipigs. Total number of spermatozoa per ejaculate was estimated by Sperm Class Analyzer (Microptic, Spain). Differences in the number of spermatozoa between individual boars were analyzed using Kruskal-Wallis test followed by Mann-Whitney U test for the *post hoc* comparison. Values of $p < 0.05$ were considered significant. The spermatozoa were prepared for *in vitro* penetration test by double centrifugation (20 min/600 g, 10 min/600 g) and the following swim-up procedure [70] provided about 1×10^6 cells for *in vitro* fertilization. The cycling minipig gilts were synchronized by Regumate (Jenssen Pharmaceuticals) and superovulated by administration of PMSG (Intervet International B.V.). Ovulation was inducted by GnRH (Intervet International B.V.). The oocyte-cumulus complexes were isolated from large antral follicles 72 h after PMSG injection at the germinal vesicle stage and they were cultured for 40–44 h up to metaphase II with the first polar body [70]. In 13 independent experiments, oocytes with intact zona pellucida were used. In some experiments, the zona pellucida was removed by incubation with 0.25% pronase. After 24 h of incubation with spermatozoa, oocytes were mounted on slides, fixed in acetic-alcohol, stained with acetic-orcein and examined with phase contrast microscopy. The penetration rate into matured pig oocytes was recorded. Differences among individuals in penetration rate were analyzed using Kruskal-Wallis test followed by Mann-Whitney U test used for the *post hoc* comparison between individual boars and values of $p < 0.05$ were considered significant.

RESULTS

Generation and characterization of TgHD minipig

The HIV1 backbone plasmid pHIV7, which contains cPPT and WPRE cis-enhancing elements (Supplementary Data S1), was used for the construction of a lentiviral vector carrying the sequence of the first 548 amino acids of human HTT protein containing 145 glutamines under the control of human HD promoter (Fig. 1A). The transduction potential of the lentiviral construct was verified on porcine zygotes using the HIV1-CMV-EGFP construct. Efficient transduction of porcine embryos was confirmed by the presence of EGFP fluorescence in embryoblasts and trophoblasts (Supplementary Data S2).

The TgHD minipigs were generated by using microinjection of HIV1-HD-548aaHTT-145Q construct into the perivitelline space of the one-cell stage porcine embryos (Supplementary Data S3). Twenty-nine injected zygotes were transferred to recipient sows via laparoscopy (Supplementary Data S4). After standard duration of gravidity (115 days), the first

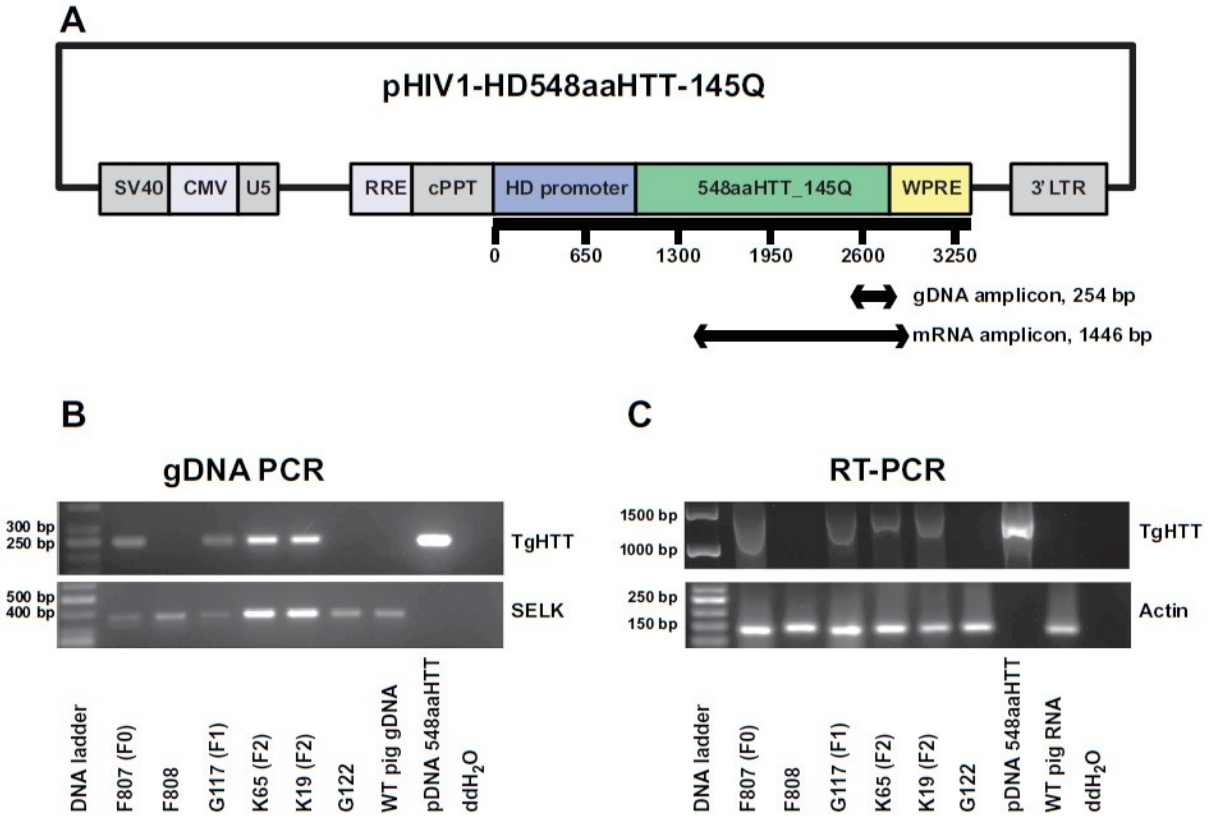

Fig. 1. Molecular characterization of TgHD minipigs. (A) Schematic of the first 548aa of human HTT cDNA fragment with the stretch of 145 glutamines ligated to human HTT promoter in the pHIV7 backbone. WPRE primer set (gDNA amplicon) was used for genotyping the animals. 548aaHTT primer set (mRNA amplicon) was used for confirmation of mRNA expression. (B) PCR of the human HTT and WPRE region (TgHTT) shows presence of transgene in porcine DNA. Amplification of SELK gene (360 bp amplicon) was used as control for the quality of DNA. (C) Expression of mRNA by RT PCR amplification of 1446 bp long amplicon spanning the region encoding human HTT and WPRE region. Amplification of actin mRNA (ACTB) was used as a control for RNA quality. Reaction mixtures without reverse transcriptase were included for each animal sample to exclude the possibility of genomic contamination (data not shown). Plasmid DNA with 548aaHTT-145Q construct was used as a positive control. WT pig genomic DNA and mRNA and ddH_2O were used as negative controls. Generation (F0, F1, F2) is indicated just for TgHD animals.

HIV1-HD-548aaHTT-145Q manipulated piglets were born. One gilt (F807) in a litter of 6 live newborns was transgenic. Two non-transgenic piglets died within 48 hours after birth (Fig. 2). The number of transgenic animals when expressed as a proportion of the number of live births or as a proportion of microinjected zygotes was 16.7% or 3.5%, respectively.

The F0 transgenic gilt was mated with its non-transgenic littermate to produce F1 generation. In the two litters of 17 newborns, five piglets were transgenic (Fig. 2). Germ line transmission to the F1 generation was 29.4%. F1 transgenic boars were sexually mature at the expected age of five months and they successfully produced offspring.

Of 92 F2 piglets born from seventeen litters – 73 survived (20.7% perinatal mortality) and 37 of these were transgenic (TgHD, black symbols, Supplementary Data S5) resulting in a 40.2% F2 generation transgenesis rate per born piglet. The number of piglets in a litter and newborn mortality was comparable between offspring of TgHD and WT animals (Supplementary Data S6). The proportion of TgHD and WT piglets in F2 generation were comparable, enabling creation of optimal experimental groups (TgHD vs. WT animals).

Five transgenic boars and one TgHD female of the F2 generation were bred and a total of 51 live WT and 30 live TgHD piglets were obtained from 23 litters. The incidence of perinatal mortality in F3 generation was 14.2% and the rate of transgenesis was 34.9%.

The F0 transgenic sow was also mated with an F1 transgenic boar. Four transgenic piglets were born in two litters (Supplementary Data S5). No homozygote TgHD transgenic offspring were obtained.

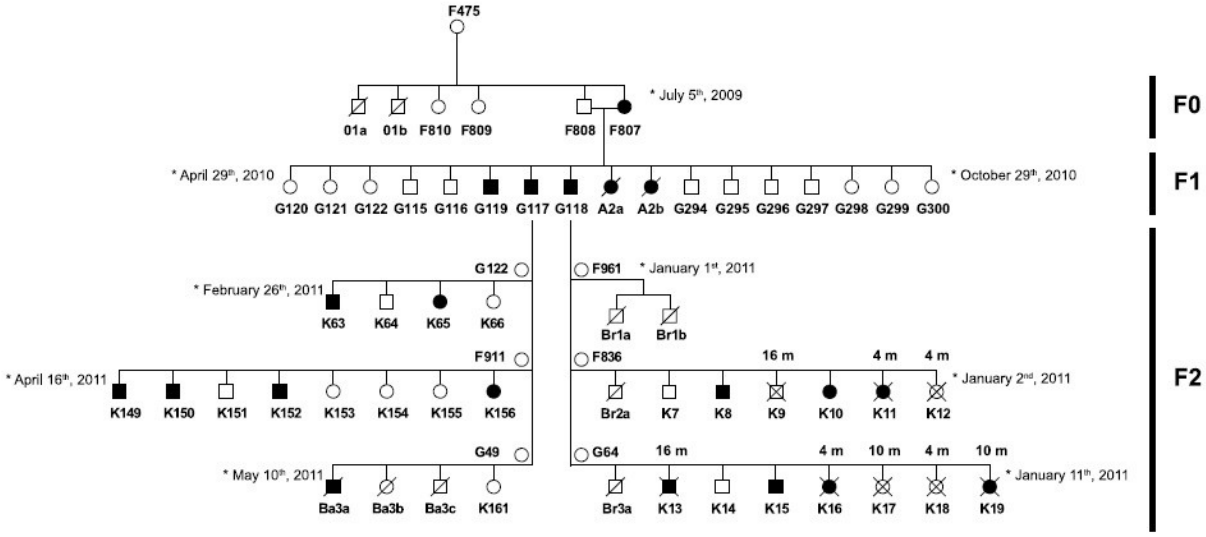

Fig. 2. Breeding and pedigrees of TgHD minipigs. Black boxes (males) and black circles (females) represent animals positively tested for the transgene in DNA extracted from biopsy of ear tissue. "/" denotes a dead minipig within the first 48 hours; "X" indicates an animal sacrificed for biochemical and microscopic studies. The F0 minipig gave birth to 5 TgHD piglets in two litters. Mendelian inheritance is indicated in the F2 generation.

DNA and RNA analysis

Genotyping was performed using PCR as described in Methods. Figure 1B demonstrates TgHD minipigs in F0, F1 and F2 generations. Expression of mRNA was confirmed by RT PCR amplification of the region encoding human HTT and WPRE region (Fig. 1C). To confirm mRNA expression of the full insert, primers were designed for amplification of the 1446 bp product from the 548aa HTT transgene. mRNA of mutant huntingtin was transcribed in all TgHD minipigs. Mutant HTT gene was detected by FISH analysis on chromosome 1 (1q24-q25) in animals from the first three generations (Fig. 3A). Microdissection of q arms of chromosomes 1 followed with non-specific DOP PCR confirmed the presence of the transgene in chromosome 1. Chromosomes 6 and 13 were used as negative controls (Fig. 3B).

Quantitative PCR was used to detect the presence of both endogenous wild type HTT gene and the mutant HTT transgene in the porcine genome. Assuming the presence of the two endogenous porcine HTT alleles, all the transgenic animals integrated 1 copy of the transgene in their genome (Fig. 3C). Furthermore, fragment analysis of the PCR amplicons of the DNA fragment containing CAG/CAA sequence showed that the integrated transgene was in frame and consisted of 124 CAG/CAA instead of the original 145 (Fig. 3D).

Development and behavior of TgHD minipigs

The development and behavior of the TgHD minipigs from F0, F1, F2 and F3 generations appeared comparable to WT. TgHD piglets looked normal at birth, were able to stand within a few minutes and their size was similar to each other and to WT. Social dominance relationships among the WT and HD littermates began forming two days after birth and as expected, changed as a consequence of weaning and sexual maturity. TgHD and WT animals of both sexes became sexually mature at the expected age of 5 months and were able to produce offspring. We noticed a decline in the fertility of the F1 generation TgHD boars beginning at about 12 months (see below). Motor deficits characteristic of HD were not evident in the TgHD animals. Lateral eye movements were smooth and vertical gaze movement was similar to WT minipigs. Saccades were not slow, facial praxis was normal, and vocalization had a normal rhythm. No involuntary movements were observed. A qualitative rating scale was developed to evaluate stance, gait, and ability to cross a barrier in TgHD and WT animals starting at age 3 months and at monthly intervals up to 30 and 40 months of age. A rating of 0 was normal and 3 was the most impaired (see Supplementary Data S7 for details). Using this rating scale, there was no difference in score for standing, gait, or crossing a barrier between WT (score = 0) and F0 TgHD minipigs (F807) up to 40 months and F1

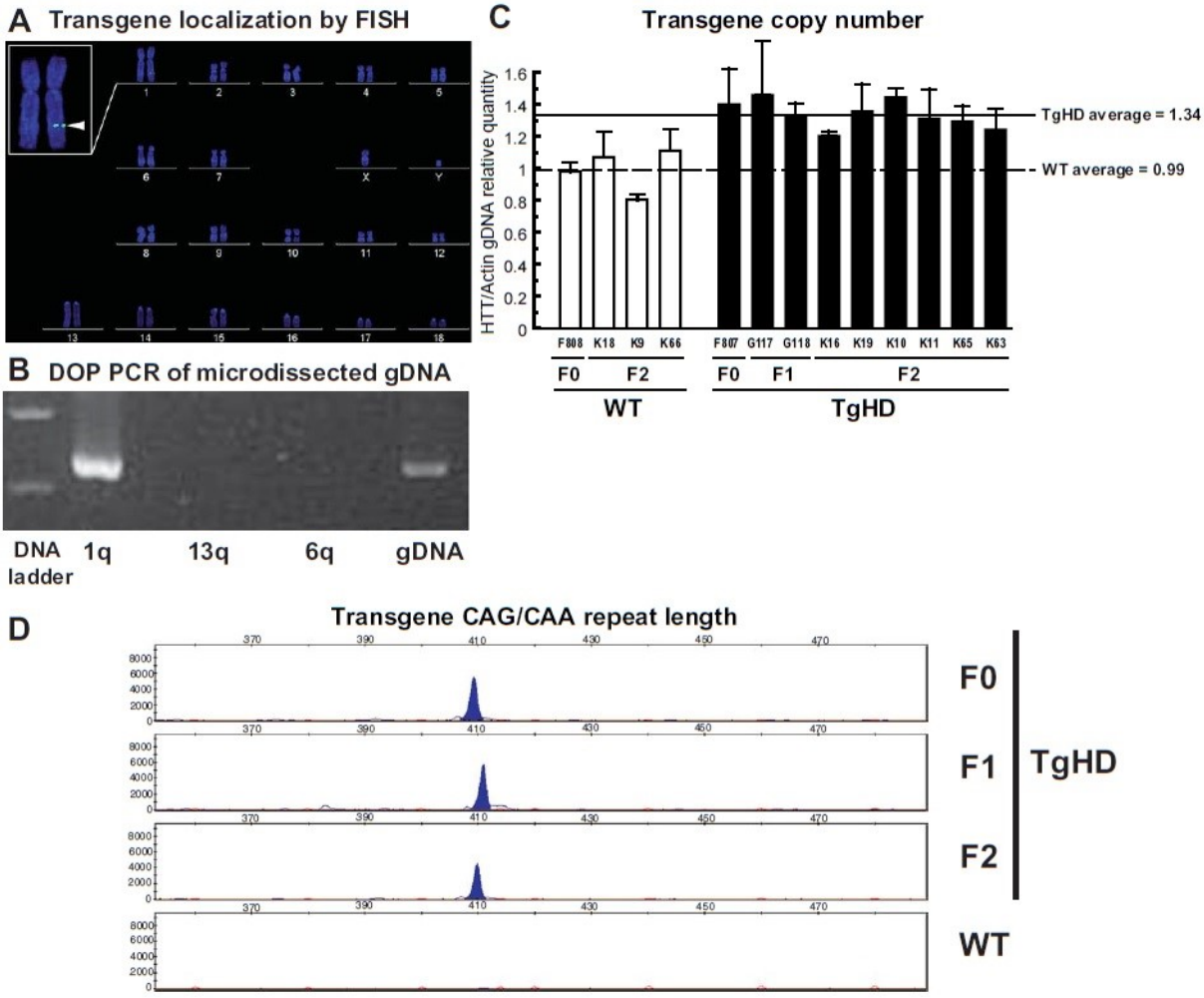

Fig. 3. Localization and copy number of mutant HTT and length of CAG/CAA repeat in TgHD minipig. (A) Incorporation of mutant HTT into the porcine genome. FISH technique shows the localization of the transgene on chromosome 1 (1q24-q25) (inset, arrowhead) of F1 TgHD male. (B) Microdissection of q arms of chromosome 1 followed by non-specific degenerate oligonucleotide primed (DOP) PCR confirms the presence of the transgene on chromosome 1 but not chromosomes 6 and 13. Genomic DNA from TgHD minipig was used as a positive control. (C) Bar graph shows quantity of HTT gDNA (both endogenous porcine HTT and human HTT transgene) in WT and TgHD animals relative to endogenous actin gDNA. Lines indicate mean values for the WT (dashed line) and transgenic animals (full line). Copy number of the transgene was determined by comparing its mean value to that of the WT. (D) The result of analysis of fragment length electrophoresis is shown. PCR amplification with primers specific for transgene shows a peak of 410 bp in TgHD animals but not in the WT. 410 bp fragment encodes both primer sequence and CAG/CAA repeat sequence encoding 124 glutamines in all three generations. CAG/CAA repeat number was similar in different porcine tissues (data not shown).

generation minipigs (G117, G118, and G122) up to 30 months of age (Scores = 0).

Expression of mutant huntingtin protein

Brain lysates were obtained from two 4 month old F2 TgHD minipigs and two WT minipigs. SDS-PAGE and Western blot analysis was performed as described in methods using antibody Ab1 to detect HTT. Mutant HTT protein fragment was detected in all regions of the CNS examined including motor cortex, putamen, caudate nucleus, hippocampus, hypothalamus, thalamus, cerebellum, and spinal cord (Fig. 4A top for one WT and one TgHD). Mutant HTT fragment migrated at the expected size of 120 kDa. Peripheral tissues including small intestine, lung, liver, kidney, ovaries and skin also expressed the TgHD protein whereas little or no transgenic HTT was present in stomach, heart, skeletal muscle and spleen (Fig. 4A bottom). With some exceptions (for example, hypothalamus), the densitometry

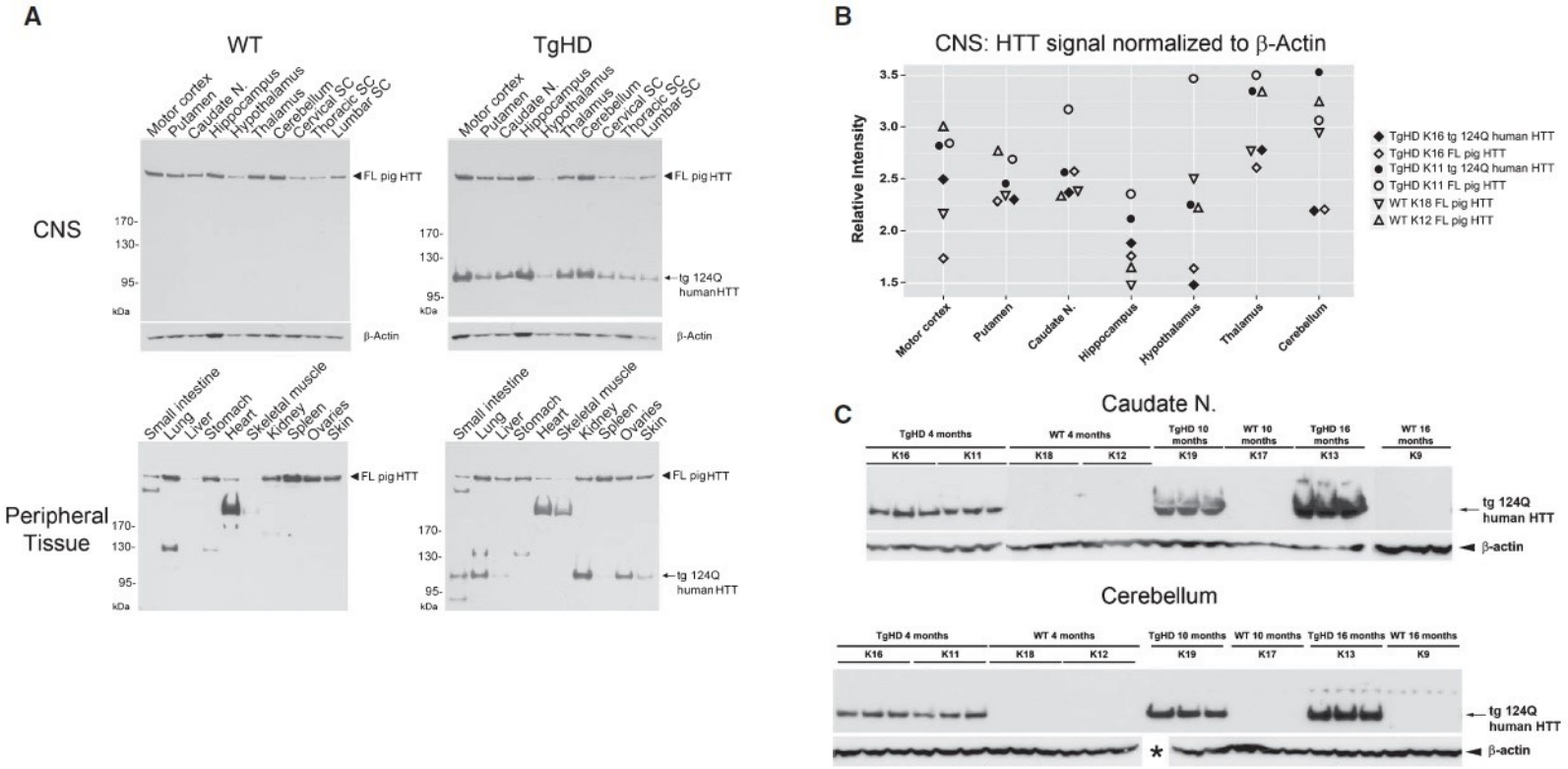

Fig. 4. Western blot analysis of mutant HTT protein in F2 WT and TgHD minipig. (A) Western blot immunoprobed with the anti-HTT1-17 antibody Ab1 shows expression of the porcine WT (FL-HTT and human HTT transgenic protein fragment (tg 124 Q human HTT) in different CNS and peripheral tissues of 4 month old minipigs. (B) Scatterplot of signal intensity values for pig huntingtin and mutant HTT relative to beta actin levels in different brain regions for WT and TgHD minipigs. (C) Western blot analysis of caudate nucleus and cerebellum from F2 – 4, 10 and 16 month old WT and TgHD minipigs. Samples of each animal are shown in triplicate. Actin is shown as loading control. Asterisk denotes missing actin band for one of triplicates of K19 cerebellum sample.

analysis showed that the levels of mutant HTT fragment in different brain regions were comparable to the levels of the endogenous porcine huntingtin seen on the same blots (see scatterplot, Fig. 4B). Further Western blot analysis of caudate nucleus and cerebellum was performed in frozen samples of brain from 8 minipigs (4 TgHD and 4 WT) ages 4, 10 and 16 months. Results showed that the mutant protein fragment was detected in the TgHD minipigs at all ages. The signals for the mutant protein migrated more broadly in SDS-PAGE in the caudate and cerebellum of the 10 and 16 months old minipigs than in the samples from the 4 month old minipig (Fig. 4C). Whether this characteristic of migration is related to an altered property of mutant HTT is unclear.

We quantified the levels of soluble mutant HTT in CNS and peripheral tissues of two sibling pairs of TgHD and WT minipigs using TR-FRET as described in Methods. Results in all brain and spinal cord regions and some peripheral tissues (lung, spleen, kidney, ovaries) showed robust HTT signal in TgHD animals compared to WT minipigs suggesting the assay was detecting mutant HTT (Fig. 5). To determine the presence of aggregated mutant HTT in TgHD minipig brain, AGERA and filter retardation assays were applied. Homogenates from motor cortex, putamen, caudate nucleus and cerebellum of WT and TgHD 16 month old minipigs were tested with mEM48 antibody. Based on these assays, aggregated mutant HTT was not present in the brain of TgHD minipig but was detected as expected in the brain of the R6/2 HD mouse (Fig. 6).

Immunohistochemistry of WT and TgHD brains

HTT immunoreactivity was examined by the immunoperoxidase method in the 4 month old minipig brain at the levels of the neostriatum using anti-HTT antibody Ab1 which detects HTT1–17. The cortex, caudate nucleus and putamen showed HTT immunoreactivity. Within these regions the gray matter was more strongly labeled than the white matter (Fig. 7). Consistent with findings in mice and human brain [71], endogenous HTT in WT minipig strongly localized to somatodendritic regions of cortical neurons and to cell bodies of neostriatal neurons. Neuropil of cortex and neostriatum was also strongly labeled. The other anti-HTT antibody which detected endogenous huntingtin in WT minipig was AB585, which was made to HTT585–725 [59]. There was no difference in the intensity of staining for HTT in TgHD minipig compared to WT minipig with anti-HTT Ab1. No nuclear inclusions were detected in the TgHD brain even though Ab1 antibody detects nuclear inclusions in the human HD cortex [72]. Antibodies MW8 and mEM48 are known to detect nuclear aggregates in other HD animal models but did not produce any staining in the TgHD minipig. Similarly no labeling was detected with MW8 in the 16 month old TgHD pigs.

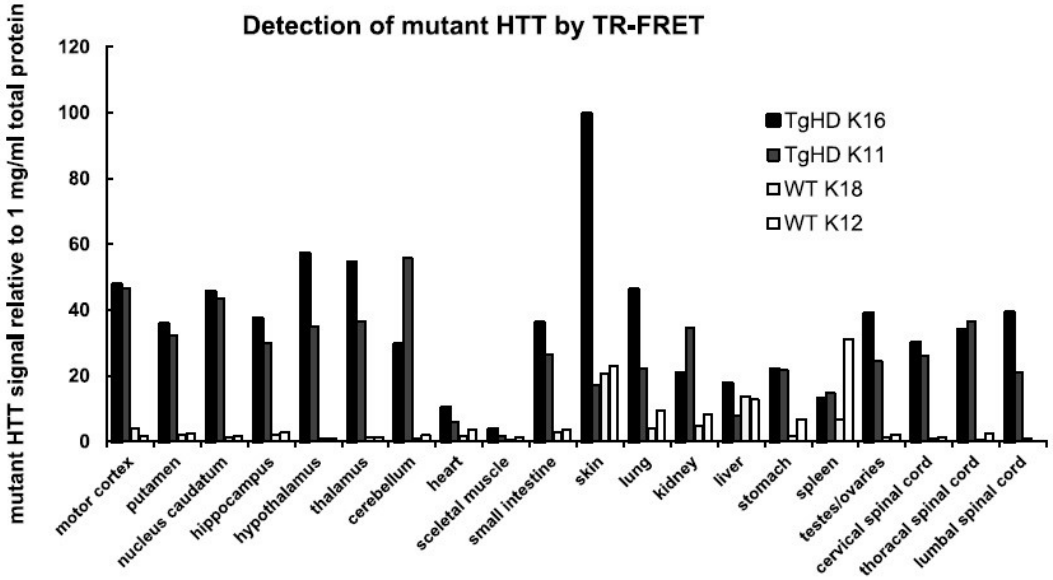

Fig. 5. TR-FRET analysis of soluble HTT protein in F2 WT and TgHD minipig. Bar graph shows results of TR-FRET analysis of soluble mutant HTT protein in TgHD and WT tissue samples (isolated from 4 month old minipigs) expressed as mutant HTT signal per 1 mg/ml total protein. Results of TR-FRET quantitative analysis correlated with western blot analysis shown in Fig. 4B.

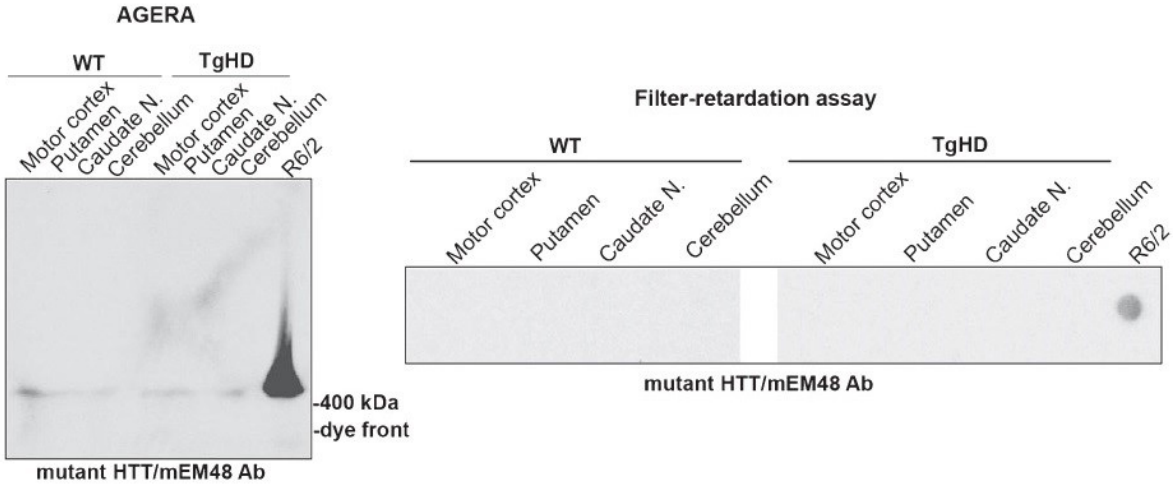

Fig. 6. Biochemical assays for detection of aggregated mutant HTT. AGERA and Filter retardation assays were performed as described in Methods using tissue from different brain regions of WT and TgHD minipig and R6/2 HD mouse. Membranes were probed with mEM48 antibody. Only R6/2 sample shows signal in both assays.

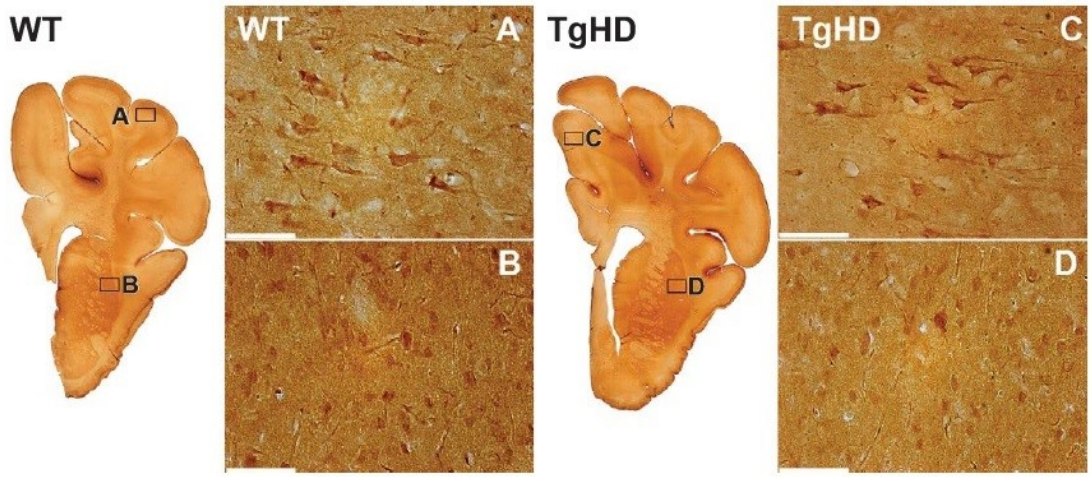

Fig. 7. HTT localization in the brain of WT and TgHD minipig. Shown are coronal sections of 4 month old WT minipig brain on the left and TgHD minipig brain on the right labeled using the immunoperoxidase method to detect HTT with anti-HTT1–17 (Ab1). Boxed regions of the cingulate cortex and the putamen are shown in images to the right of each section. HTT immunoreactivity has a strong somatodendritic localization in WT and TgHD cortex and in somata of medium sized neostriatal neurons. There is no obvious difference in labeling between WT and TgHD neurons. Scale bars 100 μm.

DARPP32 is highly localized to neuronal cell bodies and processes of the normal rodent and human neostriatum. A decline in DARPP32 immunoreactivity in the neostriatum is characteristic of HD mice [73, 74]. Immunoperoxidase labeling for DARPP32 in the neostriatum of F2 generation 16 month old WT and TgHD minipigs showed intense labeling in neuronal cell bodies and neuropil (Fig. 8A–D). Some areas of less intense DARPP32 neuropil staining were present and may be striosomes, which have been described using other neuronal markers in rodent and human striatum [75, 76] (Fig. 8B, D). Immunofluorescence analysis of caudate and putamen of F2 WT and TgHD minipigs at ages 4, 10 and 16 months also showed DARPP32 robustly expressed in neostriatal neurons and neuropil (Fig. 9A–C, shown for 16 months). A quantitative stereology analysis was performed in the sibling pair of 16 month old minipigs. Results showed that the median number of DARPP32 + neurons per mm^3 in caudate and putamen of the TgHD minipig was slightly lower compared to the WT (TgHD: 24,781 caudate neurons and 22,351 putamen neurons, and WT: 26,846 caudate

neurons and 23,863 putamen neurons) (Fig. 9C). In the TgHD brain there were reduced signal intensities for DARPP32 labeling in the caudate nucleus (11.3% reduction) and putamen (31.7% reduction) compared to the WT sibling. Although these data are highly preliminary and need confirmation in additional minipigs, the results suggest that by 16 months of age the levels of DARPP32 in TgHD minipig start to decline.

Analysis of reproductive capacity in TgHD boars

The number of spermatozoa per ejaculate was systematically evaluated in the transgenic boars from the age of 13 months to 26 months. There was a significant decline in the median number of spermatozoa in TgHD minipigs ($2.45–3.65 \times 10^9$ of spermatozoa) compared to WT ($8.15–12.48 \times 10^9$ of spermatozoa) (Fig. 10A, Kruskal-Wallis test $p<0.001$ followed by *post-hoc* Mann-Whitney U, $p<0.01$).These data suggest an impairment of spermatogenic production of the testes of TgHD minipigs. A time course analysis of the TgHD sperm samples showed that sperm number was reduced at 13 months and remained low up to 26 months (Supplementary Data S8). IVF assay showed that in WT oocytes with zona pellucida intact, the number of TgHD spermatozoa that penetrated the oocyte was lower than for the WT spermatozoa (Fig. 10B). The median percentage of WT oocytes that were penetrated by TgHD spermatozoa was significantly lower than WT oocytes penetrated by WT spermatozoa (Kruskal-Wallis test $p<0.001$ followed by *post-hoc* Mann-Whitney U, $p<0.05$) (Fig. 10C). These results indicated that the penetration activity of spermatozoa in TgHD boars was impaired compared to those of WT spermatozoa. To investigate the basis for the impaired penetration rate in TgHD, WT oocytes with zona pellucida removed were used for further analysis. Removing the zona pellucida markedly increased penetration rate in the WT and TgHD groups to 100% level (Fig. 10D). These findings suggest that the presence of the HTT gene interferes with the penetration of TgHD spermatozoa through the zona pellucida but does not

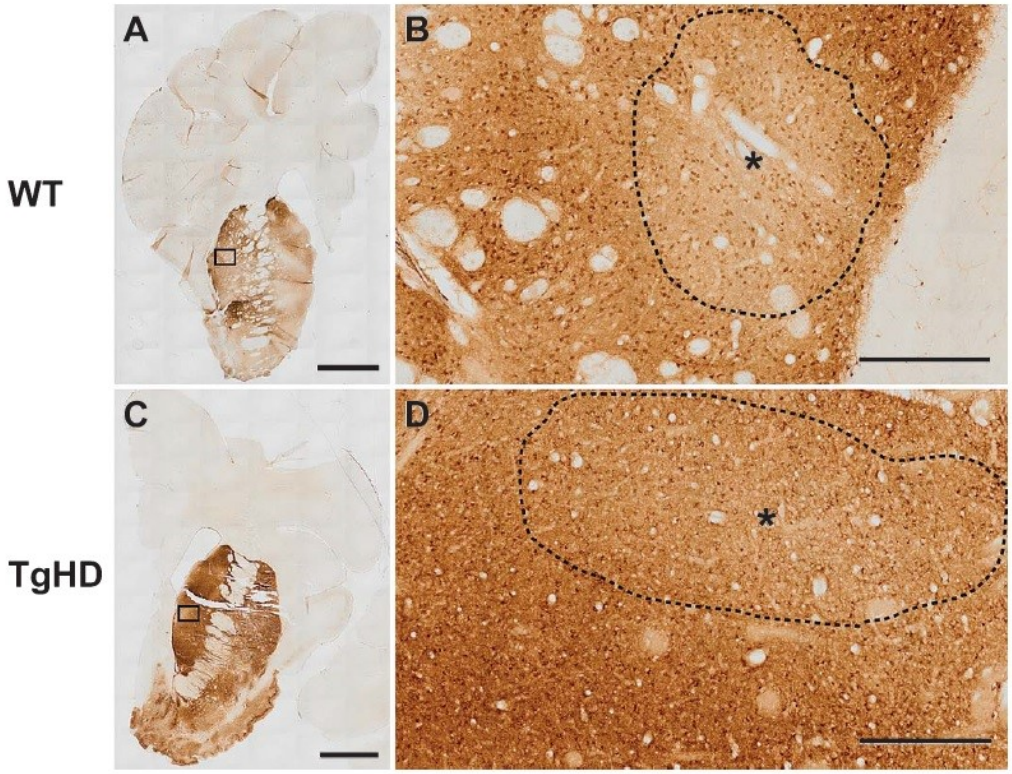

Fig. 8. DARPP32 immunoreactivity with immunoperoxidase method in 16 month old F2 WT and TgHD minipig brain. (A and C) Coronal sections through the neostriatum of WT (A) and TgHD (C) minipig show intense labeling for DARPP32 in the caudate nucleus and putamen and in the basal forebrain. Boxed areas are shown at higher magnification in B and D. (B and D) Higher magnification images show the intense labeling of neuropil and cell bodies. Areas of weaker neuropil labeling are demarcated by a dashed line and asterisk in the center and may represent striosomes. Scale bars in A and C are 5 mm and in B and D are 500 μm.

interfere with fusion of the post-acrosomal spermatozoa membrane and the cytoplasmic membrane of oocytes.

DISCUSSION

Rodent models of HD including transgenic mice expressing N-terminal fragments of mutant HTT have been very important for understanding disease mechanisms, validating targets, and testing candidate therapies, but have some limitations for modeling the human disease [2, 17]. The miniature pig (*Sus scrofa*) has similarities to humans in anatomy, physiology, and metabolism [20, 28, 29]. The size and structure of pig brain makes it amenable to neurosurgical procedures and non-invasive high resolution neuroimaging methods similar to those performed in humans [30, 34, 77]. The lifespan of minipigs and their sophisticated cognitive and motor abilities also make them useful for long-term studies of learning, memory and behavior [28, 78, 79]. In this study we show successful establishment of a transgenic minipig stably expressing N-truncated human mutant huntingtin 1–548 with 124 glutamines through multiple generations.

Transgenic HD minipigs were generated using lentiviral transduction of porcine zygotes in syngamy, at the onset of embryonic DNA synthesis. The precise timing of lentiviral transduction enhances incorporation of the transgene cDNA into embryos. The lentiviral delivery did not cause mosaicism, since the mutant HTT was revealed in all tissues tested in F1 and F2 TgHD minipigs and maintained the same number of glutamines. We found an in-frame deletion of the expanded CAG/CAA tract such that the integrated transgene encoded 124 glutamines instead of the original 145 glutamines. Similar contraction of the polyglutamine repeat has been observed in human HD [80]. The rates of transgenesis and viability of offspring in pig were higher with lentiviral delivery than with a cloning strategy reported previously [55, 81, 82]. In our experiments, the lentiviral construct that was used to transduce the minipig genome did not influence survival or normal development through multiple generations. The total neonatal mortality of our TgHD minipigs was 17.2%, which is in the range of the WT strain (16.4%, Supplementary Data S6). In contrast, the transgenic HD pigs, generated via a cloning strategy and bearing N-terminal mutant HTT (208 amino acids and 105 Q), showed a severe chorea phenotype before death and the presence of apoptotic cells in brain [55].

Both female and male transmissions of the HD transgene were confirmed in our TgHD minipigs. Two litters of F1 generation minipigs were born with a rate of transgenesis of 29.4%. The litters of F2 and F3 generations had a Mendelian inheritance of the transgene of 40.2% and 34.9%, respectively. Importantly, one single copy of exogenous HTT was found in chromosome 1 (1q24-q25) where it was maintained in F1 and F2 offspring. The TgHD minipigs of F0 –F2 generations had two alleles coding endogenous pig HTT and one allele for the N-terminal human mutant HTT. No homozygote TgHD minipigs were generated with heterozygote TgHD matings. The site of insertion of the transgene may have disrupted some essential genetic sequence that caused lethality of progeny homozygous for the HD transgene [83]. More detailed information on the exact site of insertion of the transgene in chromosome 1 may reveal more insights about potential homozygote lethality.

Mutant HTT protein expression was detected in different brain regions including cortex, caudate nucleus and putamen and in a variety of peripheral tissues and confirmed by both Western Blot analysis and TR-FRET. With one exception (hypothalamus in one of the TgHD minipigs), the data from WB and TR-FRET biochemical assays showed a good correspondence for the relative distribution of human mutant HTT in different brain regions and peripheral tissues. The expression of the transgenic protein was not confirmed in heart, stomach, spleen and skeletal muscle. *Trottier* et al. [84] determined the presence of HTT protein also in heart. Discrepancies in observed distribution of huntingtin in tissues can be influenced by the preparation of protein lysates [85]. In "bloody" tissues (liver, spleen), red color of analyte is known to artificially increase background in TR-FRET readout thus higher mutant HTT background signals in these WT tissues were likely due to this effect. The variations in the expression level of protein were expected in skin tissue due to insufficient homogenization.

Midbrain dopaminergic neurons play a critical role in basal ganglia circuitry and function including coordination of movement. Protein phosphatase 1 regulatory subunit 1B, also known as dopamine- and cAMP-regulated neuronal phosphoprotein (DARPP32), is highly expressed in caudate-putamen medium-sized spiny neurons [73, 86]. Dopamine D1 receptor stimulation enhances cyclic AMP formation, resulting in the phosphorylation of DARPP32 [86] at Thr34 by PKA [87]. A loss of DARPP32 levels in medium-sized spiny striatal neurons was observed in several rodent models of HD [74, 88], and in the globus pallidus and putamen

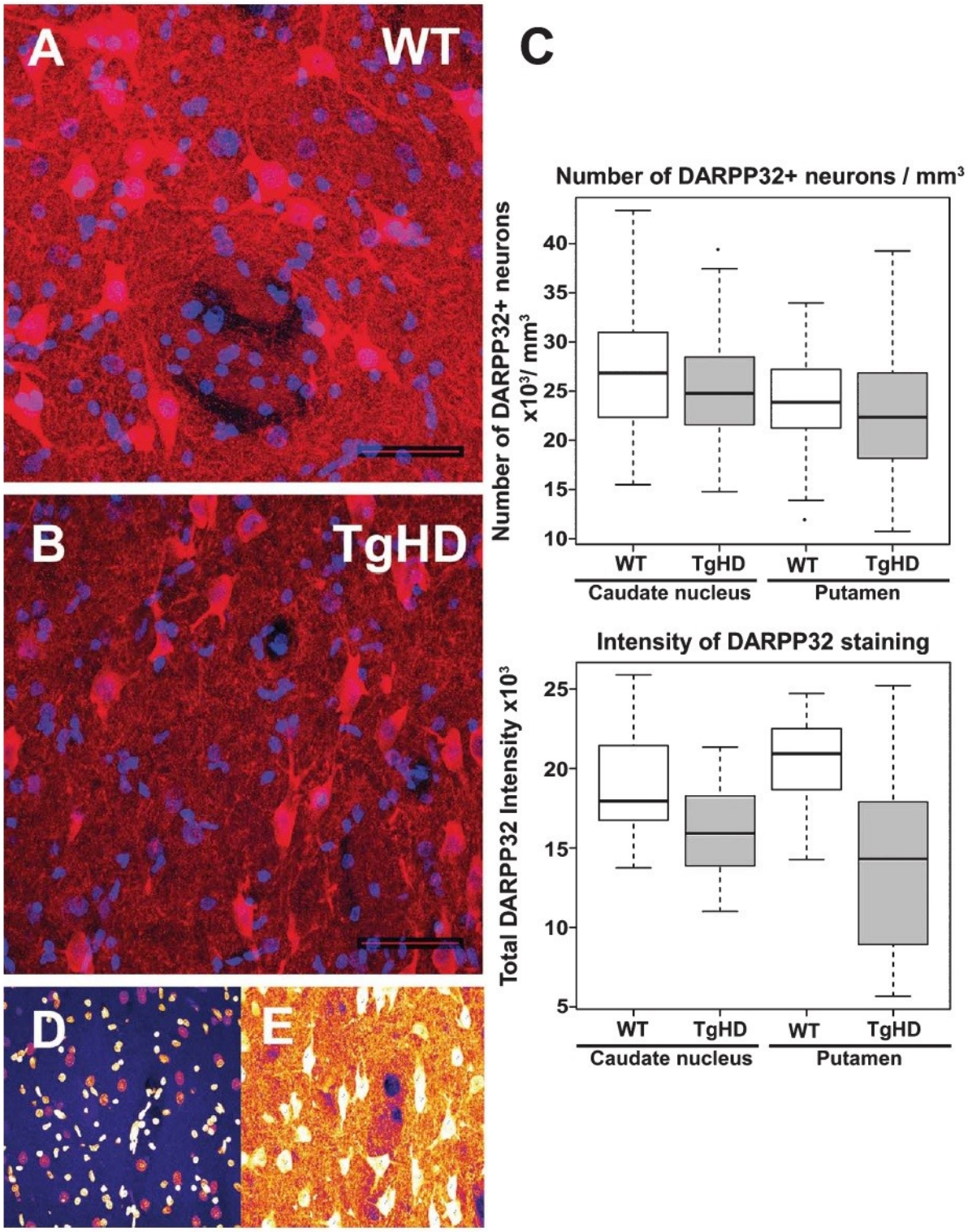
A
WT
B
TgHD
D
E
C
Number of DARPP32+ neurons / mm³
Number of DARPP32+ neurons x10³/ mm³
40
35
30
25
20
15
10
WT
TgHD
WT
TgHD
Caudate nucleus
Putamen
Intensity of DARPP32 staining
Total DARPP32 Intensity x10³
25
20
15
10
5
WT
TgHD
WT
TgHD
Caudate nucleus
Putamen

Fig. 9.

of 7 month old HD sheep [21]. A 16 month old TgHD minipig brain had a reduction compared to WT in the intensity of neuronal labeling for DARPP32 in the caudate nucleus and putamen. Clearly these findings, which are based on a detailed quantitative analysis of only one sibling pair of WT and TgHD minipigs, need to be confirmed in more animals. Nevertheless, the data suggest that changes in DARPP32 may begin in the TgHD minipig brain at around 16 months of age.

The formation of aggregates is a hallmark of HD pathology. Nuclear and cytoplasmic inclusions of mutant HTT are seen in human postmortem HD brain and in mouse models of HD [9, 72]. There was no evidence of aggregates of mutant HTT protein in the TgHD minipig up to 16 months of age based on biochemical (AGERA, filter retardation) and immunohistochemical assays with antibody to anti-HTT1-17. This antibody detects mutant HTT inclusions in the human HD brain. Other antibodies commonly used to detect nuclear inclusions of human HTT fragments in HD mice including MW8 and EM48 produced no staining in the TgHD minipigs. The absence of nuclear inclusions in the TgHD minipigs was consistent with the negative results for aggregation observed using the AGERA and filter retardations assays. Clearly study of brains from older TgHD minipigs will be needed to determine onset of aggregate formation. Many factors influence the incidence of aggregated mutant HTT including levels of mutant protein expression, polyglutamine length, the length of the mutant HTT fragment, and age of the animal [89–91]. It is noteworthy that a well studied HD mouse model BACHD which expresses full length mutant HTT with 97 glutamines encoded by CAG/CAA repeats [92] develops brain pathology and progressive motor deficits but lacks obvious intranuclear mutant HTT aggregates [93]. Some neuropil aggregates appeared in late stages (12–18 months BACHD) and were more prominent when aggressive antigen retrieval and anti-HTT antibody 3B5H10 were used in the brain sections [94], suggesting that epitopes for detecting mutant HTT aggregates may be masked. As with BACHD, the polyglutamine tract in our TgHD minipig has a mix of CAG/CAA repeats. It is possible that CAG/CAA sequence generates protein conformations that are unfavorable for immunodetection of aggregates.

A surprising finding was evidence for a decline in fertility in F1 boars caused by reduced sperm number and penetration rate. This phenotype can be easily monitored in the TgHD minipigs and therefore represents a biomarker that can be suitable for therapeutics. From 13–26 months the decline in sperm function was constant. Analysis of earlier ages might reveal a period of progressive decline that could also be a useful index for analysis of therapeutics. As only 2 F1 transgenic boars were available for detailed analysis, these findings must be considered preliminary and we are currently investigating reproductive competence in a larger cohort of F2 animals. Pathology in the germinal epithelium has been documented in human HD and YAC 128 HD mouse on histological sections where a decreased number of germ cells and reduced seminiferous tubule cross-sectional area have been observed [95]. The testicular pathology in humans was related to the presence of mutant HTT since severity was greater in patients with longer CAG repeats and testicular pathology was not present in a patient with amyotrophic lateral sclerosis. The YAC 128 HD mouse develops testicular pathology between 9 and 12 months prior to significant reduction in testosterone or GnRH levels but coinciding with changes in the brain and the appearance of motor deficits. Unlike the TgHD minipigs, problems with sperm quality and fertility have not been reported in HD patients.

No evident changes in motor function were observed in a F0 TgHD minipig up to the age of 40 months. However, only 4 animals (3 TG vs. 1 WT) were subjected to the study. A systematic quantitative study focusing on changes in motor and cognitive functions in TgHD minipigs is underway (Dr. R. Reilmann, unpublished data). In contrast to our TgHD minipigs, the short-lived transgenic piglets produced by a cloning strategy showed dyskinesia and chorea-like movements before death [55].

In summary we have developed a heterozygote TgHD minipig that expresses a human mutant HTT fragment throughout the CNS and peripheral tissues in a stable fashion through multiple generations. The TgHD minipig is healthy at birth and through early

Fig. 9. Immunofluorescence labeling of DARPP32 in WT and TgHD minipig neostriatum. (A and B) Shown are images of microscopic fields from the putamen of 16 month old WT (A) and TgHD sibling minipig (B). DARPP32 labeling in the cytoplasm is red and DAPI staining in the nucleus is in blue. (C) Upper boxplot shows median numbers of DARPP32 + neurons (mm^3) in caudate nucleus and putamen of WT and TgHD minipigs. Lower box plots shows median intensity of DARPP32 staining determined as described in Methods. (D) and (E) are pseudo-color images of DAPI stained nuclei and DARPP32 stained neurons respectively in WT putamen obtained using fire view in FiJi software as part of thresholding for the neuronal counting procedure. Scale bar 50 μm. (Colours are visible in the online version of the article; http://dx.doi.org/10.3233/JHD-130001)

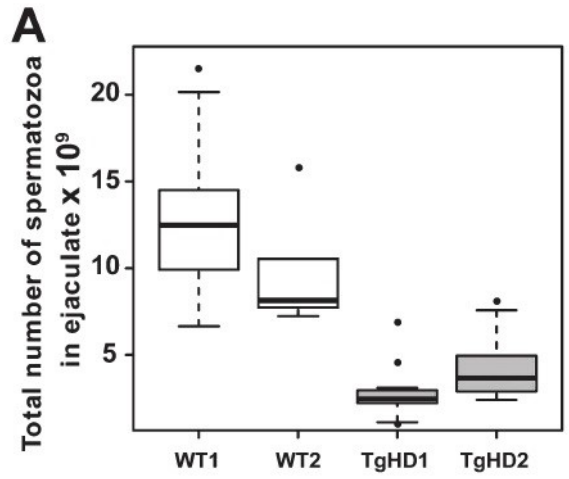

Mann-Whitney U test p-values

	TgHD1	TgHD2	WT1
TgHD2	0.0016		
WT1	8.8e-07	4.5e-07	
WT2	0.0011	0.0020	0.1090

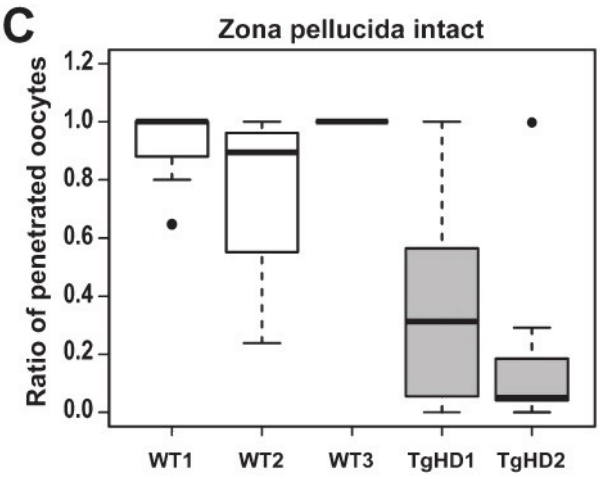

Mann-Whitney U test p-values

	WT3	WT2	WT1	TgHD1
WT2	0.11867			
WT1	0.22897	0.30008		
TgHD1	0.01761	0.08904	0.00049	
TgHD2	0.01957	0.02093	0.00021	0.11366

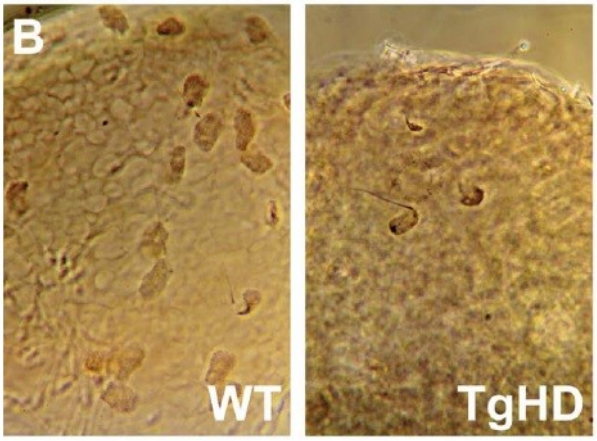

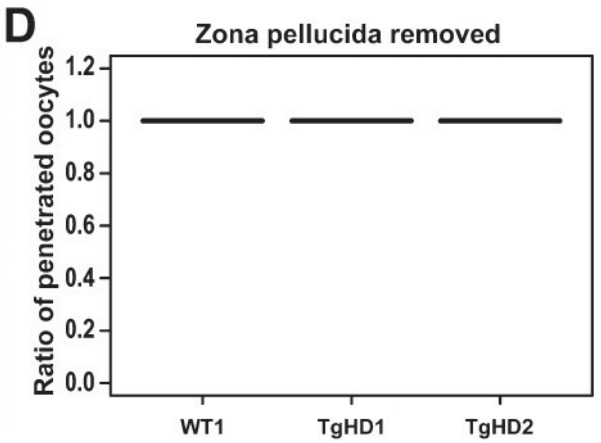

Fig. 10. Failure of reproductive capacity in TgHD boars. (A) Boxplots show number of spermatozoa per ejaculate in two WT boars and in 2 TgHD minipig boars of similar age (see methods for details). The median number of spermatozoa is reduced in TgHD minipigs compared to WT minipigs, *p*-values for all pairwise comparisons (Mann-Whitney U test) are shown in the table. (B) Left: Image of WT oocyte fertilized with WT spermatozoa *in vitro*: Note the large number of penetrated, partly de-condensed spermatozoa that are visible in intact oocyte *in vitro* fertilized with WT spermatozoa. Right: Image of WT oocyte fertilized with TgHD spermatozoa *in vitro*. Note the small number of spermatozoa. The syngamy of male and female pronuclei is visible and only one supernumerary penetrated sperm is evident. (C) Boxplots show the median ratio of intact WT oocytes (including zona pellucida) penetrated by WT or TgHD spermatozoa as determined by IVF. *P*-values for all pairwise comparisons (Mann-Whitney U test) are shown in the table below. (D) Boxplots show the median ratio of WT oocytes with zona pellucida removed penetrated by WT or TgHD spermatozoa as determined by IVF.

development and does not exhibit obvious signs of abnormal movement up to 40 months of age. However, a decline is evident at 16 months in DARPP32 immunoreactivity in the neostriatum, the region most affected in HD, as well as a decline in sperm number and penetration rate beginning at about 13 months. Formal testing of the TgHD minipigs in a battery of motor tasks is now underway.

ACKNOWLEDGMENTS

We would like to thank Patricia Jandurova, Irena Deylova and Stepan Hladky for the excellent technical assistance. We are grateful to Professor Jindrich Martinek for his help with the immunohistochemistry and virtual microscopy. We thank Jiri Jarkovsky, Institute of Biostatistics, Masaryk University, Brno, Czech Republic for advice on statistics. This work was supported by the CHDI Foundation (ID 1035), The Technical Agency of the Czech Republic (TA01011466), the project EXAM from European Regional Development Fund CZ.1.05/2.1.00/03.0124, The Grant Agency of the Charles University - Project No. 589412 and RVO 67985904.

CONFLICT OF INTEREST

One of the authors, Dr. David S. Howland is employed by CHDI Inc. which supported this research.

REFERENCES

[1] Gil JM, Rego AC. Mechanisms of neurodegeneration in Huntington's disease. The European Journal of Neuroscience. 2008;27(11):2803-20. PubMed PMID: 18588526. Epub 2008/07/01. eng.

[2] Zuccato C, Valenza M, Cattaneo E. Molecular mechanisms and potential therapeutical targets in Huntington's disease. Physiological Reviews. 2010;90(3):905-81. PubMed PMID: 20664076. Epub 2010/07/29. eng.

[3] Perez-De La Cruz V, Santamaria A. Integrative hypothesis for Huntington's disease: A brief review of experimental evidence. Physiological Research/Academia Scientiarum Bohemoslovaca. 2007;56(5):513-26. PubMed PMID: 17184144. Epub 2006/12/23. eng.

[4] Walker FO. Huntington's disease. Lancet. 2007;369(9557): 218-28. PubMed PMID: 17240289. Epub 2007/01/24. eng.

[5] The Huntington's Disease Collaborative Research Group. A novel gene containing a trinucleotide repeat that is expanded and unstable on Huntington's disease chromosomes. Cell. 1993;72(6):971-83. PubMed PMID: 8458085. Epub 1993/03/26. eng.

[6] Brinkman RR, Mezei MM, Theilmann J, Almqvist E, Hayden MR. The likelihood of being affected with Huntington disease by a particular age, for a specific CAG size. American Journal of Human Genetics. 1997;60(5):1202-10. PubMed PMID: 9150168. Pubmed Central PMCID: 1712445. Epub 1997/05/01. eng.

[7] Dunnett SB, Rosser AE. Cell transplantation for Huntington's disease Should we continue? Brain Research Bulletin. 2007;72(2-3):132-47. PubMed PMID: 17352937. Epub 2007/03/14. eng.

[8] Lee ST, Kim M. Aging and neurodegeneration. Molecular mechanisms of neuronal loss in Huntington's disease. Mechanisms of Ageing and Development. 2006;127(5):432-5. PubMed PMID: 16527334. Epub 2006/03/11. eng.

[9] Davies SW, Turmaine M, Cozens BA, DiFiglia M, Sharp AH, Ross CA, et al. Formation of neuronal intranuclear inclusions underlies the neurological dysfunction in mice transgenic for the HD mutation. Cell. 1997;90(3):537-48. PubMed PMID: 9267033. Epub 1997/08/08. eng.

[10] Mangiarini L, Sathasivam K, Seller M, Cozens B, Harper A, Hetherington C, et al. Exon 1 of the HD gene with an expanded CAG repeat is sufficient to cause a progressive neurological phenotype in transgenic mice. Cell. 1996;87(3):493-506. PubMed PMID: 8898202. Epub 1996/11/01. eng.

[11] Schilling G, Becher MW, Sharp AH, Jinnah HA, Duan K, Kotzuk JA, et al. Intranuclear inclusions and neuritic aggregates in transgenic mice expressing a mutant N-terminal fragment of huntingtin. Human Molecular Genetics. 1999; 8(3):397-407. PubMed PMID: 9949199. Epub 1999/02/09. eng.

[12] Reddy PH, Williams M, Charles V, Garrett L, Pike-Buchanan L, Whetsell WO, Jr., et al. Behavioural abnormalities and selective neuronal loss in HD transgenic mice expressing mutated full-length HD cDNA. Nature Genetics. 1998; 20(2):198-202. PubMed PMID: 9771716. Epub 1998/10/15. eng.

[13] Van Raamsdonk JM, Murphy Z, Slow EJ, Leavitt BR, Hayden MR. Selective degeneration and nuclear localization of mutant huntingtin in the YAC128 mouse model of Huntington disease. Human molecular genetics. 2005;14(24):3823-35. PubMed PMID: 16278236. Epub 2005/11/10. eng.

[14] Ariano MA, Aronin N, Difiglia M, Tagle DA, Sibley DR, Leavitt BR, et al. Striatal neurochemical changes in transgenic models of Huntington's disease. Journal of Neuroscience Research. 2002;68(6):716-29. PubMed PMID: 12111832. Epub 2002/07/12. eng.

[15] Reynolds GP, Dalton CF, Tillery CL, Mangiarini L, Davies SW, Bates GP. Brain neurotransmitter deficits in mice transgenic for the Huntington's disease mutation. Journal of Neurochemistry. 1999;72(4):1773-6. PubMed PMID: 10098889. Epub 1999/03/31. eng.

[16] Van Raamsdonk JM, Pearson J, Slow EJ, Hossain SM, Leavitt BR, Hayden MR. Cognitive dysfunction precedes neuropathology and motor abnormalities in the YAC128 mouse model of Huntington's disease. The Journal of Neuroscience : The Official Journal of the Society for Neuroscience. 2005;25(16):4169-80. PubMed PMID: 15843620. Epub 2005/04/22. eng.

[17] Yang SH, Chan AW. Transgenic animal models of huntington's disease. Current Topics in Behavioral Neurosciences. 2011;7:61-85. PubMed PMID: 21225414. Epub 2011/01/13. eng.

[18] Bendixen E, Danielsen M, Larsen K, Bendixen C. Advances in porcine genomics and proteomics–a toolbox for developing the pig as a model organism for molecular biomedical research. Briefings in Functional Genomics. 2010;9(3):208-19. PubMed PMID: 20495211. Epub 2010/05/25. eng.

[19] Casal M, Haskins M. Large animal models and gene therapy. Eur J Hum Genet. 2006;14(3):266-72. PubMed PMID: 16333317. Epub 2005/12/08. eng.

[20] Swindle MM, Makin A, Herron AJ, Clubb FJ, Jr., Frazier KS. Swine as models in biomedical research and toxicology testing. Vet Pathol. 2012;49(2):344-56. PubMed PMID: 21441112. Epub 2011/03/29. eng.

[21] Jacobsen JC, Bawden CS, Rudiger SR, McLaughlan CJ, Reid SJ, Waldvogel HJ, et al. An ovine transgenic Huntington's disease model. Human Molecular Genetics. 2010; 19(10):1873-82. PubMed PMID: 20154343. Pubmed Central PMCID: 2860888. Epub 2010/02/16. eng.

[22] Yang SH, Cheng PH, Banta H, Piotrowska-Nitsche K, Yang JJ, Cheng EC, et al. Towards a transgenic model

of Huntington's disease in a non-human primate. Nature. 2008;453(7197):921-4. PubMed PMID: 18488016. Pubmed Central PMCID: 2652570. Epub 2008/05/20. eng.

[23] Bjarkam CR, Jorgensen RL, Jensen KN, Sunde NA, Sorensen JC. Deep brain stimulation electrode anchoring using BioGlue((R)), a protective electrode covering, and a titanium microplate. Journal of Neuroscience Methods. 2008; 168(1):151-5. PubMed PMID: 17953993. Epub 2007/10/24. eng.

[24] Ettrup KS, Sorensen JC, Rodell A, Alstrup AK, Bjarkam CR. Hypothalamic deep brain stimulation influences autonomic and limbic circuitry involved in the regulation of aggression and cardiocerebrovascular control in the Gottingen minipig. Stereotactic and Functional Neurosurgery. 2012;90(5):281-91. PubMed PMID: 22797692. Epub 2012/07/17. eng.

[25] Fjord-Larsen L, Kusk P, Tornoe J, Juliusson B, Torp M, Bjarkam CR, et al. Long-term delivery of nerve growth factor by encapsulated cell biodelivery in the Gottingen minipig basal forebrain. Molecular Therapy : The Journal of the American Society of Gene Therapy. 2010;18(12):2164-72. PubMed PMID: 20664524. Pubmed Central PMCID: 2997581. Epub 2010/07/29. eng.

[26] Jensen KN, Deding D, Sorensen JC, Bjarkam CR. Long-term implantation of deep brain stimulation electrodes in the pontine micturition centre of the Gottingen minipig. Acta Neurochirurgica. 2009;151(7):785-94; discussion 94. PubMed PMID: 19404572. Epub 2009/05/01. eng.

[27] Lind NM, Moustgaard A, Jelsing J, Vajta G, Cumming P, Hansen AK. The use of pigs in neuroscience: Modeling brain disorders. Neuroscience and Biobehavioral Reviews. 2007; 31(5):728-51. PubMed PMID: 17445892. Epub 2007/04/21. eng.

[28] Lunney JK. Advances in swine biomedical model genomics. International Journal of Biological Sciences. 2007;3(3):179-84. PubMed PMID: 17384736. Pubmed Central PMCID: 1802015. Epub 2007/03/27. eng.

[29] Vodicka P, Smetana K, Jr., Dvorankova B, Emerick T, Xu YZ, Ourednik J, et al. The miniature pig as an animal model in biomedical research. Annals of the New York Academy of Sciences. 2005;1049:161-71. PubMed PMID: 15965115. Epub 2005/06/21. eng.

[30] Ishizu K, Smith DF, Bender D, Danielsen E, Hansen SB, Wong DF, et al. Positron emission tomography of radioligand binding in porcine striatum *in vivo*: Haloperidol inhibition linked to endogenous ligand release. Synapse. 2000; 38(1):87-101. PubMed PMID: 10941144. Epub 2000/08/15. eng.

[31] Rosa-Neto P, Doudet DJ, Cumming P. Gradients of dopamine D1- and D2/3-binding sites in the basal ganglia of pig and monkey measured by PET. NeuroImage. 2004;22(3):1076-83. PubMed PMID: 15219579. Epub 2004/06/29. eng.

[32] Andersen F, Watanabe H, Bjarkam C, Danielsen EH, Cumming P, DaNe XSG. Pig brain stereotaxic standard space: Mapping of cerebral blood flow normative values and effect of MPTP-lesioning. Brain Research Bulletin. 2005;66(1):17-29. PubMed PMID: 15925140. Epub 2005/06/01. eng.

[33] Duhaime AC, Saykin AJ, McDonald BC, Dodge CP, Eskey CJ, Darcey TM, et al. Functional magnetic resonance imaging of the primary somatosensory cortex in piglets. Journal of Neurosurgery. 2006;104(4 Suppl):259-64. PubMed PMID: 16619637. Epub 2006/04/20. eng.

[34] Gizewski ER, Schanze T, Bolle I, de Greiff A, Forsting M, Laube T. Visualization of the visual cortex in minipigs using fMRI. Research in Veterinary Science. 2007;82(3):281-6. PubMed PMID: 17064742. Epub 2006/10/27. eng.

[35] Watanabe H, Andersen F, Simonsen CZ, Evans SM, Gjedde A, Cumming P, et al. MR-based statistical atlas of the Gottingen minipig brain. NeuroImage. 2001;14(5):1089-96. PubMed PMID: 11697940. Epub 2001/11/08. eng.

[36] Bjarkam CR, Cancian G, Larsen M, Rosendahl F, Ettrup KS, Zeidler D, et al. A MRI-compatible stereotaxic localizer box enables high-precision stereotaxic procedures in pigs. Journal of Neuroscience Methods. 2004;139(2):293-8. PubMed PMID: 15488243. Epub 2004/10/19. eng.

[37] Rosendal F, Chakravarty MM, Sunde N, Rodell A, Jonsdottir KY, Pedersen M, et al. Defining the intercommissural plane and stereotactic coordinates for the Basal Ganglia in the Gottingen minipig brain. Stereotactic and Functional Neurosurgery. 2010;88(3):138-46. PubMed PMID: 20357521. Epub 2010/04/02. eng.

[38] Rosendal F, Frandsen J, Chakravarty MM, Bjarkam CR, Pedersen M, Sangill R, et al. New surgical technique reduces the susceptibility artefact at air-tissue interfaces on *in vivo* cerebral MRI in the Gottingen minipig. Brain Research Bulletin. 2009;80(6):403-7. PubMed PMID: 19712728. Epub 2009/08/29. eng.

[39] Rosendal F, Pedersen M, Sangill R, Stodkilde-Jorgensen H, Nielsen MS, Bjarkam CR, et al. MRI protocol for *in vivo* visualization of the Gottingen minipig brain improves targeting in experimental functional neurosurgery. Brain Research Bulletin. 2009;79(1):41-5. PubMed PMID: 19185604. Epub 2009/02/03. eng.

[40] Archibald AL, Bolund L, Churcher C, Fredholm M, Groenen MA, Harlizius B, et al. Pig genome sequence–analysis and publication strategy. BMC Genomics. 2010;11:438. PubMed PMID: 20642822. Pubmed Central PMCID: 3017778. Epub 2010/07/21. eng.

[41] Jiang Z, Rothschild MF. Swine genome science comes of age. International Journal of Biological Sciences. 2007;3(3):129-31. PubMed PMID: 17384732. Pubmed Central PMCID: 1802017. Epub 2007/03/27. eng.

[42] Jorgensen FG, Hobolth A, Hornshoj H, Bendixen C, Fredholm M, Schierup MH. Comparative analysis of protein coding sequences from human, mouse and the domesticated pig. BMC Biology. 2005;3:2. PubMed PMID: 15679890. Pubmed Central PMCID: 549206. Epub 2005/02/01. eng.

[43] Wernersson R, Schierup MH, Jorgensen FG, Gorodkin J, Panitz F, Staerfeldt HH, et al. Pigs in sequence space: A 0.66X coverage pig genome survey based on shotgun sequencing. BMC Genomics. 2005;6:70. PubMed PMID: 15885146. Pubmed Central PMCID: 1142312. Epub 2005/05/12. eng.

[44] Ramos AM, Crooijmans RP, Affara NA, Amaral AJ, Archibald AL, Beever JE, et al. Design of a high density SNP genotyping assay in the pig using SNPs identified and characterized by next generation sequencing technology. PloS One. 2009;4(8):e6524. PubMed PMID: 19654876. Pubmed Central PMCID: 2716536. Epub 2009/08/06. eng.

[45] Kim J, Cho IS, Hong JS, Choi YK, Kim H, Lee YS. Identification and characterization of new microRNAs from pig. Mammalian Genome : Official Journal of the International Mammalian Genome Society. 2008;19(7-8):570-80. PubMed PMID: 18548309. Epub 2008/06/13. eng.

[46] Li M, Xia Y, Gu Y, Zhang K, Lang Q, Chen L, et al. MicroRNAome of porcine pre- and postnatal development. PloS One. 2010;5(7):e11541. PubMed PMID: 20634961. Pubmed Central PMCID: 2902522. Epub 2010/07/17. eng.

[47] Reddy AM, Zheng Y, Jagadeeswaran G, Macmil SL, Graham WB, Roe BA, et al. Cloning, characterization and

expression analysis of porcine microRNAs. BMC Genomics. 2009;10:65. PubMed PMID: 19196471. Pubmed Central PMCID: 2644714. Epub 2009/02/07. eng.

[48] Hofmann A, Kessler B, Ewerling S, Weppert M, Vogg B, Ludwig H, et al. Efficient transgenesis in farm animals by lentiviral vectors. EMBO Reports. 2003;4(11):1054-60. PubMed PMID: 14566324. Pubmed Central PMCID: 1326377. Epub 2003/10/21. eng.

[49] Nagashima H, Fujimura T, Takahagi Y, Kurome M, Wako N, Ochiai T, et al. Development of efficient strategies for the production of genetically modified pigs. Theriogenology. 2003;59(1):95-106. PubMed PMID: 12499021. Epub 2002/12/25. eng.

[50] Kurome M, Ueda H, Tomii R, Naruse K, Nagashima H. Production of transgenic-clone pigs by the combination of ICSI-mediated gene transfer with somatic cell nuclear transfer. Transgenic Research. 2006;15(2):229-40. PubMed PMID: 16604463. Epub 2006/04/11. eng.

[51] Lavitrano M, Busnelli M, Cerrito MG, Giovannoni R, Manzini S, Vargiolu A. Sperm-mediated gene transfer. Reproduction, Fertility, and Development. 2006;18(1-2):19-23. PubMed PMID: 16478599. Epub 2006/02/16. eng.

[52] Matsuyama N, Hadano S, Onoe K, Osuga H, Showguchi-Miyata J, Gondo Y, et al. Identification and characterization of the miniature pig Huntington's disease gene homolog: Evidence for conservation and polymorphism in the CAG triplet repeat. Genomics. 2000;69(1):72-85. PubMed PMID: 11013077. Epub 2000/10/03. eng.

[53] Lin B, Rommens JM, Graham RK, Kalchman M, MacDonald H, Nasir J, et al. Differential 3′ polyadenylation of the Huntington disease gene results in two mRNA species with variable tissue expression. Human Molecular Genetics. 1993;2(10):1541-5. PubMed PMID: 7903579. Epub 1993/10/01. eng.

[54] Aigner B, Renner S, Kessler B, Klymiuk N, Kurome M, Wunsch A, et al. Transgenic pigs as models for translational biomedical research. Journal of Molecular Medicine. 2010;88(7):653-64. PubMed PMID: 20339830. Epub 2010/03/27. eng.

[55] Yang D, Wang CE, Zhao B, Li W, Ouyang Z, Liu Z, et al. Expression of Huntington's disease protein results in apoptotic neurons in the brains of cloned transgenic pigs. Human Molecular Genetics. 2010;19(20):3983-94. PubMed PMID: 20660116. Pubmed Central PMCID: 2947404. Epub 2010/07/28. eng.

[56] Motlik J, Klima J, Dvorankova B, Smetana K, Jr. Porcine epidermal stem cells as a biomedical model for wound healing and normal/malignant epithelial cell propagation. Theriogenology. 2007;67(1):105-11. PubMed PMID: 17055565. Epub 2006/10/24. eng.

[57] Trask BJ. DNA sequence localization in metaphase and interphase cells by fluorescence *in situ* hybridization. Methods in Cell Biology. 1991;35:3-35. PubMed PMID: 1779860. Epub 1991/01/01. eng.

[58] Ruijter JM, Ramakers C, Hoogaars WM, Karlen Y, Bakker O, van den Hoff MJ, et al. Amplification efficiency: Linking baseline and bias in the analysis of quantitative PCR data. Nucleic Acids Research. 2009;37(6):e45. PubMed PMID: 19237396. Pubmed Central PMCID: 2665230. Epub 2009/02/25. eng.

[59] DiFiglia M, Sapp E, Chase K, Schwarz C, Meloni A, Young C, et al. Huntingtin is a cytoplasmic protein associated with vesicles in human and rat brain neurons. Neuron. 1995;14(5):1075-81. PubMed PMID: 7748555. Epub 1995/05/01. eng.

[60] Weiss A, Klein C, Woodman B, Sathasivam K, Bibel M, Regulier E, et al. Sensitive biochemical aggregate detection reveals aggregation onset before symptom development in cellular and murine models of Huntington's disease. Journal of Neurochemistry. 2008;104(3):846-58. PubMed PMID: 17986219. Epub 2007/11/08. eng.

[61] Legleiter J, Mitchell E, Lotz GP, Sapp E, Ng C, DiFiglia M, et al. Mutant huntingtin fragments form oligomers in a polyglutamine length-dependent manner *in vitro* and *in vivo*. The Journal of Biological Chemistry. 2010;285(19):14777-90. PubMed PMID: 20220138. Pubmed Central PMCID: 2863238. Epub 2010/03/12. eng.

[62] Sontag EM, Lotz GP, Agrawal N, Tran A, Aron R, Yang G, et al. Methylene blue modulates huntingtin aggregation intermediates and is protective in Huntington's disease models. The Journal of Neuroscience : The Official Journal of the Society for Neuroscience. 2012;32(32):11109-19. PubMed PMID: 22875942. Epub 2012/08/10. eng.

[63] Sontag EM, Lotz GP, Yang G, Sontag CJ, Cummings BJ, Glabe CG, et al. Detection of mutant huntingtin aggregation conformers and modulation of SDS-soluble fibrillar oligomers by small molecules. Journal of Huntington's Disease. 2012;1(1):127-40.

[64] Scherzinger E, Lurz R, Turmaine M, Mangiarini L, Hollenbach B, Hasenbank R, et al. Huntingtin-encoded polyglutamine expansions form amyloid-like protein aggregates *in vitro* and *in vivo*. Cell. 1997;90(3):549-58. PubMed PMID: 9267034. Epub 1997/08/08. eng.

[65] Weiss A, Abramowski D, Bibel M, Bodner R, Chopra V, DiFiglia M, et al. Single-step detection of mutant huntingtin in animal and human tissues: A bioassay for Huntington's disease. Analytical Biochemistry. 2009;395(1):8-15. PubMed PMID: 19664996. Epub 2009/08/12. eng.

[66] Bjarkam CR, Pedersen M, Sorensen JC. New strategies for embedding, orientation and sectioning of small brain specimens enable direct correlation to MR-images, brain atlases, or use of unbiased stereology. Journal of Neuroscience Methods. 2001;108(2):153-9. PubMed PMID: 11478974. Epub 2001/08/02. eng.

[67] Sorensen JC, Bjarkam CR, Danielsen EH, Simonsen CZ, Geneser FA. Oriented sectioning of irregular tissue blocks in relation to computerized scanning modalities: Results from the domestic pig brain. Journal of Neuroscience Methods. 2000;104(1):93-8. PubMed PMID: 11163415. Epub 2001/02/13. eng.

[68] Guzowski JF, McNaughton BL, Barnes CA, Worley PF. Environment-specific expression of the immediate-early gene Arc in hippocampal neuronal ensembles. Nature Neuroscience. 1999;2(12):1120-4. PubMed PMID: 10570490. Epub 1999/11/26. eng.

[69] West MJ. Design-based stereological methods for counting neurons. Progress in Brain Research. 2002;135:43-51. PubMed PMID: 12143362. Epub 2002/07/30. eng.

[70] Rath D, Niemann H. *In vitro* fertilization of porcine oocytes with fresh and frozen-thawed ejaculated or frozen-thawed epididymal semen obtained from identical boars. Theriogenology. 1997;47(4):785-93. PubMed PMID: 16728028. Epub 1997/03/01. eng.

[71] Bhide PG, Day M, Sapp E, Schwarz C, Sheth A, Kim J, et al. Expression of normal and mutant huntingtin in the developing brain. The Journal of Neuroscience : The Official Journal of the Society for Neuroscience. 1996;16(17):5523-35. PubMed PMID: 8757264. Epub 1996/09/01. eng.

[72] DiFiglia M, Sapp E, Chase KO, Davies SW, Bates GP, Vonsattel JP, et al. Aggregation of huntingtin in neuronal

intranuclear inclusions and dystrophic neurites in brain. Science. 199726;277(5334):1990-3. PubMed PMID: 9302293. Epub 1997/09/26. eng.

[73] Ouimet CC, Greengard P. Distribution of DARPP-32 in the basal ganglia: An electron microscopic study. Journal of Neurocytology. 1990;19(1):39-52. PubMed PMID: 2191086. Epub 1990/02/01. eng.

[74] van Dellen A, Welch J, Dixon RM, Cordery P, York D, Styles P, et al. N-Acetylaspartate and DARPP-32 levels decrease in the corpus striatum of Huntington's disease mice. Neuroreport. 2000;11(17):3751-7. PubMed PMID: 11117485. Epub 2000/12/16. eng.

[75] Tippett LJ, Waldvogel HJ, Thomas SJ, Hogg VM, van Roon-Mom W, Synek BJ, et al. Striosomes and mood dysfunction in Huntington's disease. Brain : A Journal of Neurology. 2007;130(Pt 1):206-21. PubMed PMID: 17040921.

[76] Crittenden JR, Graybiel AM. Basal Ganglia disorders associated with imbalances in the striatal striosome and matrix compartments. Frontiers in Neuroanatomy. 2011;5:59. PubMed PMID: 21941467. Pubmed Central PMCID: 3171104.

[77] Keereman V, Fierens Y, Broux T, De Deene Y, Lonneux M, Vandenberghe S. MRI-based attenuation correction for PET/MRI using ultrashort echo time sequences. J Nucl Med. 2010;51(5):812-8. PubMed PMID: 20439508. Epub 2010/05/05. eng.

[78] Gieling ET, Nordquist RE, van der Staay FJ. Assessing learning and memory in pigs. Anim Cogn. 2011;14(2):151-73. PubMed PMID: 21203792. Pubmed Central PMCID: 3040303. Epub 2011/01/05. eng.

[79] Gieling ET, Schuurman T, Nordquist RE, van der Staay FJ. The pig as a model animal for studying cognition and neurobehavioral disorders. Current Topics in Behavioral Neurosciences. 2011;7:359-83. PubMed PMID: 21287323. Epub 2011/02/03. eng.

[80] Wheeler VC, Persichetti F, McNeil SM, Mysore JS, Mysore SS, MacDonald ME, et al. Factors associated with HD CAG repeat instability in Huntington disease. Journal of Medical Genetics. 2007;44(11):695-701. PubMed PMID: 17660463. Epub 2007/07/31. eng.

[81] Lai L, Prather RS. Creating genetically modified pigs by using nuclear transfer. Reproductive Biology and Endocrinology : RB&E. 2003;1:82. PubMed PMID: 14613542. Pubmed Central PMCID: 280726. Epub 2003/11/14. eng.

[82] Polejaeva IA, Chen SH, Vaught TD, Page RL, Mullins J, Ball S, et al. Cloned pigs produced by nuclear transfer from adult somatic cells. Nature. 2000;407(6800):86-90. PubMed PMID: 10993078. Epub 2000/09/19. eng.

[83] Park F. Lentiviral vectors: Are they the future of animal transgenesis? Physiol Genomics. 2007;31(2):159-73. PubMed PMID: 17684037. Epub 2007/08/09. eng.

[84] Trottier Y, Devys D, Imbert G, Saudou F, An I, Lutz Y, et al. Cellular localization of the Huntington's disease protein and discrimination of the normal and mutated form. Nature Genetics. 1995;10(1):104-10. PubMed PMID: 7647777. Epub 1995/05/01. eng.

[85] Wood JD, MacMillan JC, Harper PS, Lowenstein PR, Jones AL. Partial characterisation of murine huntingtin and apparent variations in the subcellular localisation of huntingtin in human, mouse and rat brain. Human Molecular Genetics. 1996;5(4):481-7. PubMed PMID: 8845840. Epub 1996/04/01. eng.

[86] Walaas SI, Greengard P. DARPP-32, a dopamine- and adenosine 3′:5′-monophosphate-regulated phosphoprotein enriched in dopamine-innervated brain regions. I. Regional and cellular distribution in the rat brain. The Journal of Neuroscience : The Official Journal of the Society for Neuroscience. 1984;4(1):84-98. PubMed PMID: 6319627. Epub 1984/01/01. eng.

[87] Hemmings HC, Jr., Greengard P, Tung HY, Cohen P. DARPP-32, a dopamine-regulated neuronal phosphoprotein, is a potent inhibitor of protein phosphatase-1. Nature. 1984;310(5977):503-5. PubMed PMID: 6087160. Epub 1984/08/09. eng.

[88] Bibb JA, Yan Z, Svenningsson P, Snyder GL, Pieribone VA, Horiuchi A, et al. Severe deficiencies in dopamine signaling in presymptomatic Huntington's disease mice. Proceedings of the National Academy of Sciences of the United States of America. 2000;97(12):6809-14. PubMed PMID: 10829080. Pubmed Central PMCID: 18747. Epub 2000/06/01. eng.

[89] Hackam AS, Singaraja R, Wellington CL, Metzler M, McCutcheon K, Zhang T, et al. The influence of huntingtin protein size on nuclear localization and cellular toxicity. The Journal of Cell Biology. 1998;141(5):1097-105. PubMed PMID: 9606203. Pubmed Central PMCID: 2137174. Epub 1998/06/12. eng.

[90] Chen S, Berthelier V, Hamilton JB, O'Nuallain B, Wetzel R. Amyloid-like features of polyglutamine aggregates and their assembly kinetics. Biochemistry. 2002;41(23):7391-9. PubMed PMID: 12044172. Epub 2002/06/05. eng.

[91] Li SH, Li XJ. Aggregation of N-terminal huntingtin is dependent on the length of its glutamine repeats. Human Molecular Genetics. 1998;7(5):777-82. PubMed PMID: 9536080. Epub 1998/05/23. eng.

[92] Gray M, Shirasaki DI, Cepeda C, Andre VM, Wilburn B, Lu XH, et al. Full-length human mutant huntingtin with a stable polyglutamine repeat can elicit progressive and selective neuropathogenesis in BACHD mice. The Journal of Neuroscience : The Official Journal of the Society for Neuroscience. 2008;28(24):6182-95. PubMed PMID: 18550760. Pubmed Central PMCID: 2630800. Epub 2008/06/14. eng.

[93] Pouladi MA, Stanek LM, Xie Y, Franciosi S, Southwell AL, Deng Y, et al. Marked differences in neurochemistry and aggregates despite similar behavioural and neuropathological features of Huntington disease in the full-length BACHD and YAC128 mice. Human Molecular Genetics. 2012;21(10):2219-32. PubMed PMID: 22328089.

[94] Miller J, Arrasate M, Brooks E, Libeu CP, Legleiter J, Hatters D, et al. Identifying polyglutamine protein species *in situ* that best predict neurodegeneration. Nature Chemical Biology. 2011;7(12):925-34. PubMed PMID: 22037470. Pubmed Central PMCID: 3271120. Epub 2011/11/01. eng.

[95] Van Raamsdonk JM, Murphy Z, Selva DM, Hamidizadeh R, Pearson J, Petersen A, et al. Testicular degeneration in Huntington disease. Neurobiology of Disease. 2007;26(3):512-20. PubMed PMID: 17433700. Epub 2007/04/17. eng.

SUPPLEMENTARY DATA

S1

Construction of HIV1-HD-548aaHTT-145Q vectors

To make N-terminal the first 548aa truncated form of human huntingtin, the following "A" and "B" oligonucleotides were synthesized, annealed and inserted in between the EcoRV and XbaI sites in the plasmid pFLmixQ145 comprising human full-length HTT cDNA with 145 CAG/CAA repeats (obtained from Coriell Cell Repositories, Camden, NJ):

"A" 5´ ATCTTGAGCCACAGCTCCAGCCAGGTCAGCGCCGTCCCATCTGACCCTGCCATGTAATAGT 3'

"B" 3´ TAGAACTCGGTGTCGAGGTCGGTCCAGTCGCGGCAGGGTAGACTGGGACGGTACATTATCAGATC 5'

The inserted oligonucleotides place two stop codons (TAATAG) after 548aa.An 860 bpBamHI-XcmI DNA fragment containing the HD promoter was isolated from the plasmid p4G6E4.0 (gift from Dr. G. Bates). N-truncated 548aa-145Q huntingtin was ligated with the HD promoter at the XcmI site, residing at the initiation codon of the HTT coding region. Right BamHI site in HD-548aa-145Q construct was created by insertion of synthetic linker (Xba-BglII-BamHI-Xba) into the XbaI site. After verifying the sequence of the HD-548aa-145Q construct, HD-548aa-145Q unit was isolated and inserted into the BamHI cloning site of the HIV1 backbone plasmid pHIV7, which contains cPPT and WPRE cis-enhancing elements. The resulting HIV1 vector plasmid was designated as pHIV1-HD-548aaHTT-145Q. Lentiviral vectors were produced by transient co-transfection of 293T cells maintained in Dulbecco's modified Eagle's medium (DMEM) with 10 % FCS. 293T cells in 150 mm dishes were co-transfected by Polyethylenimine (PEI) with each HIV1 vector plasmid, pLP1 and pLP2 (Invitrogen), and pCMV-G [1]. Conditioned media at day 2 and 3 post transfection was collected, filtered through a 0.45 μm filter, and concentrated by centrifugation at 7,000 rpm for 16 h at 4 ^{o}C with a Sorvall GS-3 rotor. The resulting pellets were re-suspended with buffer containing 10 mMTris-HCl, pH 7.8, 1 mM $MgCl_2$ and 3 % sucrose. Chromosomal DNAs from transduced cells were prepared with DNeasy Blood & Tissue kit (Qiagen) after maintaining the cells for at least 10 days with more than two passages. This procedure is to eliminate the contaminated plasmid DNAs used for virus production from the transduced cells. The infectious titers of prepared HIV1-HD-548aaHTT-145Q vectors were determined by measuring the copy numbers of the provirus in the chromosomes by quantitative real-time RT PCR using a primer set selected for the WPRE sequence. HIV1-CMV-GFP vector ($1x10^9$ IU/ml) was used as the standard.

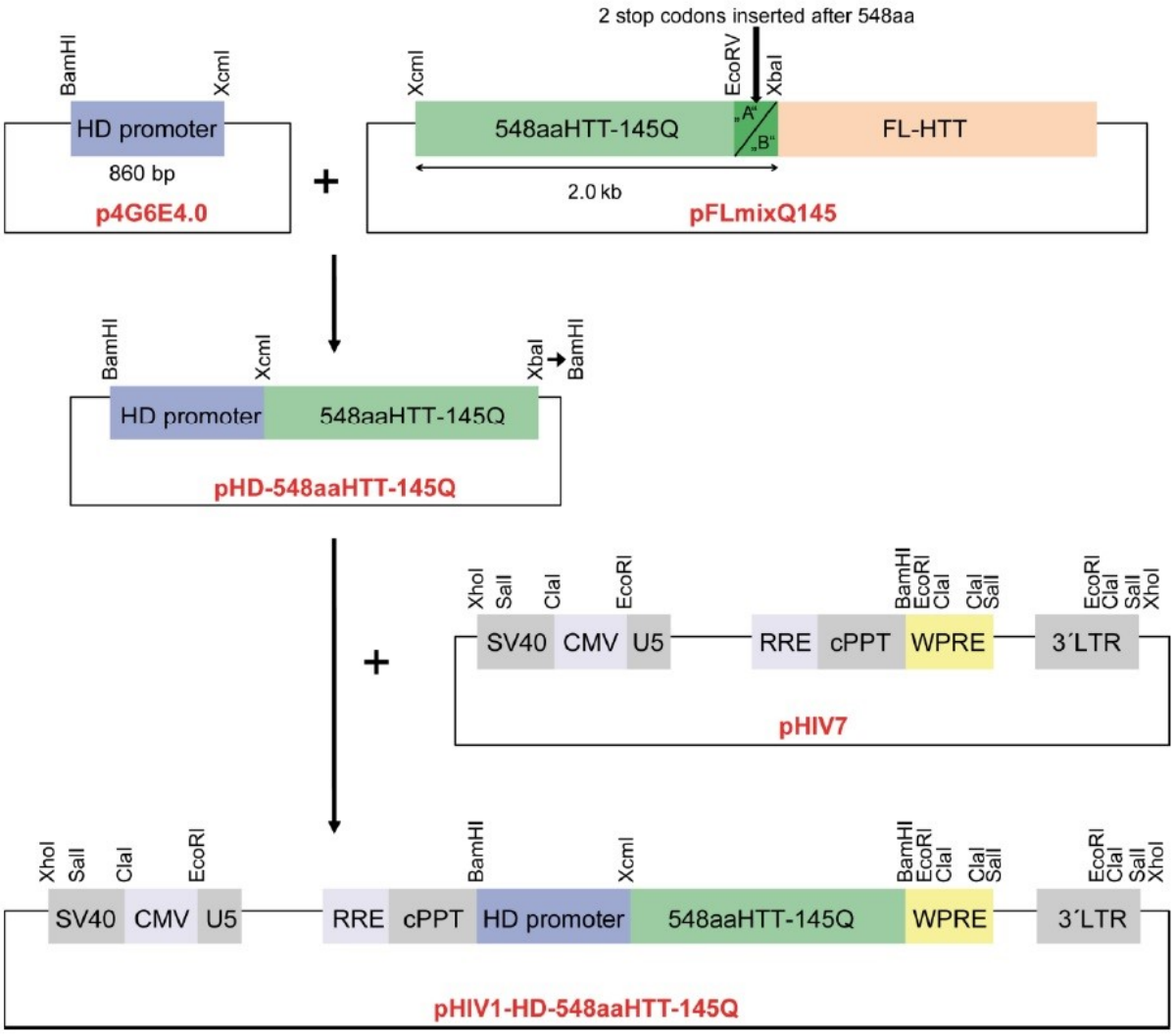
2 stop codons inserted after 548aa
BamHI
XcmI
HD promoter
860 bp
p4G6E4.0
XcmI
EcoRV
XbaI
548aaHTT-145Q
„A"
„B"
FL-HTT
2.0 kb
pFLmixQ145
BamHI
XcmI
XbaI
BamHI
HD promoter
548aaHTT-145Q
pHD-548aaHTT-145Q
XhoI
SalI
ClaI
EcoRI
BamHI
EcoRI
ClaI
ClaI
SalI
EcoRI
ClaI
SalI
XhoI
SV40
CMV
U5
RRE
cPPT
WPRE
3´LTR
pHIV7
XhoI
SalI
ClaI
EcoRI
BamHI
XcmI
BamHI
EcoRI
ClaI
ClaI
SalI
EcoRI
ClaI
SalI
XhoI
SV40
CMV
U5
RRE
cPPT
HD promoter
548aaHTT-145Q
WPRE
3´LTR
pHIV1-HD-548aaHTT-145Q

2

S2

Verification of HIV1-HD-548aa-145Q vectors in vitro

Porcine neural stem cells differentiated into neurons and glial cells [2] were transduced with HIV-HD-548aaHTT-145Q constructs ($1x10^9$ IU/ml). The immunocytological study for detection of the transgene was performed using mouse monoclonal antibody raised against the first 82aa of human recombinant huntingtin (MAB5492, Millipore). This antibody binds the human wild type and mutant huntingtin. Porcine transduced cells express mutant human huntingtin four days after transduction with HIV-HD-548aaHTT-145Q construct **(A)**. In order to test the potential of the lentiviral construct to successfully infect the porcine zygote, porcine oocytes were aspired from preovulatory follicles **(B)** by laparoscopy. **(C)** Microinjection of FITC-dextran into perivitelline space of porcine oocyte is shown to demonstrate lentivirus injection procedure. Oocytes were matured in vitro until the in vitro fertilization (IVF) was done by the frozen epididymal sperm from a selected boar. After successful IVF, embryos at the pronuclear stage **(D)** were microinjected with the HIV1-CMV-EGFP construct into the perivitelline space. Embryos were then cultured in vitro until the expanded blastocyst **(E)** and the hatched blastocyst stages **(F)**. The EGFP fluorescence is visible in cells of embryoblast (arrow) and trophoblast (arrowhead) **(F)**.

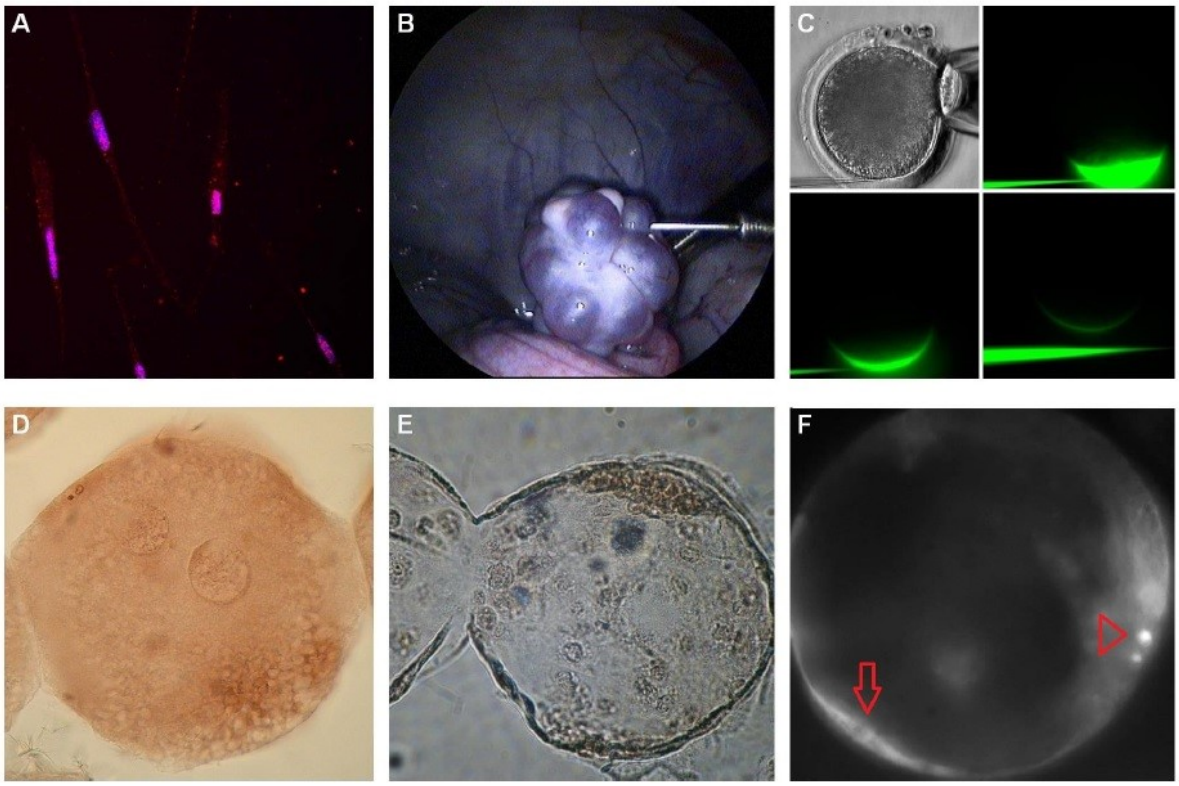

S3

Transgenesis

Libechov minipig gilts were checked for estrus daily with an experienced boar and standing estrus was recorded. In each experiment, gilts in the luteal phase of estrus cycle (4 – 5 donors and 3 recipients) were synchronized by Regumate for 15 days. The superovulation of donors started by intramuscularly administered 500 IU PMSG (Day 16) followed by induction of ovulation by intramuscularly administered injection of 500 IU hCG (Praedyn) or gnRH (Receptal, Day 19). Females were mated twice with the boars for the collection of pronuclear stage embryos. Embryos were flushed from oviducts 48 – 50 hours after injection of hCG or gnRh. Pronuclear stage embryos were microinjected into the perivitelline space with lentiviral vector (50 – 100 viral particles per zygote) at a micromanipulation workstation (Burleigh MIS-5400 piezoelectric and Narishige hydraulic micromanipulator with MDI PM2000 pressure microinjector mounted on Olympus IX70 inverted microscope). The injected embryos were then cultured for one hour in vitro in the PZM3 medium and immediately transferred laparoscopically into the fallopian tubes of recipients.

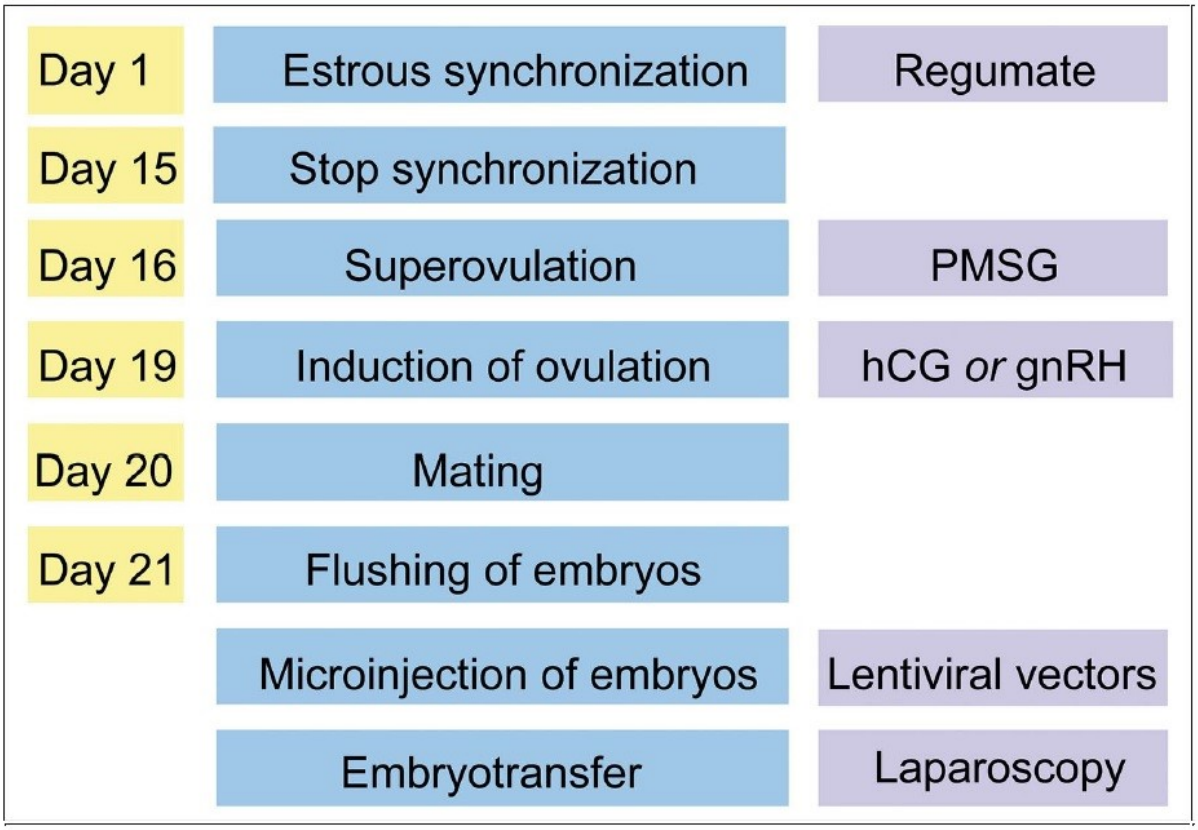

S4

Video

Laparoscopic delivery (XION medical, GmbH Berlin) of HD construct microinjected pronuclear stage embryos into the recipient oviduct.

Minipig females were positioned in dorsal recumbency for the embryo delivery procedure. After preparation and disinfection of the surgical field, a Verres needle was inserted through the umbilicus and the abdomen was inflated to 12 – 14 mm Hg with CO_2. The Verres needle was replaced by a trocar for insertion of the laparoscope. Instrumentation trocars were positioned lateral-caudal from the umbilicus. Using graspers, the left and right oviducts were prepared and fixated. After fixation of oviducts a hand-made double lumen aspiration needle was inserted through the trocar and embryos were injected into the oviduct lumen by epidural catheter (Perifix® Standard, B.Braun Medical, 18G). At the end of the procedure, the abdominal cavity was examined for hemostasis and proper tissue apposition. Following desufflation, the peritoneum, muscle, and skin layers penetrated by the trocars were closed with sutures.

S5

The complete pedigree of F0, F1 and F2 generations TgHD minipigs

Black boxes (males) and black circles (females) represent animals positively tested for the transgene in DNA extracted from biopsy of ear tissue. "/" denotes a dead minipig within the first 48 hours; "X" indicates an animal sacrificed for biochemical and microscopic studies. The F0 minipig gave birth to 5 TgHD piglets in two litters. Mendelian inheritance is indicated in the F2 generation. 37 transgenic animals were born in 17 litters. No homozygous TgHD minipigs were born.

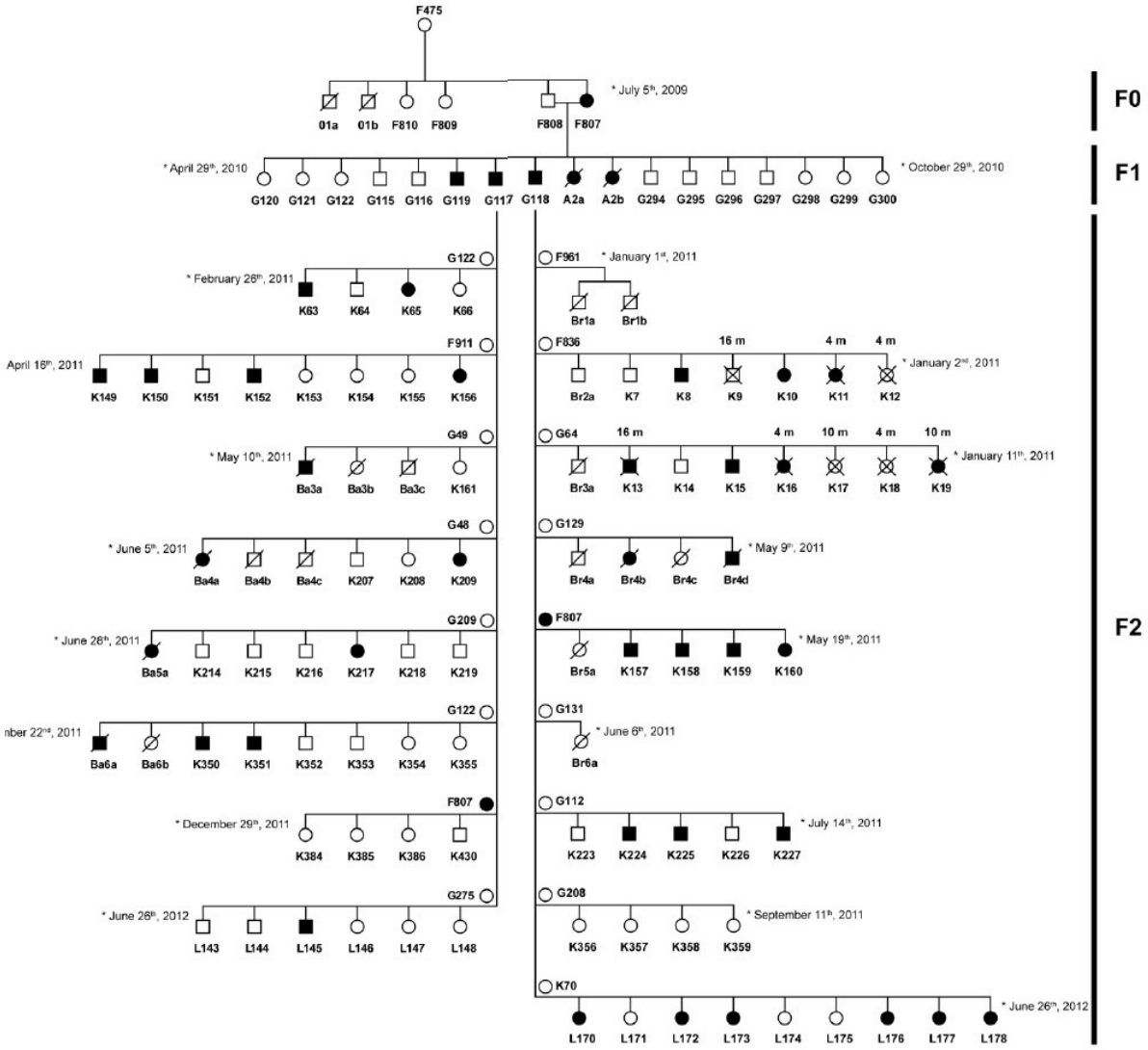

S6

Comparison of number of piglets and newborn mortality between TgHD and WT litters

(A) Average number of piglets in TgHD litters is comparable with average number of piglets in WT litters. **(B)** Newborn mortality is comparable between transgenic and wild-type litters.

(A)

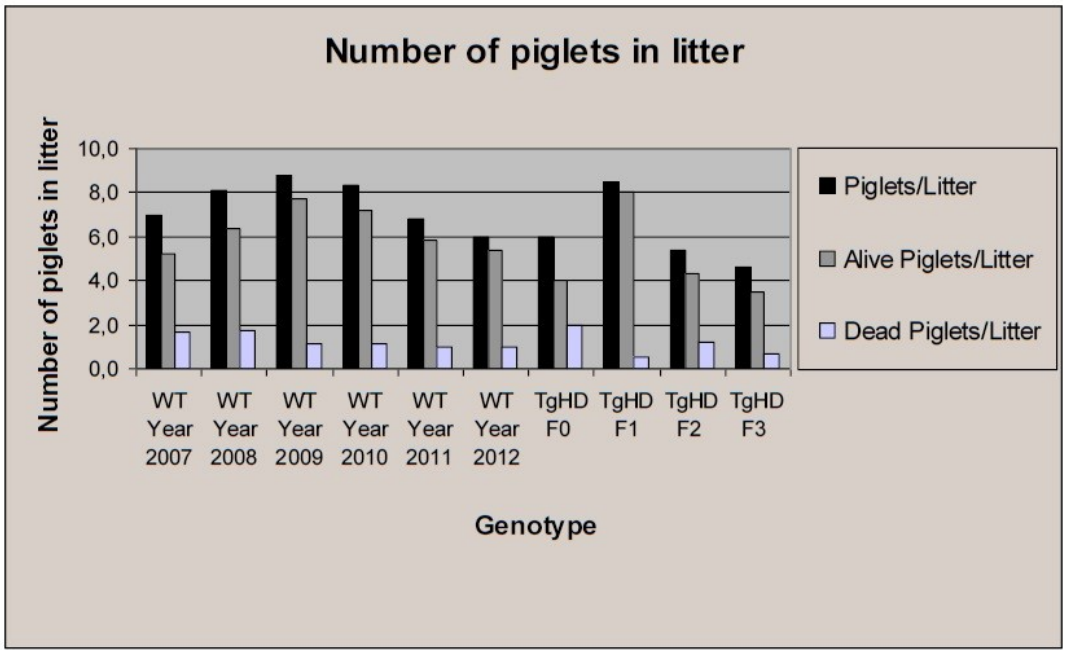

(B)

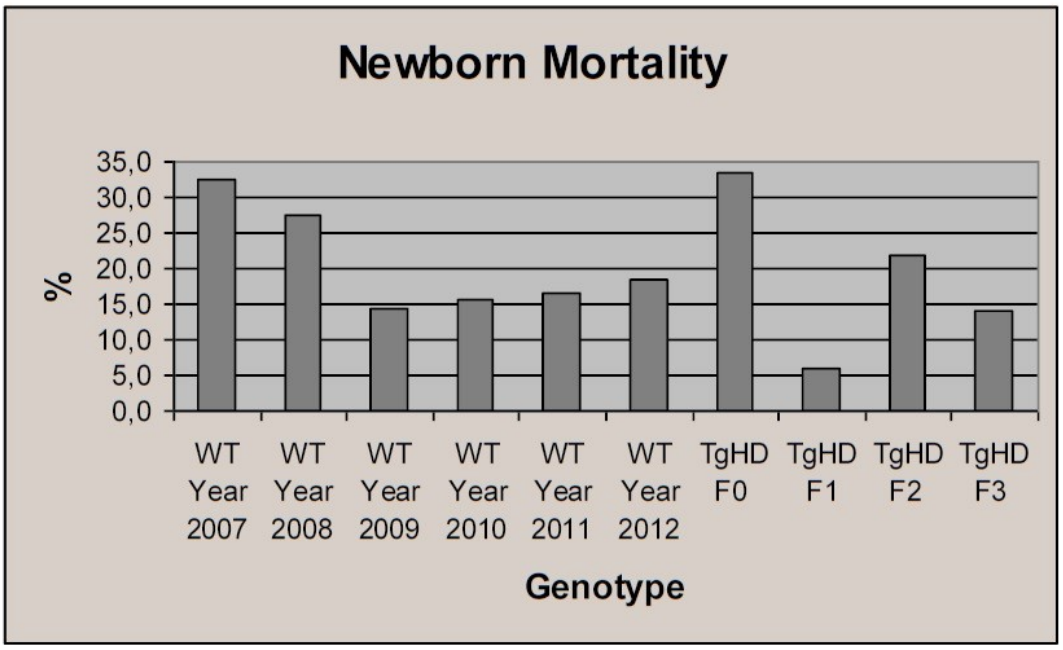

S7

Methods for motor behavior testing

Transgenic minipigs from F0 (F807) and F1 (G117, G118) generations together with wild-type controls (G122) from F1 generation were used. The minipigs were trained to be familiar with the trainer, her handling and in crossing barriers from the age of 6 weeks. Each piglet was trained daily in the morning in 15 min sessions. The training and testing areas were 3x3 m x 2x15 m. Minipigs were trained once a week until the age of 3 months. Testing began two days after the last training day in monthly intervals starting at the age of 3 months and continuing to the age of 40 months (F807) and 30 months (G117, G118, G122). Weight, eyes movements, facial praxis, vocalization, and evidence of involuntary movements were monitored before each testing. Females (F807 and G122) were not included into the testing procedure if they were within 4 weeks of expected delivery and during nursing. The scores and description of behaviors were as follows:

Points	Stand	Gait	Crossing a barrier
0	standing on 4 legs	normal gait	no problem with crossing a barrier
1	lowering of hind quarters close to the ground and placement of the forelegs under the body	ataxia (incoordinated movements)	*problem with crossing a barrier
2	kneeling on one or both forelegs	dysmetria (altered range of movement)	animal is not able to cross a barrier
3		weakness (leg dragging, collapse upon weight bearing)	

*3-9 month old piglets were trained to cross a barrier 14x20x79 cm (HxWxL) and pigs 10 months and older were trained to cross a barrier 16x36x95 cm (HxWxL)

S8

Total number of sperm in ejaculate of WT and TgHD minipigs

Sperm counts obtained in the samples collected from 2 WT and 2 TgHD minipig boars at the dates indicated.

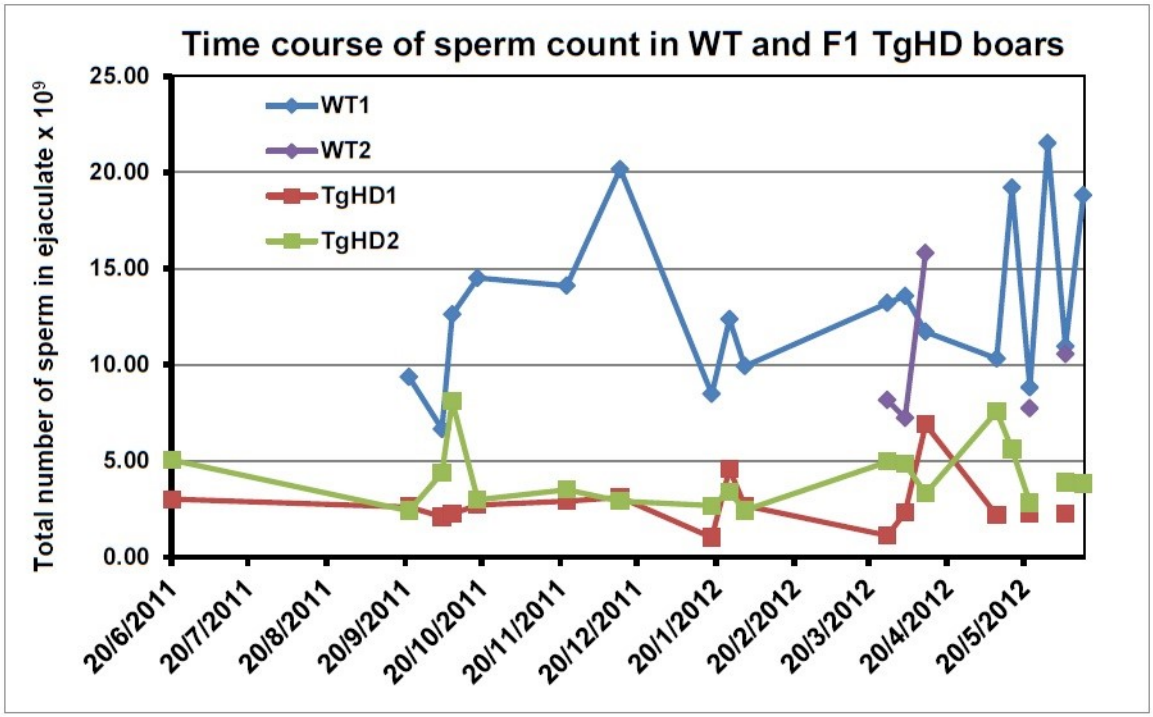

References:

1. Yee JK, Miyanohara A, LaPorte P, Bouic K, Burns JC, Friedmann T. A general method for the generation of high-titer, pantropic retroviral vectors: highly efficient infection of primary hepatocytes. Proceedings of the National Academy of Sciences of the United States of America. 1994 Sep 27;91(20):9564-8. PubMed PMID: 7937806. Pubmed Central PMCID: 44853. Epub 1994/09/27. eng.
2. Skalnikova H, Halada P, Vodicka P, Motlik J, Rehulka P, Horning O, et al. A proteomic approach to studying the differentiation of neural stem cells. Proteomics. 2007 Jun;7(11):1825-38. PubMed PMID: 17474145. Epub 2007/05/03. eng.

Paper II

Mutated Huntingtin Causes Testicular Pathology in Transgenic Minipig Boars.

Macakova, M., Bohuslavova, B., Vochozkova, P., Pavlok, A., Sedlackova, M., Vidinska, D., Vochyanova, K., Liskova, I., Valekova, I., ***Baxa, M.,*** *Ellederova, Z., Klima, J., Juhas, S., Juhasova, J., Klouckova, J., Haluzik, M., Klempir, J., Hansikova, H., Spacilova, J., Collins, R., Blumenthal, I., Talkowski, M., Gusella, J., Howland, D.S., DiFiglia, M., and Motlik, J. (2016).*

Neurodegenerative diseases 16, 245–59

IF 2.842

Motivation of the study

Even though the most prominent phenotype in HD is degeneration of neurons in the brain, the presence of mutant huntingtin affects also peripheral tissues, including testes. Previosuly (Paper I), we showed reproductive failure in 13-month-old TgHD boars. Disposing with a larger cohort of TgHD boars from F2 generation, we were interested in their reproductive parameters. We aimed to answer a question, whether the sperm and testicular pathology is caused by the primary effect of mutant huntingtin protein or whether it is a consequence of hormonal changes or interruption of any coding sequence during insertion of the lentiviral construct.

Summary

We demonstrated decreased sperm count, motility and progressivity in TgHD boars. Reproductive failures started in the age of 13 months and persisted at a low level with ageing. TgHD sperms showed continuous decreased ability to penetrate the oocytes. Moreover, we revealed structural abnormalities in TgHD spermatozoa. We observed double or triple axonemes with fused mitochondrial sheaths. Disorganized mitochondrial sheaths were frequently associated with the proximal cytoplasmic droplets.

We noticed degenerative changes in seminiferous epithelium in the TgHD boars at both 24- and 36-months of age. We observed apoptosis manifested by increased density and vacuolation of cytoplasm, dilatation of endoplasmic reticulum, structural alterations of the nuclei and swollen mitochondria in Setoli cells. Cell shrinkage, increased chromatin condensation in the nucleus, dilatation of endoplasmic reticulum and swollen mitochondria with defects of their internal structure were found in spermatogonia. Similar to HD patients we observed reduced numbers of developing spermatocytes and spermatids. Impaired spermatogenesis observed by electron microscopy was confirmed by proliferative analysis of seminiferous tubules using the proliferative markers. 90% of TgHD seminiferous tubules lacked primary spermatocytes even if their contained spermatogonia. Spermatogenesis was more affected in 36-month-old TgHD boar in comparison with the age of 24 months.

As we supposed that the sperm and testicular degeneration was caused by the expression of mtHtt, we detected the presence of mutant huntingtin protein in sperms and testicular tisssues of TgHD boars. Next, we show no difference in levels of testosterone, luteinizing hormone and inhibin-α levels and confirmed no direct disruption of any annotated gene in porcine genome. Thus, we proved that demonstrated pathological phenopyte was not

a consequence of an integration of the transgene into the porcine genome or not an effect of altered levels of fertility-related hormones.

In conclusion, we showed that insertion of the lentiviral construct did not interrupt any coding sequence in the porcine genome and levels of fertility-related hormones did not differ in TgHD and WT animals. We confirmed the expression of mtHtt in degenerated sperms and testis of TgHD boars, with a conclusion, that the decline and progressive worsening of reproductive parameters, testicular morphological abnormalities and impaired spermatogenesis is a direct harmful consequence of the expressed mutant huntingtin protein.

My contribution

I participated on experimental design and evaluation of the data obtained in this study. I wrote the draft of the manuscript.

Original Paper

Neuro–degenerative Diseases

Neurodegener Dis 2016;16:245–259
DOI: 10.1159/000443665

Received: June 1, 2015
Accepted after revision: December 23, 2015
Published online: March 10, 2016

Mutated Huntingtin Causes Testicular Pathology in Transgenic Minipig Boars

Monika Macakova[a, c] Bozena Bohuslavova[a, c] Petra Vochozkova[a, c] Antonin Pavlok[a] Miroslava Sedlackova[b] Daniela Vidinska[a, c] Klara Vochyanova[a, c] Irena Liskova[a, d] Ivona Valekova[a, c] Monika Baxa[a, c] Zdenka Ellederova[a] Jiri Klima[a] Stefan Juhas[a] Jana Juhasova[a] Jana Klouckova[e] Martin Haluzik[e] Jiri Klempir[d] Hana Hansikova[f] Jana Spacilova[f] Ryan Collins[g] Ian Blumenthal[g] Michael Talkowski[g] James F. Gusella[g] David S. Howland[i] Marian DiFiglia[h] Jan Motlik[a]

[a]Laboratory of Cell Regeneration and Plasticity, Institute of Animal Physiology and Genetics, Czech Academy of Science, Libechov, [b]Department of Histology and Embryology, Faculty of Medicine, Masaryk University in Brno, Brno, [c]Department of Cell Biology, Faculty of Science, and [d]Department of Neurology and Centre of Clinical Neuroscience, First Faculty of Medicine, Charles University in Prague, and [e]3rd Department of Medicine, Department of Endocrinology and Metabolism, and [f]Laboratory for Study of Mitochondrial Disorders, Department of Pediatrics and Adolescent Medicine, First Faculty of Medicine, Charles University and General University Hospital in Prague, Prague, Czech Republic; [g]Center for Human Genetic Research, and [h]Department of Neurology, Massachusetts General Hospital, Boston, Mass., and [i]CHDI Foundation, Princeton, N.Y., USA

Key Words
Huntington's disease · Pig model · Mutant huntingtin · Spermatozoa · Testes · Degeneration

Abstract
Background: Huntington's disease is induced by CAG expansion in a single gene coding the huntingtin protein. The mutated huntingtin (mtHtt) primarily causes degeneration of neurons in the brain, but it also affects peripheral tissues, including testes. ***Objective:*** We studied sperm and testes of transgenic boars expressing the N-terminal region of human mtHtt. ***Methods:*** In this study, measures of reproductive parameters and electron microscopy (EM) images of spermatozoa and testes of transgenic (TgHD) and wild-type (WT) boars of F1 (24–48 months old) and F2 (12–36 months old) generations were compared. In addition, immunofluorescence, immunohistochemistry, Western blot, hormonal analysis and whole-genome sequencing were done in order to elucidate the effects of mtHtt. ***Results:*** Evidence for fertility failure of both TgHD generations was observed at the age of 13 months. Reproductive parameters declined and progressively worsened with age. EM revealed numerous pathological features in sperm tails and in testicular epithelium from 24- and 36-month-old TgHD boars. Moreover, immunohistochemistry confirmed significantly lower proliferation activity of spermatogonia in transgenic testes. mtHtt was highly expressed in spermatozoa and testes of TgHD boars and localized in all cells of seminiferous tubules. Levels of fertility-related hormones did not differ in TgHD and WT siblings. Genome analysis confirmed that insertion of the lentiviral construct did not interrupt any coding sequence in the pig genome. ***Conclusions:*** The sperm and testicular degeneration of TgHD boars is caused by gain-of-function of the highly expressed mtHtt.

Monika Macakova and Bozena Bohuslavova contributed equally to this work.

KARGER

E-Mail karger@karger.com
www.karger.com/ndd

1660–2854/16/0164–0245$39.50/0

Jan Motlik
Laboratory of Cell Regeneration and Plasticity
Institute of Animal Physiology and Genetics
Rumburska 89, CZ–27721 Libechov (Czech Republic)
E-Mail motlik@iapg.cas.cz

Introduction

Huntington's disease (HD) is a neurodegenerative disorder caused by the expansion of CAG repeat in the gene encoding the huntingtin protein (Htt), which is expressed in most tissues. The onset of the disease is usually in the mid-thirties. The main target is the central nervous system, but it has an impact on the whole body. There is no available curative treatment to date. Even the pathogenesis of the disease is not well understood. Nevertheless, it is well known that mutated Htt (mtHtt) forms cytoplasmic and nuclear aggregates, particularly in the cerebral cortex, striatum and lateral hypothalamus [1]. Many rodent models of HD that express either truncated or full-length human mutant Htt display differences in the onset and severity of phenotypes. Rodent models have collectively provided valuable information related to target validation and drug therapy [2–4]. However, large animal models are expected to simulate the disease more faithfully and moreover enable the usage of medical techniques and equipment applicable for human patients [5].

Minipigs represent a desirable model for longitudinal safety studies and preclinical drug trials to fill the gap between rodent models and patients [6, 7]. The advantage of minipigs is their resemblance with the human brain as well as with the whole body in terms of size, anatomy and physiology. There is a 96% homology between porcine and human huntingtin genes and proteins [8] that provides further impetus to use the minipig as a model of HD. Therefore, a transgenic minipig model was generated using microinjection of a lentiviral vector encoding the N-terminal (1–548 aa) of human Htt containing 145 CAG/CAA repeats under the control of the human HTT promoter [9]. The mtHtt gene with 124 glutamines was incorporated into chromosome 1 (1q24–q25), and the expression of mtHtt was detected in numerous peripheral tissues. Successful germ line transmission occurred through 4 successive generations inheriting the mutation in Mendelian ratio [9].

Even though the neurological phenotype of HD patients is the most prominent, the first sign of phenotype development in TgHD boars of F1 generation was reproductive failure, starting at the age of 13 months [9]. Interestingly, among all organs, the testes display the most comparable gene expression pattern to the brain [10]. In accordance with this finding, the expression of mtHtt in R6/2 and YAC128 mouse models of HD results in atrophy of the brain and testes [11–13]. Closer examination of the testes in YAC128 mice revealed disorganized seminiferous epithelium and a reduced number of germ cells. YAC72 mice expressing mtHtt but lacking endogenous Htt ($YAC72^{-/-}$) revealed an even more severe phenotype resulting in infertility with aspermia and massive apoptotic cell death in the testes [14]. Also, a detailed testes examination in HD patients documented testicular abnormalities as well as reduced numbers of germ cells and abnormal morphology of seminiferous tubules [13].

The question arises whether the defect in testes is caused by the presence of mtHtt in testes or by a defect in neurons responsible for hormonal changes. In R6/2 mice, a secondary effect due to the decreased level of gonadotropin-releasing hormone (GnRH)-immunoreactive neurons was suggested. Only 10% of GnRH neurons remained in R6/2 mice by 9 weeks of age, while testicular atrophy and infertility were detected at 12 weeks of age together with a decrease of testosterone levels in serum and testes [11]. Nonetheless, the direct effect of mtHtt was not considered. On top of that, a previous paper showed testicular atrophy in R6/2 mice by 4 weeks of age [15], a week prior to the start of GnRH neuronal loss. In the YAC128 mouse model, testicular degeneration developed between 9 and 12 months of age, but even at 12 months, there is no evidence for decreased testosterone levels in urinary and plasma samples or loss of GnRH neurons in the hypothalamus [13].

In this paper, we followed reproductive parameters of TgHD and WT minipig boars from F1 and F2 generations in order to describe their sperm and testicular pathology phenotype. Furthermore, we investigated whether the phenotype is caused by the primary effect of mtHtt. We ruled out hormonal changes or interruption of any coding sequence during insertion of the lentiviral construct. Here we show evidence for morphological and functional defects in sperm and testes over two generations of TgHD minipigs that accrue before the neurology defects and hormonal changes, suggesting a direct toxic consequence of the expressed N-terminal mtHtt.

Materials and Methods

Animals

Transgenic minipigs with the N-terminal part of human mtHtt [9] were studied. Transgenic boars (n = 17) and their wild-type male controls (n = 13) were used in experiments. All components of this study were carried out in accordance with the Animal Care and Use Committee of the Institute of Animal Physiology and Genetics and were conducted according to current Czech regulations and guidelines for animal welfare and with approval by the State Veterinary Administration of the Czech Republic.

For an overview of the animals used in experiments see supplementary material SM 1 (for all online suppl. material, see www.karger.com/doi/10.1159/000443665).

Spermatozoa Collection, Measurement of Sperm Parameters and in vitro Fertilization Test

Semen was collected from boars of F1 (age 24–48 months, n = 4) and F2 (age 12–36 months, n = 8) generations. All samples were evaluated using a sperm cell analyzer (Microptic, Spain) immediately after collection. The number of spermatozoa per ejaculate and the motility and progressivity of the spermatozoa were assessed. In vitro fertilization tests were done as previously described [9].

Preparation of Testicular Tissue

Testicular tissue was obtained from boars of F2 generation aged 24 (n = 2) and 36 months (n = 4). Animals were perfused under deep anesthesia with cold PBS. The tissue of the right testis was fixed in 4% paraformaldehyde followed by cryoprotection in 30% sucrose in 0.1 M PBS and used for immunohistochemistry and electron microscopy (EM). The tissue of the left testis was used for SDS-PAGE and Western blot.

Electron Microscopy

Small blocks of testicular tissue and ejaculate samples were fixed in 300 mM glutaraldehyde (Sigma-Aldrich) in 100 mM cacodylate buffer for 2 h at room temperature (RT), washed in the same buffer and postfixed in 40 mM osmium tetroxide (Polysciences) in 100 mM cacodylate buffer for 1 h at RT. Samples of testicular tissue were embedded in araldite resin (Durcupan ACM; Sigma-Aldrich) after rinsing in cacodylate buffer and dehydration in ethanol. Ejaculate samples were embedded in agar blocks, dehydrated in ethanol and embedded in araldite resin (Durcupan ACM; Sigma-Aldrich).

For immunohistochemical analyses, samples of ejaculate were washed in PBS and fixed in 4% paraformaldehyde with 0.1% glutaraldehyde in PBS. The samples were embedded in agar blocks, dehydrated in ethanol and embedded in LR white resin (Sigma-Aldrich). Samples were incubated with mouse anti-polyglutamine monoclonal primary antibody (MAB1574; Millipore; 1:50) overnight at 4°C. Then the sections were rinsed in PBS and incubated with anti-mouse IgG-Gold antibody (10 nm gold particles; G7652; Sigma-Aldrich; 1:40) for 2 h at RT.

In all of the EM analyses, 60-nm-thick sections were cut using a Leica EM UC6 ultramicrotome and stained with uranyl acetate and lead citrate. Sections were examined under an FEI Morgagni 268D electron microscope (FEI Company, The Netherlands) at 70 kV.

Immunofluorescence and Immunohistochemistry

Spermatozoa were spotted onto clean slides using cytospin (800 *g*, 5 min). Spermatozoa were fixed and permeabilized with ice-cold absolute methanol for 5 min and then with acetone for 30 s. Slides were blocked with 5% goat serum and 5% milk for 30 min at RT. Sections were incubated with mouse anti-polyQ monoclonal antibody (3B5H10; Sigma Aldrich; 1:500) for 2 h at 4°C, and then Alexa Fluor 488-conjugated goat anti-mouse antibody (A21424; Invitrogen; 1:500) was applied for 1 h at RT. DAPI was added to the mounting medium.

Frozen testicular tissue was cut using a Leica CM1950 cryostat. Testicular sections (5 µm thick) were mounted on slides coated with 2% (3-aminopropyl) triethoxysilane in acetone (Sigma-Aldrich). Slides were heated for 10 min at 0.7 bar overpressure in 0.01 M sodium citrate buffer (pH 6.0) using a pressure cooker (Steba, Germany) for antigen retrieval. Sections were blocked with 10% goat or donkey serum and stained with mouse anti-PCNA monoclonal antibody (ab29; Abcam; 1:2,000) and rabbit anti-Ki67 monoclonal antibody (ab16667; Abcam; 1:1,000) or rabbit anti-Htt monoclonal antibody (EPR5526; Abcam; 1:250) overnight at 4°C. Sections stained with EPR5526 were further treated with Alexa Fluor 647-conjugated goat anti-rabbit antibody (Amersham; 1:500) for 1 h at RT and followed by mounting medium containing DAPI. Other sections were incubated with sheep anti-mouse biotinylated antibody or donkey anti-rabbit biotinylated antibody (Amersham; 1:200) for 1 h at RT followed by incubation with an avidin-peroxidase complex (Vector ABC Elite) and 3,3′-diaminobenzidine tetrahydrochloride (DAB; Sigma) chromogen. Sections were dehydrated in graded ethanol, cleared in xylene and then coverslipped using DPX. Slides were digitalized using a scanning microscope (Olympus BX) and images were edited using VS-120 software. Statistical analyses were performed using GraphPad Prism 5.0 software (one-way ANOVA with Duncan's post hoc test). PCNA-positive and Ki67-positive cells were counted in 20–30 seminiferous tubules per animal.

SDS-PAGE and Western Blot

Testes were homogenized in liquid nitrogen using a mortar. Spermatozoa and homogenized testes were lysed in RIPA buffer (150 mM NaCl, 1% NP-40, 0.5% deoxycholate, 0.1% SDS, 50 mM Tris-HCl pH 8, inhibitors of phosphatases and proteases), sonicated, and centrifuged at 10,000 *g* for 10 min at 4°C. Samples (20 µg of total protein) were loaded onto 3–8% Tris-acetate gel (EA03755; LifeTech) and run at 150 V. Gel was transferred onto nitrocellulose membrane (IB301001; LifeTech) at 250 mA. Membranes were blocked in 5% skimmed milk, and probed overnight with anti-Htt antibody (EPR5526; Abcam; 1:30,000 or AB1; Sigma Aldrich; 1:000), or anti-polyQ antibody (3B5H10; Sigma Aldrich; 1:3,000), tubulin staining was used as loading control (anti-tubulin; Sigma Aldrich; 1:10,000). Secondary antibody conjugated with HRP (anti-mouse, 711-035-152; Jackson ImmunoResearch; 1:10,000 or anti-rabbit, 711-035-152; Jackson ImmunoResearch; 1:10,000) was used. Light reaction was induced by ECL (RPN2232; GE Healthcare) and the signal was captured on CL-Xposure films (34091; Thermo Scientific).

Hormonal Assay

Blood samples were collected 5 times from age-matched TgHD (n = 15) and WT (n = 8) boars (aged 7–30 months). The samples were allowed to clot for 60 min at RT, and centrifuged twice (1,500 *g*, 10 min, 4°C). Serum levels of testosterone, luteinizing hormone (LH) and inhibin-α were determined by commercial ELISA kits (CSB-E06796p, CSB-E06791p, CSB-E12870p, CSB-EL-011718PI; CUSABIO, Wuhan, China). All measurements were performed in duplicate and according to the manufacturers' protocols. Statistical analysis was done using the Kolmogorov-Smirnov normality test followed by the unpaired t test.

Jumping Library Whole-Genome Sequencing

Customized sequencing libraries were constructed based on published protocols [16] and sequenced with paired-end 50-bp reads on an Illumina HiSeq2500. Library barcodes were demulti-

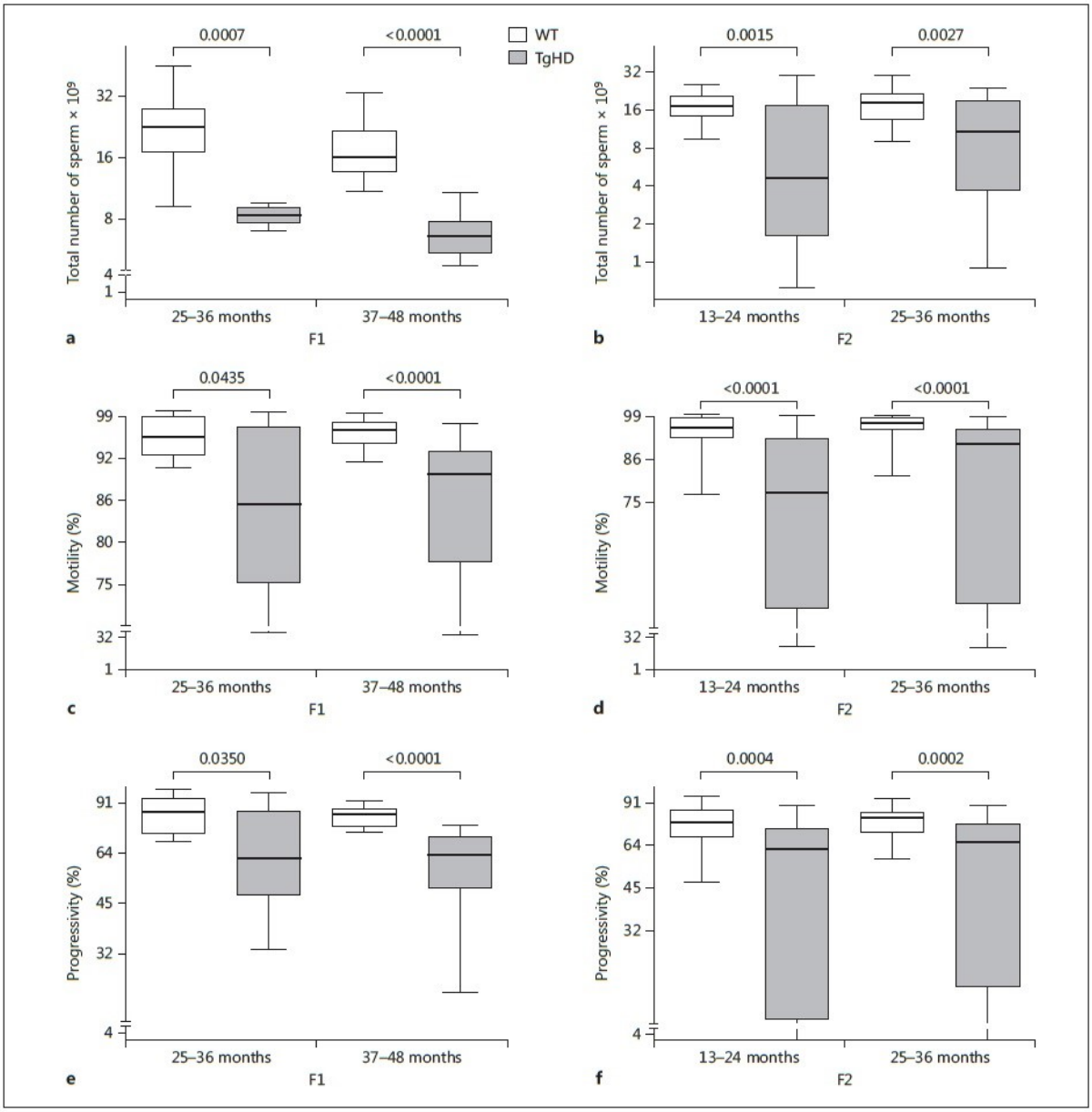

Fig. 1. Sperm parameters. **a** Sperm count in the semen samples of TgHD boars from F1 generation collected at the age of 25–36 and 37–48 months was significantly decreased in comparison with control animals. **b** Number of sperms in ejaculate of F2 TgHD boars collected at the age of 13–24 and 25–36 months was also lower in comparison with their WT littermates. Motility of the sperms was decreased in both F1 (**c**) and F2 (**d**) generations in all tested ages. Also, progressivity of the sperms was lower in TgHD animals from F1 (**e**) and F2 (**f**) generations. Data were analyzed using the Kolmogorov-Smirnov normality test followed by the Mann-Whitney U test. $p < 0.05$ was considered significant.

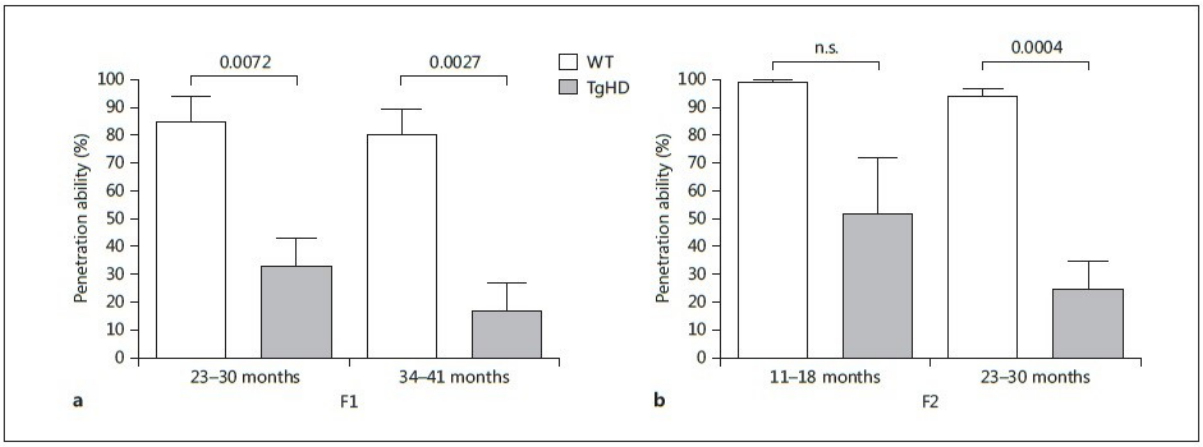

Fig. 2. Sperm penetration ability. **a** The ability to penetrate into oocytes is decreased in sperms of F1 boars at the age of 23–30 months, and also at the age of 34–41 months. The most striking difference in the penetration ability between WT and TgHD F2 boars was at the age of 23–30 months. **b** Such alterations were observed as well in animals from F2 generation who reached the age of 11–18 months ($p = 0.0608$). Each penetration test was repeated at least 5 times. Data were analyzed using the Kolmogorov-Smirnov normality test followed by the Mann-Whitney U test. $p < 0.05$ was considered significant.

plexed with CASAVA v1.7. Read quality was assessed with FastQC v0.11.2 (http://www.bioinformatics.babraham.ac.uk). Quality and adapter trimming was performed with TrimGalore v0.3.7 (http://www.bioinformatics.babraham.ac.uk). Reads were aligned to a modified version of *Sus scrofa* reference genome assembly Sscrofa10.2.74 (GCA_000003025.4; http://www.ensembl.org/Sus_scrofa) that included the full pHIV1-HD548aa-145Q vector sequence. Reads were aligned with BWA-backtrack v0.7.10-r789 [17]. Duplicates were marked with Picard Tools MarkDuplicates v0.1.111 (http://picard.sourceforge.net). All alignment manipulations, including sorting and indexing, was performed with sambamba v0.4.6 [18]. Alignment quality was assessed using Picard Tools, Samtools v1.0 and BamTools v2.2.2 [19, 20]. All chimeric read pairs mapping from endogenous reference sequences to the transgene or vector backbone sequences were isolated and clustered using our published algorithms *BamStat* and *ReadPairCluster* [21–23]. An independent algorithm, DELLY, was used to corroborate integration sites detected by principal methods [24]. Actual sequences of the integration junctions were determined by PCR and Sanger sequencing.

Results

Sperm Pathology of TgHD Boars

We showed altered reproduction parameters in 2 TgHD boars of F1 generation starting at the age of 13 months [9] as a potential HD phenotype in our porcine model. However, detailed analysis of a larger cohort of animals was needed to investigate the basis for the decline in fertility. We provided evidence on sperm reproductive parameters of TgHD and WT boars from F1 (24–36 months old) and F2 (12–36 months old) generations. Animals in the compared groups did not yet vary in weight, size or their motor movements.

Semen of TgHD and WT animals was collected and characterized using a sperm cell analyzer. Sperm count, motility and progressivity were evaluated. All parameters measured in semen samples of TgHD boars significantly decreased at around 13 months in both generations (fig. 1) and persisted at a low level with increasing age. In vitro fertilization tests showed a continuous decreased ability of TgHD sperms to penetrate the oocytes (fig. 2).

EM analysis of semen samples revealed altered morphology of spermatozoa between TgHD and WT boars. Structural anomalies of spermatozoa were much more numerous in TgHD samples. These abnormalities were more pronounced in the F2 generation. Nearly all the spermatozoa of TgHD animals of F2 generation had a cytoplasmic droplet (most often proximal; fig. 3a). Severe structural alterations in TgHD spermatozoa were localized mainly in the connecting piece and midpiece of the tail. Abnormalities were manifested as deformation of the mitochondrial sheath in the tail midpiece and also other tail structures. Common findings were folded or coiled tails, and sometimes a double or triple axoneme with fused mitochondrial sheaths (fig. 3b, d). Deformity of the

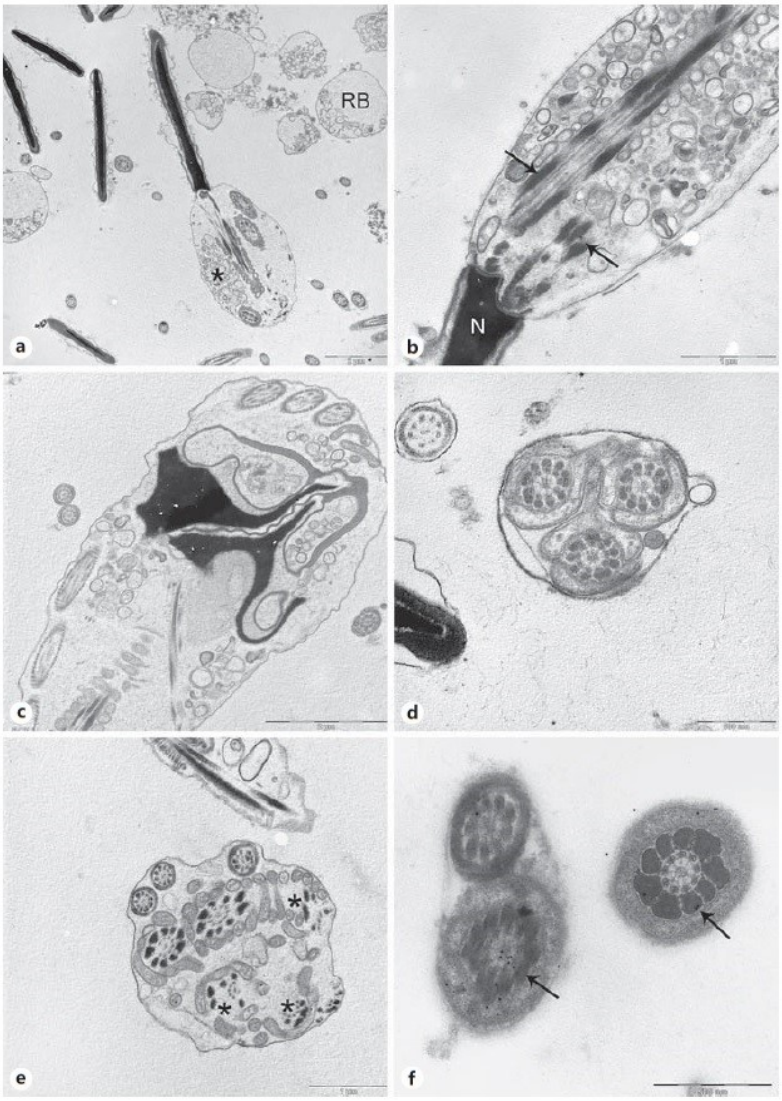

Fig. 3. Fresh ejaculate of TgHD boar. RB = Residual bodies; N = neck. **a** Spermatozoon with proximal cytoplasmic droplet (asterisk) and residual bodies. **b** Spermatozoon with cytoplasmic droplet and double neck and tail structures (arrows). **c** Fully deformed spermatozoon. **d** A tail of a spermatozoon with triple axoneme and fused mitochondrial sheaths. **e** Connecting piece of tail of a spermatozoon with multiple and totally disorganized axoneme and mitochondrial sheaths (asterisk). **f** Immunocytochemical reaction. 10-nm gold particles (arrows) indicate the presence of polyglutamine-containing proteins.

nucleus associated with incomplete chromatin condensation and abnormal acrosome occurred occasionally (fig. 3c). Instability of acrosomes was in some cases manifested by a precocious acrosomal reaction. Proximal cytoplasmic droplets were often associated with disorganized mitochondrial sheaths (fig. 3e). In the F2 generation, there was a total absence of residual bodies in the ejaculate.

Testicular Pathology of TgHD Boars

After having demonstrated the sperm pathology of TgHD boars, we sacrificed one pair of 24-month-old and 2 pairs of 36-month-old animals from the F2 generation to perform the morphological analysis of testes.

At the age of 24 months, degenerative changes in seminiferous epithelium were more frequent in the TgHD boar in comparison with the wild-type one. Apoptosis was seen in supporting Sertoli cells as well as cells of sper-

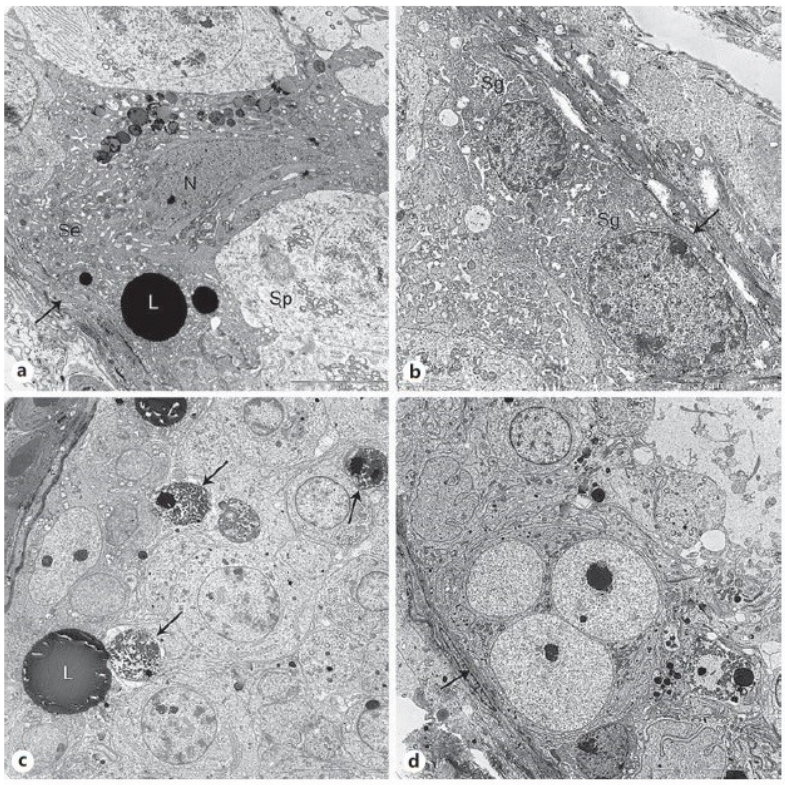

Fig. 4. Seminiferous epithelium of TgHD boar at the age of 24 months. Se = Sertoli cell undergoing apoptosis; N = nuclear structure; Sp = spermatocyte; L = lipid droplet; Sg = spermatogonia. **a** Sertoli cell undergoing apoptosis – increasing cytoplasm density, vacuolation, altered nuclear structure. Note spermatocyte and large lipid droplet. **b** Spermatogonia undergoing apoptosis. Note basal lamina (arrow). **c** Degenerated spermatocytes (arrows). Note large lipid droplet. **d** Spermatogonia with 3 nuclei. Note basal lamina (arrow).

matogenic lineage. Degeneration of Sertoli cells was characterized by increased density and vacuolation of cytoplasm, dilatation of endoplasmic reticulum, structural alterations of the nuclei and swollen mitochondria (fig. 4a). Degeneration of spermatogonia was manifested by cell shrinkage, increased chromatin condensation in the nucleus, dilatation of endoplasmic reticulum and swollen mitochondria with defects of their internal structure (fig. 4b). In addition, other cells of the spermatogenic lineage were gradually degenerated (fig. 4c). Strongly reduced epithelium of the seminiferous tubules, restricted to the Sertoli cells, spermatogonia and the sparsely occurring spermatocytes and spermatids were occasionally observed. Multinucleated spermatogenic cells including spermatogonia (fig. 4d) were frequently recognized. The thick basal lamina was made up of several layers (2–3 laminae densae).

At the age of 36 months, the rate of degenerative changes in the testicular samples of 2 transgenic individuals was different. The changes were less pronounced in boar K104 than in boar K63 and resembled those of a TgHD boar at the age 24 months. Morphology of seminiferous tubules in boar K63 showed a significant reduction of spermatogenesis. In some of the tubules, spermatogenesis was preserved (but only to a limited extent; (fig. 5a); other tubules contained only Sertoli cells (fig. 5b). In the tubules with preserved spermatogenesis, the degenerative changes were detected in both Sertoli cells (fig. 5d) and spermatogenic elements, including the spermatogonia. Degenerative changes exhibited characteristics typical for early or advanced apoptosis – the increased density of cytoplasm associated with its vacuolization, swollen mitochondria, dilated endoplasmic reticulum and clumps of heterochromatin in the nucleus. The basal lamina was thick and made up of several layers (2–3 laminae densae). Tubules without spermatogenic cells were lined with Sertoli cells exclusively, which, unlike the tubules with preserved spermatogenesis, hold signs of degeneration only in exceptional cases. Sertoli cells contained extreme amounts of endoplasmic reticulum, which

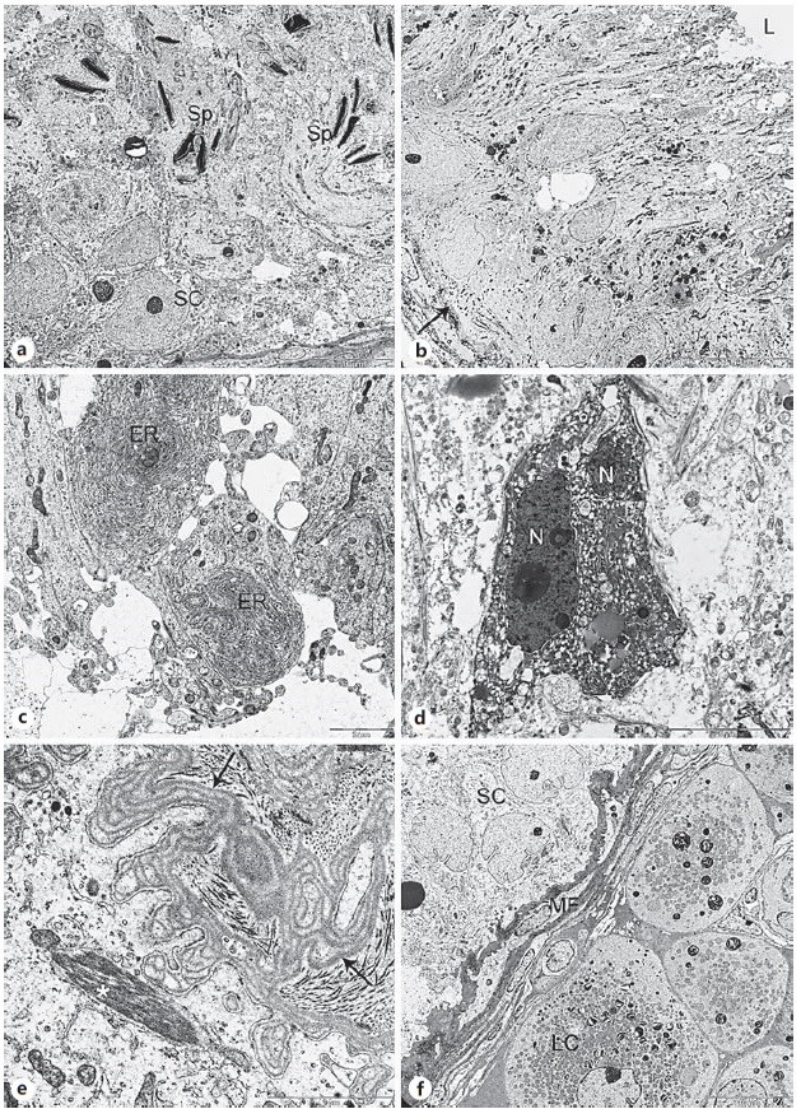

Fig. 5. Seminiferous epithelium of TgHD boar at the age of 36 months. SC = Sertoli cell; Sp = spermatids; L = lumen of tubule; ER = endoplasmic reticulum; N = nucleus of Sertoli cell; MF = myofibroblasts; LC = Leydig cells. **a** Preserved but reduced spermatogenesis. Note Sertoli cells and spermatids. **b** Seminiferous epithelium containing only intact Sertoli cells, with no spermatogenic elements. Note basal lamina (arrow) and lumen of tubule. **c** Sertoli cells of the same tubule – concentric cisternae of endoplasmic reticulum in apical cytoplasm. **d** Sertoli cell undergoing apoptosis in a tubule with preserved spermatogenesis. Note nucleus of Sertoli cell. **e** Basal part of a Sertoli cell with Charcot-Böttcher crystal (asterisk). Note split and undulated basal lamina (arrows). **f** The lamina propria of a tubule with absent spermatogenesis. Note myofibroblasts. Numerous Leydig cells occupy extended areas adjacent to the tubule.

often formed concentrically arranged cisternae (fig. 5c). Structures, known as Charcot-Böttcher crystals, were often observed in these cells (fig. 5e). The basal lamina was made up of several layers (up to 6 laminae densae) and was strongly undulated (fig. 5e), probably as a result of tubules diameter reduction in the absence of spermatogenic elements.

At both ages, 24 and 36 months, the lamina propria of seminiferous tubules was made up of 1–2 layers of myofibroblasts and occasionally occurring fibroblasts (fig. 5f). No differences were found in comparison with the control animals of the same age. Numerous Leydig cells occupying extended areas adjacent to the tubules were present in the interstitium. Their number, location and morphology were identical in both TgHD and WT animals, regardless of age (fig. 5f).

An immunohistochemical cell proliferation assay detecting Ki67 and PCNA expression was performed in order to determine the mitotic activity of spermatogonia. Ki67 protein is expressed only in the nuclei of spermato-

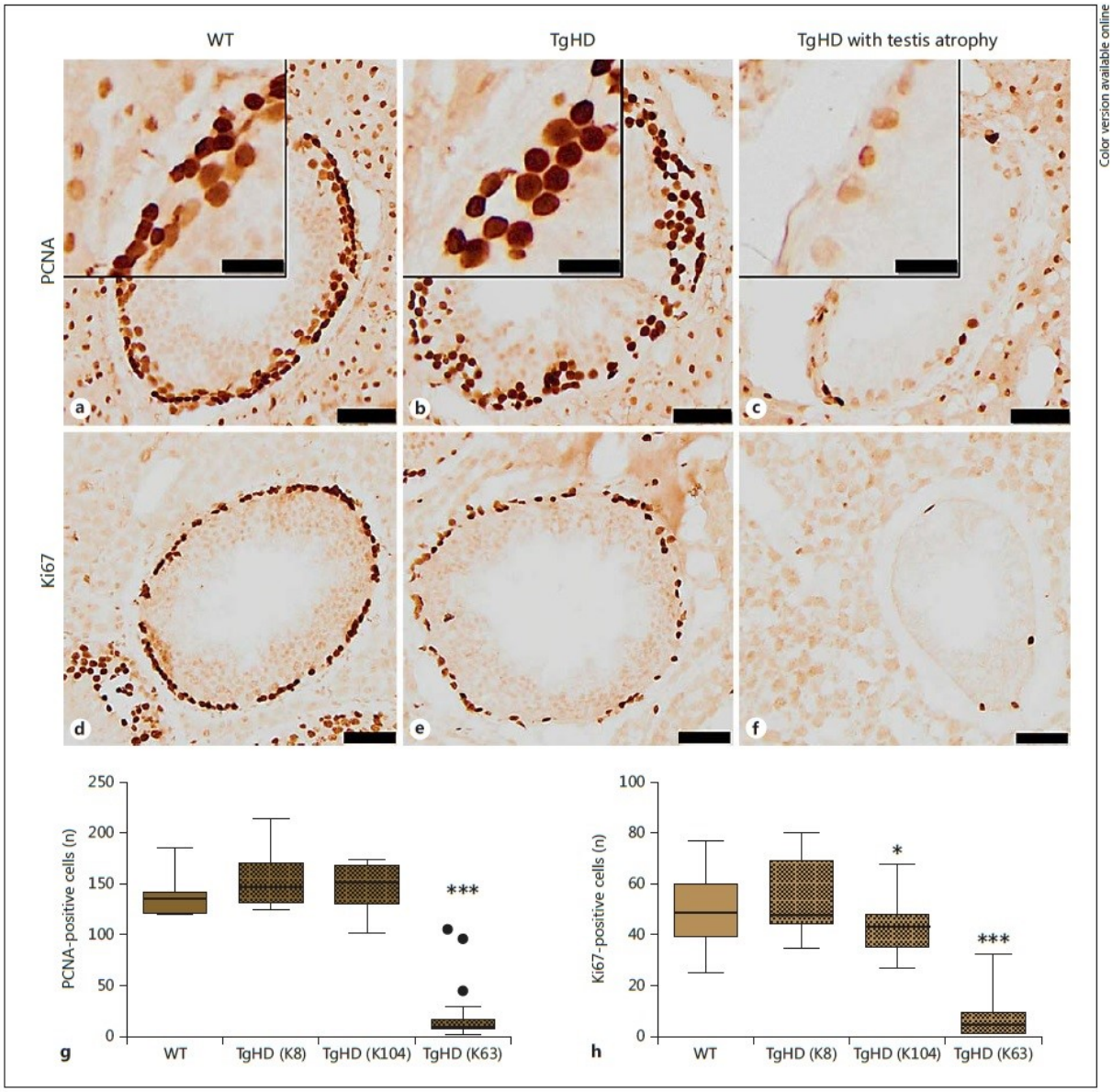

Color version available online

Fig. 6. Proliferative analysis. PCNA (**a–c**) and Ki67 (**d–f**) staining revealed decreased number of spermatocytes (**c**) and spermatogonia (**f**) in seminiferous epithelium of the TgHD boar (K63) at the age of 36 months. **g**, **h** The number of spermatogenic cells of the TgHD boar (K63) was significantly decreased compared with the WT boar ($p < 0.05$). Seminiferous tubules of the 24-month-old (**b**) and 36-month-old (**e**) transgenic boars showed similar staining of spermatogenic cells to WT (**a**, **d**). **h** The exception is testicular tissue from TgHD boar K104, in which spermatogonia (Ki67-positive cells) were determined in a significantly reduced number of seminiferous tubules compared with WT. Scale bars = 50 µm (20 µm in **insets**). Results were plotted as mean ± SD of positive cells per seminiferous tubule. $p < 0.05$ was considered significant. * $p = 0.0151$; *** $p < 0.0001$.

Neurodegener Dis 2016;16:245–259
DOI: 10.1159/000443665

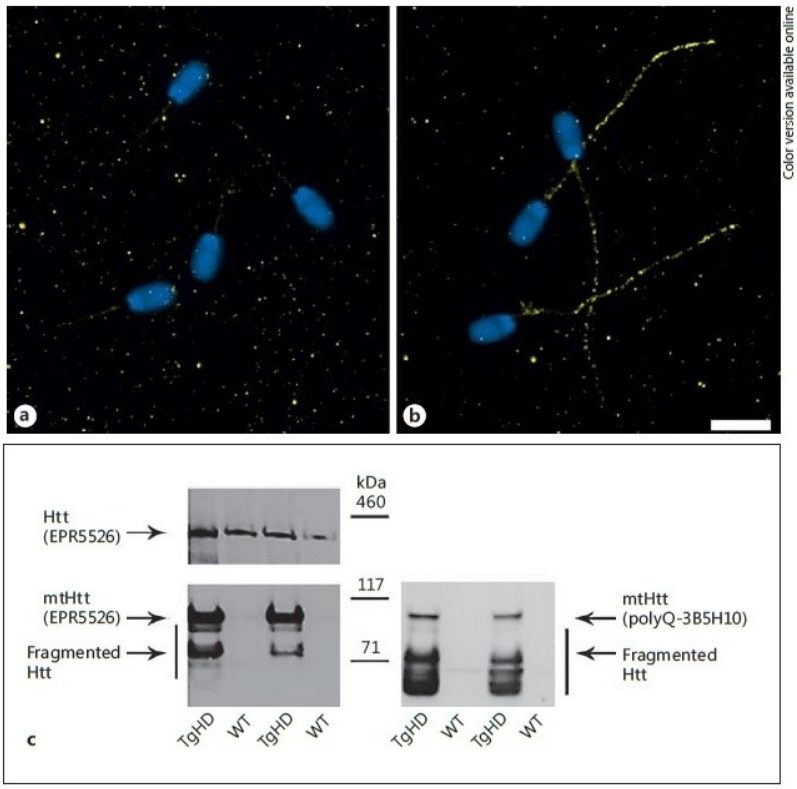

Fig. 7. Presence of Htt in spermatozoa cells. **a**, **b** Immunofluorescence dotted signal of the polyglutamine-containing proteins (3B5H10 antibody, yellow; color in online version only) was detected along whole spermatozoa tail of TgHD boars (**b**) but not in WT cells (**a**). Scale bar = 20 μm. **c** Western blot analysis detected endogenous (Htt) and transgenic (mtHtt) huntingtin by EPR5526 antibody, specific to N-terminal part of huntingtin. PolyQ antibody (3B5H10) as well as Htt antibody (EPR5526) detected fragments of mtHtt.

gonia, while PCNA occurs also in the nuclei of primary spermatocytes in normal seminiferous epithelium [25] – 90.86% (726/799) of seminiferous tubules lacked PCNA-positive cells and 90.08% (745/827) of seminiferous tubules contained no Ki67-positive cell in the testis of the 36-month-old TgHD boar (K63; fig. 6a–f). Spermatogonia serve as stem cells in the process of differentiation to spermatozoa, and their proliferative activity secures normal spermatogenesis. That means that impaired spermatogenesis involved 90% of seminiferous tubules. These results confirmed impaired spermatogenesis observed by EM (as indicated above). The remaining 10% of seminiferous tubules contained spermatogonia and spermatocytes stained by anti-PCNA and anti-Ki67 antibodies, but their number was significantly reduced in comparison with the seminiferous tubules of a WT boar. A significant decrease in the quantity of spermatogonia was also observed in the testis of the other TgHD boar at the age of 36 months (K104) in comparison with the WT one. It suggested that the spermatogonial proliferation was reduced in TgHD boars at the age of 36 months (n = 2, K104 and K63). No difference was found in the testes of the 24-month-old TgHD boar (K8; fig. 6g, h).

Sperm and Testicular Degeneration: The Direct Effect of mtHtt

Supposing that sperm pathology is caused by the toxic effect of mtHtt, experiments showing localization and expression of mtHtt were done. The presence of the polyglutamine-containing proteins was observed in structures in the spermatozoa tail of TgHD boars using 10-nm gold particles examined under EM (fig. 3f). This finding was confirmed by a dotted immunohistochemical signal detected along the whole spermatozoa tail in all tested ages of F1- and F2-generation TgHD boars (but not in WT controls) using 3B5H10 (anti-N-terminal fragment of 171 aa of human Htt with 65Q) antibody (fig. 7a). Western blot analysis using EPR5526 (anti-N-terminal fragment of Htt) confirmed highly abundant mtHtt and a slightly lower level of endogenous Htt in spermatozoa (fig. 7b). In ad-

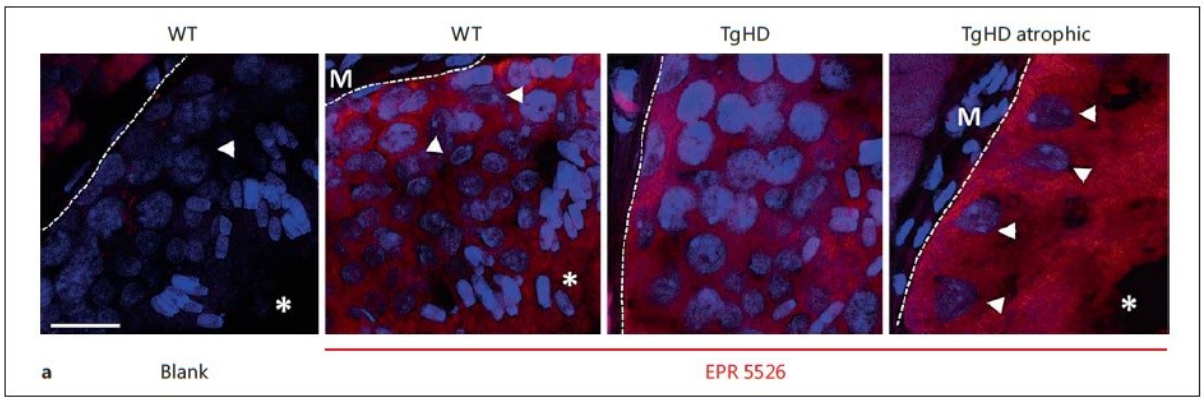

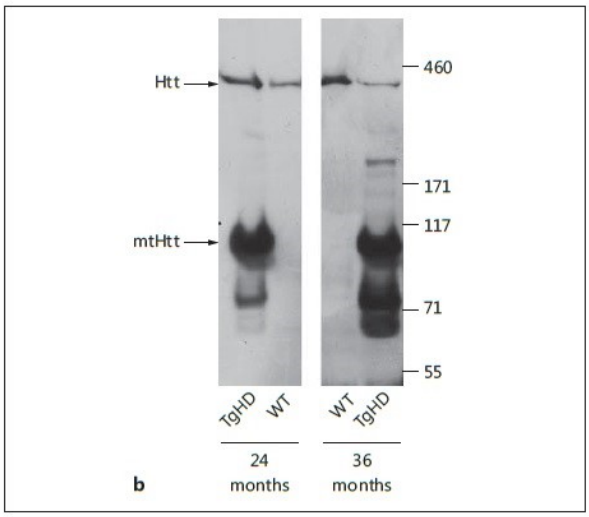

Fig. 8. Expression of Htt in testes. M = Myoid cells. **a** Total huntingtin protein was visualized immunohistochemically with EPR5526 antibody in sections of WT and transgenic (TgHD) porcine testis. EPR5526 (red; color in online version only) was detected in seminiferous epithelium demarcated by seminiferous tubule basement membrane (dashed line) and lumen (asterisk). Myoid cells were negatively stained. Cell nuclei were counterstained with DAPI (blue). Prominent Sertoli cell nuclei (arrowheads) present in atrophic seminiferous tubule (TgHD atrophic) documented the loss of germ cells. Blank, WT testis section stained only with A647-conjugated secondary antibody. Scale bar = 20 µm. **b** Western blot analysis of testis; representative sample shown. Anti-AB1 antibody detected endogenous Htt, transgenic mtHtt and fragments.

dition, anti-polyQ antibody (3B5H10) as well as anti-huntingtin antibody (EPR5526) revealed a fragmented form of mtHtt, which was reported to cause cellular toxicity [26]. Sperm samples from all tested ages in both generations (F1, F2) were analyzed, and no significant change in expression between samples was detected (only representative data from two pairs of samples are shown; fig. 7).

Consequently, we looked at Htt localization in TgHD and WT seminiferous tubules from testes of 24- and 36-month-old boars. The signal was widely spread in spermatogenic and Sertoli cells in normal as well as in the atrophic seminiferous tubules (fig. 8a). Western blot analysis showed a high expression of mtHtt form compared with endogenous Htt. The huntingtin antibody also revealed fragmented forms of mtHtt that may contribute to toxicity of the transgene (fig. 8b).

In order to eliminate the neuronal effect on the testicular phenotype, levels of fertility-related hormones were measured in the blood serum of two age groups: 7- to 17-month-old TgHD (n = 14) and WT (n = 9) boars, and 15–30-month-old TgHD (n = 11) and WT (n = 6) boars. Levels of testosterone, LH and inhibin-α were analyzed (see online suppl. material SM 2). No significant difference was observed between TgHD and WT animals.

Mapping the HIV1-HD-548aaHTT-145Q Transgene Integration

To detect any and all sites of vector integration into the pig genome in the transgenic lineage, we performed long-insert jumping library whole-genome sequencing of transgenic animals from F0 (founder female) and F2 gen-

erations in comparison with a negative control. This method, which involves sequencing the ends of genomic DNA fragments after circularization and size reduction, has previously been shown to be an effective platform for vector integration site discovery in transgenic sheep and mice [21]. Whole-genome sequencing of jumping libraries prepared from random fragments (mean size 3.6 kb) resulted in an average of 65.5× coverage of mapped inserts across each base in the haploid genome for all 3 animals. The paired-end reads were examined for the signature of vector integration into the genome: chimeric fragments consisting of pig genomic sequence on one end and a portion of the introduced vector/transgene on the other. No integrations were detected in the negative control genome, while a single identical vector integration was detected in each of the F0 and F2 generations of TgHD animals. As suggested previously from FISH analysis, the integration occurred into chromosome 1q [9]. The jumping library analysis revealed that 5.3 kb of the HIV1-HD-548aaHTT-145Q vector DNA integrated as expected via the HIV LTR sequences and harbored an intact HD-548aaHTT145Q expression cassette. Sanger sequencing of the junctions with genomic DNA showed that the integration was in reverse orientation relative to the genomic sequence, between chr1 228,641,631 and 228,641,637, with loss of the 5 intervening bases of genomic DNA. This integration does not directly disrupt any annotated gene, and no further breakpoint or integration complexity or other genomic rearrangement was apparent at the resolution of the jumping library sequencing.

Discussion

In this study we described sperm and testicular degeneration, which is a result of the presence of mtHtt protein in the testes of transgenic minipig boars expressing the N-terminal part of human mtHtt. Cohorts of TgHD and their WT controls of F1 and F2 generations were directly compared.

Previous studies on HD rodent models showed male sterility that was assumed to be due to a reduction of spermatozoa [15]. We confirmed this phenotype in a large animal model of HD, the minipig. Additionally, we reported both the reduction of spermatozoa and also their function measured by motility, progressivity and in vitro penetration assay. Spermatozoa of TgHD boars had severe problems to penetrate the minipig oocytes. The difference in values of sperm parameters was evident at 13 months and worsened with age. A comparison of animals from F1 and F2 generations of the same age (25–36 months) showed slightly worse values of all observed parameters in the F2 generation. There was also a wider variability of sperm parameters in the F2 generation, probably caused by a larger cohort of animals in the F2 group. Furthermore, EM analysis revealed deformation of the mitochondrial sheath in the tail midpiece of TgHD spermatozoa. Folded or coiled tails and a double or triple axoneme with fused mitochondrial sheaths were also observed. This can be caused by a failure of the disjunction of excess cytoplasm, which results in the presence of cytoplasmic droplets. This phenomenon, together with spermatozoa motility dysfunction, can be related to a decrease of mitochondrial energetic metabolism and functional impairment of respiratory chain complex II (unpublished observations). Occasionally, nucleus deformation associated with incomplete chromatin condensation and abnormal acrosome occurred in transgenic spermatozoa (but not in WT controls). These abnormalities were more pronounced in the F2 generation. Moreover, nearly all the spermatozoa of TgHD animals of the F2 generation contained a cytoplasmic droplet, and their ejaculate lacked residual bodies.

The testicular degeneration reported here is in agreement with observations in mice (R6/2 and Yac72) [14, 15], as well as in postmortem samples from humans [13]. Multinucleated spermatogenic cells were frequently present in the seminiferous epithelium of 24- and 36-month-old TgHD boars. The spermatogonia were shrunk and had dilated endoplasmic reticulum, swollen mitochondria and condensed chromatin in the nucleus. Spermatocytes and spermatids were observed occasionally. Reduced numbers of developing spermatocytes and spermatids were also observed in HD patients [13] and YAC128 mice [27]. Some tubules contained only Sertoli cells. Sertoli cells were characterized by increased density and vacuolization of the cytoplasm, dilatation of endoplasmic reticulum, structural alterations of the nuclei and swollen mitochondria. These are features typical for early or advanced apoptosis. Moreover, proliferative analysis of seminiferous tubules with elongated spermatozoa showed fewer cells expressing the proliferative markers PCNA and Ki67 in TgHD animals. The apoptotic nature of the cell death in a large number of degenerating spermatids with diffuse cytoplasmic vacuolization, condensed nuclei and electron-dense cytoplasm which were phagocytized and degraded by Sertoli cells was also observed in a mouse model lacking endogenous huntingtin YAC72$^{-/-}$ [14]. Similar-

ly, seminiferous tubules of YAC128 were disrupted by large vacuoles [27]. In addition, the seminiferous tubule wall was thickened in HD patients [13]. In the TgHD minipig, the thick basal lamina was made up of several layers (2–3 laminae densae) compared with the WT minipig. At the age of 36 months, spermatogenesis was more affected in comparison with the age of 24 months. Sertoli cells contained extreme amounts of endoplasmic reticulum and structures known as Charcot-Böttcher crystals. The basal lamina was made up of several layers (up to 6 laminae densae) and was strongly undulated, resulting probably from a reduction of the diameter of the tubules in the absence of spermatogenic elements. The rate of degenerative changes in the testicular samples of the 2 transgenic boars at the age of 36 months was different. The changes were less pronounced in boar K104 than in boar K63 and resembled those of the TgHD boar at the age 24 months. Boar K63 also showed more change in sperm parameters, including atrophy of seminiferous epithelium and impaired spermatogenesis. The difference in severity of pathology between age-matched boars might be a consequence of variation in the progression of the disease and genetic background of individual minipigs. The age of onset of HD depends on CAG length (around 70%), but also on other factors like polymorphism, modifier genes, etc. (30%) [28, 29]. We suggest that polymorphisms of proteins interacting with huntingtin could contribute to different degrees of testicular degeneration between transgenic boars of the same age.

After demonstrating testicular abnormalities we intended to clarify the reason for the pathological phenotype. We focused on the design of the transgenic minipig model. The number of CAG repeats was chosen in order to expect an earlier phenotype. This number of repeats imitates juvenile HD in patients. It has an earlier onset and faster progress, but the disease has the same characteristics as the adult form. Mixed CAG/CAA repeats, instead of just CAG, were used to increase the stability of the insert. This has been used in several rodent models (YAC128, BACHD mice) that also showed the phenotype [30, 31]. Therefore, the design was not a problem. We also checked whether the insertion of the lentiviral construct did not interrupt any coding sequence in the pig genome. Since the result was negative, the question was whether the defect in the testes was due to the expression of mtHtt or as a result of changed levels of fertility-related hormones.

There is evidence that the expression of mutant Htt leads to selective cellular dysfunction and degeneration [32]. The most affected cells are neurons. However, we also provided data for spermatozoa degeneration and testicular dysfunction in a minipig model of HD. We showed a high and stable expression of endogenous Htt as well as the transgenic N-truncated mutant form of human Htt in spermatozoa as well as in spermatogenic and Sertoli cells, and also in the atrophic seminiferous tubules of TgHD testes. In addition, we detected fragments of mtHtt in spermatozoa as well as in testes. It has been published that smaller fragments of mtHtt cause cellular toxicity and induce apoptosis [33, 34]. Furthermore, mutant N-terminal Htt fragments were also detected in tissues from HD patients and mouse models in the presymptomatic stage, suggesting their role in the progression of HD [35–37]. These facts also support our statement that the N-terminal part of human mtHtt causes testicular pathology in transgenic minipig boars.

Although testicular degeneration in HD is well described in mouse models (R6/2 and YAC128), it is not clear whether this phenotype is independent or a consequence of alterations of the hypothalamic-pituitary-gonadal axis (GnRH). A significant loss of GnRH neurons starting from 5 weeks of age followed by decreasing levels of plasma testosterone at 12 weeks of age was found in R6/2 mice [11], while testicular atrophy without concomitant loss of GnRH neurons was described in a YAC128 mouse model [13]. An analysis of testosterone levels in YAC128 mice did not reveal any significant difference compared with controls, even when testicular atrophy was already present [13]. Furthermore, testosterone treatment had no effect on the peripheral phenotype of HD, e.g. body weight loss or motor function in R6/2 mice [11]. An analysis of complete neuroendocrine status in HD patients showed no significant difference in the plasma levels of LH, FSH and testosterone between all male HD patients and controls [38]. However, Markianos et al. [39] observed significantly lower testosterone and LH levels in HD patients compared with healthy controls. These conflicting results suggested a detailed hormonal analysis of our porcine model. We observed no significant difference in the levels of fertility-related hormones between TgHD and control boars, and no changes in libido were observed during regular collection of semen. Moreover, in the interstitium, the number, location and morphology of the Leydig cells were identical regardless of the age or genotype of the animal, and no differences were found in the lamina propria of seminiferous tubules of the TgHD boars in both ages compared with WT controls. Similarly, unaffected Leydig cells were observed between degenerating tubules of stromal interstitial tissue in YAC72$^{-/-}$

mice [14]. Our results support the idea that testicular degeneration and fertility defects are related to mtHtt expression in testes and not to peripheral hormonal changes.

In conclusion, we demonstrated a failure in sperm parameters and extensive testicular pathology in a minipig model of HD. We showed that insertion of the lentiviral construct did not interrupt any coding sequence in the pig genome and suggest that the testicular defect was caused by the presence of mtHtt and its fragmented cytotoxic form in testicular tissue, since hormonal changes were not measured between TgHD boars and their WT controls.

Acknowledgments

This work was supported by the CHDI Foundation (A-5378), the project EXAM from the European Regional Development Fund (CZ.1.05/2.1.00/03.0124), RVO 67985904, the Norwegian Financial Mechanism 2009–2014, the Ministry of Education, Youth and Sports (project contract MSMT-28477/2014) and Charles University (grant SVV 260083), and National Sustainability Programme No. LO1609 (MEYS CR).

Disclosure Statement

One of the authors, Dr. David S. Howland is employed by the CHDI Foundation, which supported this work. Dr. Howland was not involved in designing the experiments or in writing this article, and did not make the decision to publish it. He was a consultant. The authors have no other conflicts of interest to declare.

References

1 Vonsattel JP, DiFiglia M: Huntington disease. J Neuropathol Exp Neurol 1998;57:369–384.
2 Stanek LM, Sardi SP, Mastis B, Richards AR, Treleaven CM, Taksir T, Misra K, Cheng SH, Shihabuddin LS: Silencing mutant huntingtin by adeno-associated virus-mediated RNA interference ameliorates disease manifestations in the YAC128 mouse model of Huntington's disease. Hum Gene Ther 2014;25:461–474.
3 Dufour BD, Smith CA, Clark RL, Walker TR, McBride JL: Intrajugular vein delivery of AAV9-RNAi prevents neuropathological changes and weight loss in Huntington's disease mice. Mol Ther 2014;22:797–810.
4 Squitieri F, Di Pardo A, Favellato M, Amico E, Maglione V, Frati L: Pridopidine, a dopamine stabilizer, improves motor performance and shows neuroprotective effects in Huntington disease R6/2 mouse model. J Cell Mol Med 2015;19:2540–2548.
5 Holm IE, Alstrup AK, Luo Y: Genetically modified pig models for neurodegenerative disorders. J Pathol 2016;238:267–287.
6 Dolezalova D, Hruska-Plochan M, Bjarkam CR, Sorensen JC, Cunningham M, Weingarten D, Ciacci JD, Juhas S, Juhasova J, Motlik J, Hefferan MP, Hazel T, Johe K, Carromeu C, Muotri A, Bui J, Strnadel J, Marsala M: Pig models of neurodegenerative disorders: utilization in cell replacement-based preclinical safety and efficacy studies. J Comp Neurol 2014;522:2784–2801.
7 Vodicka P, Smetana K Jr, Dvorankova B, Emerick T, Xu YZ, Ourednik J, Ourednik V, Motlik J: The miniature pig as an animal model in biomedical research. Ann NY Acad Sci 2005;1049:161–171.
8 Matsuyama N, Hadano S, Onoe K, Osuga H, Showguchi-Miyata J, Gondo Y, Ikeda JE: Identification and characterization of the miniature pig Huntington's disease gene homolog: evidence for conservation and polymorphism in the CAG triplet repeat. Genomics 2000;69:72–85.
9 Baxa M, Hruska-Plochan M, Juhas S, Vodicka P, Pavlok A, Juhasova J, Miyanohara A, Nejime T, Klima J, Macakova M, Marsala S, Weiss A, Kubickova S, Musilova P, Vrtel R, Sontag EM, Thompson LM, Schier J, Hansikova H, Howland DS, Cattaneo E, DiFiglia M, Marsala M, Motlik J: A transgenic minipig model of Huntington's disease. J Huntingtons Dis 2013;2:47–68.
10 Guo J, Zhu P, Wu C, Yu L, Zhao S, Gu X: In silico analysis indicates a similar gene expression pattern between human brain and testis. Cytogenet Genome Res 2003;103:58–62.
11 Papalexi E, Persson A, Bjorkqvist M, Petersen A, Woodman B, Bates GP, Sundler F, Mulder H, Brundin P, Popovic N: Reduction of GnRH and infertility in the R6/2 mouse model of Huntington's disease. Eur J Neurosci 2005;22:1541–1546.
12 Van Raamsdonk JM, Pearson J, Murphy Z, Hayden MR, Leavitt BR: Wild-type huntingtin ameliorates striatal neuronal atrophy but does not prevent other abnormalities in the YAC128 mouse model of Huntington disease. BMC Neurosci 2006;7:80.
13 Van Raamsdonk JM, Murphy Z, Selva DM, Hamidizadeh R, Pearson J, Petersen A, Bjorkqvist M, Muir C, Mackenzie IR, Hammond GL, Vogl AW, Hayden MR, Leavitt BR: Testicular degeneration in Huntington disease. Neurobiol Dis 2007;26:512–520.
14 Leavitt BR, Guttman JA, Hodgson JG, Kimel GH, Singaraja R, Vogl AW, Hayden MR: Wild-type huntingtin reduces the cellular toxicity of mutant huntingtin in vivo. American J Hum Genet 2001;68:313–324.
15 Sathasivam K, Hobbs C, Turmaine M, Mangiarini L, Mahal A, Bertaux F, Wanker EE, Doherty P, Davies SW, Bates GP: Formation of polyglutamine inclusions in non-CNS tissue. Hum Mol Genet 1999;8:813–822.
16 Hanscom C, Talkowski M: Design of large-insert jumping libraries for structural variant detection using Illumina sequencing. Curr Protoc Hum Genet 2014;80:7221–7229.
17 Li H, Durbin R: Fast and accurate long-read alignment with Burrows-Wheeler transform. Bioinformatics 2010;26:589–595.
18 Tarasov A, Vilella AJ, Cuppen E, Nijman IJ, Prins P: Sambamba: fast processing of NGS alignment formats. Bioinformatics 2015;31:2032–2034.
19 Li H, Handsaker B, Wysoker A, Fennell T, Ruan J, Homer N, Marth G, Abecasis G, Durbin R: The Sequence Alignment/Map format and SAMtools. Bioinformatics 2009;25:2078–2079.
20 Barnett DW, Garrison EK, Quinlan AR, Stromberg MP, Marth GT: BamTools: A c++ API and toolkit for analyzing and managing BAM files. Bioinformatics 2011;27:1691–1692.
21 Chiang C, Jacobsen JC, Ernst C, Hanscom C, Heilbut A, Blumenthal I, Mills RE, Kirby A, Lindgren AM, Rudiger SR, McLaughlan CJ, Bawden CS, Reid SJ, Faull RL, Snell RG, Hall IM, Shen Y, Ohsumi TK, Borowsky ML, Daly MJ, Lee C, Morton CC, MacDonald ME, Gusella JF, Talkowski ME: Complex reorganization and predominant non-homologous repair following chromosomal breakage in karyotypically balanced germline rearrangements and transgenic integration. Nat Genet 2012;44:390–397.
22 Brand H, Pillalamarri V, Collins RL, Eggert S, O'Dushlaine C, Braaten EB, Stone MR, Chambert K, Doty ND, Hanscom C, Rosenfeld JA, Ditmars H, Blais J, Mills R, Lee C, Gusella JF, McCarroll S, Smoller JW, Talkowski ME, Doyle AE: Cryptic and complex chromosomal aberrations in early-onset neuropsychiatric disorders. Am J Hum Genet 2014;95:454–461.

23 Talkowski ME, Rosenfeld JA, Blumenthal I, Pillalamarri V, Chiang C, Heilbut A, Ernst C, Hanscom C, Rossin E, Lindgren AM, Pereira S, Ruderfer D, Kirby A, Ripke S, Harris DJ, Lee JH, Ha K, Kim HG, Solomon BD, Gropman AL, Lucente D, Sims K, Ohsumi TK, Borowsky ML, Loranger S, Quade B, Lage K, Miles J, Wu BL, Shen Y, Neale B, Shaffer LG, Daly MJ, Morton CC, Gusella JF: Sequencing chromosomal abnormalities reveals neurodevelopmental loci that confer risk across diagnostic boundaries. Cell 2012;149:525–537.
24 Rausch T, Zichner T, Schlattl A, Stutz AM, Benes V, Korbel JO: Delly: Structural variant discovery by integrated paired-end and split-read analysis. Bioinformatics 2012;28:i333–i339.
25 Steger K, Aleithe I, Behre H, Bergmann M: The proliferation of spermatogonia in normal and pathological human seminiferous epithelium: an immunohistochemical study using monoclonal antibodies against Ki-67 protein and proliferating cell nuclear antigen. Mol Hum Reprod 1998;4:227–233.
26 Miller JP, Holcomb J, Al-Ramahi I, de Haro M, Gafni J, Zhang N, Kim E, Sanhueza M, Torcassi C, Kwak S, Botas J, Hughes RE, Ellerby LM: Matrix metalloproteinases are modifiers of huntingtin proteolysis and toxicity in Huntington's disease. Neuron 2010;67:199–212.
27 Van Raamsdonk JM, Pearson J, Rogers DA, Bissada N, Vogl AW, Hayden MR, Leavitt BR: Loss of wild-type huntingtin influences motor dysfunction and survival in the YAC128 mouse model of Huntington disease. Hum Mol Genet 2005;14:1379–1392.
28 Langbehn DR, Hayden MR, Paulsen JS: CAG-repeat length and the age of onset in Huntington disease (HD): a review and validation study of statistical approaches. Am J Med Genet B Neuropsychiatr Genet 2010;153B:397–408.
29 Tabrizi SJ, Reilmann R, Roos RA, Durr A, Leavitt B, Owen G, Jones R, Johnson H, Craufurd D, Hicks SL, Kennard C, Landwehrmeyer B, Stout JC, Borowsky B, Scahill RI, Frost C, Langbehn DR: Potential endpoints for clinical trials in premanifest and early Huntington's disease in the TRACK-HD study: analysis of 24-month observational data. Lancet Neurol 2012;11:42–53.
30 Gray M, Shirasaki DI, Cepeda C, Andre VM, Wilburn B, Lu XH, Tao J, Yamazaki I, Li SH, Sun YE, Li XJ, Levine MS, Yang XW: Full-length human mutant huntingtin with a stable polyglutamine repeat can elicit progressive and selective neuropathogenesis in BACHD mice. J Neurosci 2008;28:6182–6195.
31 Pouladi MA, Stanek LM, Xie Y, Franciosi S, Southwell AL, Deng Y, Butland S, Zhang W, Cheng SH, Shihabuddin LS, Hayden MR: Marked differences in neurochemistry and aggregates despite similar behavioural and neuropathological features of Huntington disease in the full-length BACHD and YAC128 mice. Hum Mol Genet 2012;21:2219–2232.
32 Bhide PG, Day M, Sapp E, Schwarz C, Sheth A, Kim J, Young AB, Penney J, Golden J, Aronin N, DiFiglia M: Expression of normal and mutant huntingtin in the developing brain. J Neurosci 1996;16:5523–5535.
33 Hackam AS, Singaraja R, Wellington CL, Metzler M, McCutcheon K, Zhang T, Kalchman M, Hayden MR: The influence of huntingtin protein size on nuclear localization and cellular toxicity. J Cell Biol 1998;141:1097–1105.
34 Martindale D, Hackam A, Wieczorek A, Ellerby L, Wellington C, McCutcheon K, Singaraja R, Kazemi-Esfarjani P, Devon R, Kim SU, Bredesen DE, Tufaro F, Hayden MR: Length of huntingtin and its polyglutamine tract influences localization and frequency of intracellular aggregates. Nat Genet 1998;18:150–154.
35 Mende-Mueller LM, Toneff T, Hwang SR, Chesselet MF, Hook VY: Tissue-specific proteolysis of huntingtin (Htt) in human brain: evidence of enhanced levels of N- and C-terminal Htt fragments in Huntington's disease striatum. J Neurosci 2001;21:1830–1837.
36 Wang CE, Tydlacka S, Orr AL, Yang SH, Graham RK, Hayden MR, Li S, Chan AW, Li XJ: Accumulation of N-terminal mutant huntingtin in mouse and monkey models implicated as a pathogenic mechanism in Huntington's disease. Hum Mol Genet 2008;17:2738–2751.
37 Wellington CL, Singaraja R, Ellerby L, Savill J, Roy S, Leavitt B, Cattaneo E, Hackam A, Sharp A, Thornberry N, Nicholson DW, Bredesen DE, Hayden MR: Inhibiting caspase cleavage of huntingtin reduces toxicity and aggregate formation in neuronal and nonneuronal cells. J Biol Chem 2000;275:19831–19838.
38 Saleh N, Moutereau S, Durr A, Krystkowiak P, Azulay JP, Tranchant C, Broussolle E, Morin F, Bachoud-Levi AC, Maison P: Neuroendocrine disturbances in Huntington's disease. PLoS One 2009;4:e4962.
39 Markianos M, Panas M, Kalfakis N, Vassilopoulos D: Plasma testosterone in male patients with Huntington's disease: relations to severity of illness and dementia. Ann Neurol 2005;57:520–525.

SUPPLEMETARY MATERIAL

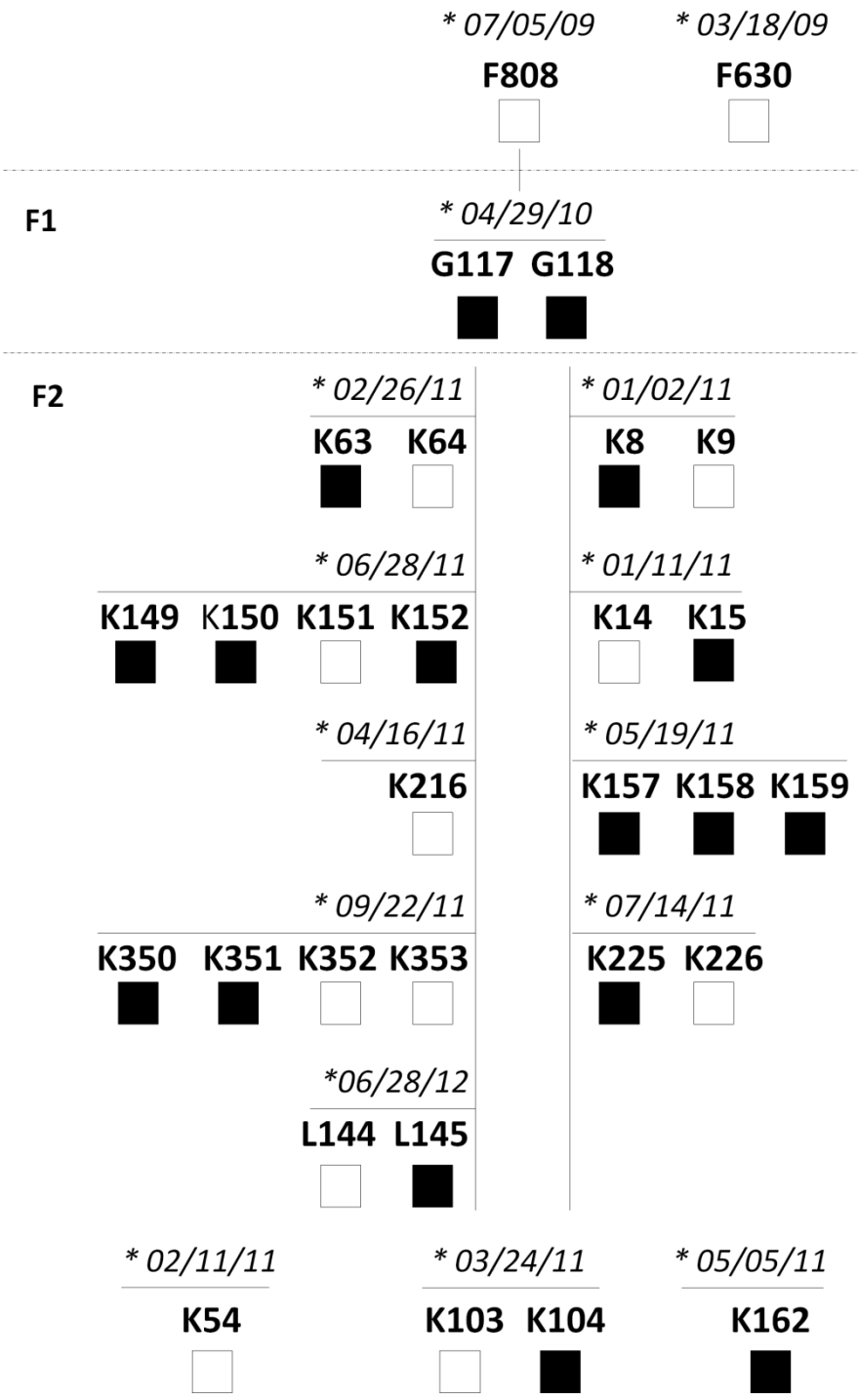

SM 1. Pedigree diagram of the minipigs in this study*. Black boxes represent transgenic animal. Paternity is not clear in K54, K103, K104 and K162 boars. Their father is G117 or G118 TgHD boar. Date of birth (*). F1 generation (F1). F2 generation (F2).*

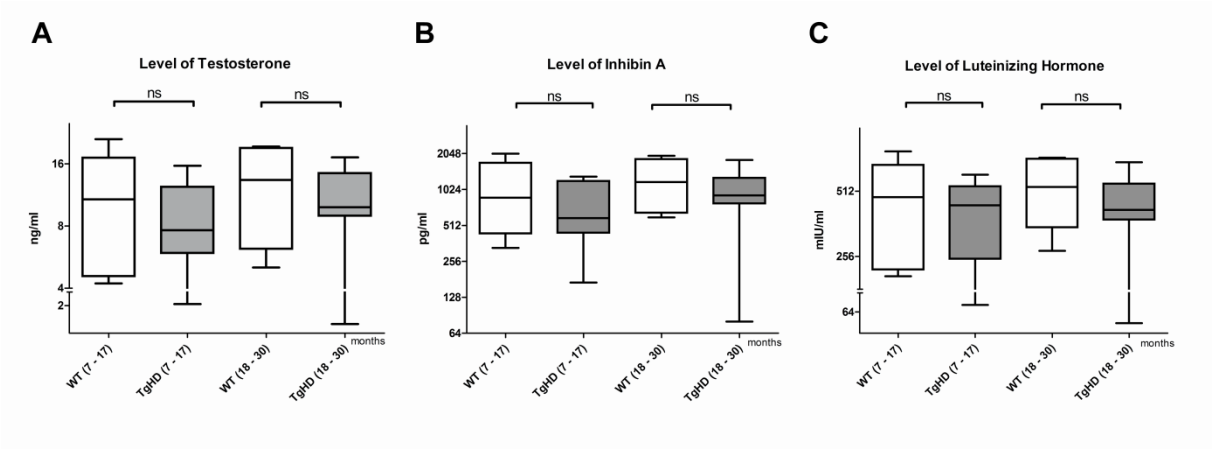

SM 2 Hormonal assay. *Levels of Testosterone, Inhibin A, and Luteinizing hormone were compared in TgHD boars and age-matched controls. No significant changes were found.*

Paper III

Gradual Phenotype Development in Huntington Disease Transgenic Minipig Model at 24 Months of Age.

Vidinská, D., Vochozková, P., Šmatlíková, P., Ardan, T., Klíma, J., Juhás, Š., Juhásová, J., Bohuslavová, B., ***Baxa, M.,*** *Valeková, I., Motlík, J., and Ellederová, Z. (2018).*

Neurodegenerative diseases 18, 107–119.

IF 2.785

Motivation of the study

Mutant huntingtin is proteolyticly cleavaged and N-terminal fragments cause neurotoxicity consistent with the disease progression. Fragments of mtHtt cluster into misfolded conformers and stepwise form aggregates. Aggregates instigate responses of inflammatory an immune apparature of central nervous system represented by microglia and astrocytes. Activated microglia predicts the onset of symptoms of HD. Hence, we were interested in wheather we could detected mtHtt aggregates in brains of 24-month-old minipigs. At this age, our pigs are considered to reach adult body and brain size.

Summary

We confirmed age-dependent fragmentation of endogenous as well as mtHtt in both brain and peripheral tissues. Three of the fragments were specifically enriched only in TgHD tissues and were mostly detectable in testes and caudate nucleus. As manifestation of HD brings diverge in Htt and mtHtt cellular localization, with the mtHtt fragments translocated into the nucleus, we fractionated lysates from testes and cortexes. We detected one of the specifically enriched (71 kDa) fragments in nuclear fraction of TgHD testicular tissue but it was not found in cortexes of 24-month-old animals. This could be attributed to the precedence of the testicular phenotype prior the brain phenotype in the TgHD minipigs.

We did not detect a presence of mtHtt aggregates in 24-month-old TgHD brains. We revealed significantly activated microglial cells and their modestly increased number in the TgHD caudate nucleus.

Finally, we showed that expression of Acyl-coenzyme A binding domain containing 3 protein (ACBD3) which mediates the cytotoxicity of mtHtt, is slightly increased both at mRNA and protein levels.

In conclusion, we observed age-related fragmentation of huntingtin in the brain and testis. The highest fragmentation was found in testes, with mtHtt fragments noticeable even in cell nuclei. Next, we showed upregulation of ACBD3 protein in testes, what was in correspondance to the previously observed testicular degeneration (Paper II). Moreover, activated microglial and slightly decreased myelination indicated proceeding pre-clinical manifestation of HD.

My contribution

I participated on processing of the brain and tissues samples from sacrificed animals. Next, I participated on WB analyses.

Original Paper

Neurodegenerative Diseases

Neurodegener Dis 2018;18:107–119
DOI: 10.1159/000488592

Received: August 17, 2017
Accepted after revision: March 20, 2018
Published online: June 5, 2018

Gradual Phenotype Development in Huntington Disease Transgenic Minipig Model at 24 Months of Age

Daniela Vidinská[a, b] Petra Vochozková[a, b] Petra Šmatlíková[a, b] Taras Ardan[a] Jiří Klíma[a] Štefan Juhás[a] Jana Juhásová[a] Božena Bohuslavová[a, b] Monika Baxa[a, b] Ivona Valeková[a] Jan Motlík[a] Zdenka Ellederová[a]

[a] Laboratory of Cell Regeneration and Plasticity, Institute of Animal Physiology and Genetics, Czech Academy of Sciences, Libechov, Czech Republic; [b] Department of Cell Biology, Faculty of Science, Charles University in Prague, Prague, Czech Republic

Keywords
Huntington disease · Pig model · Mutant huntingtin · Fragments · Aggregates · ACBD3

Abstract
Background: Huntington disease (HD) is an incurable neurodegenerative disease caused by the expansion of a polyglutamine sequence in a gene encoding the huntingtin (Htt) protein, which is expressed in almost all cells of the body. In addition to small animal models, new therapeutic approaches (including gene therapy) require large animal models as their large brains are a more realistic model for translational research. ***Objective:*** In this study, we describe phenotype development in transgenic minipigs (TgHD) expressing the N-terminal part of mutated human Htt at the age of 24 months. ***Methods:*** TgHD and wild-type littermates were compared. Western blot analysis and subcellular fractionation of different tissues was used to determine the fragmentation of Htt. Immunohistochemistry and optical analysis of coronal sections measuring aggregates, Htt expression, neuroinflammation, and myelination was applied. Furthermore, the expression of Golgi protein acyl-CoA binding domain containing 3 (ACBD3) was analyzed. ***Results:*** We found age-correlated Htt fragmentation in the brain. Among various tissues studied, the testes displayed the highest fragmentation, with Htt fragments detectable even in cell nuclei. Also, Golgi protein ACBD3 was upregulated in testes, which is in agreement with previously reported testicular degeneration in TgHD minipigs. Nevertheless, the TgHD-specific mutated Htt fragments were also present in the cytoplasm of striatum and cortex cells. Moreover, microglial cells were activated and myelination was slightly decreased, suggesting the development of a premanifest stage of neurodegeneration in TgHD minipigs. ***Conclusions:*** The gradual development of a neurodegenerative phenotype, accompanied with testicular degeneration, is observed in 24-month-old TgHD minipigs.

Introduction

Huntington disease (HD) is a currently incurable lethal monogenic neurodegenerative disorder with usual manifestation between 30–50 years of age. It is caused by

D.V. and P.V. contributed equally to this work.

E-Mail karger@karger.com
www.karger.com/ndd

Zdenka Ellederova
Institute of Animal Physiology and Genetics
Laboratory of Cell Regeneration and Plasticity
Rumburska 89, CZ–27721 Libechov (Czech Republic)
E-Mail ellederova@iapg.cas.cz

the abnormal elongation of a CAG repeat in the first exon of the huntingtin gene (HTT). The mutated form of the huntingtin protein (mHtt; containing more than 36 polyQ) has a devastating effect mainly on the central nervous system, namely basal ganglia, but it affects the whole body, as it is expressed in most tissues. HD manifestation is characterized by the presence of large inclusion bodies, i.e., aggregates, of mHtt, accumulated primarily in the striatum and cortex. Their presence is tightly correlated with disease progression [1]. However, recent studies suggest that the aggregates might have a protective role against the mHtt effects [2, 3]. Nevertheless, soluble monomers of mHtt, N-terminal fragments, and mHtt oligomers were found in affected tissues and described as toxic to cells and as a trigger of cellular dysfunction [4, 5]. Both wild-type (WT) and mHtt undergo proteolytic cleavage, but mutated N-terminal fragments cause cytotoxicity, accumulate with the progression of the disease [6–8], and their amount varies among tissues, which may correlate with cell susceptibility to HD [8–10]. In addition to the atrophy of medium spinal neurons, white matter atrophy, myelin breakdown, and changes in iron homeostasis are linked to HD [11, 12]. The pathogenesis of the disease is quite complex, since mHtt has a role in several biological processes [13, 14]. It has been reported that Golgi protein acyl-CoA binding domain containing 3 (ACBD3) is upregulated in affected tissues of HD patients and mice models as well as in the Q111 cell line [15], and that elevated ACBD3 causes cell toxicity. ACBD3 is released after cellular stress during the fragmentation of Golgi apparatus and acts as a scaffold.

Even though HD is considered a primary neurological disease, peripheral pathologies such as skeletal and heart muscle malfunction, increased proinflammatory signaling, weight loss, and metabolic changes also play an important role in disease progression. In addition, testicular degeneration was also observed in mice models and in postmortem human specimens [16–18].

Animal models are useful in clarifying HD pathogenesis as well as in validating new therapeutic approaches. Thus, in addition to the small-animal rodent models [19–21], large-animal models have been introduced [22–25]. Large animal brains are a more realistic model for the delivery issues faced with therapeutics in the clinics. The distribution of a drug in a large brain has important implications for its target engagement and eventual efficacy, and it is a much more realistic system for human patients in this regard.

In 2009, we developed one of the few large-animal models for HD – a transgenic minipig (TgHD). We did this by microinjecting a lentiviral vector encoding the N-terminal (1–548 aa) part of human Htt, which contained 124 CAG/CAA repeats under the control of the human HTT promoter [25]. Genomic analysis showed that the construct was inserted into chromosome 1 (1q24-q25) and did not interrupt any coding sequence in the pig genome [26]. At present, we have 5 generations of TgHD minipigs, with an almost equal number of transgenic and WT piglets in each litter. The first apparent defect is the reproductive failure in each generation of TgHD boars at 13 months of age [26]. The reduced sperm count and motility, which is a direct effect of overexpressed mHtt in the testes, could also be related to the significant reduction of relative phosphodiester concentration in testicular parenchyma of 24-month-old TgHD boars [27] and lower mitochondrial energy-generating parameters in TgHD boars' spermatozoa [28]. In order to obtain a significant number of animals at a clinical stage of HD, most of the animals are tested noninvasively. Magnetic resonance spectroscopy analysis showed a significant decrease of total creatine in the brains of 24-month-old TgHD animals [29]. Telemetric studies revealed differences in physical activity patterns of 36-month-old TgHD compared to WT minipigs between 4:40 and 5:30 a.m. [30]. The oldest 2 animals, starting at 60 months, manifested motoric defects in limbs and an increase in anxiety behavior [unpubl. data]. Nevertheless, more TgHD minipigs need to be studied to confirm these observations.

In this study, we have invasively analyzed various tissues from 3 pairs of 24-month-old TgHD and WT minipigs, the main focus being on the brain and HD markers. Our aim was to describe the development of the disease in this model.

Methods

Animals

TgHDs with the N-terminal part of human mHtt were studied. The genotype was determined according to Baxa et al. [25] from their skin after weaning. TgHD minipigs ($n = 3$; 2 males and 1 female) and their WT controls ($n = 3$; 2 males and 1 female) from F2 generations were perfused under deep anesthesia with ice-cold PBS at the age of 24 months, plus 1 pair of 4-, 6-, and 16-month-old animals, respectively. Various tissues were isolated and stored after being snap frozen in liquid nitrogen. The right hemisphere of each perfused brain was directly fixed for immunohistochemistry. The entire study was carried out in agreement with the Animal Care and Use Committee of the Institute of Animal Physiology and Genetics, under the Czech regulations and guidelines for animal welfare and with the approval of the Czech Academy of Sciences, protocol No. 53/2015.

SDS-PAGE and Western Blot

Tissue samples were homogenized in liquid nitrogen using a mortar and lysed in RIPA buffer (150 mM NaCl, 5 mM EDTA pH 8, 0.05% NP-40, 1% sodium deoxycholate, 0.1% SDS, 1% Triton X-100, 50 mM Tris-HCl pH 7.4, inhibitors of phosphatases and proteases), sonicated for 15 min, and centrifuged at 20,000 *g* for 15 min at 4 °C. Samples (10 µg of total protein) were loaded onto 3–8% Tris-acetate gel (EA03758, LifeTech) and run at 150 V. Gel was transferred onto nitrocellulose membrane, blocked in 5% skimmed milk, and probed overnight with anti-HTT antibody diluted in 5% milk (EPR5526, Abcam, 1:3,000), anti-polyQ antibody recognizing polyQ >39 (3B5H10, Sigma Aldrich, 1:3,000), or ACBD3 antibody (Santa Cruz, 1:500) at 4 °C. Memcode protein staining (LifeTech) and anti-tubulin (T4026, Sigma, 1:30,000) was used for the normalization of loading. Secondary antibody conjugated with HRP (anti-mouse, 711-035-152, or anti-rabbit, 711-035-152, both Jackson ImmunoResearch, 1:10,000) was used. The signal was revealed by chemiluminiscence (ECL, 28980926, APC-zech) and detected by The ChemiDoc XRS+system (Bio-Rad). The normalized volume intensity was measured by Image Lab 5.2.1 software. Normalization was done with total lane protein (different tissues) or tubulin (cortexes), and the lane background was subtracted with disk size 10.

Subcellular Fractionation

The subcellular fractionation of TgHD and WT samples was performed according to Dimauro et al. [31] with some modifications. STM buffer was replaced by TD buffer comprising 25 mM Tris pH 8.0, 2 mM $MgCl_2$, and protease and phosphatase inhibitor cocktails. NET buffer was replaced by BL buffer (comprising 10 mM Tris pH 8.0, 0.4 M LiCl, 20% glycerol, protease and phosphatase inhibitors). Proteins (4 µg) from both fractions were loaded, and Western blot analysis using anti-Htt antibody (EPR5526, Abcam, 1:3000) and anti-tubulin (T4026, Sigma, 1:30,000), a cytoplasmic marker as well as nuclear marker anti-A/C-lamin (SAB4200236, Sigma, 1:2,000) to check for the correct fractionation, was performed.

Immunohistochemistry

The right hemisphere from each animal was fixed in 4% paraformaldehyde for 24 h and then cryoprotected with 30% sucrose containing 0.01% sodium azide. Frozen coronal sections were prepared using tissue-freezing medium (Leica, 14020108926). The free-floating sections of a thickness of 40 µm were sequentially treated with formic acid, 0.3% hydrogen peroxide in MetOH, and blocking serum to unmask antigens and reduce endogenous peroxidases and unspecific binding of antibodies. The sections were incubated with the following primary antibodies: anti-Htt antibody (clone MW7 supernatant, Hybridoma Bank), anti-polyQ antibodies (clone 3B5H10, 1:1,000, P1874, Sigma, and clone 5TF1-1C2, 1:1,000, Millipore, MAB-1574) and anti-Iba1 antibody (1:200, Synaptic System GmbH, 234003). After washing, the sections were incubated with biotinylated donkey anti-rabbit or sheep anti-mouse secondary antibody (both 1:400, Amersham, UK) followed by the incubation with avidin-peroxidase complex (1:400, Sigma-Aldrich). The labeled sections by peroxidase were developed with DAB tablets (4170, Kementec Diagnostics). Negative controls were performed by omitting the primary antibody. Sections were finally dehydrated in graded ethanol, cleared in xylene, and mounted in DPX. The slides were digitalized using a virtual microscopy system (VS-120FL, Olympus, Tokyo, Japan; 20× objective).

Number and Intensity of Iba1-Positive Microglia

The whole area of the caudate nucleus (CN) was evaluated in every coronal section image (section per animal/n = 4–5). The overall intensity of Iba1 signal was measured using KS400 image analysis software (Carl Zeiss, Jena, Germany). From the estimated mean intensity, gray values ranging from 0 (white) to 255 (black), mean values for each animal were calculated for statistical analysis. The area of the CN from the same coronal section image was used to determine the number of Iba1-positive microglia. Random image fields from the CN (sections per animal/n = 4–5) with a total area of 193,000 µm^2 (7,720,000 µm^3 tissue volume) were chosen for further image analysis. Digital image processing was performed using Fiji software followed by manual counting of ≥1,500-pixel area objects using the "cell counter" plugin.

Real-Time PCR

RNA was isolated from the cortex, putamen, and testes of all pairs using Qiazol (Qiagen) and chloroform, and subsequently purified by RNeasy Plus mini-kit (Qiagen). One-step Syber Green RT PCR amplification was performed using 1 µg of total RNA in a reaction mixture of 15 µL. The primer set for *Sus scrofa* ACBD3 (109-bp amplicon) and only human HTT (73-bp amplicon) was designed using Primer3 on the intron's border to eliminate DNA amplification. GAPDH, B2M, and ACTB were used as reference genes. The reaction started with reverse transcription at 50 °C for 30 min and denaturation at 95 °C for 15 min, followed by 40 cycles of denaturation at 94 °C for 15 s, annealing at 57 °C for 30 s and elongation at 72 °C for 30 s, followed by a melting curve experiment, 50–95 °C, with 0.5 °C increments at 3 s/step.

Primer Sequences

ACBD3: fwd, 5′-GCCTGGAGGAGCTGTACG-3′, rev, 5′-TGCTTATGCAGTGCCACAAG-3′; *Human HTT*: fwd, 5′-TCAGAAATGCAGGCCTTACC-3′, rev, 5′-TGATTCTTCGGGTCTCTTGC-3′; *GAPDH*: fwd, 5′-CGTCAAGCTCATTTCCTGGTACG-3′, rev, 5′-GGGGTCTGGGATGGAAACTGGAAG-3′; *B2M*: fwd, 5′-AAACGGAAAGCCAAATTACCTGA-3′, rev, 5′-ATCTCTGTGATGCCGGTTAGTG-3′; *ACTB*: fwd, 5′-GAGAAGCTCTGCTACGTC-3′, rev, 5′-CCAGACAGCACCGTGTTGG-3′.

Statistics

All results are expressed as the mean ± standard error and were analyzed using GraphPad Prism software (GraphPad Software, San Diego, CA, USA). The *t* test and one-way analyses of variance (ANOVA) test with Bonferroni analysis as a post hoc test were applied for comparisons of the expression. The Mann-Whitney test was used to determine the differences in the quantity of Iba1+ cells between the TgHD and WT groups.

Results

Fragmentation of mHtt Is Tissue Specific and Increases with Age

In order to describe the progression of HD in TgHD minipigs, we sacrificed 3 pairs of 24-month-old TgHD and WT animals. Western blot analysis, using anti-Htt and anti-polyQ (recognizing polyQ >39) antibodies,

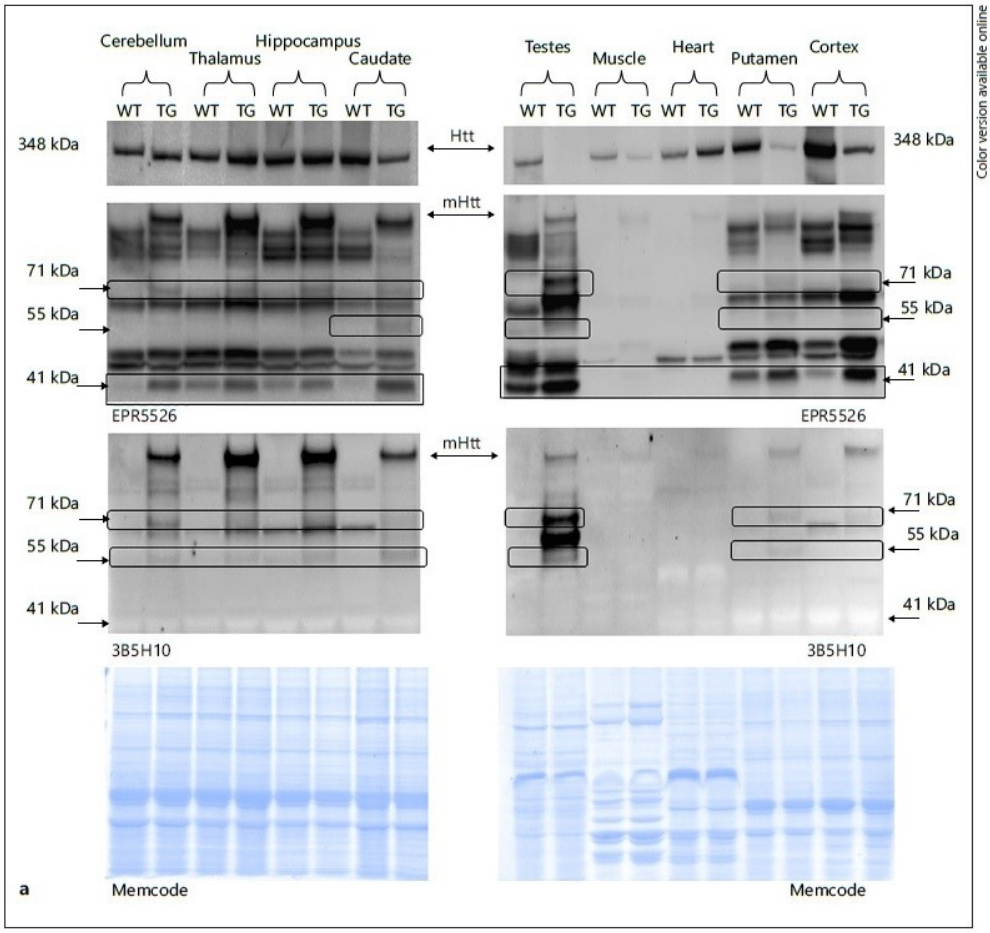

Fig. 1. Tissue-specific fragmentation of mHtt. **a** Different tissues from TgHD (TG; $n = 3$) and WT ($n = 3$) 24-month-old minipigs were run on 3–8% PAGE gel and blotted with anti-Htt antibody (EPR5526) and polyQ antibody (3B5H10). Endogenous Htt (348 kDa), mHtt (110 kDa), and several fragments (71, 55, and 41 kDa) were detected, especially in TgHD tissues compared to WT. A representative blot of 1 pair is shown. **b** Intensity of 3 fragments (71, 55, and 41 kDa) from blots of all pairs was normalized to the same exposure time and the total lane protein detected by memcode using Bio-Rad Software Image Lab 5.2.1. The mean intensity value from blots of all pairs with standard error of the mean (SEM) is shown in the graphs. The multiple unpaired *t* test was performed comparing WT and TgHD tissues. **c** The mean ratio of mHtt to endogenous Htt expression with SEM was calculated for all tissues and is shown together with the expression of mHTT mRNA determined by qPCR; one-way ANOVA and the Bonferroni multiple comparison post hoc test were applied. ** $p < 0.01$, *** $p < 0.001$, **** $p < 0.0001$.

(Figure continued on next page.)

showed tissue-specific expression of endogenous porcine Htt (approx. 348 kDa), recognized only by anti-Htt antibody, human mHtt (approx. 110 kDa) and their fragments in various tissues, namely the CN, hippocampus, thalamus, cerebellum, cortex, putamen, heart, muscle, and testes (Fig. 1a). We detected fragmentation in TgHD as well as WT samples. Three of the fragments – sizes 71, 55, and 41 kDa – were enriched or specifically expressed only in tissues from TgHD animals. The anti-polyQ antibody did not recognize the 41-kDa fragment, probably due to a low number of glutamine repeats in this fragment, highlighting that 71- and 51-kDa fragments are polyQ products. These fragments were mostly detectable in testes, but they were also present in brain tissue, main-

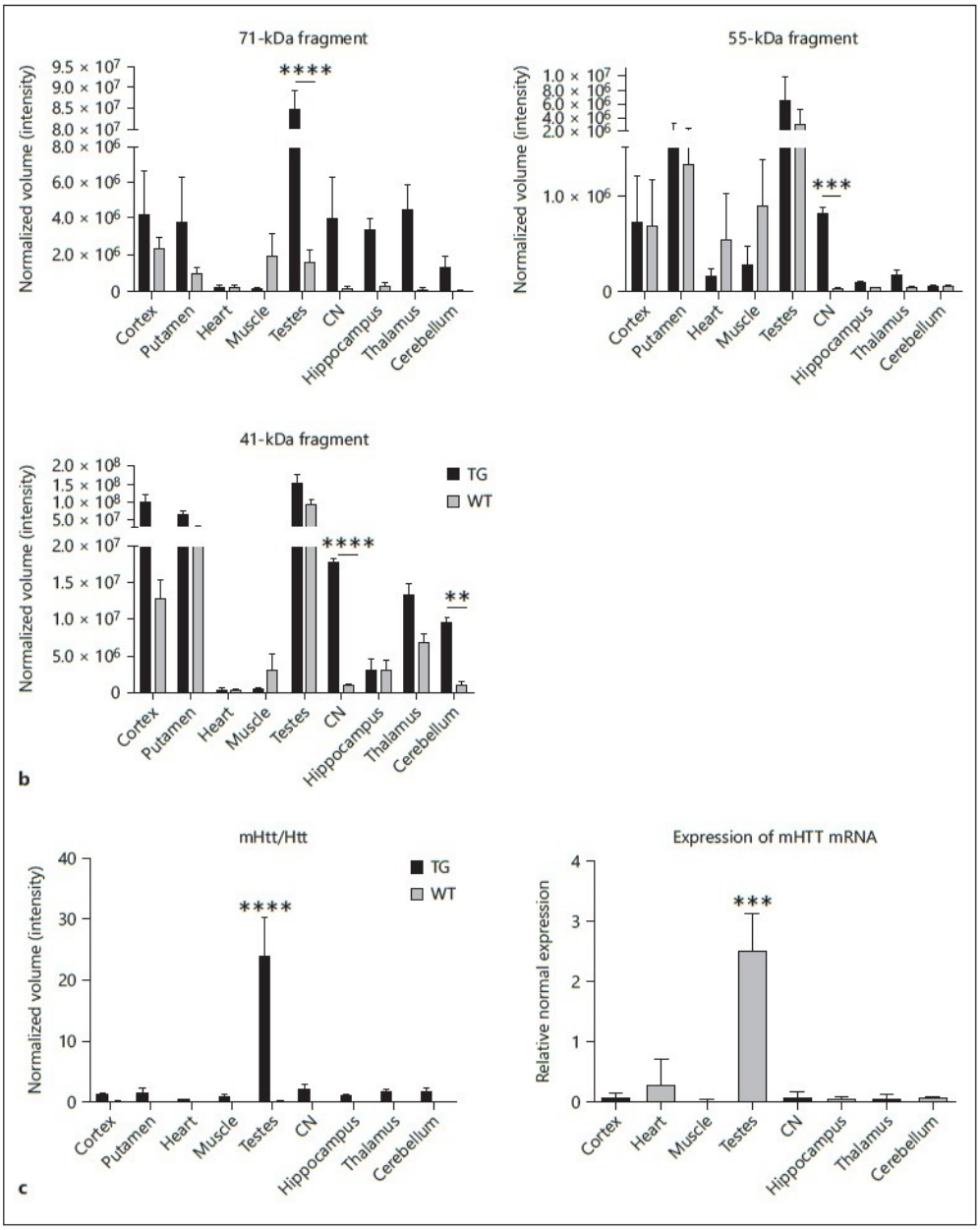

1

ly in the striatum and cortex. They were almost absent in the heart and muscle (Fig. 1b). Interestingly, multiple *t* test analysis comparing WT and TgHD samples from the same tissue revealed a significant enrichment of the 55-kDa fragment ($p < 0.0001$) as well as the 41-kDa fragment ($p < 0.001$) in the CN, the most effected tissue in patients, in TgHD minipig samples compared to WT. The 41-kDa fragment was also significantly enriched in TgHD cerebellum ($p = 0.00132$), and the 71-kDa fragment was significantly enriched in testes ($p < 0.0001$; Fig. 1b). Next

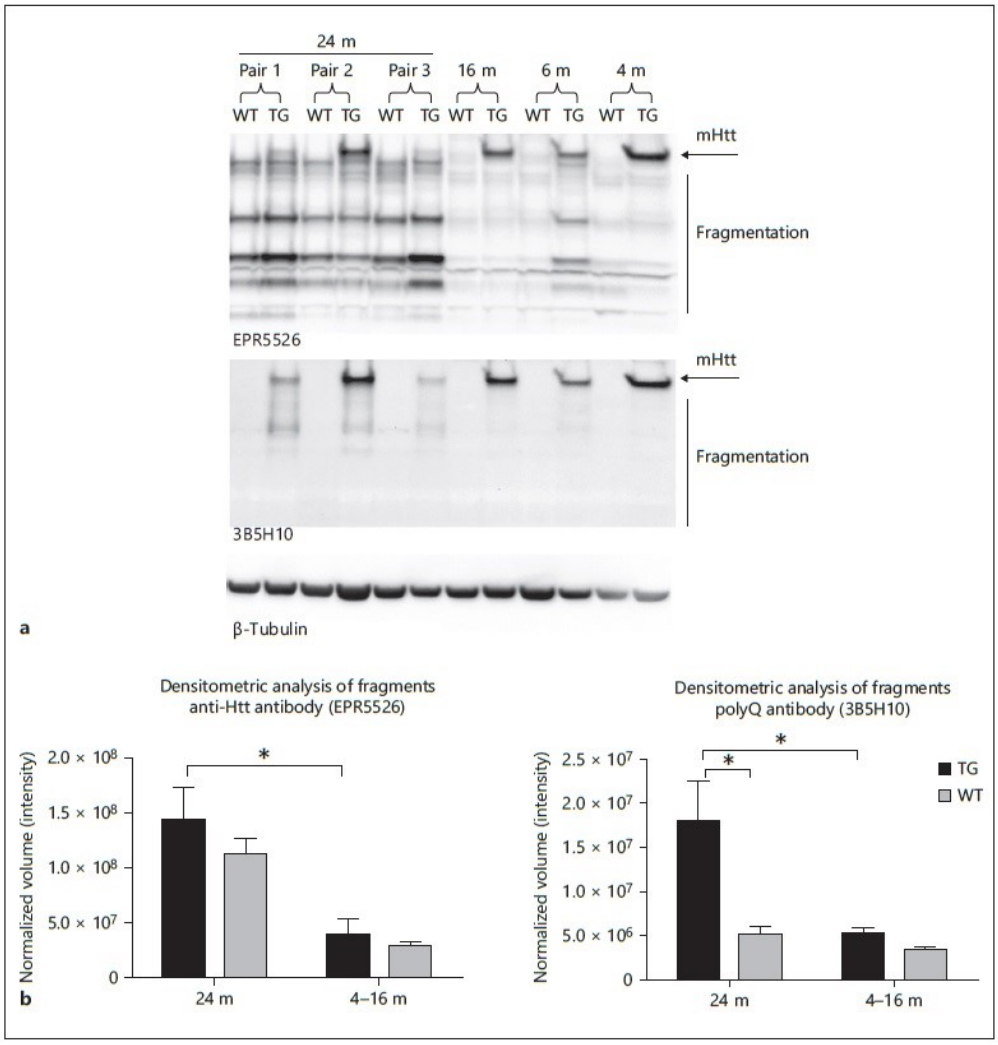

Fig. 2. Increased fragmentation in the cortex of 24-month-old TgHD (TG) versus WT minipigs compared to younger animals. **a** Western blot of cortexes from 1 pair of TgHD and WT animals sacrificed at 4 months (4 m), 6 months (6 m), and 16 months (16 m), and 3 pairs at 24 months (24 m) performed with anti-Htt antibody (EPR5526) and anti-polyQ antibody (3B5H10). β-Tubulin was used as a loading control. **b** Densitometry analysis of fragments normalized to the total lane protein detected by memcode using Bio-Rad Software Image Lab 5.2.1 is shown with mean values and SEM. One-way ANOVA and the Bonferroni multiple comparison post hoc test were applied. * $p < 0.05$.

we noticed that the expression of endogenous Htt and mHtt varied among the different tissues. It is still unclear whether the effect of mHtt is one of gain of function or loss of function [32], and it is assumed that mHtt and Htt compete for targets. Therefore, we analyzed the mHtt/Htt ratio in all tissues (Fig. 1c), detecting the highest ratio in the testes (significance $p < 0.0001$). In particular, TgHD testes from both boars expressed very low endogenous Htt. This is in agreement with a previously reported degeneration of testes and infertility of TgHD minipigs starting at 13 months of age [26]. Brain tissues, especially the CN and putamen, also showed a higher but not significant mHtt/Htt ratio compared to muscle and heart, in which the phenotype seems to be always delayed. The rea-

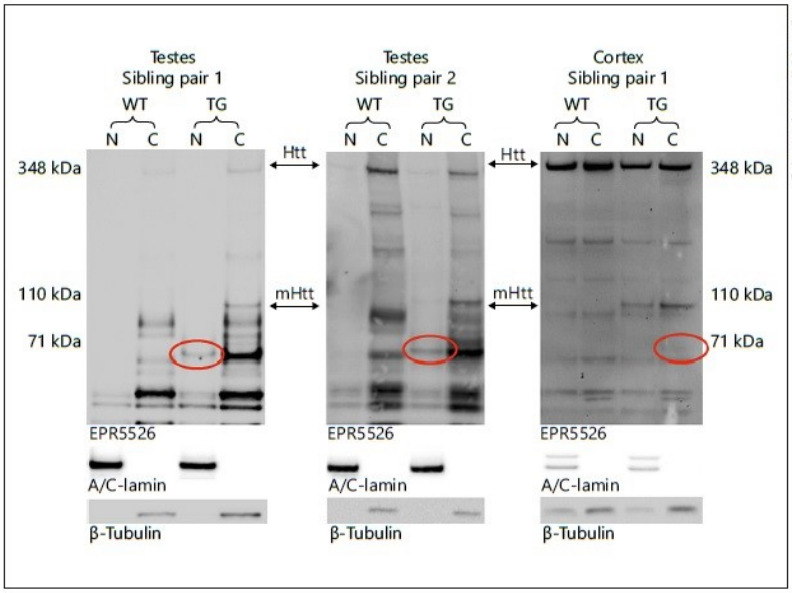

Fig. 3. Htt and its fragments after subcellular fractionation of testes and cortexes from TgHD (TG) and WT minipigs. Cortexes and testes from 2 pairs of 24-month-old boars were fractionated, and the Western blot was incubated with anti-Htt antibody (EPR5526). β-Tubulin (cytoplasmic marker) and A/C-lamin (nuclear marker) were used as a control of efficient fractionation.

son why there is the most mHtt and intense fragments in testes could be explained by the most abundant mHTT mRNA expression in testes compared to other tissues ($p < 0.001$; Fig. 1c).

The next question was whether the fragmentation changes with the age of the animals. Thus, we analyzed cortexes from 4-, 6-, 16-, and 24-month-old animals for fragmentation using anti-Htt and anti-polyQ antibodies (Fig. 2). We found that fragmentation increased at 24 months, which may indicate disease progression. Considering the importance of the amount of mHtt and its forms in nuclear versus cytoplasmic fractions in disease progression [33], we fractionated lysates from testes and cortexes (Fig. 3). It has been previously reported that when neurotoxicity is manifested, Htt and mHtt diverge in cellular localization, with the mHtt fragments translocating into the nucleus [34–36]. We found that the 71-kDa fragment can be detected in nuclear fractions in testes but not in cortexes of 24-month-old animals (Fig. 3). This may be related to the fact that the testicular phenotype precedes the brain phenotype in the TgHD minipigs [26].

Absence of mHtt Aggregate Formation in Brains of 24-Month-Old TgHD Minipigs

The hallmark of HD is the presence of mHtt aggregates in the brain. We performed filter retardation assay [37] and immunohistochemical staining with various anti-Htt antibodies (EM-48, MW7,8, S830) to check for aggregates in 24-month-old animals. None of the techniques with antibodies mentioned above could reveal mHtt aggregates. Immunostaining with MW7 antibody is shown for illustration (Fig. 4a–d, x). Using anti-polyglutamine-specific antibodies such as 3B5H10 and/or 1C2, we showed a significant increase in polyQ signal in the brain, particularly in the CN and cortex (Fig. 4f–o, t–w); however, no mHtt aggregates were detected at this age (Fig. 4d). Nevertheless, the myelination in fibers of the internal capsule (capsula interna) measured by Luxol fast blue staining was slightly decreased ($p = 0.0556$) in TgHD compared to WT (Fig. 4p–s, y).

Microglia Activation in TgHD CN

Iba1 is a calcium-binding protein specifically expressed in microglia. The optical analysis of Iba1-immunolabeled brain coronal sections revealed a significant increase of Iba1 expression ($p = 0.0258$) in the CN of TgHD animals compared to WT littermates (Fig. 5). This result indicates that microglial cells in the TgHD brain are in a more activated state. Moreover, we observed a moderate but nonsignificant ($p = 0.4$) increase in the number/amount of ≥1,500-pixel-sized Iba1-stained cells in the CN of TgHD animals compared to their WT littermates (Fig. 5).

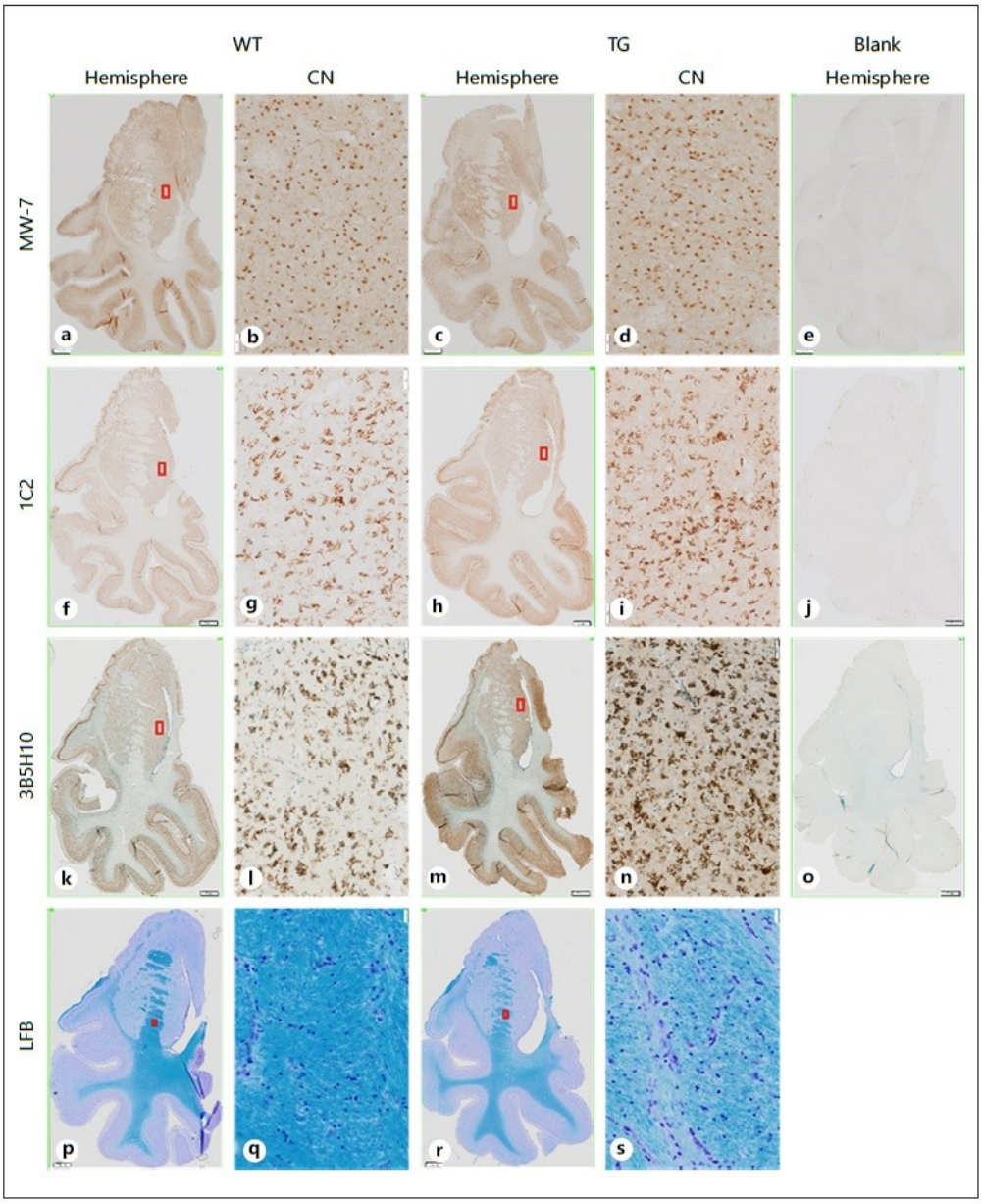

Fig. 4. No aggregate formation but higher mHtt expression and limited demyelination in TgHD (TG) brains. Representative images of MW7 antibody-immunohistochemical labeling recognizing Htt aggregates (**a–e**), 1C2-polyglutamine antibody (**f–j**), 3B5H10-polyglutamine antibody (**k–o**), and Luxol fast blue detecting the myelination (**p–s**). **t–y** Optical analysis of all pairs in the CN or motor cortex. * $p < 0.05$, *** $p < 0.001$; $n = 3$ for each group. 24 m, 24 months.

(Figure continued on next page.)

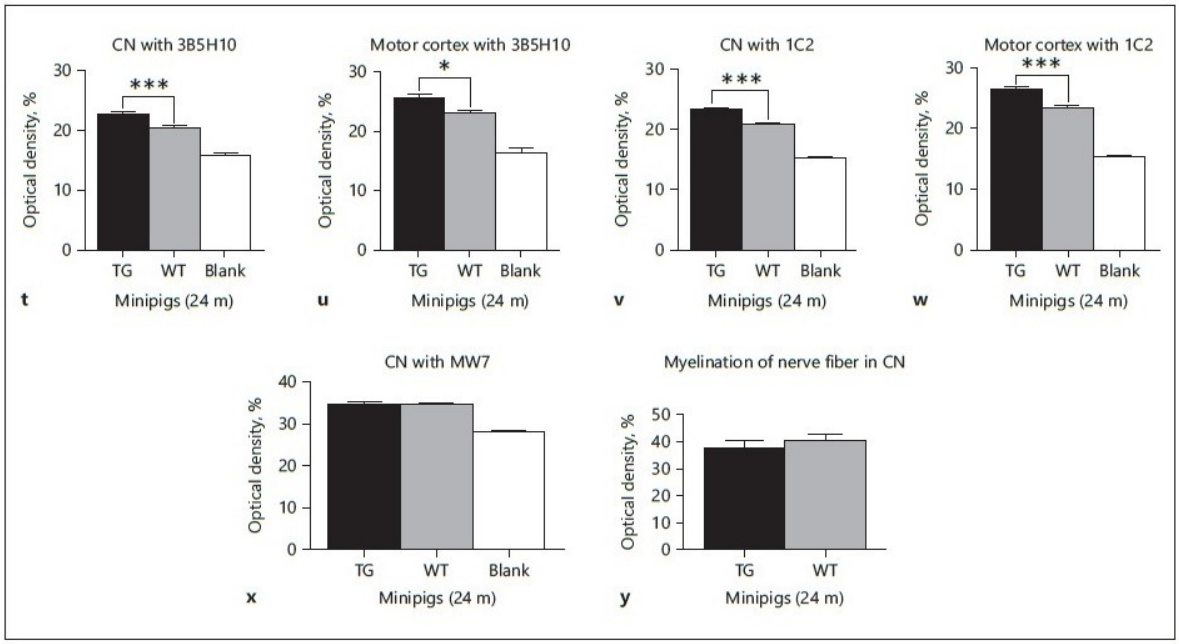

4

ACBD3 Dysregulation in Testes of 24-Month-Old TgHD Minipigs

It has been reported that the Golgi scaffold protein ACBD3 mediates the cytotoxicity of mHtt, and its higher expression is associated with the disease progression. It is elevated in disease-affected tissues of HD patients, HD mice, and mHtt-expressing cell lines [15]. We found that the expression of ACBD3 in the brain was slightly decreased, albeit insignificantly, at the mRNA (Fig. 6a) and in protein levels (Fig. 6b). Nevertheless, its expression was elevated in the testes at the protein level ($p = 0.058$; Fig. 6a, b). The mRNA was also elevated, but not significantly. These findings correlate with the highest abundance of mHtt fragments detected in the testes. It provides more evidence that the HD phenotype in the testes precedes neurodegeneration in this HD model.

Discussion

Recent promising HD treatments require preclinical testing in large animals. Minipigs are a suitable species because of their large gyrencephalic brain, adult body weight of 70–90 kg, long lifespan, and other anatomical, physiological, and metabolic similarities to humans [38, 39]. Here, we tested the phenotype development in our 24-month-old TgHD minipigs containing the N-terminal part of human mHtt (548 aa, Q124). At this age, the pigs have reached their adult size both in terms their body and their brain; 24-month-old minipigs have also been used in preclinical studies for proof-of-concept and safety of compound application [unpubl. data]. Therefore, further detailed phenotypic characterizations of this model at this age are desired.

It has been postulated that the hallmark of HD is aggregate formation in the brain. In the commonly used HD mouse models (R6/2, *Hdh*Q150, and zQ175 knock-in) the proportion of neurons with aggregates is around 40–50% [40]. Nevertheless, the percentage of neurons with aggregates in postmortem HD patient brain samples did not exceed 0.3% [40]. Likewise, we have not detected aggregates in whole brain sections of TgHD minipigs at 24 months of age. However, we expect some in older age since recent brain MRI data of 3 tested TgHD animals, 6–7 years old, showed ventricle enlargement compared to WT minipigs of the same sex and age. Moreover, older TgHD minipigs, starting from the age of 5–6 years, show motoric and behavioral deficiency [unpubl. data]. Nevertheless, at 24 months we detected the accumulation of age-dependent putative Htt fragments, with some of

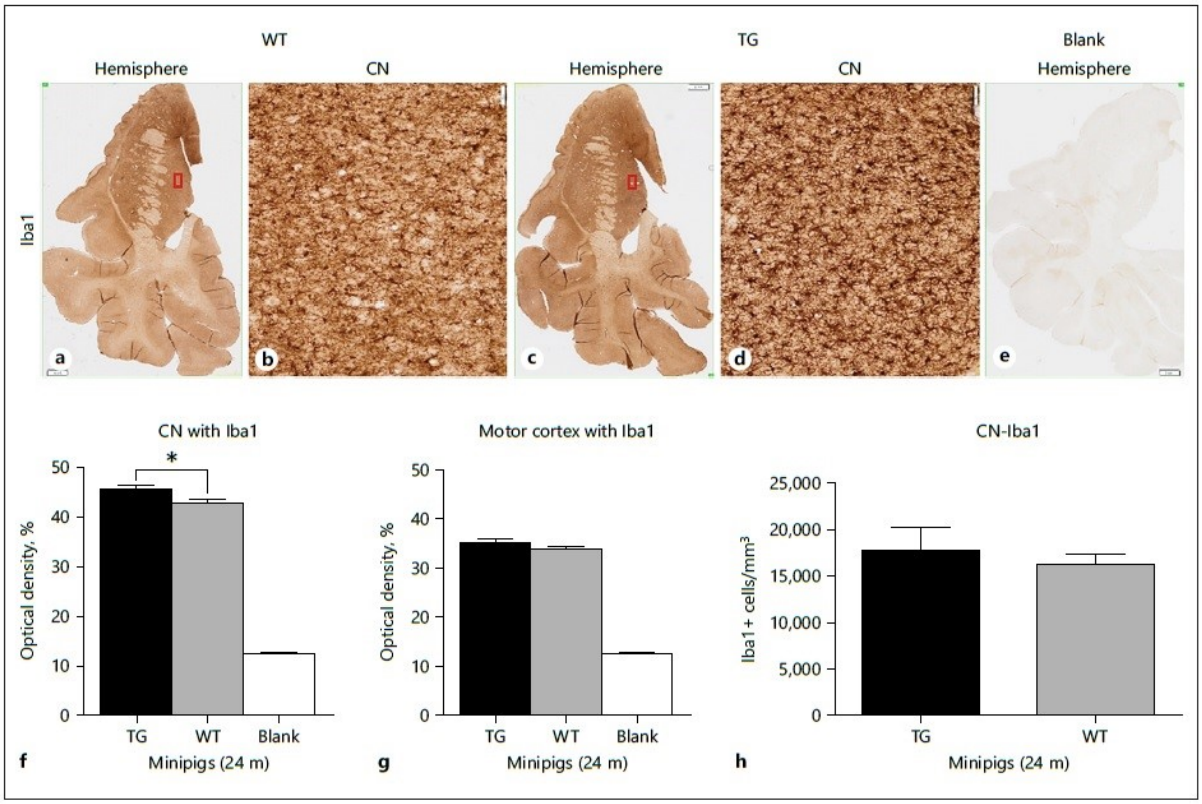

Fig. 5. Number and intensity of Iba1-positive microglia. **a–e** Representative images of Iba1 immunohistochemical labeling of coronal sections of porcine brains, including detailed views of the CN of WT (**b**) and CN of TgHD (TG) animals (**d**). Optical density analysis of Iba1 in the CN (**f**), optical density analysis of Iba1 in the motor cortex (**g**), and number of microglia in the CN (**h**). * $p < 0.05$; $n = 3$ for each group. 24 m, 24 months.

them enriched only in tissues from TgHD animals. It has been reported that the fragmentation of N-terminal mHtt causes toxicity and correlates with disease progression [8]. We found that the fragmentation is tissue specific, with most fragments present in the testes, followed by the brain (particularly in the striatum and cortex); however, we could detect almost no fragments in the heart and muscle of TgHD minipigs. Furthermore, we detected 2 fragments (around 55 and 41 kDa) significantly expressed only in the CN of TgHD minipigs. Although Htt is expressed in nearly all cells of the body, some tissues are more susceptible to the presence of the mutated form than others [41, 42]. This might be explained by the amount of toxic fragments produced [8–10]. The first phenotype observed in TgHD minipigs was boar infertility and testes degeneration at 13 months of age [26], which is in agreement with the very high abundance of mHtt fragments found in the testes. Our data also suggest progression of the disease-related phenotype in the brain of TgHD minipigs. However, the specific mHtt fragments in the brain at 24 months were not found in the nuclear fraction, in contrast to the testes, in which we detected the mHtt fragments in both the cytoplasmic and nuclear fractions.

Moreover, we found that microglial cells were significantly activated and their number in the CN was increased, though not significantly. It was recently shown that activated microglia induce the production of A1 astrocytes. A1 astrocytes fail to support growth and neuron survival; in fact, they are toxic to neurons and oligodendrocytes and cause their death. Their increased production has been described in many neurodegenerative dis-

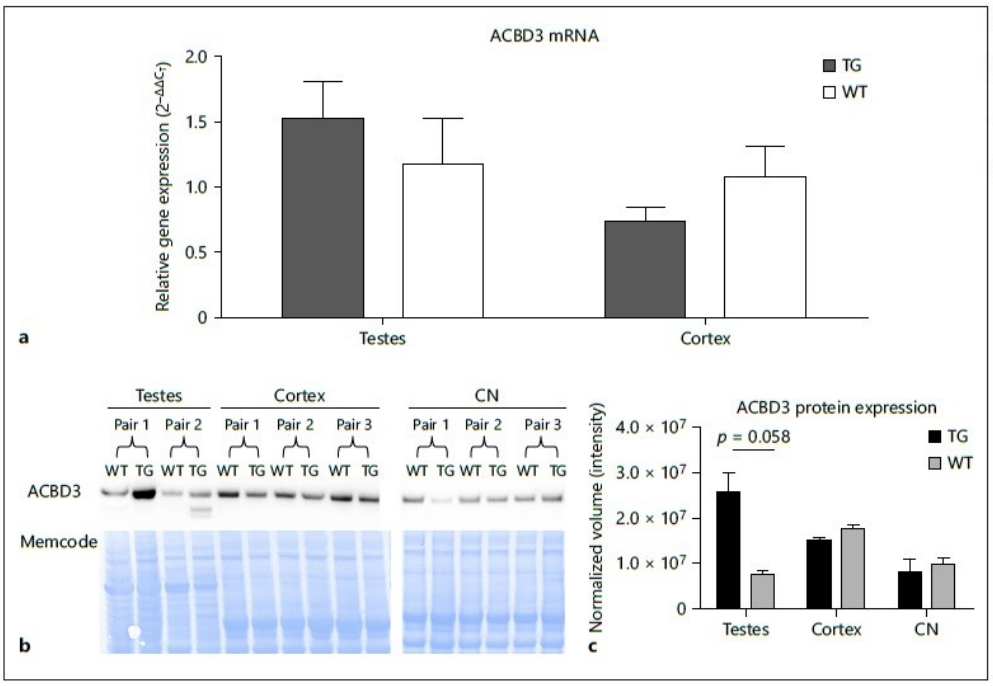

Fig. 6. Upregulation of ACBD3 in testes of TgHD (TG) minipigs. **a** Real-time PCR using ACBD3 primers and RNA from 3 sibling pairs (24 months old, 4 boars and 2 females). Expression of ACBD3 was normalized to GAPDH, B2M, and ACTB expression. **b** Western blot with ACBD3 antibody. **c** Densitometry analysis of ACBD3 band normalized to the total lane protein detected by memcode using Bio-Rad Software Image Lab 5.2.1 presented as mean values and SEM. The multiple unpaired *t* test was performed comparing WT and TgHD tissues.

eases, including HD [43]. We have previously evaluated the central nervous system immune response in our TgHD minipigs by measuring cytokine expression in the secretome of microglial cells and also cerebrospinal fluid (CSF). CSF can reflect optimal changes in the brain tissue, leading us to use it as a source of biomarkers. We found decreased levels of IFNα and IL-10 in CSF and microglia secretome and increased levels of IL-8 and IL-1β only in microglial secretome in TgHD compared to WT controls [44]. Increased levels of IL-8 and IL-1β in plasma were also found in premanifest HD gene carriers and were correlated with increased central microglial activation [45].

Furthermore, we detected demyelination, which occurs prior to neuronal loss in mice models of HD (YAC128 and BACHD) [46], in TgHD minipigs at 24 months. This indicates an ongoing premanifest stage in TgHD minipigs at this age. Interestingly, demyelination can be caused by microglia-induced damage to oligodendrocytes via proinflammatory mediators (iNOS, TNFα, TLRs, and HLA-DR) expressed in activated microglia [47].

In HD, several proteins change expression and thus may serve as biomarkers of disease progression. It has recently been reported that ACBD3 levels are considerably elevated in HD patients and in mice models, and thus augment cellular toxicity. Furthermore, HD-related neurotoxicity is suppressed by ACBD3 depletion and elevated by ACBD3 overexpression [15]. Here, we demonstrated that ACBD3 was elevated in 24-month-old TgHD testes, in which we previously described degeneration caused by mHtt expression [26]. Interestingly, the mRNA and protein expression levels of ACBD3 in the brain are lower, albeit insignificantly, in TgHD minipigs at 24 months, suggesting a possible protective adaptation or a defense mechanism.

In conclusion, testicular degeneration precedes the initiation of the neurodegenerative phenotype in 24-month-old TgHD minipigs. We detected no aggregates

but found that mHtt fragments increased at this age, with the highest number of fragments found in the testes and brain. In the testes, the total amount of mHtt fragments was particularly high and was also detectable in nuclear fractions, unlike in the brain. This corresponds to the previously described testicular degeneration and compromised fertility at this age. Also, the ACBD3 overexpression is in accordance with the HD testicular-degenerative phenotype. Furthermore, the microglial cells were activated and myelination was slightly decreased, which suggests the progression of a premanifest stage of HD. At this stage, ACBD3 was downregulated, suggesting possible adaptive neuroprotection. Taken together, these results suggest that the TgHD minipig is not just a suitable large animal model for safety studies, but also a promising model for investigating the efficacy of therapeutic preclinical testing.

Acknowledgments

Lenka Travnickova and Patricie Jandurova provided technical assistance with the immunohistochemical experiments. This work was supported by the National Sustainability Programme, project No. LO1609 (Czech Ministry of Education, Youth and Sports).

Disclosure Statement

The authors declare that they have no competing interests.

Author Contributions

Z.E., J.K., and J.M. conceived the experiments, D.V., P.V., P.S., M.B., B.B., I.V., and J.J. conducted the experiments. T.A. and S.J. analyzed the results. All authors read and approved the final manuscript.

References

1 DiFiglia M, Sapp E, Chase KO, Davies SW, Bates GP, Vonsattel JP, Aronin N: Aggregation of huntingtin in neuronal intranuclear inclusions and dystrophic neurites in brain. Science 1997;277:1990–1993.

2 Arrasate M, Mitra S, Schweitzer ES, Segal MR, Finkbeiner S: Inclusion body formation reduces levels of mutant huntingtin and the risk of neuronal death. Nature 2004;431:805–810.

3 Nucifora LG, Burke KA, Feng X, Arbez N, Zhu S, Miller J, Yang G, Ratovitski T, Delannoy M, Muchowski PJ, Finkbeiner S, Legleiter J, Ross CA, Poirier MA: Identification of novel potentially toxic oligomers formed in vitro from mammalian-derived expanded huntingtin exon-1 protein. J Biol Chem 2012;287:16017–16028.

4 Hoffner G, Souès S, Djian P: Aggregation of expanded huntingtin in the brains of patients with Huntington disease. Prion 2007;1:26–31.

5 Lajoie P, Snapp EL: Formation and toxicity of soluble polyglutamine oligomers in living cells. PLoS One 2010;5:e15245.

6 Davies SW, Scherzinger E: Nuclear inclusions in Huntington's disease. Trends Cell Biol 1997;7:422.

7 Kim M, Lee HS, LaForet G, McIntyre C, Martin EJ, Chang P, Kim TW, Williams M, Reddy PH, Tagle D, Boyce FM, Won L, Heller A, Aronin N, DiFiglia M: Mutant huntingtin expression in clonal striatal cells: dissociation of inclusion formation and neuronal survival by caspase inhibition. J Neurosci 1999;19:964–973.

8 Mende-Mueller LM, Toneff T, Hwang SR, Chesselet MF, Hook VY: Tissue-specific proteolysis of Huntingtin (htt) in human brain: evidence of enhanced levels of N- and C-terminal htt fragments in Huntington's disease striatum. J Neurosci 2001;21:1830–1837.

9 Toneff T, Mende-Mueller L, Wu Y, Hwang S-R, Bundey R, Thompson LM, Chesselet M-F, Hook V: Comparison of huntingtin proteolytic fragments in human lymphoblast cell lines and human brain. J Neurochem 2002;82:84–92.

10 Wellington CL, Ellerby LM, Gutekunst C-A, Rogers D, Warby S, Graham RK, Loubser O, van Raamsdonk J, Singaraja R, Yang Y-Z, Gafni J, Bredesen D, Hersch SM, Leavitt BR, Roy S, Nicholson DW, Hayden MR: Caspase cleavage of mutant huntingtin precedes neurodegeneration in Huntington's disease. J Neurosci 2002;22:7862–7872.

11 Bartzokis G, Lu PH, Tishler TA, Fong SM, Oluwadara B, Finn JP, Huang D, Bordelon Y, Mintz J, Perlman S: Myelin breakdown and iron changes in Huntington's disease: pathogenesis and treatment implications. Neurochem Res 2007;32:1655–1664.

12 Paulsen JS: Early detection of Huntington's disease. Future Neurol 2010;5:85–104.

13 Cattaneo E, Zuccato C, Tartari M: Normal huntingtin function: an alternative approach to Huntington's disease. Nat Rev Neurosci 2005;6:919–930.

14 Jimenez-Sanchez M, Licitra F, Underwood BR, Rubinsztein DC: Huntington's disease: mechanisms of pathogenesis and therapeutic strategies. Cold Spring Harb Perspect Med 2017;7:a024240.

15 Sbodio JI, Paul BD, Machamer CE, Snyder SH: Golgi protein ACBD3 mediates neurotoxicity associated with Huntington's disease. Cell Rep 2013;4:890–897.

16 Papalexi E, Persson A, Björkqvist M, Petersén A, Woodman B, Bates GP, Sundler F, Mulder H, Brundin P, Popovic N: Reduction of GnRH and infertility in the R6/2 mouse model of Huntington's disease. Eur J Neurosci 2005;22:1541–1546.

17 Van Raamsdonk JM, Pearson J, Murphy Z, Hayden MR, Leavitt BR: Wild-type huntingtin ameliorates striatal neuronal atrophy but does not prevent other abnormalities in the YAC128 mouse model of Huntington disease. BMC Neurosci 2006;7:80.

18 Van Raamsdonk JM, Murphy Z, Selva DM, Hamidizadeh R, Pearson J, Petersén A, Björkqvist M, Muir C, Mackenzie IR, Hammond GL, Vogl AW, Hayden MR, Leavitt BR: Testicular degeneration in Huntington disease. Neurobiol Dis 2007;26:512–520.

19 Stanek LM, Yang W, Angus S, Sardi PS, Hayden MR, Hung GH, Bennett CF, Cheng SH, Shihabuddin LS: Antisense oligonucleotide-mediated correction of transcriptional dysregulation is correlated with behavioral benefits in the YAC128 mouse model of Huntington's disease. J Huntingtons Dis 2013;2:217–228.

20 Stanek LM, Sardi SP, Mastis B, Richards AR, Treleaven CM, Taksir T, Misra K, Cheng SH, Shihabuddin LS: Silencing mutant huntingtin by adeno-associated virus-mediated RNA interference ameliorates disease manifestations in the YAC128 mouse model of Huntington's disease. Hum Gene Ther 2014;25:461–474.

21 Squitieri F, Di Pardo A, Favellato M, Amico E, Maglione V, Frati L: Pridopidine, a dopamine stabilizer, improves motor performance and shows neuroprotective effects in Huntington disease R6/2 mouse model. J Cell Mol Med 2015;19:2540–2548.
22 Yang D, Wang CE, Zhao B, Li W, Ouyang Z, Liu Z, Yang H, Fan P, O'Neill A, Gu W, Yi H, Li S, Lai L, Li XJ: Expression of Huntington's disease protein results in apoptotic neurons in the brains of cloned transgenic pigs. Hum Mol Genet 2010;19:3983–3994.
23 Uchida M, Shimatsu Y, Onoe K, Matsuyama N, Niki R, Ikeda JE, Imai H: Production of transgenic miniature pigs by pronuclear microinjection. Transgenic Res 2001;10:577–582.
24 Jacobsen JC, Bawden CS, Rudiger SR, McLaughlan CJ, Reid SJ, Waldvogel HJ, MacDonald ME, Gusella JF, Walker SK, Kelly JM, Webb GC, Faull RLM, Rees MI, Snell RG: An ovine transgenic Huntington's disease model. Hum Mol Genet 2010;19:1873–1882.
25 Baxa M, Hruska-Plochan M, Juhas S, Vodicka P, Pavlok A, Juhasova J, et al: A transgenic minipig model of Huntington's disease. J Huntingtons Dis 2013;2:47–68.
26 Macakova M, Bohuslavova B, Vochozkova P, Pavlok A, Sedlackova M, Vidinska D, et al: Mutated huntingtin causes testicular pathology in transgenic minipig boars. Neurodegener Dis 2016;16:245–259.
27 Jozefovičová M, Herynek V, Jírů F, Dezortová M, Juhásová J, Juhás Š, Klíma J, Bohuslavová B, Motlík J, Hájek M: 31P MR spectroscopy of the testes and immunohistochemical analysis of sperm of transgenic boars carried N-terminal part of human mutated Huntingtin. Česká Slov Neurol Neurochir 2015;78:28–33.
28 Krizova J, Stufkova H, Rodinova M, Macakova M, Bohuslavova B, Vidinska D, Klima J, Ellederova Z, Pavlok A, Howland DS, Zeman J, Motlik J, Hansikova H: Mitochondrial metabolism in a large-animal model of Huntington disease: the hunt for biomarkers in the spermatozoa of presymptomatic minipigs. Neurodegener Dis 2017;17:213–226.
29 Jozefovicova M, Herynek V, Jiru F, Dezortova M, Juhasova J, Juhas S, Motlik J, Hajek M: Minipig model of Huntington's disease: ^{1}H magnetic resonance spectroscopy of the brain. Physiol Res 2016;65:155–163.
30 Pokorny M, Juhas S, Juhasova J, Klima J, Motlik J, Klempir J, Havlik J: Telemetry physical activity monitoring in minipig's model of Huntington's disease. Česká Slov Neurol Neurochir 2015;78:39–42.
31 Dimauro I, Pearson T, Caporossi D, Jackson MJ: A simple protocol for the subcellular fractionation of skeletal muscle cells and tissue. BMC Res Notes 2012;5:513.
32 Saudou F, Humbert S: The biology of huntingtin. Neuron 2016;89:910–926.
33 Liu K-Y, Shyu Y-C, Barbaro BA, Lin Y-T, Chern Y, Thompson LM, James Shen C-K, Marsh JL: Disruption of the nuclear membrane by perinuclear inclusions of mutant huntingtin causes cell-cycle re-entry and striatal cell death in mouse and cell models of Huntington's disease. Hum Mol Genet 2015;24:1602–1616.
34 Velier J, Kim M, Schwarz C, Kim TW, Sapp E, Chase K, Aronin N, DiFiglia M: Wild-type and mutant huntingtins function in vesicle trafficking in the secretory and endocytic pathways. Exp Neurol 1998;152:34–40.
35 DiFiglia M, Sapp E, Chase K, Schwarz C, Meloni A, Young C, Martin E, Vonsattel JP, Carraway R, Reeves SA: Huntingtin is a cytoplasmic protein associated with vesicles in human and rat brain neurons. Neuron 1995;14:1075–1081.
36 Saudou F, Finkbeiner S, Devys D, Greenberg ME: Huntingtin acts in the nucleus to induce apoptosis but death does not correlate with the formation of intranuclear inclusions. Cell 1998;95:55–66.
37 Wanker EE, Scherzinger E, Heiser V, Sittler A, Eickhoff H, Lehrach H: Membrane filter assay for detection of amyloid-like polyglutamine-containing protein aggregates. Methods Enzymol 1999;309:375–386.
38 Schramke S, Schubert R, Frank F, Wirsig M, Fels M, Kemper N, Schuldenzucker V, Reilmann R: The Libechov minipig as a large animal model for preclinical research in Huntington's disease – thoughts and perspectives. Česká Slov Neurol Neurochir 2015;78:55–60.
39 Vodicka P, Smetana K, Dvoránková B, Emerick T, Xu YZ, Ourednik J, Ourednik V, Motlík J: The miniature pig as an animal model in biomedical research. Ann NY Acad Sci 2005;1049:161–171.
40 Jansen AHP, van Hal M, Op den Kelder IC, Meier RT, de Ruiter A-A, Schut MH, Smith DL, Grit C, Brouwer N, Kamphuis W, Boddeke HWGM, den Dunnen WFA, van Roon WMC, Bates GP, Hol EM, Reits EA: Frequency of nuclear mutant huntingtin inclusion formation in neurons and glia is cell-type-specific. Glia 2017;65:50–61.
41 Byers RK, Gilles FH, Fung C: Huntington's disease in children: neuropathologic study of four cases. Neurology 1973;23:561–569.
42 Graveland GA, Williams RS, DiFiglia M: Evidence for degenerative and regenerative changes in neostriatal spiny neurons in Huntington's disease. Science 1985;227:770–773.
43 Liddelow SA, Guttenplan KA, Clarke LE, Bennett FC, Bohlen CJ, Schirmer L, et al: Neurotoxic reactive astrocytes are induced by activated microglia. Nature 2017;541:481–487.
44 Valekova I, Jarkovska K, Kotrcova E, Bucci J, Ellederova Z, Juhas S, Motlik J, Gadher SJ, Kovarova H: Revelation of the IFNα, IL-10, IL-8 and IL-1β as promising biomarkers reflecting immuno-pathological mechanisms in porcine Huntington's disease model. J Neuroimmunol 2016;293:71–81.
45 Politis M, Lahiri N, Niccolini F, Su P, Wu K, Giannetti P, Scahill RI, Turkheimer FE, Tabrizi SJ, Piccini P: Increased central microglial activation associated with peripheral cytokine levels in premanifest Huntington's disease gene carriers. Neurobiol Dis 2015;83:115–121.
46 Teo RTY, Hong X, Yu-Taeger L, Huang Y, Tan LJ, Xie Y, To XV, Guo L, Rajendran R, Novati A, Calaminus C, Riess O, Hayden MR, Nguyen HP, Chuang K-H, Pouladi MA: Structural and molecular myelination deficits occur prior to neuronal loss in the YAC128 and BACHD models of Huntington disease. Hum Mol Genet 2016;25:ddw122.
47 Peferoen L, Kipp M, van der Valk P, van Noort JM, Amor S: Oligodendrocyte-microglia cross-talk in the central nervous system. Immunology 2014;141:302–313.

Paper IV

A transgenic minipig model of Huntington's disease shows early signs of behavioral and molecular pathologies.

Askeland, G., Rodinova, M., Štufková, H., Dosoudilova, Z., ***Baxa, M.****, Smatlikova, P., Bohuslavova, B., Klempir, J., Nguyen, T. D., Kuśnierczyk, A., Bjoras, M., Klungland, A., Hansikova, H., Ellederova, Z., and Eide, L. (2018).*

Disease Models & Mechanisms 11, dmm035949

IF 4.398

Motivation of the study

Data from both patients and HD mice models showed that the elongated CAG repetition in the mtHTT gene is genetically unstable, and gets prolonged in a tissue-specific manner with age. Studies from mouse models demonstrated that age-correlated tissue-dependent CAG mutagenesis is catalyzed by faulty DNA repair. Somatic mutagenesis contributes to the neurodegeneration as indicated in mice models of HD. Diminished genome integrity was observed in caudate region of post-mortem brains of HD patients. DNA repair factors impact the alteration of mitochondrial DNA (mtDNA) upon metabolic manipulations and mtDNA reflects modifications in mitochondrial metabolism. Mitochondrial changes were proved in HD patient´s samples. Mutant Htt could directly inhibit mitochondrial functions by triggering the oxidative stress. Signs of reduced mitochondrial activity were discovered in peripheral blood mononuclear cells (PBMC) of HD patients thus making them an easily obtainable material for studying HD progression using this biomarker.

Summary

We assessed DNA integrity, DNA repair, oxidative stress and mitochondrial capacity in basal ganglia, frontal cortex and peripheral blood mononuclear cells (PBMC) of 24-, 36- and 48-month-old TgHD minipigs. We did not detect any age-associated changes. Therefore, we decided to pool age groups for TgHD and WT animals in order to consider the potential impact of genotype.

The pooled samples showed no significant change in nuclear DNA damage. However, we observed reduced level of mtDNA damage, a tendency to more mtDNA mutations and increased mtDNA copy number in TgHD basal ganglia. Conversely, we detected decreased mtDNA copy number in TgHD frontal cortex. No alteration in PBMC was observed.

Since the reduction in mtDNA damage observed in TgHD basal ganglia could be an attribute of decreased mitochondrial activity and associated oxidative stress, we decided to figure out the status of oxidative stress using 8-oxoguanine (8-oxo-G) and malondialdehyde. Even if we observed a tendency to increased levels of 8-oxo-G in brain regions, the validation with malondialdehyde showed no significant difference. Thus, we did not prove an evidence of oxidative stress in TgHD brains up to 48 months of age. Since, the level of 8-oxo-G was remarkably increased in TgHD PBMC we assesd the level of 5-hydroxycytosine and detected no difference between TgHD and WT samples. Therefore, we supposed that the altered 8-oxo-G level is a consequence of an altered DNA repair activity in TgHD PBMCs.

We did not confirm changes in DNA repair activity in TgHD PBMCs, but we showed a potential defect in DNA repair of oxidative DNA damage in TgHD brain.

The evaluation of putative impact of mitochondrial perturbation indicated normal carbohydrate oxidation since there was no change in pyruvate dehydrogenase activity in TgHD brains. Moreover, similar citrate synthase activity indicated no impact of mtHtt on mitochondrial capacity in TgHD brains and PBMCs.

Next, we confirmed age-dependent elevation of expression levels of mtHtt in 24-, 36- and 48-month-old brains. The different situation was observed in expression of endogenous Htt which accumulated in age-dependent manner in frontal cortex of both TgHD and WT animals, but the levels of endogenous Htt significantly decreased in TgHD as well as in WT animals at the age of 48 months. Little or no mHtt fragments were expressed in PBMCs.

Lastly, we observed general tendency for reduced performance in tests monitoring potential behavioral, motor and cognitive changes at the age of 48 months.

In conclusion, we observed altered mtDNA integrity in TgHD brains but we did not prove the connection with oxidative stress or mitochondrial bionergetics. The different manifestation of mtDNA damage, frequency of mtDNA mutations and mtDNA copy number indicated different rate of mtHtt activity in basal ganglia and frontal cortex. This assumption was supported by the different expression levels of endogenous Htt in these two brain regions at the age of 48 months, what led to different ratios in mtHtt/Htt as the expression levels of mtHtt increased with age. 48-month-old TgHD animals showed decline in locomotor functions. Except of potential defect in DNA repair, we detected no changes in PBMCs, probably due to a minimal expression level of mtHtt in these cells.

My contribution

I participated on the experimental design for monitoring of behavioral, motor and cognitive changes. I conducted behavioral testing and processed the data obtained from tests used for assessing the behavior and motor and cognitive performance.

© 2018. Published by The Company of Biologists Ltd | Disease Models & Mechanisms (2018) 11, dmm035949. doi:10.1242/dmm.035949

RESEARCH ARTICLE

A transgenic minipig model of Huntington's disease shows early signs of behavioral and molecular pathologies

Georgina Askeland[1,2], Marie Rodinova[3], Hana Štufková[3], Zaneta Dosoudilova[3], Monika Baxa[3], Petra Smatlikova[4], Bozena Bohuslavova[4,5], Jiri Klempir[6], The Duong Nguyen[4,5], Anna Kuśnierczyk[7], Magnar Bjørås[2,7], Arne Klungland[2], Hana Hansikova[3], Zdenka Ellederova[4,*,‡] and Lars Eide[1,*,‡]

ABSTRACT

Huntington's disease (HD) is a monogenic, progressive, neurodegenerative disorder with currently no available treatment. The Libechov transgenic minipig model for HD (TgHD) displays neuroanatomical similarities to humans and exhibits slow disease progression, and is therefore more powerful than available mouse models for the development of therapy. The phenotypic characterization of this model is still ongoing, and it is essential to validate biomarkers to monitor disease progression and intervention. In this study, the behavioral phenotype (cognitive, motor and behavior) of the TgHD model was assessed, along with biomarkers for mitochondrial capacity, oxidative stress, DNA integrity and DNA repair at different ages (24, 36 and 48 months), and compared with age-matched controls. The TgHD minipigs showed progressive accumulation of the mutant huntingtin (mHTT) fragment in brain tissue and exhibited locomotor functional decline at 48 months. Interestingly, this neuropathology progressed without any significant age-dependent changes in any of the other biomarkers assessed. Rather, we observed genotype-specific effects on mitochondrial DNA (mtDNA) damage, mtDNA copy number, 8-oxoguanine DNA glycosylase activity and global level of the epigenetic marker 5-methylcytosine that we believe is indicative of a metabolic alteration that manifests in progressive neuropathology. Peripheral blood mononuclear cells (PBMCs) were relatively spared in the TgHD minipig, probably due to the lack of detectable mHTT. Our data demonstrate that neuropathology in the TgHD model has an age of onset of 48 months, and that oxidative damage and electron transport chain impairment represent later states of the disease that are not optimal for assessing interventions.

This article has an associated First Person interview with the first author of the paper.

KEY WORDS: Huntington's disease, Mitochondrial function, DNA damage, DNA repair, HD large animal model

INTRODUCTION

Huntington's disease (HD) is a devastating neurodegenerative disease for which there are currently no disease-modifying treatments. HD is inherited in an autosomal-dominant manner and caused by a trinucleotide CAG expansion in exon 1 of the huntingtin gene (*HTT*), resulting in the expression of mutant huntingtin (mHTT). It is clinically characterized by cognitive, psychiatric and motor dysfunctions, along with weight loss and muscle wasting. These symptoms stem from the characteristic striatal neurodegeneration, thought to be the neuropathological hallmark of the disease. The CAG repeat size negatively correlates with the age of onset of the disease and explains most of the variation in age at motor onset, with the remaining variance being currently unidentified genetic and environmental factors.

The *HTT* gene is essential for viability, and the CAG expansion mutation might cause neurodegeneration via a toxic effect of the mHTT protein, reduction of endogenous HTT function or a combination of both. Fragments of mHTT are identified in both patient brains and HD rodent models (Davies et al., 1997; DiFiglia et al., 1997) and fragmentation correlates with disease progression (Mende-Mueller et al., 2001). The fragments can be produced by proteolytic cleavage of the full-length mHTT or alternative splicing (Miller et al., 2010; Sathasivam et al., 2013).

A genetic hallmark of expanded CAG repeats is that they are able to spontaneously form hairpin structures that act as intermediate structures in somatic expansions. In mouse models, it has been demonstrated that faulty DNA repair catalyzes age-correlated CAG mutagenesis in a tissue-dependent manner (Jonson et al., 2013; Kovtun et al., 2007; Mollersen et al., 2012). Preliminary data from a mouse model of HD indicate that the somatic mutagenesis actually contributes to the neurodegeneration, possibly in a crosstalk mechanism between mismatch DNA repair and base excision DNA repair (Lai et al., 2016; Pinto et al., 2013).

The underlying mechanistic cause of HD progression by mHTT is still under investigation. As indicated above, DNA damage and repair is involved in somatic mutagenesis, and some studies have identified elevated levels of the oxidative DNA damage marker 8-oxoguanine (8-oxoG) in HD (Bogdanov et al., 2001; Long et al., 2012; Polidori et al., 1999), although we (Askeland et al., 2018) and others (Borowsky et al., 2013) could not confirm these findings in peripheral blood mononuclear cells (PBMCs) from HD patients.

[1]Department of Medical Biochemistry, Institute of Clinical Medicine, University of Oslo, 0372 Oslo, Norway. [2]Department of Microbiology, Oslo University Hospital, 0372 Oslo, Norway. [3]Department of Pediatrics and Adolescent Medicine, First Faculty of Medicine, Charles University in Prague and General University Hospital in Prague, Prague 12808, Czech Republic. [4]Laboratory of Cell Regeneration and Plasticity, Institute of Animal Physiology and Genetics, Czech Academy of Science, Libechov 27721, Czech Republic. [5]Department of Cell Biology, Faculty of Science, Charles University in Prague, Prague 12843, Czech Republic. [6]Department of Neurology and Centre of Clinical Neuroscience, First Faculty of Medicine, Charles University in Prague and General University Hospital in Prague, Prague 12821, Czech Republic. [7]Proteomics and Metabolomics Core Facility, PROMEC, Department of Clinical and Molecular Medicine, Norwegian University of Science and Technology, 7491 Trondheim, Norway.
*These authors contributed equally to this work

‡Authors for correspondence (ellederova@iapg.cas.cz; lars.eide@medisin.uio.no)

M.B., 0000-0002-5048-5857; J.K., 0000-0002-0735-7155; T.D.N., 0000-0001-9799-5785; M.B., 0000-0001-8759-1170; A.K., 0000-0001-7274-3661; H.H., 0000-0002-2734-225X; Z.E., 0000-0001-6695-6345; L.E., 0000-0003-3948-5183

Received 31 May 2018; Accepted 12 September 2018

It has been proposed that mHTT directly inhibits mitochondrial function by inducing oxidative stress and correlates with increasing CAG length (Hands et al., 2011). Postmortem striatum samples from advanced-stage HD patients showed reduced activity of complexes II, III and IV (Browne et al., 1997; Gu et al., 1996), while the R6/2 HD mouse model has shown reduced aconitase activity in the striatum and reduced complex IV activities in the striatum and cerebral cortex (Tabrizi et al., 2000). In a recent study, we discovered signs of reduced mitochondrial activity in PBMCs from HD patients, despite normal biochemical complex activities (Askeland et al., 2018).

Mouse models of HD, like the R6/2 model, have been used to test compounds that might be neuroprotective, such as the mitochondrial coenzyme Q10 (coQ10), especially in combination with remacemide (Ferrante et al., 2002). However, in follow-up clinical testing in HD patients, coQ10 failed to show a significant slowing of functional decline in early-stage HD patients, even at very high doses (Huntington Study Group, 2001; McGarry et al., 2017). Similarly, clinical trials for the use of creatine in early-stage HD patients also failed (Hersch et al., 2017), even though striking results were seen in the preclinical studies in R6/2 mice (Dedeoglu et al., 2003; Ferrante et al., 2000). This raises an important question of whether preclinical testing in current HD animal models can accurately reflect efficacy in humans. In addition, current biomarkers used in clinical trials are suboptimal owing to variability (Unified Huntington's Disease Rating Scale) or long response time MRI, and there is a particular need for reliable markers for pre-manifest HD. To accelerate the discovery of effective treatments for HD, a two-pronged approach might be needed, developing both better models and more accurate biomarkers.

In 2013, the Libechov transgenic minipig model for HD (TgHD) was first described (Baxa et al., 2013). A lentiviral approach was used to insert a truncated N-terminal fragment of exon 1 of human mHTT (1-548 amino acids). This was under the control of the human *HTT* promotor and contained 124 glutamines (CAGCAA repeats). This was the first transgenic HD pig model with successful germline transmission. The phenotype of the TgHD model is apparently mild. No aggregate formation is seen in brain tissue up to 16 months, and developmental or motor deficits are absent up to an age of 40 months (Baxa et al., 2013). However, levels of DARP32, a marker of medium spiny neurons (Gustafson et al., 1992), were reduced in the neostriatum at an age of 16 months. At 13 months, TgHD minipigs exhibited reduced fertility and lower sperm count, implying that a HD phenotype manifests prior to motor deficits. Characterization of the model is ongoing, as the original and subsequent generations of TgHD minipigs age, to provide a detailed description of the model. A battery of novel tests has recently been developed to assess the phenotype of the TgHD minipig model. These include a gait test, a hurdle test and a startbox back-and-forth test (Schramke et al., 2016). Effective preclinical testing in this model would be greatly promoted by a quantifiable and reliable phenotype.

We postulate that the TgHD pig model is a good representation of the human HD pathology, and that molecular parameters in this model are likely candidates to monitor disease progression and therapeutic interventions in humans. In order to test this hypothesis, we applied a repertoire of molecular and functional analyses to correlate with the HD phenotype and determined the age of onset.

RESULTS

The TgHD minipig model recapitulates behavioral abnormalities consistent with HD

A battery of novel behavioral tests designed for minipigs has been established (Schramke et al., 2016). Stance, gait and ability to cross a barrier were normal in F0 and F1 generations of TgHD minipigs up to 40 months of age, although fertility was affected (Baxa et al., 2013; Schuldenzucker et al., 2017). We investigated motor performance, cognitive performance and/or behavior deficit in 48-month-old minipigs and detected a significant decline in the ability to perform the tunnel test in the TgHD minipigs (Fig. 1, P=0.04). There was also a general tendency for reduced performance in the other tests (nonsignificant). Thus, these results showed the onset of locomotor/neurological impairment in the TgHD minipig model at the age of 48 months.

Genome integrity is affected in HD minipigs

We recently identified genome integrity as an early biomarker in peripheral PBMCs from HD patients (Askeland et al., 2018). The corresponding cells, in addition to brain regions from TgHD minipigs and their controls, were therefore assessed for DNA damage, mitochondrial copy number and DNA repair activity. Surprisingly, we did not identify any age-associated alterations in any of the parameters assessed (data not shown). In order to search for impact of the genotype, the different age groups were pooled for each genotype prior to reanalyses. The pooled samples revealed a reduced level of mitochondrial DNA (mtDNA) damage in the basal ganglia in TgHD minipigs, whereas the corresponding levels in the frontal cortex and in PBMCs were normal (Fig. 2A, P=0.01). Nuclear DNA (nDNA) damage was not significantly altered in any of the tested tissues in TgHD minipigs (Fig. 2B), thereby contrasting the situation seen in human PBMCs. We followed up on the level of mtDNA, and found lower mtDNA copy number in the frontal cortex in TgHD than in wild type (WT), but higher copy number in the basal ganglia in TgHD than in WT (Fig. 2C, P=0.04 and P=0.01, respectively). The differences in level and integrity of mtDNA in the basal ganglia might imply that mitophagy is disturbed in the basal ganglia of TgHD. We followed up on this point by assessing mtDNA mutation frequency. Although there was no indication of any altered mtDNA mutation frequency in PBMCs and cortex, there appeared to be a tendency to more mtDNA mutations in the basal ganglia in TgHD than in WT (Fig. 2D, nonsignificant), which could be an indication of ineffective mitophagy in the basal ganglia. 5-Methylcytosine [5-me(dC)] is a base modification that regulates gene regulation and global 5-me(dC) alters with differentiation, during development and with differences in aerobic activity. This epigenetic mark is found altered in untranslated regions in HD (Villar-Menéndez et al., 2013). When we assessed global 5-me(dC) levels in WT and TgHD minipigs, we found a modest, but significant, increase in the frontal cortex in TgHD minipigs (Fig. 2E, P=0.047), whereas PBMCs and basal ganglia displayed normal levels. 5-Hydroxymethylcytosine, another epigenetic marker, was not affected in TgHD minipigs (Fig. S2A). The different impact of mHTT on mtDNA copy number and mtDNA damage in the basal ganglia and cortex is indicative of the two brain regions being differentially affected. In contrast to the human situation, PBMCs were unaffected in the TgHD minipig.

Tissue-specific variations in level of and DNA repair capacity towards 8-oxoG in HD minipigs

The reduction in mtDNA damage observed in the basal ganglia of TgHD could be ascribed to reduced mitochondrial activity and associated oxidative stress. To assess the status of oxidative stress in the TgHD, we first measured the level of 8-oxoG, a frequently used marker of oxidative stress. There was a tendency towards increased 8-oxoG levels in all tissues, but this change was statistically significant only in PBMCs (Fig. 3A, P=0.03). We validated the

Disease Models & Mechanisms (2018) 11, dmm035949. doi:10.1242/dmm.035949

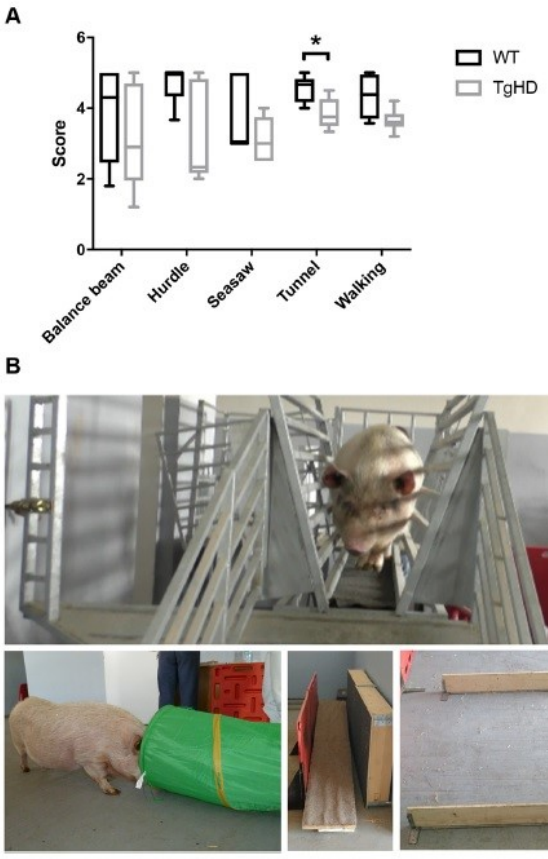

Fig. 1. The TgHD minipig model shows behavioral abnormalities consistent with early neurodegeneration. (A) Behavioral testing with tests specially designed for minipigs revealed a deficit in performing the tunnel test (P=0.04) and indications of a deficit in walking (nonsignificant). (B) Representative images (clockwise from top) of the balance beam, hurdle, seesaw and tunnel tests. Mann–Whitney test and two-way ANOVA, *P<0.05. Box plots and whiskers indicate minimum to maximum values, with hinges representing the 25th and 75th percentiles and the median indicated by the centerline. Sample size [female (F)+male (M)] distribution: balance beam, WT 4F+2M, TgHD 4F+2M; hurdle, WT 3F+2M, TgHD 4F+1M; seesaw, WT 3F+2M, TgHD 3F+2M; tunnel, WT 3F+2M, TgHD 4F+1M; walking, WT 4F+2M, TgHD 4F+2M.

results by assessing levels of malondialdehyde (MDA), another marker of oxidative stress that is produced by lipid peroxidation. We tested several brain subregions, but found no significant differences in the levels of MDA (Fig. 3B) and conclude that the TgHD minipigs do not show evidence of oxidative stress in the brain up to 48 months of age. We followed up on the increased level of 8-oxoG in PBMCs by measuring the level of another oxidized base lesion, 5-hydroxycytosine. Interestingly, whereas 5-hydroxycytosine levels varied greatly between PBMCs and the brain subregions, there was no significant difference between WT and TgHD minipigs (Fig. S2B). The elevated level of 8-oxoG is therefore indicative of an altered repair activity towards this lesion in TgHD PBMCs. The main source of 8-oxoG removal is by 8-oxoG DNA glycosylase activity. We assessed the DNA glycosylase activity against 8-oxoG in cell-free extracts and found significantly reduced levels in the frontal cortex (Fig. 3D, P=0.03), whereas PBMCs, as well as other brain regions, exhibited normal DNA glycosylase activities.

Unperturbed mitochondrial bioenergetics in HD minipigs

We recently identified mitochondrial aberrations in peripheral tissue from HD patients, including reduction of the subunit B of succinate dehydrogenase (SDHB) after onset of disease, which did not correlate with total functional score, an estimate for disease progression. To evaluate the putative impact of mitochondrial aberrations in the minipig model, we assessed mitochondrial parameters in TgHD and WT minipigs in two brain regions, and in PBMCs. First, pyruvate dehydrogenase (PDH) activity was unchanged in the frontal cortex and basal ganglia, indicating normal carbohydrate oxidation (Fig. 4B,D). Citrate synthase (CS) activity is a marker of mitochondrial volume, and was also similar between WT and TgHD minipigs in the two brain regions and PBMCs examined, indicating that mitochondrial capacity in the brain regions, as well as in PBMCs, is not affected in the TgHD model (Fig. 4B,D,E). These findings were consistent with the similar mitochondrial electron transport chain (ETC) complex activities in TgHD and WT in the basal ganglia, frontal cortex and PBMCs (Fig. 4A,C,E). To evaluate whether mitochondrial protein levels were altered, despite normal ETC activity, as in human HD PBMCs (Askeland et al., 2018), western blot analyses were performed but revealed normal expression levels in the frontal cortex and PBMCs in WT and TgHD minipigs (Fig. S3).

The tissue-specific changes in mtDNA copy number in TgHD minipigs combined with the similar CS activities (Figs 2C and 4) could be indicative of different genotype-specific mitochondrial composition. We followed up on this possibility by first comparing cytochrome c oxidase (COX) activity in isolated mitochondria with that in tissue homogenates (Fig. S4). The results did not imply any difference in COX activity in isolated mitochondria. We then assessed coupled activities of ETC complex I+II and II+III. As shown in Fig. S5, the coupled activities confirmed the data obtained by measuring the single complex activities (Fig. 4).

Disease Models & Mechanisms (2018) 11, dmm035949. doi:10.1242/dmm.035949

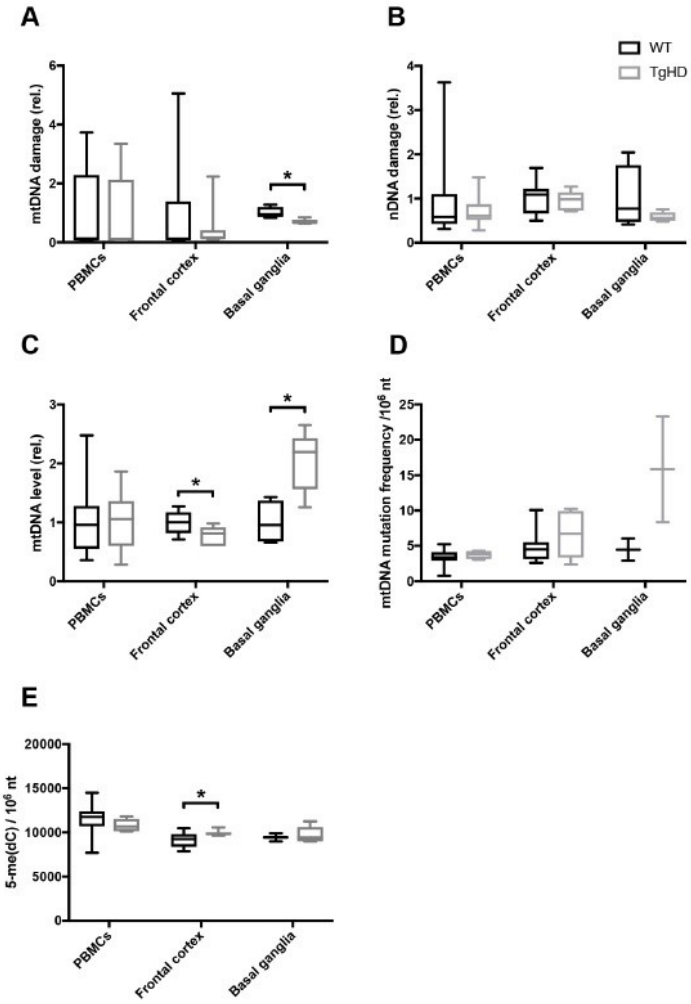

Fig. 2. Tissue-specific changes in genome integrity in the TgHD minipig model. (A) mtDNA damage analysis revealed lower damage levels in the basal ganglia in TgHD than in WT (P=0.01), but no changes in PBMCs or the frontal cortex. (B) nDNA damage analysis demonstrated that nDNA integrity is apparently unaffected in the TgHD model. (C) Quantification of mtDNA copy number shows a significant decrease in the frontal cortex (P=0.04) and, in contrast, an increase in the basal ganglia (P=0.01) in the TgHD minipigs, relative to WT. No differences were seen in PBMCs. (D) mtDNA mutation frequency analysis indicates higher levels in the basal ganglia in TgHD (nonsignificant) than in WT, but normal levels in PBMCs and the frontal cortex. (E) The methylation mark 5-me(dC) was increased in the frontal cortex in TgHD compared with WT (P=0.047). No differences in 5-me(dC) levels were seen in PBMCs or the basal ganglia. Student's t-test, *P<0.05. Box plots and whiskers indicate minimum to maximum values, with hinges representing the 25th and 75th percentiles and the median indicated by the centerline. Sample sizes: (A) basal ganglia, WT n=4, TgHD n=5; PBMCs, WT n=17, TgHD n=14; frontal cortex, WT n=10, TgHD n=7; (B) PBMCs, WT n=17, TgHD n=14; frontal cortex, WT n=10, TgHD n=7; basal ganglia, WT n=4, TgHD n=5; (C) frontal cortex, WT n=10, TgHD n=5; basal ganglia, WT n=4, TgHD n=5; PBMCs, WT n=17, TgHD n=13; (D) basal ganglia, WT n=2, TgHD n=2; PBMCs, WT n=7, TgHD n=4; frontal cortex, WT n=10, TgHD n=6; (E) frontal cortex, WT n=10, TgHD n=7; PBMCs, WT n=10, TgHD n=6; basal ganglia, WT n=2, TgHD n=5.

mHTT and HTT accumulate in an age- and tissue-specific manner in the TgHD minipig model

The results shown herein are indicative of subtle effects of the transgene on molecular biomarkers. To follow up on the putative impact of mHTT, we addressed the accumulation of mHTT and endogenous WT HTT protein in the tissues of interest. The transgene encoding the mHTT fragment was confirmed in the TgHD minipig, and was absent in WT minipigs (Fig. S1). As expected, in capillary electrophoresis, we observed a distinct peak representing 121 CAG/CAA repeats (Fig. S1B,C), which is different from the multiple peaks seen from repetitive CAG repeats that result in somatic expansions (Mollersen et al., 2012). To investigate the fate of endogenous HTT and transgene mHTT, we performed western blot analyses using specific antibodies against polyglutamine (PolyQ), mHTT and HTT. The N-terminal mHTT fragment accumulated with age in both the putamen and cortex (Fig. 5). The endogenous minipig HTT protein accumulated with age in the frontal cortex in both genotypes (Fig. 5A,B), but interestingly became depleted in the putamen at 48 months compared with 36 months (Fig. 5C,D). Importantly, the age-dependent accumulation of HTT was significantly different between TgHD and WT minipigs (ANOVA, P<0.001). Thus, the putamen from TgHD minipigs demonstrates a combination of reduced endogenous HTT protein with accumulation of mHTT fragment at the age of onset (48 months). PBMCs were recently shown to present important biomarkers for HD progression (Askeland et al., 2018). Cell-free extracts from PBMCs of minipigs at the affected age (48 months) were consequently analyzed for expression of mHTT. In contrast to human PBMCs, minipig TgHD PBMCs were found to express little or no mHTT fragments (Fig. 5E), thus explaining the relative inertness of these cells from the TgHD model.

In general, the relatively low impact of mHTT on the molecular parameters investigated so far is in coherence with the mild phenotype of the TgHD model. However, the most striking difference between human and the minipig model is the apparent lack of mHTT in TgHD PBMCs, which also makes PBMCs a less suitable biomaterial for studying disease progression in the TgHD model. Together, these results indicate that the mitochondrial

Disease Models & Mechanisms (2018) 11, dmm035949. doi:10.1242/dmm.035949

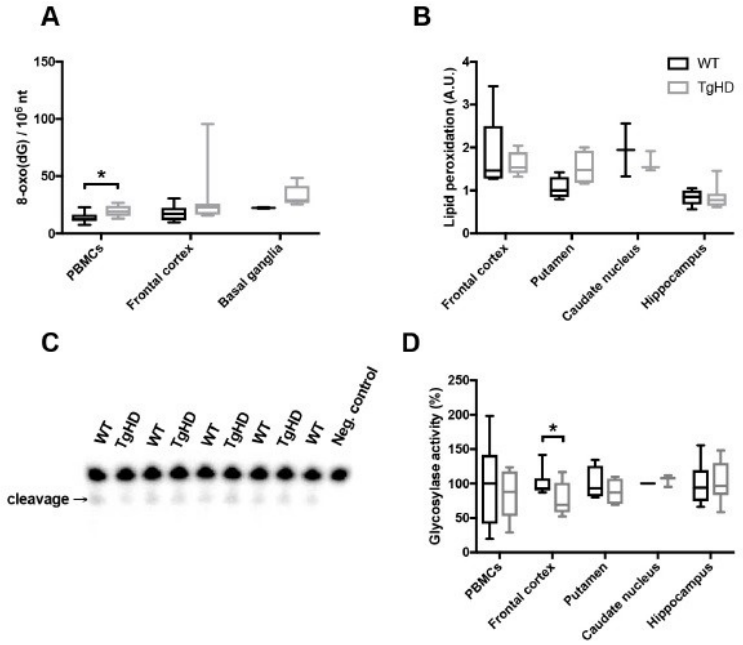

Fig. 3. Tissue-specific alterations in oxidative DNA damage and repair in TgHD minipigs. (A) Mass spectrometry analysis of the oxidative damage marker 8-oxoG [as nucleoside 8-oxo(dG)] showed increased levels of PBMCs in TgHD relative to WT (P=0.03), whereas the frontal cortex and basal ganglia displayed similar levels in the two genotypes. (B) The level of malondialdehyde (MDA) was determined in the specified brain subregions. No significant differences were found between WT and TgHD in any of the groups. Arbitrary units (A.U.) represent levels of MDA (μg), showing the extent of lipid peroxidation. (C) Representative image of the DNA glycosylase activity assay, showing incision of 8-oxoG containing ^{32}P-endlabeled oligonucleotide. Extracts were collected from individual animals. (D) DNA glycosylase activity toward 8-oxoG in nuclear protein extracts from PBMCs and different brain subregions. The analysis of substrate cleavage by DNA glycosylase enzyme OGG1 revealed reduced activity in the frontal cortex in TgHD (P=0.03), and indicates a defect in DNA repair of oxidative DNA damage. No genotype differences were seen in other brain regions. Data are presented as relative to the average of the WT activities. Student's t-test, *P<0.05. Box plots and whiskers indicate minimum to maximum values, with hinges representing the 25th and 75th percentiles and the median indicated by the centerline. Samples sizes: (A) PBMCs, WT n=10, TgHD n=6; frontal cortex, WT n=10, TgHD n=7; basal ganglia, WT n=2, TgHD n=5; (B) frontal cortex, WT n=9, TgHD n=9; putamen, WT n=4, TgHD n=4; caudate nucleus, WT n=2, TgHD n=3; hippocampus, WT n=7, TgHD n=7; (D) PBMCs, WT n=7, TgHD n=8; frontal cortex, WT n=9, TgHD n=10; putamen, WT n=4, TgHD n=4; caudate nucleus, WT n=2, TgHD n=3; hippocampus, WT n=7, TgHD n=8.

capacity in the TgHD minipig model is not affected in the tested tissues before the age of 48 months.

DISCUSSION

The TgHD minipig is a powerful HD model for use in intervention studies. Previous studies have demonstrated the toxic impact of mHTT protein on peripheral tissue and our study is the first to demonstrate neurological impairment, measured as decreased locomotor activity that initiates at an age of onset of 48 months. Hence, the TgHD minipig model could be an excellent model to capture and monitor biomarkers in response to interventions, in the pre-onset age up to 48 months.

The neurological phenotype in the TgHD model emerges subsequent to the reduced sperm count and motility (Macakova et al., 2016) in concordance with significantly diminished mitochondrial parameters (Krizova et al., 2017) and muscle ultrastructural alterations (M.R. and H.H., unpublished). The locomotor impairments that we identified here are partly in conflict with what was reported by Schuldenzucker and coworkers, who could not detect abnormal behavioral phenotype among female TgHD minipigs up to 48 months (Schuldenzucker et al., 2017). In our study, we did not investigate the impact of sex because of limited group size, but the change in the motor ability of TgHD boars compared with the WT controls appeared to be more pronounced than in TgHD sows compared with WT controls at the age of 48 months (data not shown), thereby providing a plausible explanation for the contradictory conclusions from the two studies. It should be noted, however, that the test repertoire was different in the two studies, except for the hurdle test, which in both studies did not show any statistical differences.

Prior to data analyses, we performed ANOVA to check for age association among the biomarkers for oxidative stress, DNA repair, genome integrity and mitochondrial function. We found no age association for any of these parameters and consequently pooled the samples into genotypes independent of age. It is a possibility that a larger cohort might indicate age-dependent effects for one or more of these parameters. However, currently the age correlation is too weak for these biomarkers to be used for monitoring. In contrast to the genomic and mitochondrial parameters, the expression of (m)HTT peptides in brain subregions varied with age. The N-terminal mHTT fragment accumulated strongly with increasing age in both the frontal cortex and basal ganglia, thus putatively exerting a toxic gain-of-effect in these brain subregions. The endogenous HTT protein displayed completely different tissue-dependent fates, in that the expression in the frontal cortex increased, whereas the expression in the basal ganglia became

Disease Models & Mechanisms (2018) 11, dmm035949. doi:10.1242/dmm.035949

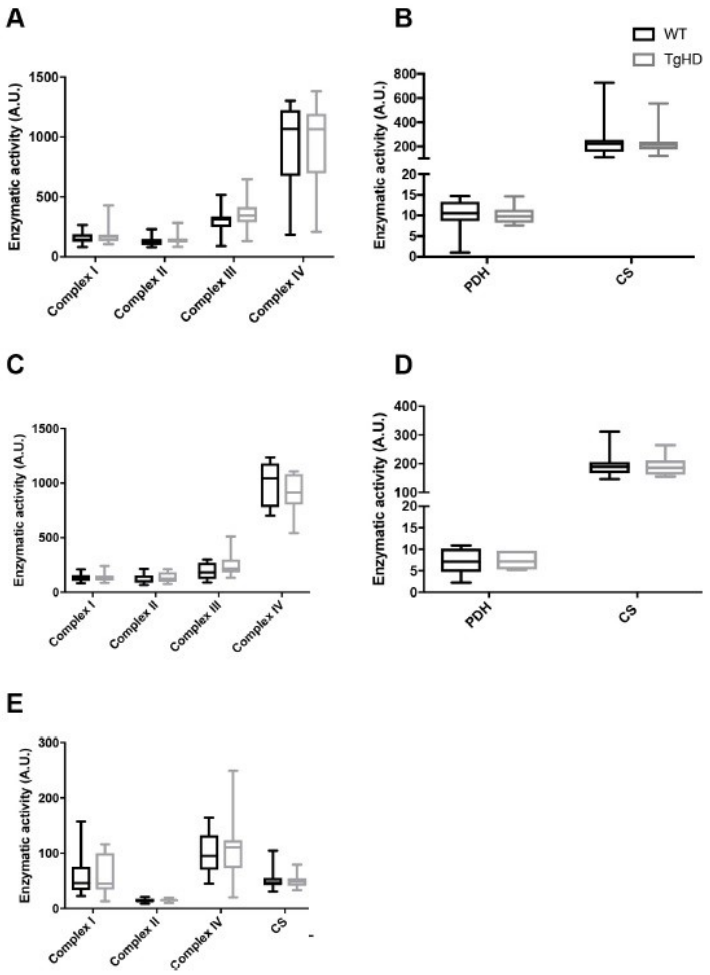

Fig. 4. Mitochondrial status in TgHD minipig brain subregions and PBMCs. (A,B) Mitochondrial ETC complexes I-IV (A), pyruvate dehydrogenase (PDH) and citrate synthase (CS) (B) all showed normal activity in TgHD compared with WT in the frontal cortex. (C,D) In the basal ganglia, mitochondrial ETC complexes I-IV (C), PDH and CS (D) all showed normal activity in TgHD compared with WT. (E) In addition, mitochondrial ETC complexes I, II and IV and CS showed normal activity in TgHD compared with WT in PBMCs. Arbitrary units (A.U.) represent enzymatic activity in nmol/min/mg. Student's *t*-test was used to assess significance. Box plots and whiskers indicate minimum to maximum values, with hinges representing the 25th and 75th percentiles and the median indicated by the centerline. Sample sizes: (A,B) frontal cortex: complex I, WT n=19, TgHD n=20; complex II, III and IV, all WT n=19, TgHD n=21; PDH, WT n=16, TgHD n=17; CS, WT n=19, TgHD n=21; (C,D) basal ganglia: complex I-IV, all WT n=10, TgHD n=9; PDH, WT n=9, TgHD n=7; CS, WT n=10, TgHD n=9; (E) PBMCs: complex I, II and IV and CS, all WT n=18, TgHD n=19.

reduced at 48 months relative to 36 months of age. Interestingly, two-way ANOVA revealed a significant genotype difference with respect to age-dependent expression. Thus, the neurological phenotype could potentially be attributed to increased accumulation of toxic N-terminal mHTT fragments, or decreased expression of endogenous HTT protein, or a combination of both. Although HTT is essential for life, conditional knockout of gene function in adulthood is more tolerable. Wang and co-workers investigated the effect of knocking out *Htt* at various ages in mice, and found no neurological phenotype, but tendency to develop pancreatitis only at a young age (Wang et al., 2016a). This implies that the age-associated decline in endogenous HTT in the putamen is not responsible for the neurological phenotype in TgHD minipigs.

The PBMCs were relatively spared in the TgHD model, in contrast to what we have recently found in PBMCs from human patients. Time-resolved Förster resonance energy transfer (TR-FRET) as well as mRNA quantification methods have been used to confirm the expression of HTT and mHTT in immune cells from human patients (Björkqvist et al., 2008; Weiss et al., 2012), as well as in this study (Fig. 5E). The analogous mHTT fragments were also detected in lymphoid cells from the R6/2 mouse model (Träger et al., 2015), as analyzed by the TR-FRET method. Thus, our results imply that the minipig is different from humans and rodents in that minipig PBMCs do not accumulate mHTT to significant levels. This finding is in line with previously reported low mHTT levels in spleen from the TgHD minipig (Baxa et al., 2013). Consequentially, other types of peripheral tissue should be considered for monitoring biomarkers during interventions. Although we could not confirm mHTT expression in PBMCs, the 8-oxoG levels were elevated. Because medium components influence genomic integrity, it cannot be excluded that the increased 8-oxoG in TgHD PBMCs relates to different metabolite composition in the serum, as is the case for human patients (Underwood et al., 2006).

The TgHD minipig model is unique in that the PolyQ peptide is not encoded by repetitive CAG repeats. PolyQ repeats with CAG interruptions have been shown to be stable *in vivo* (Choudhry et al., 2001; Pearson et al., 1998), and this is supported by our findings (Fig. S1C). Previously, a similar strategy was used to generate a murine HD model expressing a stable PolyQ peptide (Gray et al., 2008), and thereby demonstrated that somatic instability is not required for neuropathology. Despite that several DNA repair functions have been demonstrated to catalyze somatic expansions,

Disease Models & Mechanisms (2018) 11, dmm035949. doi:10.1242/dmm.035949

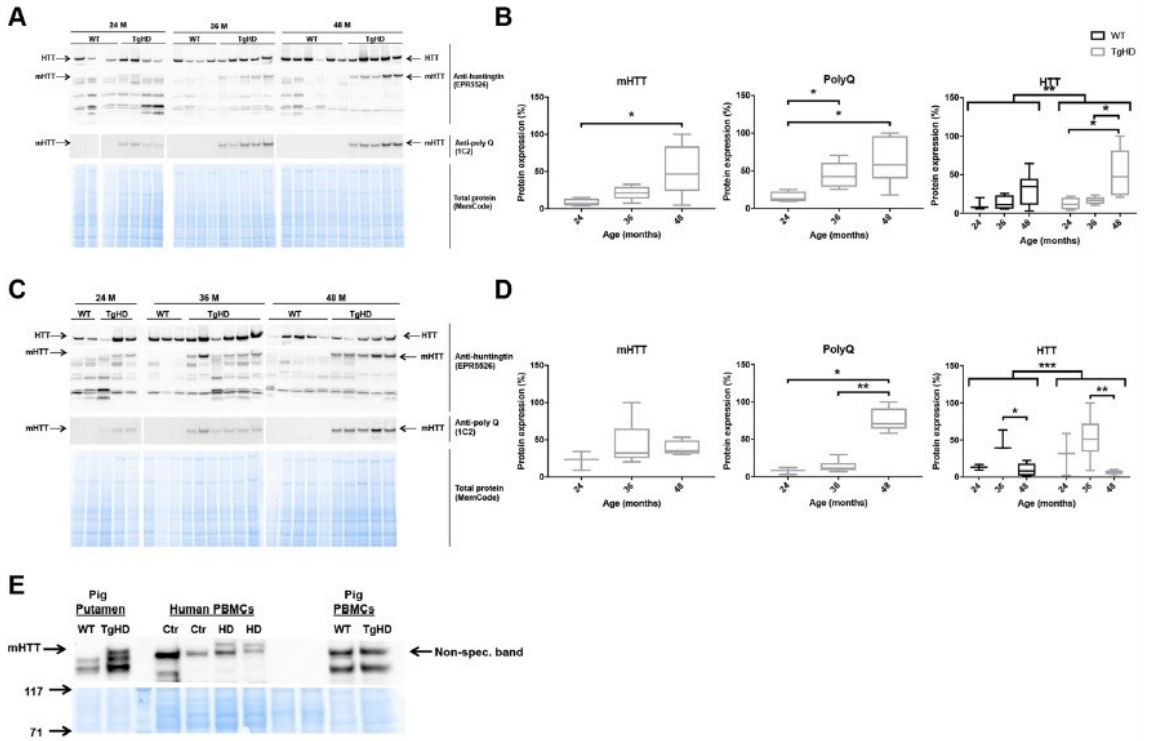

Fig. 5. TgHD minipig PBMCs do not express mHTT. (A-D) Western blot analyses of individual minipigs and subsequent quantification revealed that mHTT and endogenous HTT were expressed in a tissue- and age-specific manner in the frontal cortex (A,B) (mHTT: TgHD 24 vs 48 months, P=0.04; PolyQ: TgHD 24 vs 48 months, P=0.02; TgHD 24 vs 36 months, P=0.02; HTT: TgHD 24 vs 48 months, P=0.03; TgHD 36 vs 48 months, P=0.02; ANOVA WT vs TgHD, P=0.004) and putamen (C,D) (PolyQ: TgHD 24 vs 48 months, P=0.04; TgHD 36 vs 48 months, P=0.004; HTT: WT 36 vs 48 months, P=0.04; TgHD 36 vs 48 months, P=0.009; ANOVA WT vs TgHD, P=0.001) in TgHD minipigs, and confirmed the absence of mHTT and PolyQ in WT animals. (E) mHTT was not expressed in minipig TgHD PBMCs. Representative western blot of mHTT in PBMCs from HD patients (HD) and controls (Ctr), and PBMCs from WT and TgHD minipigs, as indicated. Three distinct antibodies were used to identify mHTT and PolyQ fragments and endogenous HTT protein (see Materials and Methods). Mann–Whitney test and ANOVA, *P<0.05, **P<0.01, ***P<0.001. Sample sizes: (A,B) mHTT and PolyQ: TgHD 24 months, n=4; TgHD 36 months, n=5; TgHD 48 months, n=6; HTT: WT 24 months, n=3; WT 36 months, n=4; WT 48 months, n=6; TgHD 24 months, n=4; TgHD 36 months, n=5; TgHD 48 months, n=5; (C,D) mHTT and PolyQ: TgHD 24 months, n=3; TgHD 36 months, n=6; TgHD 48 months, n=5; HTT: WT 24 months, n=2; 36 months, n=3; 48 months, n=5; TgHD 24 months, n=3; 36 months: n=6, 48 months, n=5.

reports of the corresponding disease phenotype of the mouse mutants lacking these functions are still awaited. However, a mitochondrial superoxide quencher was used to delay onset of pathophysiology with a parallel reduction in somatic expansions (Budworth et al., 2015). Whether the therapeutic effects are caused by reduced oxidative stress or dampened CAG expansions – or a combination of both – remains to be tested. Although we did not detect evidence of general elevation of oxidative stress in the TgHD model, mitochondrial superoxide might still underlie neuropathology. As an example, the mtDNA mutator mouse that dies prematurely was not found to generate increased oxidative stress. In general, however, more refined measurement of mitochondrial subcompartments *in vivo* did reveal increased production of peroxide with age in this mouse model (Logan et al., 2014; Trifunovic et al., 2005). We identified lower mtDNA damage in the basal ganglia of the TgHD model, which suggests that mitochondrial peroxide stress should be lower rather than higher. In a recent study, we found lower mtDNA damage in human HD patients than in controls, which we believe is indicative of reduced mitochondrial activity (Askeland et al., 2018) and could be attributed to a similar bioenergetics dysfunction in human HD patients and TgHD minipigs.

The mtDNA copy number was differentially affected by mHTT expression in the frontal cortex and basal ganglia. A reduction in mtDNA copy number has been found in grade 3 postmortem HD brains (Siddiqui et al., 2012) and thereby supports the finding in the frontal cortex, although different brain regions were not compared. The reason for the increased mtDNA copy number in the basal ganglia is less obvious. It is a possibility that mitochondrial morphology differences could underlie the mtDNA:CS variations. Although we did not detect ETC activity differences, more experiments are needed to investigate mitochondrial fragmentation in the affected tissue (frontal cortex and basal ganglia). Using (1)H magnetic resonance spectroscopy, evidence was found of altered energy metabolism at pre-onset age in the TgHD minipig (Jozefovicova et al., 2016). DNA repair capacity, mtDNA integrity and metabolism are interdependent (Yuzefovych et al., 2013); therefore, the subtle alterations in the two former parameters found here might be an indication of altered metabolism in the TgHD minipig.

It is worth noting that the methylation marker 5-me(dC) was significantly increased in the frontal cortex in TgHD compared with WT. This might be an indication of an altered methylation state, reflected in the transcriptional dysregulation seen in HD (Benn et al., 2008). Epigenetic modifications, including DNA methylation and histone methylation, have been found in HD patients and animal models and show the emerging role of epigenetics in HD (Ferrante et al., 2003; Lee et al., 2013; Ng et al., 2013).

In conclusion, our characterization of the TgHD minipig model up to 48 months of age reveals the age of neuropathological onset. Further follow-up as the animals age will be crucial to map the pathological process in this novel HD model. It is interesting to note that HD biomarkers found in rodent models – such as oxidative stress, DNA damage and mitochondrial activity – were largely unaffected, suggesting that extrapolating data from evolutionarily distant models should be done with care. These findings also demonstrate the complexity of the disease and a need for additional biomarkers than those assessed here to monitor disease progression at the preclinical stage in this model, and potentially also in human patients to investigate future interventions.

MATERIALS AND METHODS

Minipig material and sample collection

Transgenic minipigs (*Sus scrofa domesticus*, Linnaeus) with the N-terminal part of human mutated huntingtin and their WT siblings (Baxa et al., 2013) were bred and studied in agreement with the Animal Care and Use Committee of the Institute of Animal Physiology and Genetics, under the Czech regulations and guidelines for animal welfare and with the approval of the Czech Academy of Sciences (protocol number 53/2015). After weaning, all piglets were genotyped as previously described (Baxa et al., 2013). At 24, 36 and 48 months of age, a cohort of the TgHD and WT minipigs was perfused under deep anesthesia with ice-cold PBS. The brain tissue was dissected and subregions such as the basal ganglia and frontal cortex were isolated and stored at −80°C after snap freezing in liquid nitrogen. In addition, the peripheral blood was collected with heparin-coated syringes. Within 1-2 h after collection, the whole fraction of intact lymphocytes was isolated from EDTA-blood by density centrifugation at 25°C, using HistopaqueR1077 Hybri-Max™ (Sigma-Aldrich) following a standard protocol. Briefly, 6 ml blood was layered on top of 3 ml Histopaque and centrifuged at 800 ***g*** for 30 min at 25°C. The separated mononuclear band was carefully collected (~1 ml), resuspended in 10 ml PBS (137 mM NaCl, 2.7 mM KCl, 4.3 mM $Na_2HPO_4.12H_2O$, 1.5 mM KH_2PO_4) and centrifuged again at 800 ***g*** for 20 min. The pellet was washed twice in the same conditions. Finally, the dry pellet was stored at −80°C until use. For enzymatic protein and DNA analyses, samples from identical isolation of cells were used.

For isolation of the mitochondrial fraction, 5% homogenate (W/V) was prepared from the frozen tissue using Potter-Elvehjem homogenizer in KTEA medium (150 mM KCl, 50 mM Tris-HCl, 2 mM EDTA, pH 7.4, 0.2 µg/ml aprotininin) at 40°C. Mitochondria were sedimented by centrifugation of 600 g postnuclear supernatant at 10,000 ***g*** for 10 min at 4°C. The pellets were washed with KTEA medium and centrifuged again in the same conditions. Finally, the pellets were resuspended in KTEA medium to a protein concentration of ~20 mg/ml. Measurement of mitochondrial enzymes was performed immediately after isolation. For western blotting and measurements of PDH activity, frozen aliquots were used.

Human biomaterial

Use of human samples (PBMCs) was approved by the Ethical Committee of the General University Hospital in Prague [approved project COST LD15099 (2015-2017)] and the Czech-Norwegian Research Program (CZ09) 7F14308 (2014-2017). Written informed consent was obtained from patients as well as control subjects. The project was carried out in accordance with the principles expressed in the World Medical Association Declaration of Helsinki.

DNA isolation and analysis

Total DNA was isolated using the DNeasy Blood and Tissue kit (Qiagen) following the manufacturer's protocol with minor modifications. DNA purity and concentration was determined using a spectrophotometer (Epoch microplate spectrophotometer) and adjusted to correct concentrations for DNA integrity analysis (20 ng/µl for nDNA, 2 ng/µl for mtDNA). DNA integrity was assessed by the ability of a restriction enzyme to digest the DNA, using an in-house-developed quantitative PCR (qPCR)-based method as described previously (Wang et al., 2016b). Briefly, the DNA template was incubated with the *Taq*αI restriction enzyme, and primers flanking the *Taq*αI sites in the mtDNA and nDNA were subsequently used to amplify a PCR product. The ability to amplify across the restriction site is proportional to the amount of mtDNA and nDNA damage. Primer sequences are provided in Table S1.

CAG sizing was performed by PCR using primers (Table S1) with a fluorescent tag designed to flank the region of the CAG repeats. PCR products were run on a 1.2% agarose gel, and the resulting band was cut out and separated by capillary electrophoresis. The lengths of the PCR products were determined by fragment analysis on an Applied Biosystems 3130 Genetic Analyzer. Data analysis was performed by GeneMapper® software V2.6.4.

mtDNA copy number analysis was carried by qPCR amplification of a nuclear (*HBB*) and a mitochondrial (*MT-RNR1*) amplicon. Relative mtDNA content was calculated based on the ratio of mtDNA product over nuclear DNA products, using standard curves.

DNA base modifications were determined using liquid chromatography-mass spectrometry/mass spectrometry (LC-MS/MS) at the PROMEC proteomics and metabolomics core facility [Norwegian University of Science and Technology (NTNU), Trondheim], as described previously (Askeland et al., 2018).

The mutation frequency in mtDNA was determined as described previously (Wang et al., 2015). Briefly, total DNA was mixed with S1 nuclease (Qiagen; 10 U) for 15 min at 37°C and later digested using *Taq*αI restriction enzyme (New England Biolabs; 100 U, 65°C for 15 min). The resistant mutated *Taq*αI restriction sites were quantified by qPCR using the specific primers listed in Table S1. To ensure complete digestion, an additional *Taq*αI treatment (100 U; 65°C for 15 min) was performed on the digested DNA samples prior to qPCR. Mutation frequency was calculated as $(2\exp(CT^{TaqI}-CT^{NT})\times 4)^{-1}$ per nucleotide. Primer sequences are provided in Table S1.

Western blot analyses

Cell lysates of PBMC pellets were obtained using RIPA buffer (150 mM NaCl, 5 mM EDTA pH 8, 0.05% NP-40, 1% sodium deoxycholate, 0.1% SDS, 1% Triton X-100, 50 mM Tris-HCl pH 7.4, inhibitors of phosphatases and proteases) and protein concentration determined. Frozen tissues were homogenized in liquid nitrogen using a mortar and lysed in RIPA buffer, sonicated for 15 min at 0°C and centrifuged at 15,000 ***g*** for 15 min at 4°C. The concentration of protein was determined, and same amount of total protein was loaded onto a 3-8% Tris-acetate gel (EA03758, LifeTech). After electrophoresis, proteins were transferred to nitrocellulose membrane and stained with MemCode (LifeTech) to visualize total protein.

The membranes were blocked in blocking buffer and incubated with primary antibodies (see below) overnight at 4°C. Secondary detection was carried out with horseradish peroxidase (HRP)-conjugated secondary antibodies (see below). The antibody-bound proteins were visualized with the Super Signal West Femto Maximum Sensitivity Substrate (Thermo Fisher Scientific) using a Syngene Imaging System, and the intensity of the signal was quantified using Quantity One 1-D Analysis Software (Bio-Rad).

For huntingtin detection, anti-HTT antibody (EPR5526, Abcam, 1:2000) and anti-PolyQ (clone 5TF1-1C2, MAB1574, Millipore, 1:2000) were incubated overnight at 4°C. Corresponding secondary antibodies conjugated to HRP (anti-mouse, 711-035-152, Jackson ImmunoResearch, 1:10,000 or anti-rabbit, 711-035-152, Jackson ImmunoResearch, 1:10,000) were used. The signal was detected by chemiluminescence (ECL, 28980926, APCzech) and proteins were detected by a ChemiDoc XRS+System (Bio-Rad). MemCode (1858784, Thermo Fisher Scientific) total protein

staining was used for normalization of loading. For details of antibodies used in western blotting, see Table S2.

Mitochondrial enzyme activities

The activities of the respiratory chain complexes NADH:ubiquinone oxidoreductase (NQR, complex I), succinate:CoQ reductase (SQR, complex II), ubiquinol:cytochrome c oxidoreductase (QCCR, complex III), cytochrome c oxidase (COX, complex IV), NADH:cytochrome c reductase (NCCR, complex I+III), succinate:cytochrome c reductase (SCCR, complex II+III) were measured spectrophotometrically at 37°C in tissue homogenate and/or isolated mitochondria (Rustin et al., 1994) and CS according to Srere (1969). Protein concentration was measured according to Lowry et al. (1951). PDH activity was determined by measuring $^{14}CO_2$ production by decarboxylation from [1-14C]pyruvate according to Cahova et al. (2015). Analysis of respiratory chain complexes I, II, IV and CS in PBMCs has previously been described in detail (Askeland et al., 2018).

DNA repair activity

DNA glycosylase activity in cell-free nuclear protein extracts was performed as described previously (Klungland et al., 1999). Briefly, nuclear extracts were prepared by osmotic extraction, and 0.5-10 µg was added to a reaction mixture containing 50 mM MOPS pH7.5, 1 mM EDTA, 5% glycerol, 1 mM DTT and 1 fmol ^{32}P-endlabeled 8-oxoG-containing duplex and incubated for 2 h at 37°C. The reaction was terminated by addition of formamide/loading dye mixture, and denaturing at 85°C for 3 min. The incised product was separated from substrate oligonucleotide by electrophoresis on a 15% urea-PAGE gel. The gels were dried and subjected to phosphoimaging using a Typhoon 9410 Variable Mode Imager. The DNA glycosylase activity was calculated based on the ratio of incised oligonucleotide (product) over incised oligonucleotide+remaining substrate, and related to protein amount. The calculated activity was normalized to that of the average of controls, and presented with box plots displaying the 25th and 75th percentiles.

Lipid peroxidation assay

The lipid peroxidation assay was carried out using a TBARS assay kit (Cayman Chemical). Tissue homogenates were prepared from small amounts of tissue (~25 mg) using RIPA buffer. The assay was performed according to the manufacturer's protocol using fluorometric standards and a Wallac VICTOR2™ 1420 multilabel counter. The results were presented as MDA formed (A.U.), according to the manufacturer.

Motor control assessment

TgHD boars (n=2) and their WT controls (n=2) together with TgHD sows (n=4) and their WT controls (n=4) at 48 months of age were used for motor assessment. The animals were starved and a biscuit treat was used to stimulate the animals to perform the test. The following tests were performed: balance beam, hurdle, seesaw, gait and tunnel test.

The balance beam consisted of 2.5 m long inclined plane, 3.0 m long beam and extended plane (1.15×1.3 m). The animal is expected to step up to an inclined plane, cross the beam, turn back in the extended part and return back down. Scoring was as follows: 5 points for passing across the whole beam, turning in the extended part and going back down; 4 points for passing across the whole beam, not turning in the extended part and retreating; 3 points for stepping on (any part of) the beam; 2 points for stepping on the inclined plane with all four legs; 1 point for stepping on the inclined plane with two (fore)legs; 0 points if the animal refused to perform the test.

In the hurdle test, the animals were expected to pass the hurdle (height, 15 cm; width, 100 cm). Scoring was as follows: 5 points for passing across the hurdle without touching; 4 points for passing across the hurdle with touching of one leg; 3 points for passing across the hurdle with touching of two legs; 2 points for passing across the hurdle with touching of three legs; 1 point for passing across the hurdle with touching of four legs; 0 points if the animal refused to perform the test.

During the seesaw test, the pig was expected to pass over the seesaw (length, 3.0 m; width, 0.4 m). Scoring was as follows: 5 points for passing across the whole seesaw; 4 points for passing to the equilibrium position and retreating; 3 points for stepping onto and walking on the seesaw with all four legs (the equilibrium position is not reached); 2 points for stepping on the seesaw and retreating; 1 point for stepping on the seesaw with only two (fore)legs; 0 points if the animal refused to perform the test.

During the gait test, changes (difficulties) in walking were observed by walking the animal on a dry, straight floor. Scoring was as follows: 5 points for no visible gait problem and fluent walking; 4 points for slightly uneven weight bearing on one or more legs; 3 points for obvious deviation in weight bearing on one or more legs, with clear difficulties in walking; 2 points for lowering of hind quarters close to the ground, placement of hind legs under the body; 1 point for sliding the legs out of the symmetry; 0 points if the pig was unable to move and perform the test.

During the tunnel test, three biscuits were placed in different spots in the tunnel (diameter, 0.5 m; length, 1.5 m). The animal was expected to eat all the biscuits. Scoring was as follows: 5 points if three biscuits were eaten; 4 points if two biscuits were eaten; 3 points if only one biscuit was eaten; 2 points for entering the tunnel but not eating any biscuits; 1 point for showing no fear to enter but not entering the tunnel; 0 points if the animal refused to perform the test.

The tests were genotype blinded, meaning that the evaluators did not know the genotype of the animal.

Statistics

All statistics were carried out in GraphPad Prism. Calculation of statistical significance was performed using Student's t-test, Mann–Whitney or two-way ANOVA, as stated. We used the Holm–Sidak method for adjustment for multiple comparisons, where applicable.

Acknowledgements

Special thanks to Daniela Sedlackova and Suzana Knopova for technical support.

Competing interests

The authors declare no competing or financial interests.

Author contributions

Conceptualization: G.A., H.H., Z.E., L.E.; Methodology: G.A., M.R., Z.D., M. Baxa, P.S., B.B., J.K., T.D.N., A. Kusnierczyk, H.H., Z.E., L.E.; Validation: G.A., Z.D., P.S., H.H., Z.E., L.E.; Formal analysis: G.A., M.R., B.B., J.K., T.D.N.; Investigation: G.A., M.R., H.S., Z.D., M. Baxa, P.S., B.B., T.D.N., A. Kusnierczyk, Z.E.; Resources: M. Bjoras, Z.E.; Data curation: M.R., H.S., Z.D., M. Baxa, B.B., T.D.N., A. Kusnierczyk, M. Bjoras, H.H., L.E.; Writing - original draft: G.A., Z.E., L.E.; Writing - review & editing: A. Klungland, M. Bjoras, H.H., Z.E., L.E.; Supervision: J.K., H.H., Z.E., L.E.; Project administration: H.H., A. Klungland, Z.E., L.E.; Funding acquisition: A. Klungland, H.H., Z.E., L.E.

Funding

This work was funded by Norges Forskningsråd (MSMT-28477/2014) and Ministerstvo Školství, Mládeže a Tělovýchovy (COST LD15099 and LO1609), and by institutional research support from Univerzita Karlova v Praze (PROGRES Q26/LF1/3). The PROMEC proteomics and metabolomics core facility is supported by Helse Midt-Norge and Norges Teknisk-Naturvitenskapelige Universitet (NTNU; 46040500).

Supplementary information

Supplementary information available online at
http://dmm.biologists.org/lookup/doi/10.1242/dmm.035949.supplemental

References

Askeland, G., Dosoudilova, Z., Rodinova, M., Klempir, J., Liskova, I., Kuśnierczyk, A., Bjørås, M., Nesse, G., Klungland, A., Hansikova, H. et al. (2018). Increased nuclear DNA damage precedes mitochondrial dysfunction in peripheral blood mononuclear cells from Huntington's disease patients. *Sci. Rep.* **8**, 9817.

Baxa, M., Hruska-Plochan, M., Juhas, S., Vodicka, P., Pavlok, A., Juhasova, J., Miyanohara, A., Nejime, T., Klima, J., Macakova, M. et al. (2013). A transgenic minipig model of Huntington's Disease. *J. Huntingtons Dis.* **2**, 47-68.

Benn, C. L., Sun, T., Sadri-Vakili, G., McFarland, K. N., DiRocco, D. P., Yohrling, G. J., Clark, T. W., Bouzou, B. and Cha, J.-H. J. (2008). Huntingtin modulates transcription, occupies gene promoters in vivo, and binds directly to DNA in a polyglutamine-dependent manner. *J. Neurosci.* **28**, 10720-10733.

Björkqvist, M., Wild, E. J., Thiele, J., Silvestroni, A., Andre, R., Lahiri, N., Raibon, E., Lee, R. V., Benn, C. L., Soulet, D. et al. (2008). A novel pathogenic

pathway of immune activation detectable before clinical onset in Huntington's disease. *J. Exp. Med.* **205**, 1869-1877.
Bogdanov, M. B., Andreassen, O. A., Dedeoglu, A., Ferrante, R. J. and Beal, M. F. (2001). Increased oxidative damage to DNA in a transgenic mouse model of Huntington's disease. *J. Neurochem.* **79**, 1246-1249.
Borowsky, B., Warner, J., Leavitt, B. R., Tabrizi, S. J., Roos, R. A. C., Durr, A., Becker, C., Sampaio, C., Tobin, A. J. and Schulman, H. (2013). 8OHdG is not a biomarker for Huntington disease state or progression. *Neurology* **80**, 1934-1941.
Browne, S. E., Bowling, A. C., MacGarvey, U., Baik, M. J., Berger, S. C., Muquit, M. M. K., Bird, E. D. and Beal, M. F. (1997). Oxidative damage and metabolic dysfunction in Huntington's disease: selective vulnerability of the basal ganglia. *Ann. Neurol.* **41**, 646-653.
Budworth, H., Harris, F. R., Williams, P., Lee, D. Y., Holt, A., Pahnke, J., Szczesny, B., Acevedo-Torres, K., Ayala-Peña, S. and McMurray, C. T. (2015). Suppression of somatic expansion delays the onset of pathophysiology in a mouse model of Huntington's disease. *PLoS Genet.* **11**, e1005267.
Cahova, M., Chrastina, P., Hansikova, H., Drahota, Z., Trnovska, J., Skop, V., Spacilova, J., Malinska, H., Oliyarnyk, O., Papackova, Z. et al. (2015). Carnitine supplementation alleviates lipid metabolism derangements and protects against oxidative stress in non-obese hereditary hypertriglyceridemic rats. *Appl. Physiol. Nutr. Metab.* **40**, 280-291.
Choudhry, S., Mukerji, M., Srivastava, A. K., Jain, S. and Brahmachari, S. K. (2001). CAG repeat instability at SCA2 locus: anchoring CAA interruptions and linked single nucleotide polymorphisms. *Hum. Mol. Genet.* **10**, 2437-2446.
Davies, S. W., Turmaine, M., Cozens, B. A., DiFiglia, M., Sharp, A. H., Ross, C. A., Scherzinger, E., Wanker, E. E., Mangiarini, L. and Bates, G. P. (1997). Formation of neuronal intranuclear inclusions underlies the neurological dysfunction in mice transgenic for the HD mutation. *Cell* **90**, 537-548.
Dedeoglu, A., Kubilus, J. K., Yang, L., Ferrante, K. L., Hersch, S. M., Beal, M. F. and Ferrante, R. J. (2003). Creatine therapy provides neuroprotection after onset of clinical symptoms in Huntington's disease transgenic mice. *J. Neurochem.* **85**, 1359-1367.
DiFiglia, M., Sapp, E., Chase, K. O., Davies, S. W., Bates, G. P., Vonsattel, J. P. and Aronin, N. (1997). Aggregation of huntingtin in neuronal intranuclear inclusions and dystrophic neurites in brain. *Science* **277**, 1990-1993.
Ferrante, R. J., Andreassen, O. A., Jenkins, B. G., Dedeoglu, A., Kuemmerle, S., Kubilus, J. K., Kaddurah-Daouk, R., Hersch, S. M. and Beal, M. F. (2000). Neuroprotective effects of creatine in a transgenic mouse model of Huntington's disease. *J. Neurosci.* **20**, 4389-4397.
Ferrante, R. J., Andreassen, O. A., Dedeoglu, A., Ferrante, K. L., Jenkins, B. G., Hersch, S. M. and Beal, M. F. (2002). Therapeutic effects of coenzyme Q10 and remacemide in transgenic mouse models of Huntington's disease. *J. Neurosci.* **22**, 1592-1599.
Ferrante, R. J., Kubilus, J. K., Lee, J., Ryu, H., Beesen, A., Zucker, B., Smith, K., Kowall, N. W., Ratan, R. R., Luthi-Carter, R. et al. (2003). Histone deacetylase inhibition by sodium butyrate chemotherapy ameliorates the neurodegenerative phenotype in Huntington's disease mice. *J. Neurosci.* **23**, 9418-9427.
Gray, M., Shirasaki, D. I., Cepeda, C., Andre, V. M., Wilburn, B., Lu, X.-H., Tao, J., Yamazaki, I., Li, S.-H., Sun, Y. E. et al. (2008). Full-length human mutant huntingtin with a stable polyglutamine repeat can elicit progressive and selective neuropathogenesis in BACHD mice. *J. Neurosci.* **28**, 6182-6195.
Gu, M., Gash, M. T., Mann, V. M., Javoy-Agid, F., Cooper, J. M. and Schapira, A. H. V. (1996). Mitochondrial defect in Huntington's disease caudate nucleus. *Ann. Neurol.* **39**, 385-389.
Gustafson, E. L., Ehrlich, M. E., Trivedi, P. and Greengard, P. (1992). Developmental regulation of phosphoprotein gene expression in the caudate-putamen of rat: an in situ hybridization study. *Neuroscience* **51**, 65-75.
Hands, S., Sajjad, M. U., Newton, M. J. and Wyttenbach, A. (2011). In vitro and in vivo aggregation of a fragment of huntingtin protein directly causes free radical production. *J. Biol. Chem.* **286**, 44512-44520.
Hersch, S. M., Schifitto, G., Oakes, D., Bredlau, A.-L., Meyers, C. M., Nahin, R., Rosas, H. D. and Huntington Study Group CREST-E Investigators and Coordinators. (2017). The CREST-E study of creatine for Huntington disease: a randomized controlled trial. *Neurology* **89**, 594-601.
Huntington Study Group. (2001). A randomized, placebo-controlled trial of coenzyme Q10 and remacemide in Huntington's disease. *Neurology* **57**, 397-404.
Jonson, I., Ougland, R., Klungland, A. and Larsen, E. (2013). Oxidative stress causes DNA triplet expansion in Huntington's disease mouse embryonic stem cells. *Stem Cell Res.* **11**, 1264-1271.
Jozefovicova, M., Herynek, V., Jiru, F., Dezortova, M., Juhasova, J., Juhas, S., Motlik, J. and Hajek, M. (2016). Minipig model of Huntington's disease: (1)H magnetic resonance spectroscopy of the brain. *Physiol. Res.* **65**, 155-163.
Klungland, A., Rosewell, I., Hollenbach, S., Larsen, E., Daly, G., Epe, B., Seeberg, E., Lindahl, T. and Barnes, D. E. (1999). Accumulation of premutagenic DNA lesions in mice defective in removal of oxidative base damage. *Proc. Natl. Acad. Sci. USA* **96**, 13300-13305.
Kovtun, I. V., Liu, Y., Bjoras, M., Klungland, A., Wilson, S. H. and McMurray, C. T. (2007). OGG1 initiates age-dependent CAG trinucleotide expansion in somatic cells. *Nature* **447**, 447-452.
Krizova, J., Stufkova, H., Rodinova, M., Macakova, M., Bohuslavova, B., Vidinska, D., Klima, J., Ellederova, Z., Pavlok, A., Howland, D. S. et al. (2017). Mitochondrial metabolism in a large-animal model of Huntington disease: the hunt for biomarkers in the spermatozoa of Presymptomatic Minipigs. *Neurodegener. Dis.* **17**, 213-226.
Lai, Y., Budworth, H., Beaver, J. M., Chan, N. L. S., Zhang, Z., McMurray, C. T. and Liu, Y. (2016). Crosstalk between MSH2-MSH3 and polβ promotes trinucleotide repeat expansion during base excision repair. *Nat. Commun.* **7**, 12465.
Lee, J., Hwang, Y. J., Kim, K. Y., Kowall, N. W. and Ryu, H. (2013). Epigenetic mechanisms of neurodegeneration in Huntington's disease. *Neurotherapeutics* **10**, 664-676.
Logan, A., Shabalina, I. G., Prime, T. A., Rogatti, S., Kalinovich, A. V., Hartley, R. C., Budd, R. C., Cannon, B. and Murphy, M. P. (2014). In vivo levels of mitochondrial hydrogen peroxide increase with age in mtDNA mutator mice. *Aging Cell* **13**, 765-768.
Long, J. D., Matson, W. R., Juhl, A. R., Leavitt, B. R., Paulsen, J. S., PREDICT-HD Investigators and Coordinators of the Huntington Study Group. (2012). 8OHdG as a marker for Huntington disease progression. *Neurobiol. Dis.* **46**, 625-634.
Lowry, O. H., Rosebrough, N. J., Farr, A. L. and Randall, R. J. (1951). Protein measurement with the Folin phenol reagent. *J. Biol. Chem.* **193**, 265-275.
Macakova, M., Bohuslavova, B., Vochozkova, P., Pavlok, A., Sedlackova, M., Vidinska, D., Vochyanova, K., Liskova, I., Valekova, I., Baxa, M. et al. (2016). Mutated Huntingtin causes testicular pathology in transgenic minipig boars. *Neurodegener. Dis.* **16**, 245-259.
McGarry, A., McDermott, M., Kieburtz, K., de Blieck, E. A., Beal, F., Marder, K., Ross, C., Shoulson, I., Gilbert, P., Mallonee, W. M. et al. (2017). A randomized, double-blind, placebo-controlled trial of coenzyme Q10 in Huntington disease. *Neurology* **88**, 152-159.
Mende-Mueller, L. M., Toneff, T., Hwang, S.-R., Chesselet, M.-F. and Hook, V. Y. H. (2001). Tissue-specific proteolysis of Huntingtin (htt) in human brain: evidence of enhanced levels of N- and C-terminal htt fragments in Huntington's disease striatum. *J. Neurosci.* **21**, 1830-1837.
Miller, J. P., Holcomb, J., Al-Ramahi, I., de Haro, M., Gafni, J., Zhang, N., Kim, E., Sanhueza, M., Torcassi, C., Kwak, S. et al. (2010). Matrix metalloproteinases are modifiers of huntingtin proteolysis and toxicity in Huntington's disease. *Neuron* **67**, 199-212.
Mollersen, L., Rowe, A. D., Illuzzi, J. L., Hildrestrand, G. A., Gerhold, K. J., Tveteras, L., Bjolgerud, A., Wilson, D. M., III, Bjoras, M. and Klungland, A. (2012). Neil1 is a genetic modifier of somatic and germline CAG trinucleotide repeat instability in R6/1 mice. *Hum. Mol. Genet.* **21**, 4939-4947.
Ng, C. W., Yildirim, F., Yap, Y. S., Dalin, S., Matthews, B. J., Velez, P. J., Labadorf, A., Housman, D. E. and Fraenkel, E. (2013). Extensive changes in DNA methylation are associated with expression of mutant huntingtin. *Proc. Natl. Acad. Sci. USA* **110**, 2354-2359.
Pearson, C. E., Eichler, E. E., Lorenzetti, D., Kramer, S. F., Zoghbi, H. Y., Nelson, D. L. and Sinden, R. R. (1998). Interruptions in the triplet repeats of SCA1 and FRAXA reduce the propensity and complexity of slipped strand DNA (S-DNA) formation. *Biochemistry* **37**, 2701-2708.
Pinto, R. M., Dragileva, E., Kirby, A., Lloret, A., Lopez, E., St Claire, J., Panigrahi, G. B., Hou, C., Holloway, K., Gillis, T. et al. (2013). Mismatch repair genes Mlh1 and Mlh3 modify CAG instability in Huntington's disease mice: genome-wide and candidate approaches. *PLoS Genet.* **9**, e1003930.
Polidori, M. C., Mecocci, P., Browne, S. E., Senin, U. and Beal, M. F. (1999). Oxidative damage to mitochondrial DNA in Huntington's disease parietal cortex. *Neurosci. Lett.* **272**, 53-56.
Rustin, P., Chretien, D., Bourgeron, T., Gérard, B., Rötig, A., Saudubray, J. M. and Munnich, A. (1994). Biochemical and molecular investigations in respiratory chain deficiencies. *Clin. Chim. Acta* **228**, 35-51.
Sathasivam, K., Neueder, A., Gipson, T. A., Landles, C., Benjamin, A. C., Bondulich, M. K., Smith, D. L., Faull, R. L. M., Roos, R. A. C., Howland, D. et al. (2013). Aberrant splicing of HTT generates the pathogenic exon 1 protein in Huntington disease. *Proc. Natl. Acad. Sci. USA* **110**, 2366-2370.
Schramke, S., Schuldenzucker, V., Schubert, R., Frank, F., Wirsig, M., Ott, S., Motlik, J., Fels, M., Kemper, N., Hölzner, E. et al. (2016). Behavioral phenotyping of minipigs transgenic for the Huntington gene. *J. Neurosci. Methods* **265**, 34-45.
Schuldenzucker, V., Schubert, R., Muratori, L. M., Freisfeld, F., Rieke, L., Matheis, T., Schramke, S., Motlik, J., Kemper, N., Radespiel, U. et al. (2017). Behavioral testing of minipigs transgenic for the Huntington gene-A three-year observational study. *PLoS ONE* **12**, e0185970.
Siddiqui, A., Rivera-Sánchez, S., Castro, M. R., Acevedo-Torres, K., Rane, A., Torres-Ramos, C. A., Nicholls, D. G., Andersen, J. K. and Ayala-Torres, S. (2012). Mitochondrial DNA damage is associated with reduced mitochondrial bioenergetics in Huntington's disease. *Free Radic. Biol. Med.* **53**, 1478-1488.
Srere, P. A. (1969). Citrate synthase: [EC 4.1.3.7. Citrate oxaloacetate-lyase (CoA-acetylating)]. *Methods Enzymol.* **13**, 3-11.

Tabrizi, S. J., Workman, J., Hart, P. E., Mangiarini, L., Mahal, A., Bates, G., Cooper, J. M. and Schapira, A. H. V. (2000). Mitochondrial dysfunction and free radical damage in the Huntington R6/2 transgenic mouse. *Ann. Neurol.* **47**, 80-86.

Träger, U., Andre, R., Magnusson-Lind, A., Miller, J. R. C., Connolly, C., Weiss, A., Grueninger, S., Silajdžić, E., Smith, D. L., Leavitt, B. R. et al. (2015). Characterisation of immune cell function in fragment and full-length Huntington's disease mouse models. *Neurobiol. Dis.* **73**, 388-398.

Trifunovic, A., Hansson, A., Wredenberg, A., Rovio, A. T., Dufour, E., Khvorostov, I., Spelbrink, J. N., Wibom, R., Jacobs, H. T. and Larsson, N.-G. (2005). Somatic mtDNA mutations cause aging phenotypes without affecting reactive oxygen species production. *Proc. Natl. Acad. Sci. USA* **102**, 17993-17998.

Underwood, B. R., Broadhurst, D., Dunn, W. B., Ellis, D. I., Michell, A. W., Vacher, C., Mosedale, D. E., Kell, D. B., Barker, R. A., Grainger, D. J. et al. (2006). Huntington disease patients and transgenic mice have similar pro-catabolic serum metabolite profiles. *Brain* **129**, 877-886.

Villar-Menéndez, I., Blanch, M., Tyebji, S., Pereira-Veiga, T., Albasanz, J. L., Martín, M., Ferrer, I., Pérez-Navarro, E. and Barrachina, M. (2013). Increased 5-methylcytosine and decreased 5-hydroxymethylcytosine levels are associated with reduced striatal A2AR levels in Huntington's disease. *Neuromolecular Med.* **15**, 295-309.

Wang, W., Esbensen, Y., Scheffler, K. and Eide, L. (2015). Analysis of mitochondrial DNA and RNA integrity by a real-time qPCR-based method. *Methods Mol. Biol.* **1264**, 97-106.

Wang, G., Liu, X., Gaertig, M. A., Li, S. and Li, X.-J. (2016a). Ablation of huntingtin in adult neurons is nondeleterious but its depletion in young mice causes acute pancreatitis. *Proc. Natl. Acad. Sci. USA* **113**, 3359-3364.

Wang, W., Scheffler, K., Esbensen, Y. and Eide, L. (2016b). Quantification of DNA damage by real-time qPCR. *Methods Mol. Biol.* **1351**, 27-32.

Weiss, A., Träger, U., Wild, E. J., Grueninger, S., Farmer, R., Landles, C., Scahill, R. I., Lahiri, N., Haider, S., Macdonald, D. et al. (2012). Mutant huntingtin fragmentation in immune cells tracks Huntington's disease progression. *J. Clin. Invest.* **122**, 3731-3736.

Yuzefovych, L. V., Schuler, A. M., Chen, J., Alvarez, D. F., Eide, L., Ledoux, S. P., Wilson, G. L. and Rachek, L. I. (2013). Alteration of mitochondrial function and insulin sensitivity in primary mouse skeletal muscle cells isolated from transgenic and knockout mice: role of ogg1. *Endocrinology* **154**, 2640-2649.

Table S1. Primer sequences used in this study.

Loci	Forward	Reverse	Purpose
HBB	CTCCTGGGCAACGTGATAGT	GGTTCAGAGGAAAAAGGGCTCCTCCT	Copy number
HTT	ATGAAGGCCTTCGAGTCCCTCAAGTCCTTC	CGGCGGCGGTGGCGGTTGCTGTTGCTGCTG	CAG sizing
MT-RNR1	TCGCAACTGCCTAAAACTCA	GAATTGGCAAGGGTTGGTAA	mtDNA damage/copy number/mutation frequency
NDUFA9	GTTGTGAATGGTGCTAACTGCT	ACCAGAGACAATAAAGCAGAGGAG	nDNA damage

The table shows sequences of primers used for various experimental methods as indicated in right column.

Table S2. Information about antibodies used in supplementary western blotting (Fig.S3)

Target	Name	Manufacturer	Catalogue no.	Species raised in	Dilution
PDH E1α, PDH E1β, PDH E2, PDH E2/E3bp, OSCP	PDH antibody cocktail	Mitosciences	MSP02	Mouse	1:2000
	Complex III subunit Core 2 monoclonal antibody	Mitosciences	MS304	Mouse	1:10000
NDUFA9	Anti-NDUFA9 antibody [20C11B11B11]	Abcam	ab14713	Mouse	1:3000
SDH70	Anti-SDHA antibody [2E3GC12FB2AE2]	Abcam	ab14715	Mouse	1:5000
SDH30	Complex II subunit 30 kDa	Mitosciences	MS203		1:2000
CORE1	Anti-Ubiquinol-Cytochrome C Reductase Core Protein I antibody [16D10AD9AH5]	Abcam	ab110252	Mouse	1:5000
COX1	Anti-MTCO1 antibody [1D6E1A8]	Abcam	ab14705	Mouse	1:2000
COX5A	Anti-COX5A antibody [6E9B12D5]	Abcam	ab110262	Mouse	1:2000
ATPA	Anti-ATP5A antibody [7H10BD4F9]	Abcam	ab110273	Mouse	1:1000
Mitofilin	Anti-Mitofilin antibody [2E4AD5] - Mitochondrial Marker	Abcam	ab110329	Mouse	1:1000
Aconitase	Anti-Aconitase 2 antibody [6F12BD9]	Abcam	ab110321	Mouse	1:2000
OPA1	Purified Mouse Anti-OPA1 Clone 18/OPA1	BD Biosciences	612606	Mouse	1:2000
Porin	Anti-VDAC1 / Porin antibody [20B12AF2]		ab14734	Mouse	1:2000
ATPβ	Anti-ATPB antibody [3D5] - Mitochondrial Marker	Abcam	ab14730	Mouse	1:1000
COX2	Anti-MTCO2 antibody [12C4F12]	Abcam	ab110258	Mouse	1:10000
CS	Anti-Citrate synthetase antibody [2H8BB6]	Abcam	ab128564	Mouse	1:2500
GAPDH	Anti-GAPDH antibody [6C5]	Abcam	ab8245	Mouse	1:3333
MRPS31	Anti-MRPS31 antibody [EPR10707]	Abcam	ab167406	Rabbit	1:3333
Anti-rabbit IgG	Anti-Rabbit IgG (whole molecule)–Peroxidase antibody produced in goat	Sigma-Aldrich	*A0545*	Goat	1:2500
Anti-mouse IgG	Anti-Mouse IgG (whole molecule)–Peroxidase antibody produced in goat	Sigma-Aldrich	*A8924*	Goat	1:2500

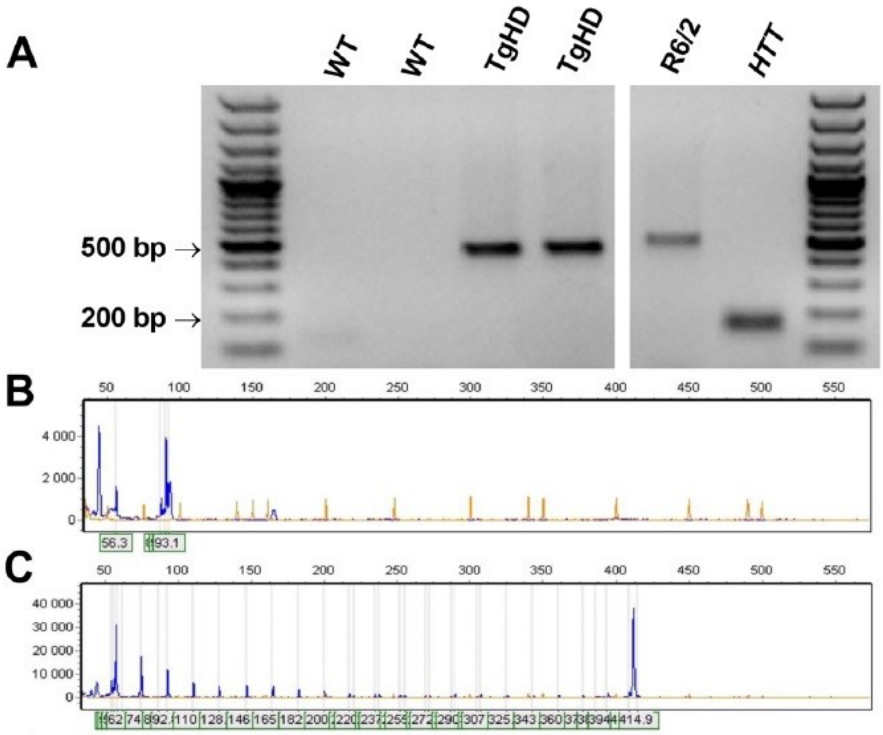

Fig. S1. Validation of TgHD minipig model. (A) PCR-mediated genotyping of the TgHD model transgene. Electrophoretic separation of PCR products made using *HTT* specific primers confirmed the presence of the expanded CAG repeat in TgHD minipigs. (B) Size determination of CAG repeat tracts. Capilliary electrophoresis and fragment analysis using size standards (yellow) and GeneMapper® software confirmed the absence of polyQ *mHTT* in WT minipigs (C) and showed presence of *mHTT* with ~121 CAG repeats in TgHD minipigs. Representative samples shown.

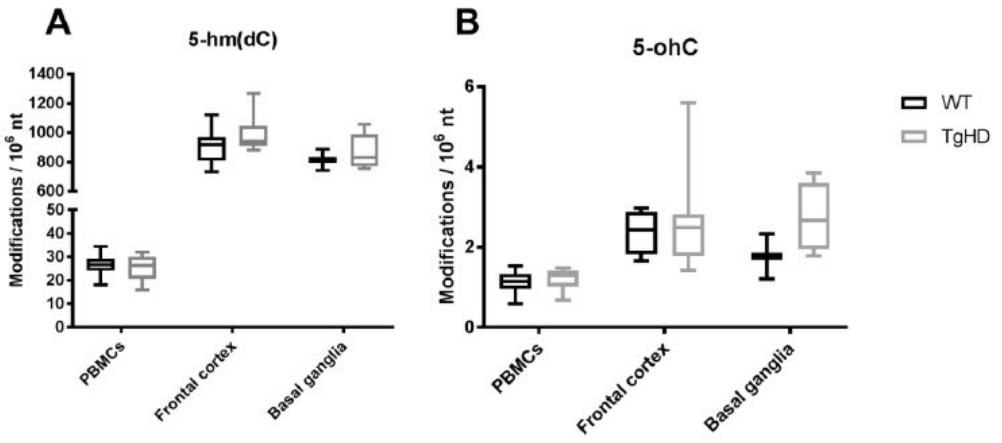

Fig. S2. Base modifications in the TgHD minipig model. LC-/MS/MS analysis of DNA showed normal levels of 5-hm(dC) and 5-ohC in all tissues (A, B). Student's t-test. Box plot whiskers indicate minimum to maximum values, with hinges representing the 25th and 75th percentile and median indicated by the center line. Sample sizes: PBMCs: WT n=10, TgHD n=6; frontal cortex: WT n=10, TgHD n=7; basal ganglia: WT n=2, TgHD n=5.

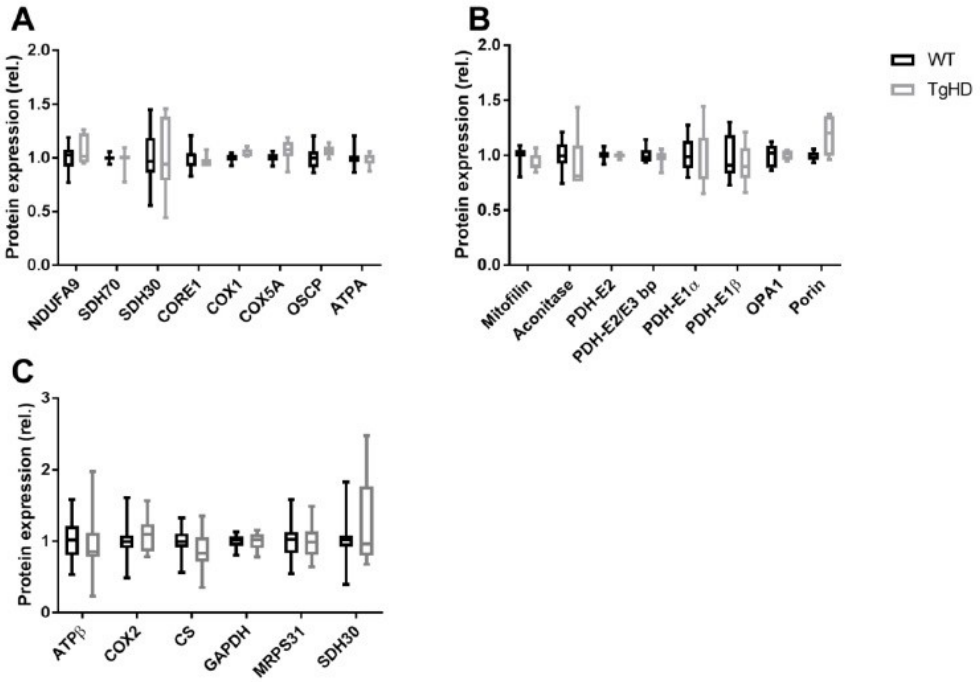

Fig. S3. Mitochondria-related protein expression in the TgHD minipig model. Western analysis showed normal levels of mitochondria associated proteins in frontal cortex (A,B) and PBMCs (C). Box plot whiskers indicate minimum to maximum values, with hinges representing the 25th and 75th percentile and median indicated by the center line. Student's t-test, adjusted for multiple comparisons using the Holm-Sidak method. Sample sizes: Frontal cortex: WT n=9, TgHD n=7, except OPA1 and Porin WT n=6, TgHD n=4; PBMCs: WT n=13, TgHD n=13, except CS WT n=13, TgHD n=12, MRPS31 WT n=11, TgHD n=12, SDH30 WT n=13, TgHD n=12.

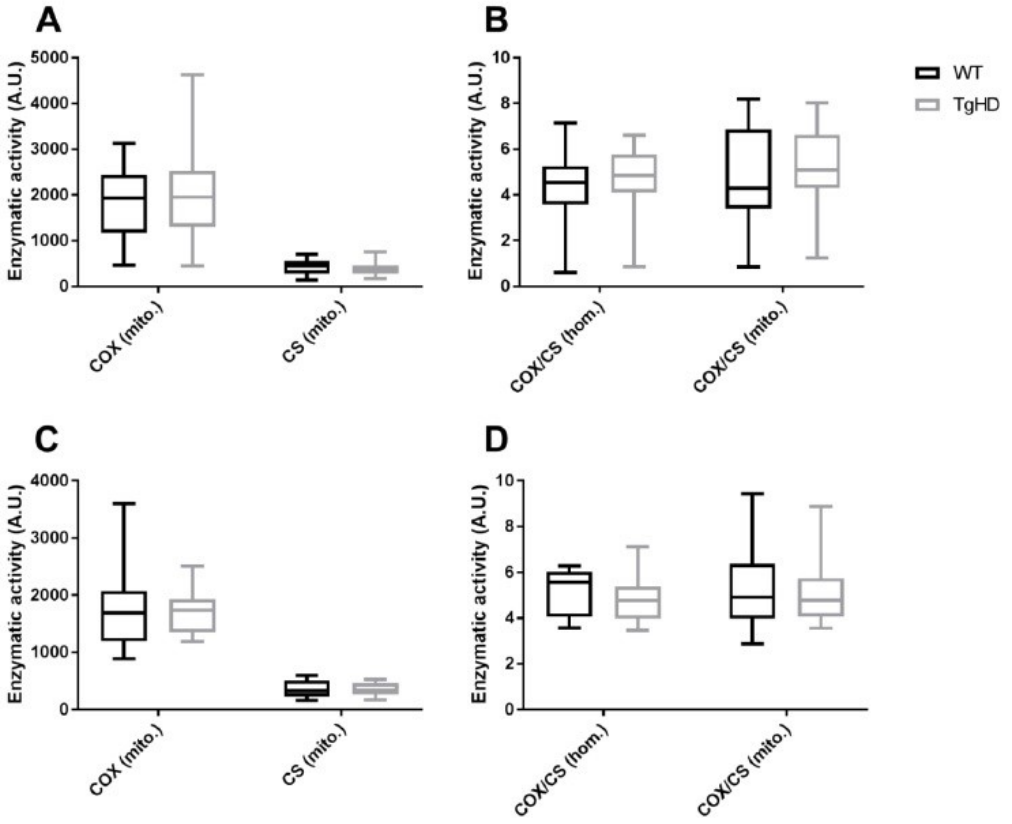

Fig. S4. Cytochrome c oxidase (COX) and citrate synthase (CS) activity in homogenates and isolated mitochondria from TgHD minipig brain. COX and CS activity unchanged in mitochondrial isolates in frontal cortex (A) and after normalizing to CS (B). COX and CS activity unchanged in mitochondrial isolates in basal ganglia (C) and after normalizing to CS (D). Arbitrary units (A.U.) represent enzymatic activity as nmol/min/mg. Student's t-test. Box plot whiskers indicate minimum to maximum values, with hinges representing the 25th and 75th percentile and median indicated by the center line. Sample sizes: Frontal cortex: COX (mito.) WT n=19, TgHD n=21, CS (mito.) WT n=19, TgHD n=21, COX/CS (hom.) WT n=19, TgHD n=21, COX/CS (mito.) WT n=19, TgHD n=21; basal ganglia: COX (mito.) WT n=10, TgHD n=9, CS (mito.) WT n=10, TgHD n=9, COX/CS (hom.) WT n=10, TgHD n=9, COX/CS (mito.) WT n=10, TgHD n=9. «mito": isolated mitochondria; "hom": homogenate.

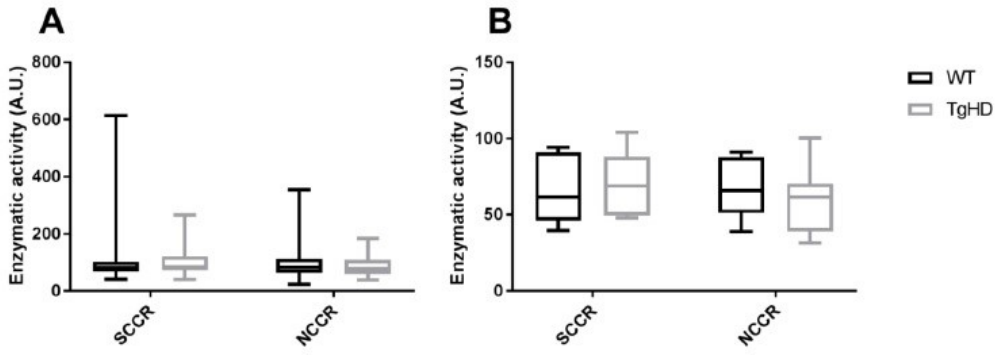

Fig. S5. Coupled activity of mitochondrial complex II+III and I+III in TgHD minipig model brain. SCCR activity (II+III) and NCCR activity (I+III) in frontal cortex (A) and basal ganglia (B) showed normal levels compared to WT animals. Arbitrary units (A.U.) represent enzymatic activity as nmol/min/mg. Student's t-test. Box plot whiskers indicate minimum to maximum values, with hinges representing the 25th and 75th percentile and median indicated by the center line. Sample sizes: Frontal cortex: SCCR WT n=19, TgHD n=21, NCCR WT n=19, TgHD n=21; basal ganglia: SCCR WT n=10, TgHD n=9, NCCR WT n=10, TgHD n=9. SCCR- succinate cytochrome c oxidase, NCCR- rotenone sensitive NADH cytochrome c oxidase.

Paper V

Transgenic minipig model of Huntington's disease exhibiting gradually progressing neurodegeneration.

*Ardan, T., **Baxa, M.,** Levinska, B., Sedlackova, M., Nguyen, T.D., Klima, J., Juhas, S., Juhasova, J., Smatlikova, P., Vochozkova, P., Motlik, J., and Ellederova, Z.*

Submitted in Disease Models & Mechanisms; MS ID#: DMM/2019/041319

IF 4.398

Motivation of the study

Misfolded mtHtt undergoes disease-specific enhanced proteolysis leading to mtHtt fragmentation. Soluble mtHtt monomers, N-terminal fragments incurred by proteolysis and mtHtt oligomers inchmeal form aggregates which are one of the main characteristics of the brains of HD affected individuals. Inclusions associated with axonal degeneration were confirmed in axons in HD mice. Mostly vulnerable and lost are medium-sized spiny neurons in striatum and the pyramidal cells in the cortex. Moreover, activated microglial cells and demyelination are associated with HD. Activated microglia induce the production of A1 astrocytes. One of the easily observable attribute of HD progression is weight loss and decreased body mass index of HD patients. We detected a reduction of DARPP32 expression, a selective marker of striatal medium spiny neurons, and microglial activation in 24-month-old TgHD animals (Paper III). Therefore, we were interested in how does the HD phenotype progress in 4 to 6-year-old TgHD minipigs.

Summary

We investigated the brain tissues of 48- and 60-70-month-old TgHD minipigs and detected the huntingtin expression mainly in spiny neurons of striatum and in cortical pyramidal neurons. We proved severe fragmentation of mHtt in putamens of 48-month-old TgHD minipigs but less mtHtt fragments were presented in 60-70-month-old TgHD putamens. Moreover, WB detected smears at the high molecular weight in 60-70-month-old TgHD putamen which could represent oligomeric structures of mtHtt. We assumed that these findings correspond to the aggregation process, where fragments start to form oligomeric structures. We did not prove a difference in a presence of potential Htt aggregates in TgHD and WT minipigs by immunohistochemistry. However, specific inclusions in the neuronal axons were detected by transmission electron microscopy in 60-70-month-old TgHD brains. There was no change observed in neuronal bodies, but neurites disclosed a mild neurodegeneration of TgHD brain.

We observed age-related progressive reduction of medium-sized spiny neurons in TgHD brains with a significant relevance in putamen.

Next, we demonstrated activated microglia at 48-month-old brains, while no significant difference in microglial activation was showed at the age of 60-70 months. Vice versa, no activation of astrocytes was detected at 48 months while a significant increase of activated astrocytes was observed in 60-70-month-old brains. It was showed that activated microglia induce the production of A1 astrocytes, which fail to support neuronal survival and

can trigger neuronal degeneration, Therefore, we supposed that activation of actrocytes at 60-70 months is a respond to microglial activation at the age of 48 months. However, a production of A1 astrocytes was not investigated in TgHD minipigs, and thus this assumption needs to be further validated. Futhermore, it was showed that activated microglia cause damage of oligodendrocytes what leads to demyelination of white matter in mice models. We demonstated significantly decreased myelination of nerve fibres in striatum and subcortical white matter of TgHD minipig at 48 months but no change was observed in 60-70-month-old TgHD brains. Moreover, we confirmed significantly decreased cellularity in 60-70-month-old TgHD brains, while no diference in cellularity was detected at 48 months. These findings indicated genotype- and age-specific loss of cells in TgHD minipig brains.

Lastly, we monitored the weight of the animals longitudinally from the age of 1 to 7 years. We decided to calculate the animal body mass index (ABMI), a weight correlated by height and length of the animal, because we faced the problem of individual and sex variabilities. ABMI increased up to the 4 years of age. Then ABMI of sows started to decrease and a significant weight loss was observed at the 6-7 years. ABMI of boars older than 4 years oscilated in the same level and showed a slight non-significant decrease at 6-7 years of age.

Taken together, we confirmed the mutant huntingtin expression in striatal spiny neurons and in pyramidal neurons of cortex. We demonstrated age-dependent loss of striatal neurons and fragmentation of mtHtt. We showed a potential linkage of microglial activation with demyelination of brain white matter and activation of A1 astrocytes. At 60-70 months, we detected clusters of structures accumulating in the neurites of some neurons, a sign of their degeneration and reduced cellularity in basal ganglia and cortex. The appearance of axonal inclusions, age-dependent cellular degeneration and dwindled ABMI foreshadowed slow but proceeding neurodegeneration in TgHD minipigs.

My contribution

I conducted the monitoring of weight loss of minipigs and processed the weight loss data validation. I participated on processing of the brain samples from sacrificed animals.

Transgenic minipig model of Huntington's disease exhibiting gradually progressing neurodegeneration

[1]Taras Ardan, [1]Monika Baxa, [1]Božena Levinská, [1,2]Miroslava Sedláčková, [1]The Duong Nguyen, [1]Jiří Klíma, [1]Štefan Juhás, [1]Jana Juhásová, [1]Petra Šmatlíková, [1]Petra Vochozková, [1]Jan Motlík and [1]Zdenka Ellederová*

[1]Laboratory of Cell Regeneration and Plasticity, Institute of Animal Physiology and Genetics, Czech Academy of Science, Libechov, Czech Republic; [2]Department of Histology and Embryology, Masaryk University in Brno, Faculty of Medicine, Brno, Czech Republic

*corresponding author:
Zdenka Ellederova,
Address: Rumburska 89, 27721 Libechov, Czech Republic, Tel: +420315639565,
email: ellederova@iapg.cas.cz

Keywords: Huntington's disease, HD large animal model, neurodegeneration

Abbreviations

HD: Huntington's Disease; HTT: huntingtin gene; HTT: huntingtin protein; mHTT: mutant HTT; TgHD: transgenic for Huntington's disease; WT: wild type; ABMI: animal body mass index; Iba1: ionized calcium-binding adapter molecule 1; GFAP: glial fibrillary acidic protein; IHC: immunohistochemistry; DARPP32: dopamine-regulated neuronal phosphoprotein; TEM: transmission electron microscopy; EM: electron microscopy; ROI: region of interest;

Summary statement

Longitudinal phenotyping studies of the minipig model for Huntington's disease demonstrated a slow and age-dependent neurodegeneration. The experimental data of the phenotype progression form a background for effective preclinical studies of gene or disease modifying therapy.

ABSTRACT

Recently developed therapeutic approaches for the treatment of Huntington's disease (HD) require pre-clinical testing in large animal models. Minipig is a suitable experimental animal because of its large gyrencephalic brain, body weight of 70 – 100 kg, long lifespan, and anatomical, physiological and metabolic resemblance to humans. The Libechov transgenic minipig model for HD (TgHD) has been proven useful for proof of concept of developing new therapies. However, to evaluate the efficacy of different therapies on the disease progression a broader phenotypic characterization of the TgHD minipig is needed.

In this study, we analysed the brain tissues of TgHD minipigs at the age of 48 and 60-70 months and compared them to wild type (WT) animals. We were able to demonstrate not only an accumulation of different forms of mutant huntingtin (mHTT) in TgHD brain, but also pathological changes associated with cellular damage caused by mHTT. At 48 months, we detected pathological changes including the demyelination of brain white matter, loss of function of striatal neurons in the putamen and activation of microglia. At 60-70 months, we found a clear marker of neurodegeneration, a significant cell loss detected in the caudate nucleus, putamen and cortex. This was accompanied by clusters of structures accumulating in the neurites of some neurons, a sign of their degeneration also seen in Alzheimer's disease, and a significant activation of astrocytes. In summary, our data demonstrate age dependent neuropathology with later onset of neurodegeneration in the TgHD minipigs.

INTRODUCTION

Huntington's disease (HD) is an inherited progressive neurodegenerative disease without current effective treatment. It is caused by CAG triplet expansion in exon 1 of the huntingtin gene (HTT) encoding mutant huntingtin protein (mHTT). HD patients suffer from involuntary chorea-like movements, poor balance, cognitive dysfunction, emotional disturbances and weight loss. HD manifests typically between thirty and fifty years of age correlating with CAG repeat size and genetic and environmental modifiers (Genetic Modifiers of Huntington's Disease (GeM-HD) Consortium et al., 2015; Gusella et al., 2014).

Even though HD is a monogenic disease, the pathogenesis is rather complicated due to the important role of huntingtin protein (HTT) in diverse cellular processes including transcription, RNA splicing, endocytosis, trafficking, anti-apoptotic processes, and cellular homeostasis (Harjes and Wanker, 2003). It is believed that misfolded mHTT undergoes disease-specific enhanced proteolysis leading to mHTT fragmentation (Mende-Mueller et al., 2001). Soluble mHTT monomers, N-terminal fragments and mHTT oligomers, so called

mHTT intermediates of the aggregation pathway, were described as a trigger of cellular dysfunction in the affected tissues (Hoffner et al., 2007; Lajoie and Snapp, 2010).

The most affected organ in HD is the brain, especially vulnerable are the medium size spiny neurons in the striatum and the pyramidal cells in the cortex (Zuccato et al., 2010). In addition to the atrophy of medium spiny neurons, white matter atrophy, myelin breakdown and microglia activation are connected to HD (Bartzokis et al., 2007; Paulsen, 2010). Even though the brain pathology appears before the clinical onset of the disease, widespread neuronal loss occurs at later stage of HD (Rosas et al., 2008).

The primary goal of HD research is to develop disease-modifying treatment that will prevent or postpone the onset and slow the progression of clinical symptoms in HD patients. Unfortunately, several promising therapies with powerful results in HD mouse models failed to be efficient in humans, such as the mitochondrial coenzyme Q10 (coQ10) (Huntington Study Group, 2001; McGarry et al., 2017) and creatine (Hersch et al., 2017). The rodent's small brain size, differences in neuroanatomy relative to humans and short life span limit their application for detailed modelling of the pathogenic features of human neurodegenerative diseases. Therefore, large animal models are desired especially for safety, tolerability, and efficacy tests of potential therapeutics and longitudinal studies of HD. To this end several large animal models have been generated such as non-human primates, sheep, and pigs (Baxa et al., 2013; Jacobsen et al., 2010; Uchida et al., 2001; D. Yang et al., 2010; S.-H. Yang et al., 2008). The advantages of pigs, especially the minipigs, are the relatively large gyrencephalic brain with similar neuroanatomy to humans, white to gray matter ratio (60:40) comparable to humans, adult body weight of 70 – 100 kg, longer life span of 12 – 15 years, relatively low cost, and lesser ethical problems (Vodicka et al., 2005). Moreover, minipigs are easy to be maintained in controlled conditions, their litter size is usually six to eight piglets, thus providing good experimental groups with similar genetic background.

The transgenic HD minipig (TgHD) model was generated in Libechov by the use of a lentiviral vector expressing N-terminal part of the human mHTT (N548-124CAG/CAA) under the control of human HTT promoter injected into one cell embryos (Baxa et al. 2013). Pigs from subsequent generations express human mHTT in all tissues with the highest level detected in the brain and testes (Macakova et al., 2016; Vidinská et al., 2018). Previously, sperm and testicular degeneration, impairments of mitochondrial metabolism and glycolysis, reduction of DARPP32, and other markers of neurological phenotype progression were demonstrated (Askeland et al., 2018; Krizova et al., 2017; Macakova et al., 2016; Vidinská et al., 2018).

The TgHD minipig model was proven to be useful in preclinical testing of HTT-lowering gene therapy showing the wide-spread vector distribution and considerable HTT lowering (Evers et al., 2018). Several injected TgHD animals and age-matched TgHD non-injected controls from the following longitudinal study are still alive and are being monitored. Therefore, a detailed characterization of TgHD minipig's phenotype is required to detect the therapeutic effect of HTT lowering as well as of other therapeutic interventions.

Here, we aimed to further characterize the neuropathological phenotype as the TgHD experimental animals age. We examined the brain tissue in terms of ultrastructure and biochemical and histochemical manifestation of important markers of neurodegeneration at 48 months (4 years) and 60-70 months (5-5.8 years).

RESULTS

Genotype and gender-specific weight loss in TgHD minipigs

Previously, we investigated the motor and cognitive performance of 48-month-old minipigs and detected a general tendency for reduced performance in all tests with a significant decline in the ability to perform the tunnel test in the TgHD minipigs (Askeland et al., 2018). Because motor and cognitive phenotype is connected with weight loss we also measured the animal body mass index (ABMI), a weight correlated by height and length of the animal. Animals at the age of 1 year (Y), 2Y, 3Y, 4Y, 5Y, 6Y and 7Y were measured. In order to have enough animals in each group to perform statistical analysis we pooled age 1-3.9Y, 4-5.9Y, and 6-7.9Y (Fig. 1A); the number of monitored animals, age, sex, and genotype are indicated under the graphs (Fig.1B). The ABMI values of boars increase up to the age of 4 years. From the age of 4 years, ABMI of boars remains on the same level. ABMI of both WT and TgHD sows increases up to the age of 4 years. From the age of 5 years the ABMI of TgHD sows decreases, while the change in AMBI of WT sows is minimal. While just a slight non-significant decrease was revealed in ABMI of TgHD compared to WT boars at 6-7 years, a significant decrease was measured at 6-7 years old TgHD sows (6Y: p=0,0286; 7Y: p=0.0357, 6-7Y: p=0.0002) in comparison to the WT controls.

A

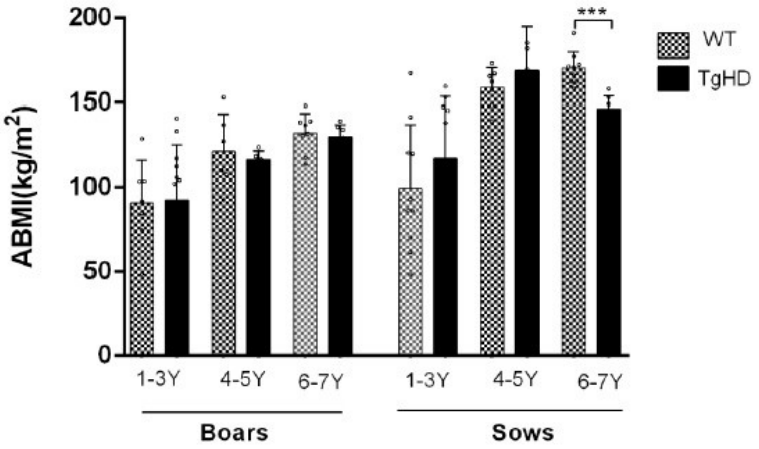

B

Animal/Age	1Y	2Y	3Y	4Y	5Y	6Y	7Y
WT ♂	2	2	3	3	3	4	4
TG ♂	4	4	4	1	4	4	3
WT ♀	4	3	3	2	5	4	5
TG ♀	3	3	4	4	4	4	3

Figure 1: The animal body mass index (ABMI) meausurement of TgHD and WT minipigs at different ages (A) a graf of ABMI devided by sex into three groups 1-3Y (years old), 4-5Y and 6-7Y, *** $p<0.001$ (B) Number of animals measured at certain age

mHTT intermediates of the aggregation pathway accumulate in age and brain region-specific manner in the TgHD minipig model

We suppose that the changes between WT and TgHD brain tissue are caused by the expression of mHTT. The expression of the N-terminal part of human mHTT in the TgHD minipigs and its absence in WT minipigs was confirmed at all ages (from 1-4 years) and different generations by us previously (Askeland et al., 2018; Baxa et al., 2013; Vidinská et al., 2018). Here, we evaluated the expression of mHTT, endogenous HTT and its forms by Western blot using an HTT-specific antibody in the brain of 48-month-old and 60-70-month-old minipigs. We detected an expression of mHTT, and its several smaller fragments, mainly in 48 month-old TgHD putamen samples (Fig. 2A). Using a different percentage gel (4-12%) we detected also smears with two bands at the high molecular weight in 60-70 month-old TgHD putamen samples presumably showing oligomeric structures (Fig. 2B). Based on this and our previous results we conclude that the forms of HTT change during aging.

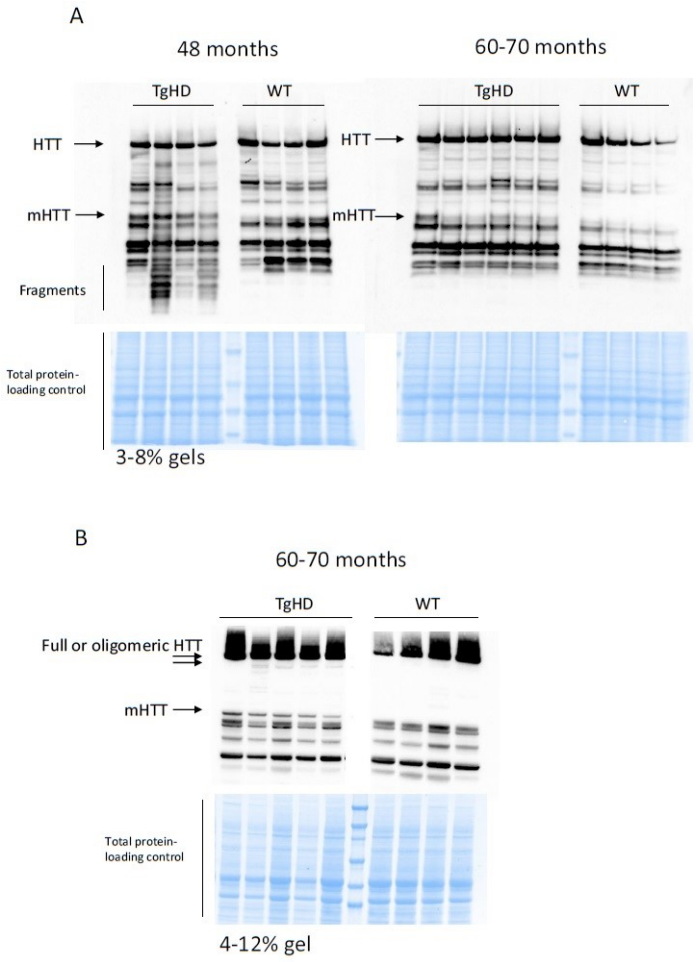

Figure 2: Western blot analysis of HTT forms (A). Detection of fragmented HTT in putaments from 48 and 60-70 month-old minipigs using 3-8% gel and EPR-5526 anti-HTT antibody (B) Detection of oligomeric forms of HTT in putamens from 60-70 moth-old minipigs using 4-12% gels and EPR-5526 anti-HTT antibody. A representative blots from different TgHD and WT animals are shown.

For the identification and localization of HTT and possible inclusions/aggregates by immunohistochemistry, the following commercially available primary antibodies were used: BML-PW0595, EPR5526 and MW8. A majority of the huntingtin expression was localized in the spiny neurons of striatum and in the cortical pyramidal neurons. MW8 antibody was used to reveal potential aggregates. Even when using this antibody, we detected a few structures with various sizes in diameter in all TgHD basal ganglia, which were comparable to aggregates observed in HD human brain. Very similar aggregate formations were also observed in WT basal ganglia. Therefore, we were not able to draw a definitive conclusion from these results. Since a recent manuscript (Jansen et al., 2017) shows that the

percentage of neurons having aggregates in post-mortem HD patient brain samples does not exceed 0.3%, it is possible that the aggregates in TgHD brain were under the detection limit.

Age and genotype-specific shift of characteristic markers of neurodegeneration (cellular damage)

In order to recognize specific markers of cell damage, we stained brain coronal sections of 48 and 60-70 month-old minipigs with anti-Iba1, anti-GFAP, and anti-DARPP32 antibodies.

At 48 months, the ionized calcium-binding adapter molecule 1 (Iba1), a specific marker of microglia and their activation state, revealed a more intense staining in the central part of caudate nucleus in comparison with rather lightly stained fibre-like structures of branching processes. The semi-quantitative image analysis of Iba1 immunostaining showed higher, statistically significant expression in insular ($p=0.0117$), and somatosensory cortex ($p=0.0414$) of 48-month-old TgHD minipigs compared to WT (Fig. 3). Reactivated astrocytes and their proliferation activity were determined by glial fibrillary acidic protein (GFAP) staining. The GFAP is an astrocyte-specific intermediate filament protein, its expression is required for normal function of fibrous astrocytes (Liedtke et al., 1996). Of note, the majority of protoplastic astrocytes do not express enough GFAP to stain positive with routine immunohistochemical (IHC) methods (Chen and Swanson, 2003; Walz, 2000), and consequently most astrocytes in grey matter are GFAP-negative with routine staining. This corresponds to our finding in which astrocytes were clearly stained in the white matter whereas the gray matter structures were less intensively labelled. The image analysis of GFAP staining demonstrated no significant changes between WT and TgHD minipigs in the 48-month-old brain substructures of interest (Fig.3). Last, we examined the expression of DARPP32 in minipig striatum and cortex. DARPP32 is the selective marker of striatal medium spiny neurons and a potent inhibitor of protein phosphatase 1, which plays an important role in dopaminergic and glutamatergic signalling. Neurons in the striatum exhibited very strong DARPP32 staining whereas neurons located in the cortex had a weaker signal. The results of image analysis of DARPP32 labelling showed a reduced level of expression in the striatum with a significant relevance in putamen ($p<0.05$) of TgHD compared to WT animals (Fig.3). Since DARPP32 is a selective marker of striatal medium spiny neurons, our finding suggests the loss of function of these neurons with consequences on dopaminergic signalling in striatum of TgHD minipig brain.

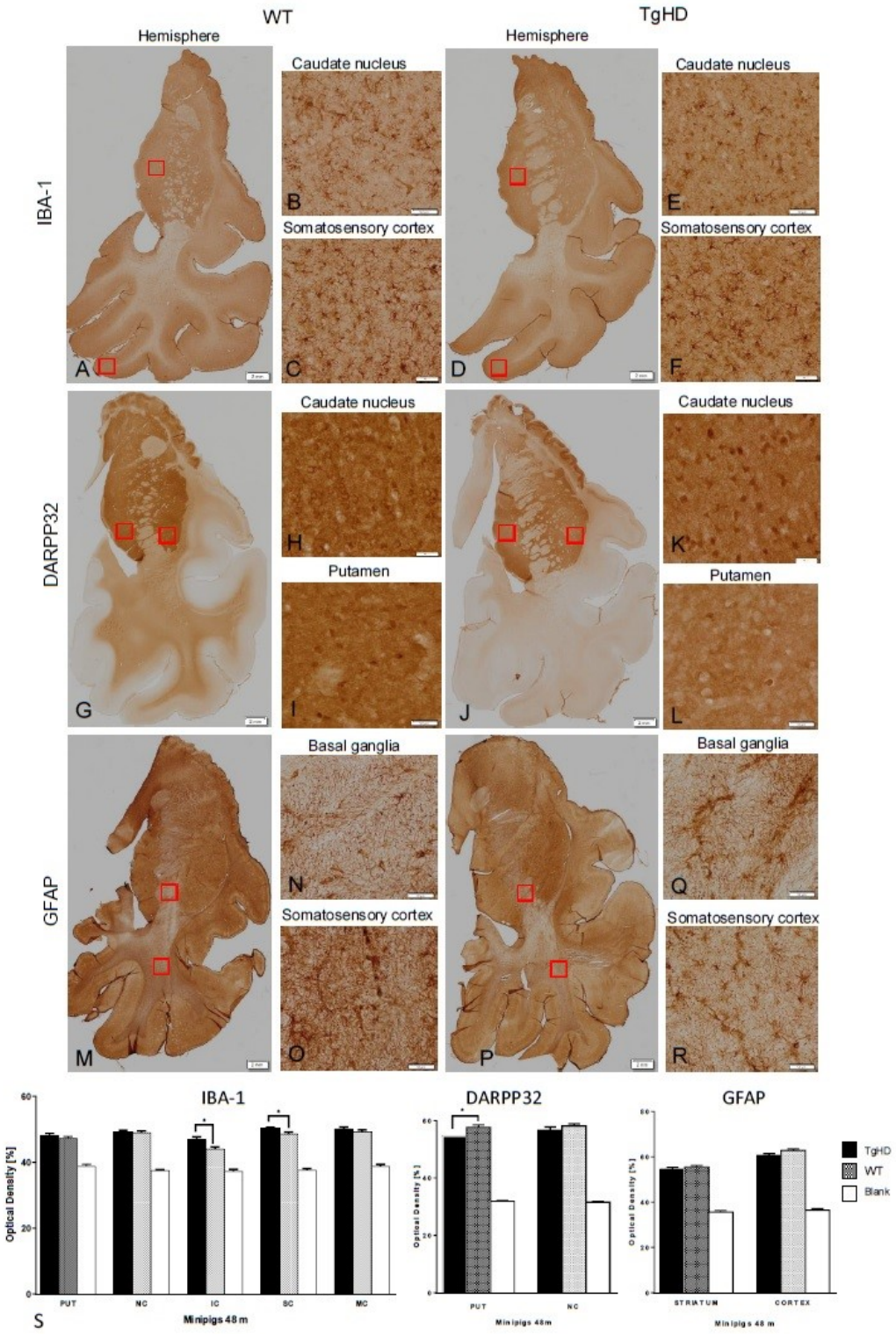

Figure 3: Immunohistochemical investigation of expressions of IBA-1 (A-F), DARPP32 (G-L) and GFAP (M-R) in the brain sections of 48m old animals. The image analysis of the immunohistochemical staining demonstrated significantly increased IBA-1 expression in insular and somatosensory cortex and significantly decreased DARPP32 expression in putamen of TgHD animals (S, * significance, PUT - putamen, NC – caudate nucleus, IC - insular cortex, SC - somatosensory cortex, MC - motor cortex). Scalebar 1 (hemispheres) – 2mm, scalebar 2 (enlargements of brain structures) – 50µm.

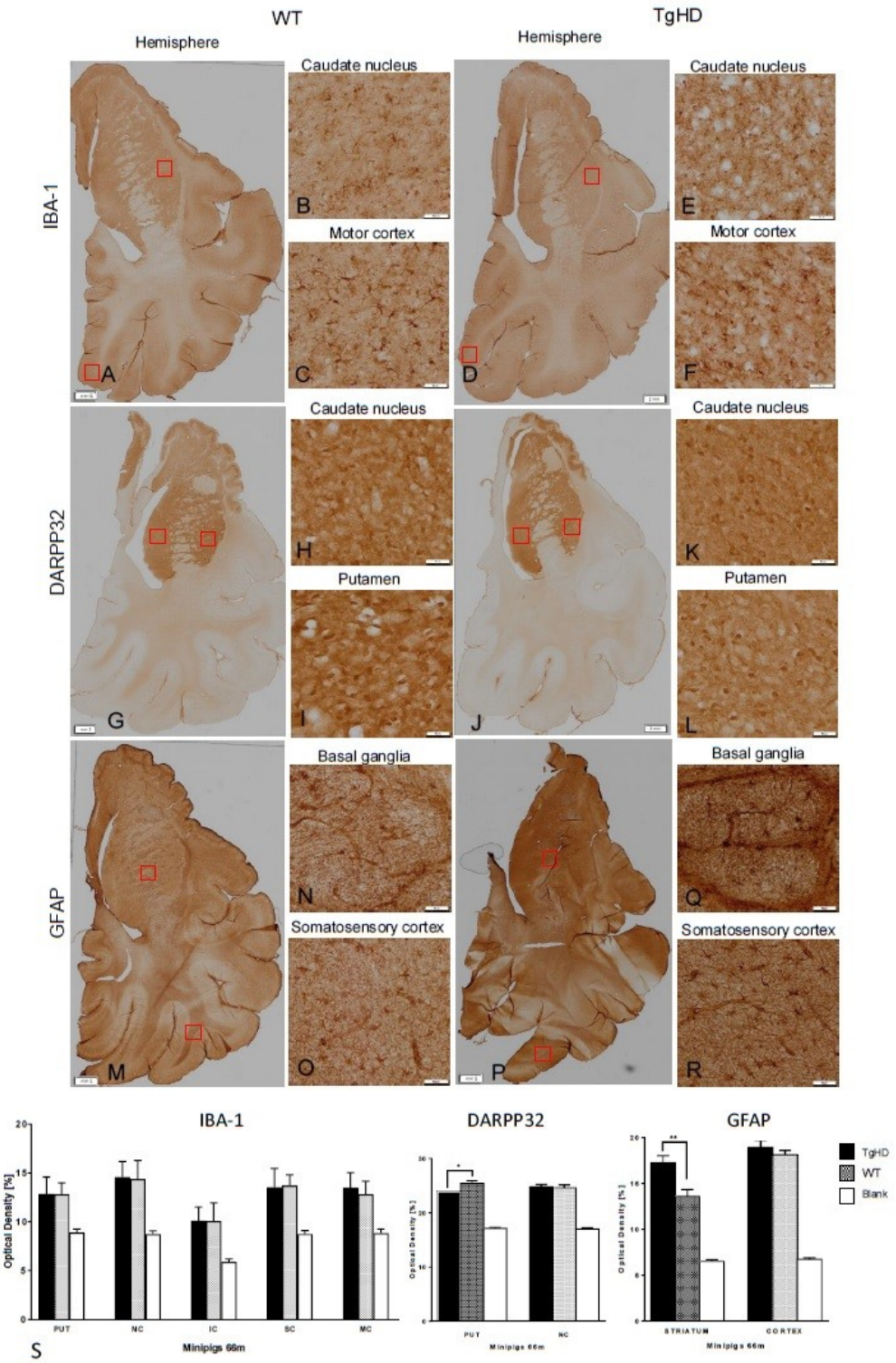

Figure 4: Immunohistochemical investigation of expressions of IBA-1 (A-F), DARPP32 (G-L) and GFAP (M-R) in the brain sections of 66m old animals. The image analysis of the immunohistochemical staining a demonstrated significantly increased GFAP expression in striatum and significantly decreased DARPP32 expression in putamen of TgHD animals (S, * significance, PUT - putamen, NC – caudate nucleus, IC - insular cortex, SC - somatosensory cortex, MC - motor cortex). Scalebar 1 (hemispheres) – 2mm, scalebar 2 (enlargements of brain structures) – 50µm.

At 60-70 months, the IHC brain sections staining of Iba1 indicated only a slightly increased expression in the motor cortex of TgHD minipig brain; however, the image analysis of Iba1 immunostaining did not show any statistically significant differences between WT and TgHD minipigs (Fig. 4). Unlike to 48-month coronal sections, we detected a significantly increased expression of astrocyte marker GFAP in the white matter near striatum ($p<0.01$), and also increased (non-significantly) expression in the somatosensory cortex in TgHD 60-70 month–old minipigs compared to WT (Fig. 4). The image analysis of DARPP32 labelling showed consistent significantly reduced level of its expression in the putamen ($p=0.02$) of TgHD compared to WT, similar to those from 48-months old animals (Fig.4).

For the histochemical demonstration of myelin, Luxol fast blue staining was employed. Results of this staining showed a significantly decreased myelination of nerve fibres in striatum ($p=0.003$) and in the subcortical white matter ($p<0.0001$) of TgHD minipig in comparison to WT at 48 months (Fig. 5), but no change in older minipigs at 60-70 months.

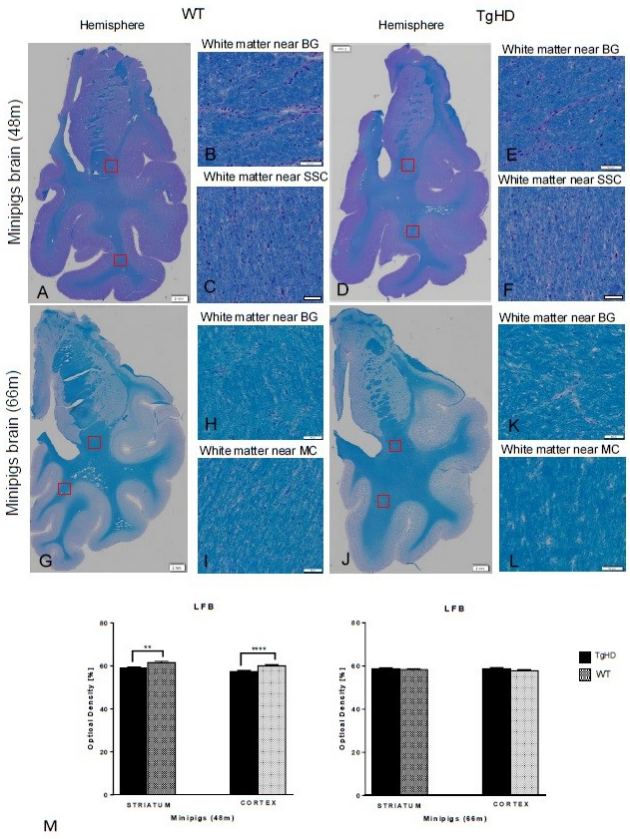

Figure 5: Luxol fast blue (LFB) histochemical staining of pig brains (A-L) and quantification of myelinization in white matter on minipig coronal brain sections of 48m and 60-70m old animals (M). The significantly decreased intensity of myelin staining was detected in a white matter of striatum (E) and somatosensory cortex (F) of TgHD 48m old animals (*significance). No changes of myelinization were detected in 60-70 old minipigs (G-M). Scalebar 1 (hemispheres) – 2mm, scalebar 2 (enlargements of brain structures) – 50µm.

Altered ultrastructure and cellular loss in the brain of 60-70 months old TgHD minipigs

To visualize the ultrastructure of the striatum and cortex, all 60-70 month-old brain sections were processed for transmission electron microscopy (TEM). An initial observation pointing to signs of degeneration was the presence of light and dark neurons, assuming the dark ones to be actually degenerating as previously described in HD mice (Turmaine et al., 2000). However, these neurons were found in TgHD as well as in WT samples, and referring to the literature, the dark cells were eventually evaluated as artefacts that arose during tissue manipulation and processing (Jortner, 2006). Previously, TEM analysis of HD mice revealed inclusions of huntingtin in the nuclei as well as in the cytoplasm of the neurons (dark and light), and in the glia (Davies et al., 1997). But just as in IHC analysis, we could see a few inclusion-like structures in TgHD as well as in WT samples. There were perhaps a few more inclusions in the TgHD samples of the cortex, which could possibly be interpreted as lipofuscin. We also examined the shape and structure of the nucleus. In TgHD neurons, the folds of the nucleus were seen more often, but sometimes they were seen also in WT. However, clusters of structures accumulating in the neurites of some neurons which are probably a sign of their degeneration were detected only in TgHD samples (Fig.6). These structures are morphologically identical to those detected in Alzheimer's disease (Nixon et al., 2005). Neuronal bodies are not affected, but neurites are revealing a mild neurodegeneration of TgHD brain.

Further, we employed toluidine blue staining for the determination of cellularity in WT and TgHD pig's basal ganglia and cortex. The changes in cellularity were measured on segmented images using an image analysis method and the cellularity was calculated as the percentage of nuclei staining in the selected region of interest (ROI). Results of statistical analysis, where unpaired t-test was applied, showed no significant differences in cellularity between WT and TgHD basal ganglia at 48 months. However, it showed significantly decreased cellularity of TgHD in both striatal areas (caudate nucleus $p=0.0198$ and putamen, $p=0.0245$) and motor cortex ($p=0.0355$) at 60-70 months (Fig. 7). These results indicate genotype and age-specific loss of cells in TgHD minipig brains.

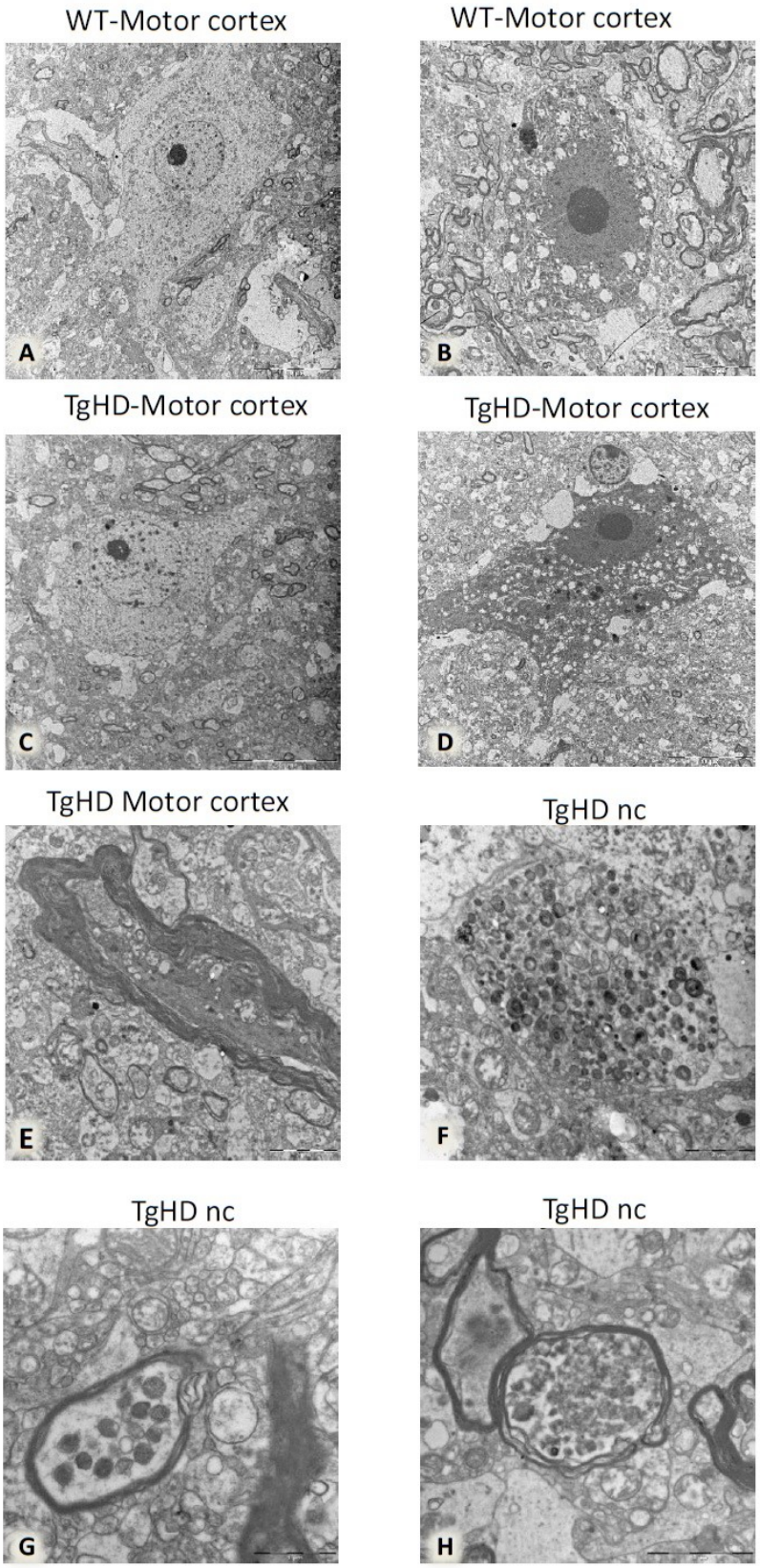

Figure 6: Electron microscopy of motoric cortex and caudate nucleus. Light (A, C) and dark (B, D) neurons. Dystrophic neurite (E). Accumulation of multilamellar bodies in unmyelinated neuronal process (F). Dense bodies in myelinated process are probably remnants of degenerated mitochondria (G). Autophagic vacuoles in a myelinated process (H).

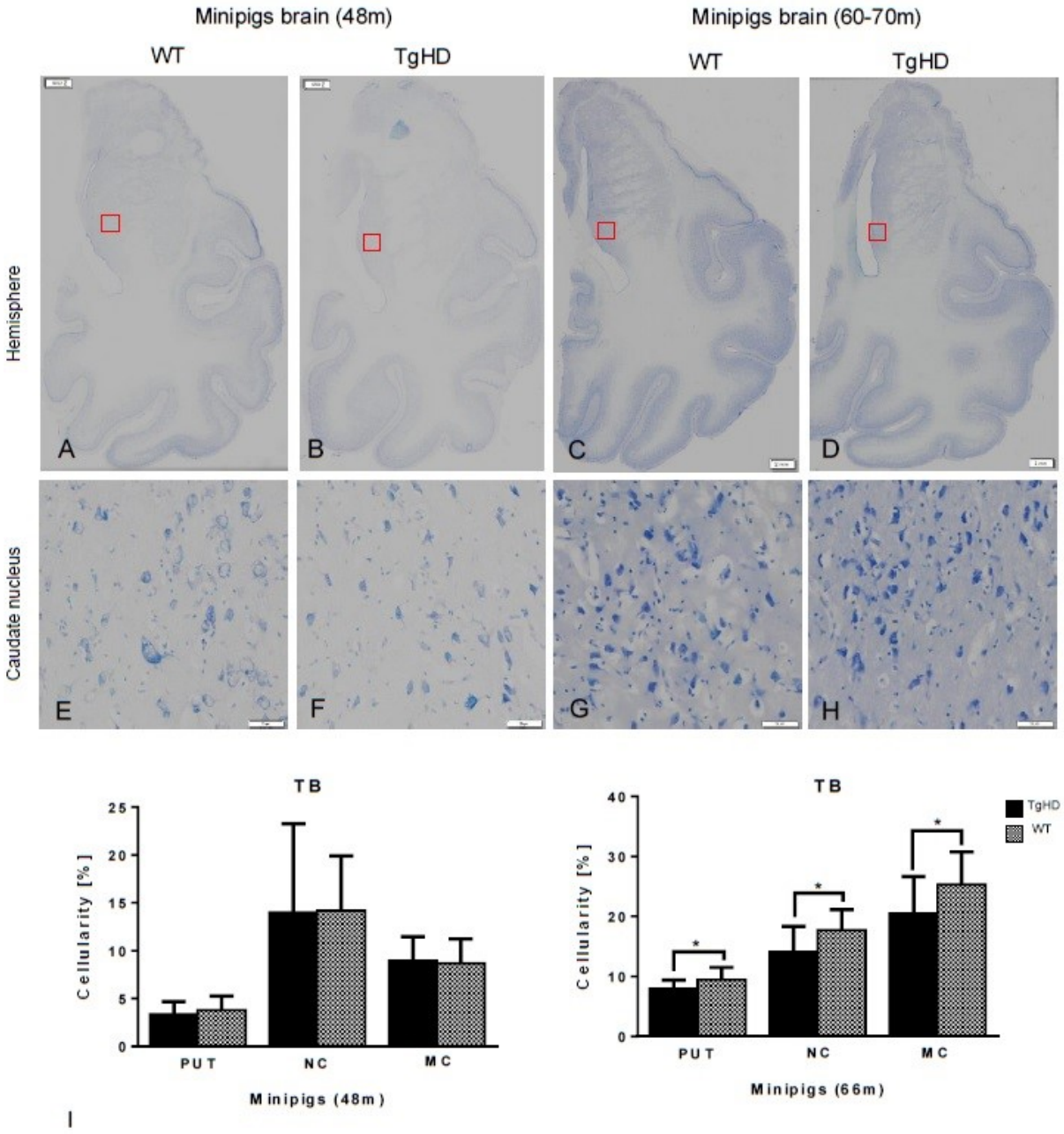

Figure 7: Toluidine blue histochemical staining in hemispheres (A-D) and caudate nucleus (E-H) and quantification of cellularity in striatum and motor cortex of minipig brain sections of both 48-month and 66-month-old animals using image analysis methods (I). The significantly decreased cellularity was detected in putamen (PU), caudate nucleus (NC) and motor cortex (MC) of TgHD 66 month-old animals (I, * significance). Scalebar 1 (hemispheres) – 2mm, scalebar 2 (enlargements of brain structures) – 50µm.

DISCUSSION

The TgHD minipig is an important biomedical model primarily designated for testing therapeutic interventions. It can overcome the gap between rodent models and human patients to gain more preliminary knowledge before proceeding with demanding and expensive clinical trials. For this reason, an extensive phenotypical characterization of the TgHD minipig model is highly warranted. The previous characterization showed locomotor functional decline together with genotype-specific effects on mitochondrial DNA (mtDNA) damage, mtDNA copy number, and markers of a metabolic alteration that manifest in a progressive neuropathology at 48 months (Askeland et al., 2018). In the present study, we extended our observations and tested older animals for weight loss. Weight loss is a hallmark of HD progression, the decrease in patients' body mass index (BMI) is associated with functional, motor, and cognitive decline (van Der Burg et al. 2017). Accordingly, we found a significant decrease in ABMI of 6-7 years old sows and a slight non-significant decrease was revealed in ABMI of TgHD boars compared to WT boars at the same age (Fig.1). This is also consistent with our previous data of a perturbed mitochondrial phenotype in TgHD minipig muscle tissue starting at 36 months prior to the development of mitochondrial ultrastructural changes and locomotor impairment beginning at the age of 48 months (Rodinova et al., in press).

There is strong evidence that HTT is fragmented in affected individuals (Bates et al., 2015) and the N-terminal mHTT fragments accumulate with the disease progression, translocate into the nucleus and cause aberrant protein interaction leading to cellular dysfunction (Benn et al., 2005; Graham et al., 2006; Saudou et al., 1998). mHTT also forms aggregates that were initially described as being the toxic trigger in HD (Davies et al., 1997). However, the later studies suggest also a protective role of aggregates, as they reduce the level of the toxic soluble protein (Miller et al., 2010; Saudou et al., 1998). Thus soluble intermediates of the aggregation pathway, oligomers forming from mHTT fragments, are described as the most reactive harmful species (Truant et al., 2008). We previously reported tissue-specific and age-correlated progressive HTT fragmentation in different tissues collected from animals up to 24 months (Vidinská et al., 2018). Here we show severe mHTT fragmentation at 48 months but less fragmentation occurring at 60-70 months (Fig.2A). It can be explained by the aggregation process, where fragments at certain point start to form oligomeric structures (Fig.2B). This age-dependent process has been previously seen in R6/2 and knock-in HD mice (Sathasivam et al., 2010).

In this study we also demonstrate the age related changes in markers of neurodegeneration in TgHD brains at two time points, 48 months and 60-70 months. Reduction of DARPP32, an integrator of neurotransmission, has been described in different HD models well before the onset of the behavioural phenotype (Heng et al., 2007; Woodman et al., 2007). Also in our TgHD minipig model, we previously reported downregulation of DARPP32 at 16 and 24 months (Baxa et al., 2013; Vidinská et al., 2018). Consistently, here we report the downregulation of DARPP32 at 48 months as well as at 60-70 months.

We also show microglial activation at 48 months. This result is in line with microglial activation at 24 month-old TgHD minipig brain sections (Vidinská et al., 2018), together with decreased levels of IFNα and IL-10 and increased levels of IL-8 and IL-1β in the microglial secretome in TgHD compared to WT controls (Valekova et al., 2016). The increased levels of IL-8 and IL-1β were also found in plasma of pre-manifest HD patients and were linked to increased central microglial activation (Politis et al., 2015). It was recently revealed that the activated microglia induce the production of A1 astrocytes (Liddelow et al., 2017). In the present study, we used GFAP as a marker of astrocytes' activation, and we did not detect activation of astrocytes at 48 months but a significant increase of activation at 60-70 months, which could be an effect of high microglial activation at 48 months. It was shown that A1 astrocytes fail to support neuronal survival; in contrast, they can trigger neuronal degeneration (Liddelow et al., 2017). Their increased number was demonstrated in HD as well as in other neurodegenerative diseases (Hinkle et al., 2019). However, the higher presence of A1 astrocytes specifically was not measured in TgHD minipigs. Therefore it is just an assumption that our detection of activated astrocytes reflects a higher production of harmful A1 astrocytes, and it needs to be further validated.

Additionally, we detected demyelination at 48 months similarly as in our previous study, where we examined brain sections from 24 month-old TgHD animals compared to WT (Vidinská et al., 2018). Also in different mice models the demyelination occurs before neurodegeneration (Teo et al., 2016). Activated microglia expressing proinflammatory mediators damage oligodendrocytes and consequently cause demyelination of white matter (Peferoen et al., 2014). It is interesting that both microglia activation and demyelination were significant at 48 months but not at 60-70 months, where astrocyte activation takes place.

As previously discussed, no genotype-specific aggregates were found in the brains of TgHD minipigs by IHC. However, the TEM analysis revealed TgHD-specific inclusions in the axons of some neurons (Fig.6). Inclusions in axons were also detected in HD mice and associated with axonal degeneration (Li et al., 2001). Inclusions can block axonal transport and thus

contribute to the degeneration of mitochondria and other organelles and ultimately lead to neuronal degeneration. However, it is also possible that mHTT directly binds to synaptic vesicles and affects synaptic transmission before forming large aggregates (Usdin et al., 1999). We also found age and genotype-related cellular loss in basal ganglia and cortex (Fig.7). Cellular degeneration particularly in basal ganglia and cortex is the hallmark of HD progression (Zuccato et al., 2010). Our finding of axonal inclusions together with the age-dependent cellular degeneration is one of the main findings of this study and shows slow but progressive neurodegeneration in the TgHD minipig model with N-terminal part of human mHTT. The slow progression observed in this model is surprising since the triplet repeat lenght is 124 thus modelling a juvenile form of the disease. It is possible that the slow progression is due to the CAG/CAA mix of the repeat region of mHTT. This design aimed for a better stability of the construct when generating this TgHD minipig model in 2008 (Baxa et al., 2013). Nevertheless, later on it was revealed that there is a dramatic striatal-specific somatic repeat expansion in HD patients causing the striatal cells to be more vulnerable to the effect of mHTT (Swami et al., 2009). However, the slow progression of the TgHD minipig model with the currently and previously described HD specific biomarkers of disease progression can serve for evaluation of HD treatment efficacy.

MATERIALS AND METHODS

Minipig material and sample collection

Transgenic minipigs with the N-terminal part of human mHTT were studied. The genotype was determined by PCR according to Baxa et al. (2013) from DNA isolated from minipigs skin biopsies after weaning. 48 month-old TgHD minipigs (n =6) and their WT controls (n = 6) and 60-70 month-old TgHD minipigs (n =6) and their WT controls (n = 4) from F2 generations were perfused under deep anaesthesia with ice cold PBS. Various tissues were isolated and stored after snap freezing in liquid nitrogen. The right hemisphere of each perfused brain was directly fixed for immunohistochemistry. The entire study was carried out in agreement with the Animal Care and Use Committee of the Institute of Animal Physiology and Genetics, under the Czech regulations and guidelines for animal welfare and with the approval of Czech Academy of Sciences, protocol number: 53/2015

The body mass index calculation

Animals are weight regularly in the same hour of the daz. Their body mass indexes (ABMI) were calculated as follows: ABMI= m/h*l; m = weight of animal, h = height of animal

in withers, l = length of animal from withers to tailbone.The results were evaluated using GraphPad Prism 6 by t-test/Mann-Whitney test.

SDS-PAGE and Western blot

Tissue samples were homogenized in liquid nitrogen using a mortar and lysed in RIPA buffer (150 mM NaCl, 5mM EDTA pH 8, 0.05% NP-40, 1% sodium deoxycholate, 0.1% SDS, 1% Triton X-100, 50 mM Tris-HCl pH 7.4, inhibitors of phosphatases and proteases), sonicated for 15 min, and centrifuged at 20000 g, 15 min, at 4°C. Samples (10 µg of total protein) were loaded onto 3 – 8% or 4-12% Tris-acetate gel (#EA03758, LifeTech) and run at 150 V. Gel was transferred onto nitrocellulose membrane, blocked in 5% skimmed milk, and probed overnight with anti-HTT antibody diluted in 5% milk (EPR5526, Abcam, 1:3000), diluted in 5% milk, at 4°C at 4°C. Memcode protein staining (LifeTech) was used for normalization of loading. Secondary antibody conjugated with HRP (anti-mouse, #711-035-152, Jackson ImmunoResearch, 1:10000 or anti-rabbit, #711-035-152, Jackson ImmunoResearch, 1:10000) was used. The signal was revealed by chemiluminiscence (ECL, #28980926, APCzech) and detected by The ChemiDoc XRS+system (Biorad).

Immunohistochemistry

Right hemisphere from each animal was fixed in 4% paraformaldehyde for 24 hours and then cryoprotected with 30% sucrose containing 0.01% sodium azide. Frozen coronal sections were prepared using tissue freezing medium (Leica, 14020108926). The free-floating sections (three per animal) of a thickness 40 µm were sequentially treated with formic acid, 0.3% hydrogen peroxide in MetOH and blocking serum to unmask antigens and reduce endogenous peroxidases and unspecific binding of antibodies. The sections were incubated with the following commercially available primary antibodies: Iba1 (AIF1, Synaptic System), GFAP (G3893, Sigma Aldrich), DARPP32 (ab40801, Abcam), anti-HTT (BML-PW0595, Enzo Life Science; EPR5526, Abcam; and MW8) diluted in 5% milk (all 1:250), at 4°C. The specificity of primary antibodies was verified by Western Blot and/or comparative immunohistochemistry of mouse WT and TgHD (R6/2, 12 weeks old) brain sections in the previous study. After washing, sections were incubated with biotinylated donkey anti-rabbit or sheep anti-mouse secondary antibody (both 1:400, Amersham, Buckinghamshire, UK) followed by the incubation with avidin-peroxidase complex (1:400, Sigma-Aldrich). The labelled sections by peroxidase were developed with DAB tablets (#4170, Kementec Diagnostics). The specificity of secondary antibodies was confirmed by using negative controls. The evaluation and quantification of immunoreactivity was performed using a densitometry measurement of staining by image analysis software VS-Desktop (Olympus,

Tokyo, Japan) and ImageJ (Rasband, W.S., U. S. National Institutes of Health, Bethesda, Maryland, USA). According to the 3D view model of pig brain (from program 3D Slicer; slicer.org) optical sections were divided into substructures: basal ganglia (caudate nucleus, putamen) and cortex (motor and somatosensory and insular), in which the mean of intensity was measured. For statistical analysis an unpaired t-test or a one-way ANOVA test with Bonferroni's (or Tukey's) multiple comparison post-test was employed using GraphPad PRISM software (GraphPad Software, San Diego, CA, USA).

Histochemical examination of brain tissue

For histochemical demonstration of myelin Luxol fast blue staining was employed. Toluidine blue staining was used for the determination of cellularity in WT and TgHD pig caudate nucleus. The changes in cellularity were measured on segmented images using image analysis method and the cellularity was calculated as percentage of nuclei staining in selected region of interest (ROI). Unpaired t-test was applied.

Electron microscopy (EM)

Small blocks of motor cortex and striatum were fixed in 300 mM glutaraldehyde (Sigma-Aldrich) in 100 mM cacodylate buffer for 2 h at room temperature (RT), washed in the same buffer and post-fixed in 40 mM osmium tetroxide (Polysciences) in 100 mM cacodylate buffer for 1 h at RT. After rinsing in cacodylate buffer and dehydratation in ethanol the samples were embedded in araldite resin (Durcupan ACM, Sigma-Aldrich). 60 nm thick sections were cut using Leica EM UC6 ultramicrotome and stained with uranyl acetate and lead citrate. Sections were examined under FEI Morgagni 268D electron microscope (FEI Company, The Netherlands) at 70 kV.

ACKNOWLEDGMENTS

Special thanks to Patricia Jandurová, Lenka Trávníčková and Hana Říhová for technical support.

CONFLICT OF INTEREST

The authors have no conflict of interest to report.

FUNDING

The research leading to these results has received funding from National Sustainability Programme, project number LO1609 (Czech Ministry of Education, Youth and Sports), and CHDI foundation (RA: A11609).

AUTHOR CONTRIBUTION STATEMENT

MB, BL, TDN, PS, PV, JJ, SJ performed the experiments. MS performed and analysed EM, TA analysed the IHC data, ZE, JM, TA, JK designed the experiments and interpreted results. ZE, TA wrote the manuscript and JK revised it.

REFERENCES

Askeland, G., Rodinova, M., Štufková, H., Dosoudilova, Z., Baxa, M., Smatlikova, P., Bohuslavova, B., Klempir, J., Nguyen, T. D., Kuśnierczyk, A., et al. (2018). A transgenic minipig model of Huntington's disease shows early signs of behavioral and molecular pathologies. *Disease Models & Mechanisms* **11**, dmm035949.

Bartzokis, G., Lu, P. H., Tishler, T. A., Fong, S. M., Oluwadara, B., Finn, J. P., Huang, D., Bordelon, Y., Mintz, J. and Perlman, S. (2007). Myelin Breakdown and Iron Changes in Huntington's Disease: Pathogenesis and Treatment Implications. *Neurochemical Research* **32**, 1655–1664.

Bates, G. P., Dorsey, R., Gusella, J. F., Hayden, M. R., Kay, C., Leavitt, B. R., Nance, M., Ross, C. A., Scahill, R. I., Wetzel, R., et al. (2015). Huntington disease. *Nature Reviews Disease Primers* **1**, 15005.

Baxa, M., Hruska-Plochan, M., Juhas, S., Vodicka, P., Pavlok, A., Juhasova, J., Miyanohara, A., Nejime, T., Klima, J., Macakova, M., et al. (2013). A Transgenic Minipig Model of Huntington's Disease. *Journal of Huntington's disease* **2**, 47–68.

Benn, C. L., Landles, C., Li, H., Strand, A. D., Woodman, B., Sathasivam, K., Li, S.-H., Ghazi-Noori, S., Hockly, E., Faruque, S. M. N. N., et al. (2005). Contribution of nuclear and extranuclear polyQ to neurological phenotypes in mouse models of Huntington's disease. *Human molecular genetics* **14**, 3065–78.

Chen, Y. and Swanson, R. A. (2003). Astrocytes and Brain Injury. *Journal of Cerebral Blood Flow & Metabolism* **23**, 137–149.

Davies, S. W., Turmaine, M., Cozens, B. A., DiFiglia, M., Sharp, A. H., Ross, C. A., Scherzinger, E., Wanker, E. E., Mangiarini, L. and Bates, G. P. (1997). Formation of neuronal intranuclear inclusions underlies the neurological dysfunction in mice transgenic for the HD mutation. *Cell* **90**, 537–48.

Evers, M. M., Miniarikova, J., Juhas, S., Vallès, A., Bohuslavova, B., Juhasova, J., Skalnikova, H. K., Vodicka, P., Valekova, I., Brouwers, C., et al. (2018). AAV5-miHTT Gene Therapy Demonstrates Broad Distribution and Strong Human Mutant Huntingtin Lowering in a Huntington's Disease Minipig Model. *Molecular Therapy*.

Genetic Modifiers of Huntington's Disease (GeM-HD) Consortium, J.-M., Wheeler, V. C., Chao, M. J., Vonsattel, J. P. G., Pinto, R. M., Lucente, D., Abu-Elneel, K., Ramos, E. M., Mysore, J. S., Gillis, T., et al. (2015). Identification of Genetic Factors that Modify Clinical Onset of Huntington's Disease. *Cell* **162**, 516–26.

Graham, R. K., Slow, E. J., Deng, Y., Bissada, N., Lu, G., Pearson, J., Shehadeh, J., Leavitt, B. R., Raymond, L. A. and Hayden, M. R. (2006). Levels of mutant huntingtin influence the phenotypic severity of Huntington disease in YAC128 mouse models. *Neurobiology of Disease* **21**, 444–455.

Gusella, J. F., Macdonald, M. E. and Lee, J. M. (2014). Genetic modifiers of Huntington's disease. *Movement Disorders*.

Heng, M. Y., Tallaksen-Greene, S. J., Detloff, P. J. and Albin, R. L. (2007). Longitudinal evaluation of the Hdh(CAG)150 knock-in murine model of Huntington's disease. *The Journal of neuroscience : the official journal of the Society for Neuroscience* **27**, 8989–98.

Hersch, S. M., Schifitto, G., Oakes, D., Bredlau, A.-L., Meyers, C. M., Nahin, R., Rosas, H. D. and Huntington Study Group CREST-E Investigators and Coordinators (2017). The CREST-E study of creatine for Huntington disease: A randomized controlled trial. *Neurology* **89**, 594–601.

Hinkle, J. T., Dawson, V. L. and Dawson, T. M. (2019). The A1 astrocyte paradigm: New avenues for pharmacological intervention in neurodegeneration. *Movement Disorders* mds.27718.

Hoffner, G., Souès, S. and Djian, P. (2007). Aggregation of expanded huntingtin in the brains of patients with Huntington disease. *Prion* **1**, 26–31.

Huntington Study Group (2001). A randomized, placebo-controlled trial of coenzyme Q10 and remacemide in Huntington's disease. *Neurology* **57**, 397–404.

Jansen, A. H. P., van Hal, M., Op den Kelder, I. C., Meier, R. T., de Ruiter, A.-A., Schut, M. H., Smith, D. L., Grit, C., Brouwer, N., Kamphuis, W., et al. (2017). Frequency of nuclear mutant huntingtin inclusion formation in neurons and glia is cell-type-specific. *Glia* **65**, 50–61.

Jortner, B. S. (2006). The return of the dark neuron. A histological artifact complicating contemporary neurotoxicologic evaluation. *NeuroToxicology* **27**, 628–634.

Krizova, J., Stufkova, H., Rodinova, M., Macakova, M., Bohuslavova, B., Vidinska, D., Klima, J., Ellederova, Z., Pavlok, A., Howland, D. S., et al. (2017). Mitochondrial Metabolism in a Large-Animal Model of Huntington Disease: The Hunt for Biomarkers

in the Spermatozoa of Presymptomatic Minipigs. *Neurodegenerative Diseases* **17**, 213–226.

Lajoie, P. and Snapp, E. L. (2010). Formation and Toxicity of Soluble Polyglutamine Oligomers in Living Cells. *PLoS ONE* **5**, e15245.

Li, H., Li, S. H., Yu, Z. X., Shelbourne, P. and Li, X. J. (2001). Huntingtin aggregate-associated axonal degeneration is an early pathological event in Huntington's disease mice. *The Journal of neuroscience : the official journal of the Society for Neuroscience* **21**, 8473–81.

Liddelow, S. A., Guttenplan, K. A., Clarke, L. E., Bennett, F. C., Bohlen, C. J., Schirmer, L., Bennett, M. L., Münch, A. E., Chung, W.-S., Peterson, T. C., et al. (2017). Neurotoxic reactive astrocytes are induced by activated microglia. *Nature* **541**, 481–487.

Liedtke, W., Edelmann, W., Bieri, P. L., Chiu, F. C., Cowan, N. J., Kucherlapati, R. and Raine, C. S. (1996). GFAP is necessary for the integrity of CNS white matter architecture and long-term maintenance of myelination. *Neuron* **17**, 607–15.

Macakova, M., Bohuslavova, B., Vochozkova, P., Pavlok, A., Sedlackova, M., Vidinska, D., Vochyanova, K., Liskova, I., Valekova, I., Baxa, M., et al. (2016). Mutated Huntingtin Causes Testicular Pathology in Transgenic Minipig Boars. *Neuro-degenerative diseases* **16**, 245–59.

McGarry, A., McDermott, M., Kieburtz, K., de Blieck, E. A., Beal, F., Marder, K., Ross, C., Shoulson, I., Gilbert, P., Mallonee, W. M., et al. (2017). A randomized, double-blind, placebo-controlled trial of coenzyme Q10 in Huntington disease. *Neurology* **88**, 152–159.

Mende-Mueller, L. M., Toneff, T., Hwang, S. R., Chesselet, M. F. and Hook, V. Y. (2001). Tissue-specific proteolysis of Huntingtin (htt) in human brain: evidence of enhanced levels of N- and C-terminal htt fragments in Huntington's disease striatum. *The Journal of neuroscience : the official journal of the Society for Neuroscience* **21**, 1830–7.

Miller, J. P., Holcomb, J., Al-Ramahi, I., de Haro, M., Gafni, J., Zhang, N., Kim, E., Sanhueza, M., Torcassi, C., Kwak, S., et al. (2010). Matrix Metalloproteinases Are Modifiers of Huntingtin Proteolysis and Toxicity in Huntington's Disease. *Neuron* **67**, 199–212.

Nixon, R. A., Wegiel, J., Kumar, A., Yu, W. H., Peterhoff, C., Cataldo, A. and Cuervo, A. M. (2005). Extensive involvement of autophagy in Alzheimer disease: an immuno-electron microscopy study. *Journal of neuropathology and experimental neurology* **64**,

113–22.

Paulsen, J. S. (2010). Early detection of Huntington's disease. *Future Neurology* **5**, 85–104.

Peferoen, L., Kipp, M., van der Valk, P., van Noort, J. M. and Amor, S. (2014). Oligodendrocyte-microglia cross-talk in the central nervous system. *Immunology* **141**, 302–13.

Politis, M., Lahiri, N., Niccolini, F., Su, P., Wu, K., Giannetti, P., Scahill, R. I., Turkheimer, F. E., Tabrizi, S. J. and Piccini, P. (2015). Increased central microglial activation associated with peripheral cytokine levels in premanifest Huntington's disease gene carriers. *Neurobiology of disease* **83**, 115–21.

Rodinova, M., Krizova, J., Stufkova, H., Bohuslavova, B., Askeland, G., Dosoudilova, Z., Juhas, S., Juhasova, J., Ellederova, Z., Zeman, J., et al. (2019). Skeletal muscle in an early manifest transgenic minipig model of Huntington's disease revealed deterioration of mitochondrial bioenergetics and ultrastructure impairment. *Disease Models and Mechanisms* **DMM/2018/0**,.

Rosas, H. D., Salat, D. H., Lee, S. Y., Zaleta, A. K., Hevelone, N. and Hersch, S. M. (2008). Complexity and heterogeneity: what drives the ever-changing brain in Huntington's disease? *Annals of the New York Academy of Sciences* **1147**, 196–205.

Sathasivam, K., Lane, A., Legleiter, J., Warley, A., Woodman, B., Finkbeiner, S., Paganetti, P., Muchowski, P. J., Wilson, S. and Bates, G. P. (2010). Identical oligomeric and fibrillar structures captured from the brains of R6/2 and knock-in mouse models of Huntington's disease. *Human Molecular Genetics* **19**, 65–78.

Saudou, F., Finkbeiner, S., Devys, D. and Greenberg, M. E. (1998). Huntingtin acts in the nucleus to induce apoptosis but death does not correlate with the formation of intranuclear inclusions. *Cell* **95**, 55–66.

Swami, M., Hendricks, A. E., Gillis, T., Massood, T., Mysore, J., Myers, R. H. and Wheeler, V. C. (2009). Somatic expansion of the Huntington's disease CAG repeat in the brain is associated with an earlier age of disease onset. *Human Molecular Genetics* **18**, 3039–3047.

Teo, R. T. Y., Hong, X., Yu-Taeger, L., Huang, Y., Tan, L. J., Xie, Y., To, X. V., Guo, L., Rajendran, R., Novati, A., et al. (2016). Structural and molecular myelination deficits occur prior to neuronal loss in the YAC128 and BACHD models of Huntington disease. *Human Molecular Genetics* **25**, ddw122.

Truant, R., Atwal, R. S., Desmond, C., Munsie, L. and Tran, T. (2008). Huntington's disease: revisiting the aggregation hypothesis in polyglutamine neurodegenerative

diseases. *FEBS Journal* **275**, 4252–4262.

Turmaine, M., Raza, A., Mahal, A., Mangiarini, L., Bates, G. P. and Davies, S. W. (2000). Nonapoptotic neurodegeneration in a transgenic mouse model of Huntington's disease. *Proceedings of the National Academy of Sciences of the United States of America* **97**, 8093–7.

Usdin, M. T., Shelbourne, P. F., Myers, R. M. and Madison, D. V. (1999). Impaired Synaptic Plasticity in Mice Carrying the Huntington's Disease Mutation. *Human Molecular Genetics* **8**, 839–846.

Valekova, I., Jarkovska, K., Kotrcova, E., Bucci, J., Ellederova, Z., Juhas, S., Motlik, J., Gadher, S. J. and Kovarova, H. (2016). Revelation of the IFNalpha, IL-10, IL-8 and IL-1beta as promising biomarkers reflecting immuno-pathological mechanisms in porcine Huntington's disease model. *Journal of neuroimmunology* **293**, 71–81.

Vidinská, D., Vochozková, P., Šmatlíková, P., Ardan, T., Klíma, J., Juhás, Š., Juhásová, J., Bohuslavová, B., Baxa, M., Valeková, I., et al. (2018). Gradual Phenotype Development in Huntington Disease Transgenic Minipig Model at 24 Months of Age. *Neurodegenerative Diseases* **18**, 107–119.

Vodicka, P., Smetana, K., Dvoránková, B., Emerick, T., Xu, Y. Z., Ourednik, J., Ourednik, V. and Motlík, J. (2005). The miniature pig as an animal model in biomedical research. *Annals of the New York Academy of Sciences* **1049**, 161–71.

Walz, W. (2000). Role of astrocytes in the clearance of excess extracellular potassium. *Neurochemistry international* **36**, 291–300.

Woodman, B., Butler, R., Landles, C., Lupton, M. K., Tse, J., Hockly, E., Moffitt, H., Sathasivam, K. and Bates, G. P. (2007). The Hdh(Q150/Q150) knock-in mouse model of HD and the R6/2 exon 1 model develop comparable and widespread molecular phenotypes. *Brain research bulletin* **72**, 83–97.

Zuccato, C., Valenza, M. and Cattaneo, E. (2010). Molecular Mechanisms and Potential Therapeutical Targets in Huntington ' s Disease. *Physiol Rev* **90**, 905–981.

Paper VI

Longitudinal study revealed motor, cognitive, and behavioral decline in transgenic minipig model of Huntington's disease.

Baxa, M., *Levinska, B., Skrivankova, M., Pokorny, M., Juhasova, J., Klima, J., Klempir, J., Motlik, J., Juhas, S., and Ellederova, Z.*

Submitted in Disease Models & Mechanisms; MS ID#: DMM/2019/041293

IF 4.398

Motivation of the study

We demonstrated pre-clinical HD-like phenotype in our TgHD model. Firstly, we proved sperm and testicular degeneration (Papers I and II). Next, we showed age-related transformation of mHtt intermediates with inclusions in the axons of some neurons, loss of medium sized spiny neurons, activation of microglia and demyelination of white matter (Papers III and V). Moreover, we observed changes in mtDNA integrity (Paper IV). We were also interested in the manifestation of clinical symptoms of HD. Unsteady gait and worsened movement coordination ability, as well as impaired tongue protrusion were observed in HD individuals. Morover, cognitive deficits influenced an ability to learn the tasks and spatial navigation. Next, disturbances in sleep and circadian rhythm projecting into altered physical activity during the day were confirmed in HD patients. Therefore, we aimed to longitudinally monitor motor, cognitive and behavioral phenotype of TgHD minipigs.

Summary

We established the tests for monitoring of potential cognitive changes and stress-induced performance. Morover, motor activity was assesed. Next, we investigated physical activity by telemetric system adapted for minipigs. We explored a cohort of 30 animals at the age of 4-7.9 years during the 4 following years.

We assessed the gait of minipigs on the straight dry floor as well as in the test challenged by obstacle. Significantly decreased walking score was evident in 6-7.9-year-old TgHD boars when they manifested different movements of hind-legs in comparison to WT males. Conversely, we detected remarkable deceased walking score in 4-5.9-year-old TgHD sows, while the decline was not such obvious in TgHD sows at 6-7.9 years. In Hurdle test, age-dependent (non-significant) impairment was observed in TgHD boars while (non-signifiant) improvement was detected in 6-7.9-year-old TgHD females. We supposed that the different body constitution of males and females caused sex-related differences in both tests. Morover, lower ABMI of 6-7-year-old TgHD females could facilitace their movement performance, and therefore older TgHD sows showed similar or improved score in Walking and Hurdle tests. Pull back test was performed to estimate the reaction of animals to unexpected disruption of their balance. TgHD boars revealed disturbed balance and longer corrective response to unexpected shove. The Tongue test was assesed to monitor fine motor skills. TgHD boars reached significantly decreased score in reaching the treats from the holeboard while TgHD sows obtained very similar score to WT ones.

Cognitive decline was investigated by Skittles and Cover pan tests. TgHD boars showed age-dependent diminution in cognitive performance. TgHD sows showed more effort to perform the tests and their scores were similar to WT females.

Stress-induced tests required courage to succeed in the task. Thus, the response to stress stimuli and a recollection of memories reflected the abilities and characters and emotions of the individual animals. Balance beam and Seesaw tests revealed continuous age-dependent decline in TgHD animals, significant in 6-7.9-year-old TgHD boars.

The physical activity was investigated by telemetric assessment in three different day intervals: Morning, Lunch and Afternoon. We revealed non-significantly reduced physical activity in TgHD boars of younger ages (2.6-4.5 years). However, from the age of 4.6 years the physical activity was decreased only in the morning period while increased during the lunch time and in the afternoon. Remarkably increased physical activity was observed between younger and older TgHD boars what could be ascribed to the manifestation of the disease progression.

In conclusion, all of the tests revealed perspicuous sex-related differences. Genotype-related impairment was observed in some motor tests and tests monitoring the stress-induced performance at the age of 6-7.9 years. We demonstated slow progression of clinical phenotype in adult TgHD minipigs.

My contribution

I participated on experimental design. I conducted experiments monitoring behavior and changes in motor and cognitive functions. I evaluated all of the data and interpreted the results. I wrote the draft of the manuscript.

Longitudinal study revealed motor, cognitive and behavioral decline in transgenic minipig model of Huntington's disease

[1,2]Monika Baxa, [1,2]Bozena Levinska, [1,2]Monika Skrivankova, [1,3]Matous Pokorny, [1]Jana Juhasova, [1]Jiri Klima, [1, 4]Jiri Klempir, [1]Stefan Juhas* and [1]Zdenka Ellederova*

[1]Laboratory of Cell Regeneration and Plasticity, Institute of Animal Physiology and Genetics, Czech Academy of Science, Libechov, Czech Republic, [2]Department of Cell Biology, Faculty of Science, Charles University in Prague, Prague, Czech Republic, [3]Department of Circuit Theory, Faculty of Electrical Engineering, Czech Technical University in Prague, Prague, Czech Republic, [4]Department of Neurology and Centre of Clinical Neuroscience, First Faculty of Medicine, Charles University in Prague and General University Hospital in Prague, Prague, Czech Republic

*Shared correspondence authors:

Zdenka Ellederova
E-mail: ellederova@iapg.cas.cz
Tel: +420315639565
Address: Rumburska 89, 27721 Libechov, Czech Republic

Stefan Juhas
E-mail: juhas@iapg.cas.cz
Tel: +420315639555
Address: Rumburska 89, 27721 Libechov, Czech Republic

Keywords

Huntington's disease; large animal model; phenotyping; motor, cognitive and behavioral studies

Abbreviations

HD: Huntington's disease; HTT: huntingtin gene; mHTT: mutant huntingtin gene; TgHD: Transgenic for N-truncated mutant human huntingtin gene, WT: Wild-type

Summary statement

The transgenic minipig model of Huntington's disease demonstrates slowly progressive motor, cognitive and behavioral phenotype with later onset in adulthood.

ABSTRACT

Huntington´s disease (HD) is an inherited devastating neurodegenerative disease with no cure up to date. Several therapeutic treatments for HD are in development, nevertheless their safety, tolerability and efficacy need to be tested before translation to bedside. The monogenetic nature of this disorder enabled generation of transgenic animal models carrying mutant huntingtin gene (mHTT) causing HD. Large animal model reflecting disease progression in humans would be beneficial for testing the potential therapeutic approaches. Progression of motor, cognitive and behavioral phenotype was monitored in transgenic Huntington's disease minipigs (TgHD) expressing N-terminal part of human mHTT. New tests were established to investigate a physical activity by telemetry, and to explore stress induced behavior and cognitive changes in minipigs. The longitudinal study revealed significant differences in the 6 - 8 year-old TgHD animals compared to WT controls in majority of the tests. The telemetric study showed remarkable increased physical activity of 4.6 - 6.5 year-old TgHD boars during the lunch time as well as in the afternoon. The present phenotypic study showed progression of the disease in adult TgHD minipigs and therefore this model can be suitable for longstanding preclinical studies.

INTRODUCTION

The clinical symptoms of neurodegenerative Huntington‘s disease (HD) are motor, cognitive and behavioral impairments manifesting typically in mid-thirties (Nance, 1998). Motor problems include involuntary chorea like movement, poor balance, and disturbed fine motor skills (Beighton and Hayden, 1981; David et al., 1987). Most prominent cognitive symptoms include impaired judgment, the inability to initiate, sustain attention, and complete a task, and also difficulty with tasks requiring flexibility or speed (Brandt et al., 1984; Lai et al., 2018). The behavioral disturbances include anxiety, depression, irritability, obsessiveness, and impulsive and aggressive behavior interchanging with apathy (Eddy et al., 2016). HD is induced by abnormal polyglutamine elongation of the gene encoding the huntingtin protein (HTT). Even though, the cause was discovered in 1993, HD is still incurable and necessarily needs a suitable model for testing potential therapies. Large animal models can provide better preclinical outcomes including safety, biodistribution, longitudinal assessment, and efficacy of novel therapeutic approaches compared to rodents (Howland and Munoz-Sanjuan, 2014). Therefore, large animal models such a non-human primate (Kocerha et al., 2013; Yang et al., 2008), sheep (Jacobsen et al., 2010), and pigs or minipigs (Baxa et al., 2013; Uchida et al., 2001; Yan et al., 2018; Yang et al., 2010), have been generated.

Among them minipigs represent a good economical and ethical choice (Morton and Howland, 2013). Their brain is quite large and similarly structured as in humans. Their similar metabolism, body weight, longevity of 15-20 years, and high reproduction make them suitable for translational research (Vodička et al., 2005).

In 2009, transgenic minipig model for HD (TgHD) expressing N-terminal part of human mutated huntingtin (mHTT, 548 amino acids, 124 Q) was generated (Baxa et al., 2013). Generally, all tissues isolated from TgHD minipigs from different generations expressed human mHTT as well as endogenous HTT (Macakova et al., 2016; Vidinská et al., 2018). Broad phenotypic studies of TgHD minipigs compared to wild type (WT) siblings are ongoing. The phenotype development of the model was rather slow and the first clear phenotype preceding the neurodegenerative one was sperm and testicular degeneration linked with mitochondria metabolism and glycolytic impairment starting at 13 months of age (Krizova et al., 2017; Macakova et al., 2016). However, reduction of DARPP32, a marker of a proper function of spiny neurons, has been detected from 16 to 70 months (Baxa et al., 2013; Vidinská et al., 2018; Ardan et al., unpublished data). Also, other markers of neurodegeneration such as activation of microglia, and demyelination of white matter together with mHTT gradual fragmentation were revealed at 24 months (Vidinská et al., 2018). Next, mitochondrial DNA damage, and marker of metabolic alternation were detected at 48 months (Askeland et al., 2018). Furthermore, a perturbed mitochondrial function was detected in TgHD minipig muscle tissue starting at 36 months before alternation in muscle mitochondria ultrastructure and the first locomotor decline at the age of 48 months (Askeland et al., 2018; Rodinova et al., 2019 in press). A TgHD genotype specific significant cellular lost detected in striatum and cortex together with inclusions in the axons of some neurons were detected at 60-70 months (5-5.8 years) (Ardan et al., unpublished data).

This study aimed to longitudinally monitor motor, cognitive and behavioral phenotype of TgHD minipigs up to eight years. Gait, Hurdle and a Startbox back and forth tests using TgHD minipigs were established in George-Huntington's Institute in Muenster (Schramke et al., 2016; Schuldenzucker et al., 2017). Activity measured by telemetric system adapted for minipigs, and cover and skittle toys for cognitive measures and balance beam and seesaw for stress induced tests were established by us. Within the 4 following years 4 - 7.9 year-old (4-7.9Y) TgHD minipigs (n = 8) and their WT controls (n = 10) were monitored using motor, cognitive and behavioral tests and simultaneously, physical activity of TgHD boars (n = 6) and their WT siblings (n = 6) at the age of 2.5 - 6.5 years was investigated by telemetry.

RESULTS

Motor impairment

Since the clearest clinical hallmark of HD is movement detriment, unsteady gait and lack of coordination are perceived in patients (Caron et al., 1993; Vuong et al., 2018) the gait of minipigs was examined. The Walking test was performed on straight dry floor while the Hurdle test was challenged with an obstacle. Walking test (Fig. 1A) revealed impairment in TgHD animals. The decrease in walking score was significant in TgHD boars at the age of 6 - 7.9 years ($p = 0.013$) and in TgHD sows at 4 - 5.9 years ($p = 0.015$) compared side by side with their age matched WT controls. More evident changes in walking were observed among TgHD boars. TgHD animals exhibited different movement of hind legs. Tiptoes of TgHD boars tended centrically under their abdomen. Moreover, the movement of their ankles resembled the movement copying the arc shape (Suppl. 1). Remarkable sex related differences were observed between TgHD boars and TgHD sows in both younger (4 - 5.9Y) and older (6 - 7.9Y) animals ($p = 0.003$ and $p = 0.024$, respectively).

Both TgHD boars and TgHD sows reached lower (non-significant) score in the Hurdle test (Fig. 1B) related to their WT controls at the age of 4 - 5.9 years. Sex related difference was observed between 6 - 7.9 year-old TgHD boars and sows. TgHD boars showed continuing deterioration within ageing in comparison to WT animals while TgHD sows showed better test score at the age of 6 - 7.9 years.

Corrective responses to externally generated force pulses were disturbed in HD patients (Smith et al., 2000), therefore Pull back test (Suppl. 2) was introduced in minipigs. This test simulated unexpected disruption of animal´s balance. When 6 year-old TgHD boars were shoved in the haunch area, they lost their balance, hind legs got to slip and moved together aside in an opposite direction from which the sudden pulse occurred. Their front legs got to wider position in the effort to keep stability and not to fall. Control WT animals got balanced in a fleeting moment with no problem concerning their legs.

Next, fine motor skills were investigated. Motor impersistence manifesting as a difficulty to keep the tongue fully protruded for a few seconds was observed in HD patients (Huntington Study Group., 1996), therefore Tongue test was introduced to monitor the protrusion persistence of the animals. The number of reached treats test (Fig. 2A) showed significantly ($p = 0.004$) decreased score in TgHD boars but very similar score in TgHD sows in comparison to their WT controls. The Deepest reached hole test (Fig. 2B) revealed the decreased score in TgHD boars but almost the same score in TgHD sows compared to WT ones.

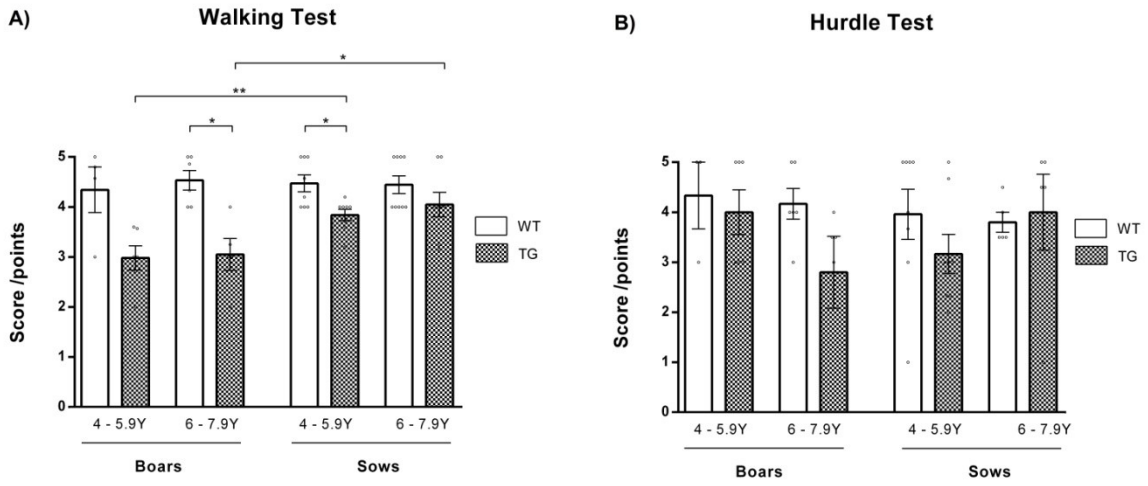

Fig. 1 Motor impairment. A) Walking test. The impairment in gait was observed in TgHD animals. The difference was significant in 6-7.9 year-old TgHD boars (p = 0.013) and 4-5.9 year-old TgHD sows (p = 0.015) in comparison to their WT controls. The decline was more obvious in TgHD boars than TgHD sows. Clear sex related differences were noticed between TgHD boars and TgHD sows of matching ages (p = 0.003 and p = 0.024, respectively). WT ♂ 4-5.9Y n = 4, WT ♂ 6-7.9Y n = 6, TgHD ♂ 4-5.9Y n = 6, TgHD ♂ 6-7.9Y n = 5, WT ♀ 4-5.9Y n = 8, WT ♀ 6-7.9Y n = 9, TgHD ♀ 4-5.9Y n = 8, TgHD ♀ 6-7.9Y n = 8. B) Hurdle test. The ability to cross the barrier declined in TgHD boars with the age. TgHD sows obtained worse score at the age of 4-5.9 years, while better score at the age of 6-7.9 years in comparison to their age matched WT controls. The difference was observed between TgHD boars and TgHD sows at the age of 6-7.9 years. WT ♂ 4-5.9Y n = 3, WT ♂ 6-7.9Y n = 6, TgHD ♂ 4-5.9Y n = 6, TgHD ♂ 6-7.9Y n = 5, WT ♀ 4-5.9Y n = 8, WT ♀ 6-7.9Y n = 5, TgHD ♀ 4-5.9Y n = 8, TgHD ♀ 6-7.9Y n = 5.

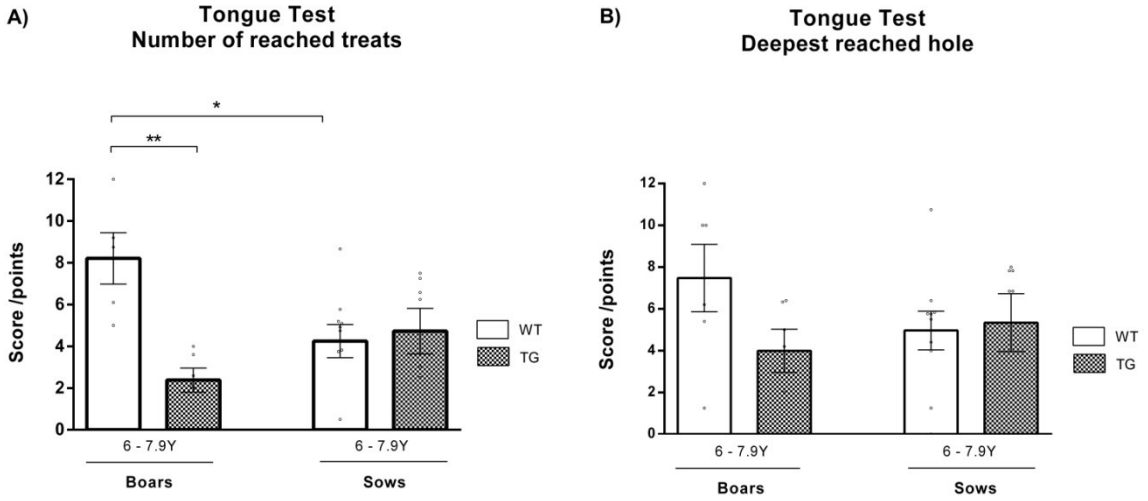

Fig. 2 Tongue protrusion persistence. A) Number of reached treats test revealed notably (p = 0.004) lower score in TgHD boars. B) The Deepest hole test showed decreased score in TgHD boars and the similar score in TgHD sows in comparison to their WT controls. WT ♂ 6-7.9Y n = 5, TgHD ♂ 6-7.9Y n = 6, WT ♀ 6-7.9Y n = 0, TgHD ♀ 6-7.9Y n = 7.

Cognitive changes

Cognitive deficits emerge in HD and ordinarily influence also ability to learn the tasks, spatial navigation and working memory. Hence, new tests for monitoring of these functions in minipigs were developed in this study. Skittles test consisted of a pan with 7 holes concealed by 7 different skittles. Pigs were expected to flip as many skittles as possible. The treats were hidden under the skittles. Cover pan test consisted of a pan with 6 holes closed by 6 different movable covers. Animals were expected to move the cover and to reach the treat hidden under it. Skittles test (Fig. 3A) showed notable ($p = 0.03$) lower score in TgHD boars in the age of 6 - 7.9 years than in their WT controls while TgHD females showed similar results to WT ones. Similarly, 6 - 7.9 year-old TgHD males obtained lower score in Cover pan test (Fig. 3B), while the scores of TgHD and WT females were comparable. The decline in score was observed in TgHD animals at the age of 6 - 7.9 years.

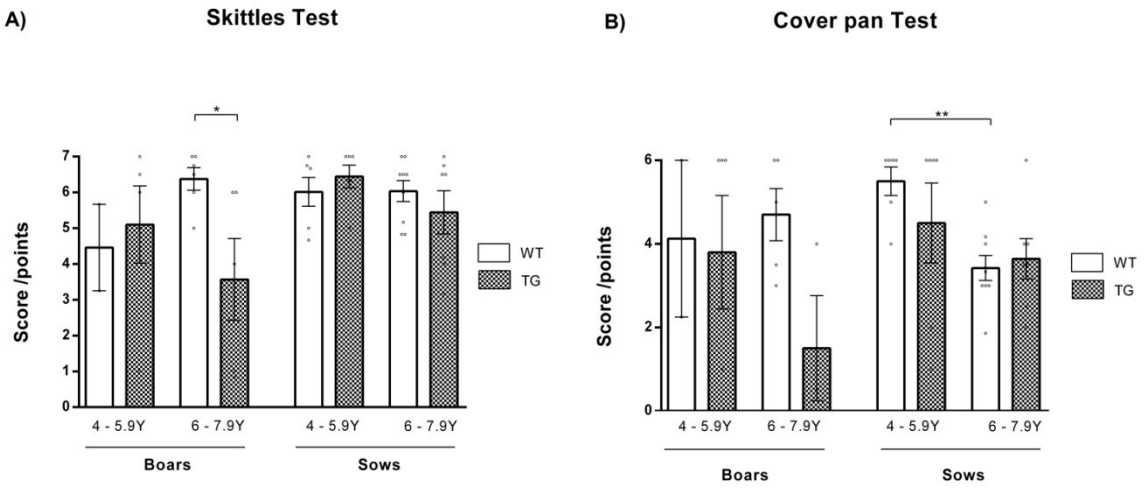

Fig. 3 Cognitive changes. A) Skittles test. Significantly ($p = 0.03$) decreased score was detected in TgHD boars compared to WT ones in the age of 6-7.9 years, but similar score among all sows. WT ♂ 4-5.9Y n = 2, WT ♂ 6-7.9Y n = 6, TgHD ♂ 4-5.9Y n = 5, TgHD ♂ 6-7.9Y n = 5, WT ♀ 4-5.9Y n = 6, WT ♀ 6-7.9Y n = 9, TgHD ♀ 4-5.9Y n = 6, TgHD ♀ 6-7.9Y n = 7. B) Cover pan test. Difference was revealed between 6-7.9 year-old TgHD boars and their WT controls. The impairment of the ability to perform the test within the ageing was observed. WT ♂ 4-5.9Y n = 2, WT ♂ 6-7.9Y n = 5, TgHD ♂ 4-5.9Y n = 5, TgHD ♂ 6-7.9Y n = 3, WT ♀ 4-5.9Y n = 6, WT ♀ 6-7.9Y n = 9, TgHD ♀ 4-5.9Y n = 6, TgHD ♀ 6-7.9Y n = 7.

Decline in stress induced performance

HD patients have difficulties in coping of stressful situations. Therefore, the tests inducing stress were also investigated. The Balance beam test (Fig. 4A) was previously applied in pig model of ataxia telangiectasia (Beraldi et al., 2015). Seesaw test (Fig. 4B) was newly

established in this study. Both tests showed lower score obtained by TgHD animals in comparison to WT controls. Significant alterations were detected between 6 - 7.9 year-old TgHD and WT boars in Balance beam and Seesaw tests ($p = 0.033$ and $p = 0.004$, respectively). The impairment worsened with the age, mainly in TgHD sows performing Seesaw test ($p = 0.024$). Boars obtained higher score in both tests compared to sows.

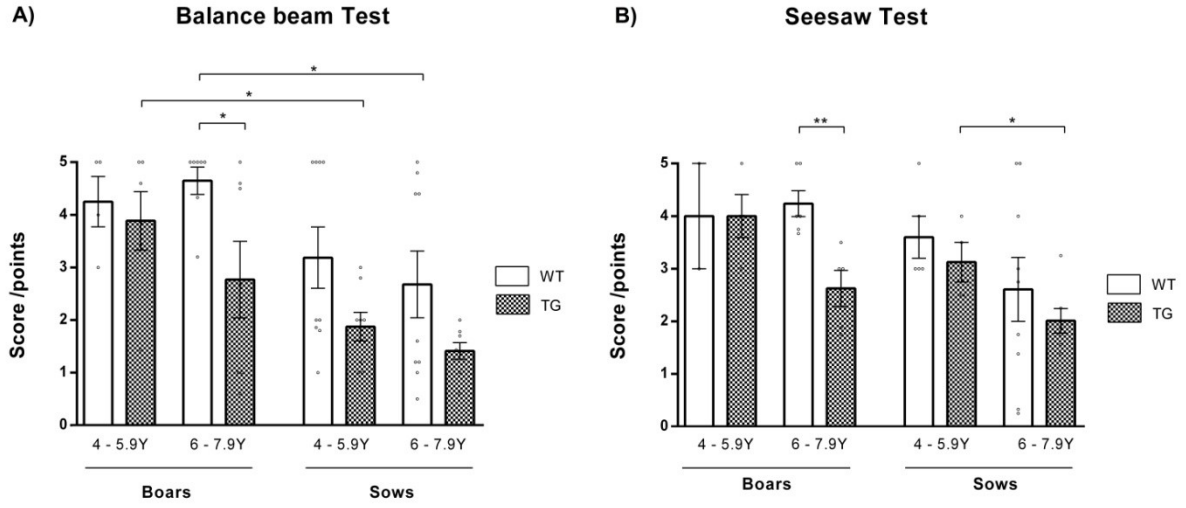

Fig. 4 Decline in stress induced performance. A) Balance beam test. Significant ($p = 0.033$) deterioration was observed in TgHD boars at the age of 6-7.9 years. Both TgHD and WT sows reached notable lower score than boars in older age ($p = 0.012$ and $p = 0.021$, respectively). The ability to pass the assessment decreased with the age in all TgHD animals. WT ♂ 4-5.9Y n = 4, WT ♂ 6-7.9Y n = 7, TgHD ♂ 4-5.9Y n = 6, TgHD ♂ 6-7.9Y n = 7, WT ♀ 4-5.9Y n = 9, WT ♀ 6-7.9Y n = 9, TgHD ♀ 4-5.9Y n = 8, TgHD ♀ 6-7.9Y n = 8. B) Seesaw test. TgHD boars obtained remarkably ($p = 0.004$) lower score than their WT controls. The reached score decreased within the ageing in all TgHD animals, significantly ($p = 0.024$) in TgHD sows. WT ♂ 4-5.9Y n = 2, WT ♂ 6-7.9Y n = 6, TgHD ♂ 4-5.9Y n = 4, TgHD ♂ 6-7.9Y n = 5, WT ♀ 4-5.9Y n = 5, WT ♀ 6-7.9Y n = 9, TgHD ♀ 4-5.9Y n = 4, TgHD ♀ 6-7.9Y n = 7.

Altered physical activity

People with HD tend to be less physically active in the morning while more active in the afternoon and evening what is considered to be concerned with sleep disturbances and shifted circadian rhythm of HD individuals (Herzog–Krzywoszanska and Krzywoszanski, 2019). The physical activity of minipigs was investigated by telemetric assessment. TgHD boars were monitored during one-week period in six different sessions. Physical activity was evaluated in three different day intervals: Morning (2:30-4:30 AM, before morning feeding), Lunch (9:40-12:00 AM, no external activity) and Afternoon (2:50-3:50 PM, before afternoon feeding). Total acceleration computed by telemetric system was averaged in 10 minute intervals. Evaluation of the Morning data (Fig. 5A) revealed decreased (non-significant)

activity in TgHD compared to WT controls. During the Lunch time (Fig. 5B) the physical activity of 2.6 - 4.5 year-old TgHD boars was comparable to WT ones while the physical activity of 4.6 - 6.5 year-old TgHD animals was significantly ($p = 0.026$) increased in comparison to WT controls. Accruement in the physical activity was notable ($p = 0.003$) also between 2.6 - 4.5 year-old and 4.6 - 6.5 year-old TgHD boars. Likewise, in the Afternoon (Fig. 5C) the physical activity was similar in younger animals (age 2.6 - 4.5 years) and increased in the older animals (age 4.6 - 6.5 years). The difference in the physical activity of TgHD animals during Lunch time and in the Afternoon was remarkably ($p = 0.003$ and $p = 0.002$, respectively) increased with the age.

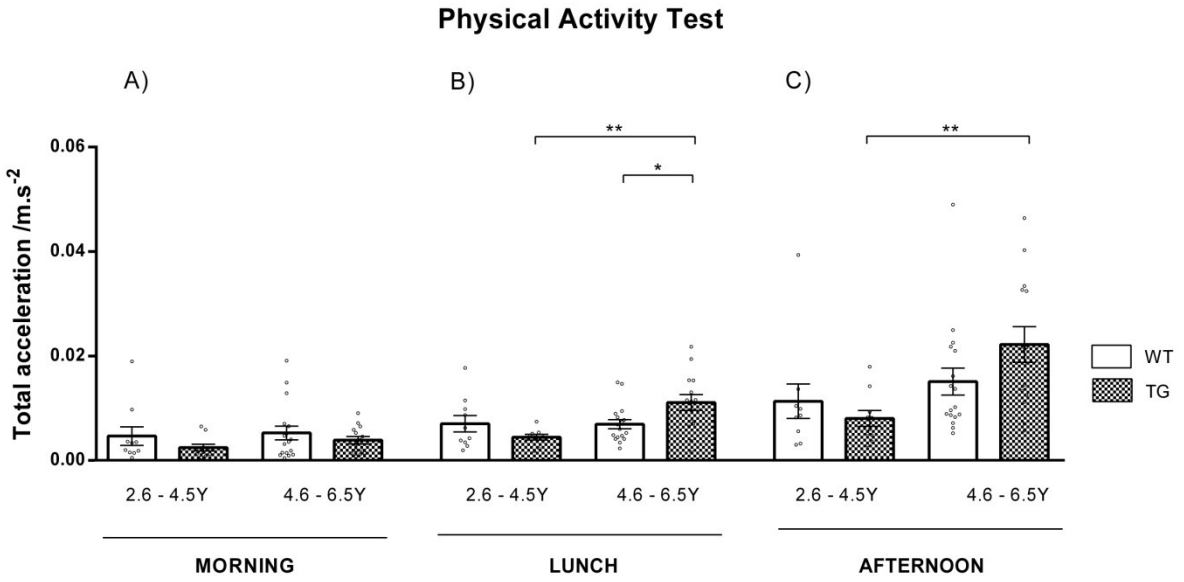

Fig. 5 Altered physical activity. A) Physical activity was lower in TgHD animals in the Morning. B) During the Lunch time, 2.6-4.5 year-old TgHD animals had comparable physical activity to their WT controls. The activity of 4.6-6.5 year-old animals was significantly ($p = 0.026$) higher than the controls. The activity notably ($p = 0.003$) increased with the age of TgHD animals. C) In the Afternoon, 2.6-4.5 year-old TgHD animals had a bit decreased physical activity in comparison to their WT controls while the activity of 4.6-6.5 year-old animals was higher than the controls. Increase in the physical activity was notable ($p = 0.002$) within ageing in TgHD animals. WT ♂ 2.6-4.5Y n = 7, WT ♂ 4.6-6.5Y n = 17, TgHD ♂ 2.6-4.5Y n = 10, TgHD ♂ 4.6-6.5Y n = 14.

DISCUSSION

Transgenic minipigs encoding truncated human mutant (124 Q) huntingtin (Baxa et al., 2013) were monitored in longitudinal phenotypic study utilizing motor, cognitive and behavioral tests. Previously, no significant difference was observed between TgHD and WT sows

up to 40 months of age (Schuldenzucker et al., 2017). A significant decline in the ability to perform the Tunnel test and a general tendency (non-significant) for reduced accomplishment in the other motor, behavioral and cognitive tests was detected in a mixed group of TgHD males and females at the age of 48 months (Askeland et al., 2018).
In this study Walking, Hurdle, Pull back, Tongue, Skittles, Cover pan, Balance beam, Seesaw, and Physical Activity tests were performed with a larger groups of animals at the age of 4 - 5.9 and 6 - 7.9 years whereas the impact of sex was taken into account. The overview of the test´s outcomes is illustrated in Table 1. The data obtained from the 4 following years enabled to compare the progress of the observed changes with the age of animals (age: x, x + 1, x + 2 and x + 3 years).

Table 1 Overview of the test´s outcomes. TgHD animals were compared to their sex- and age- matched controls. The impairment (↓), the improvement (↑) or the similarity (↔) in test performing is illustrated. (-) the test was not performed. Significance: * $p \leq 0.05$, ** $p \leq 0.01$, n = non-significant.

	TgHD ♂			TgHD ♀	
	4-5.9Y	6-7.9Y		4-5.9Y	6-7.9Y
Walking Test	$\downarrow^{n}$	$\downarrow^{*}$		$\downarrow^{*}$	$\downarrow^{n}$
Hurdle Test	$\downarrow^{n}$	$\downarrow^{n}$		$\downarrow^{n}$	↔
Tongue Test	-	$\downarrow^{**}$		-	↔
Pull back Test	-	$\downarrow^{n}$		-	-
Skittles Test	$\uparrow^{n}$	$\downarrow^{*}$		$\uparrow^{n}$	$\downarrow^{n}$
Cover pan test	$\downarrow^{n}$	$\downarrow^{n}$		$\downarrow^{n}$	↔
Balance beam Test	$\downarrow^{n}$	$\downarrow^{*}$		$\downarrow^{n}$	$\downarrow^{n}$
Seesaw Test	↔	$\downarrow^{**}$		$\downarrow^{n}$	$\downarrow^{n}$
Physical Activity Morning	$\downarrow^{n}$	$\downarrow^{n}$		-	-
Physical Activity Lunch	$\downarrow^{n}$	$\uparrow^{*}$		-	-
Physical Activity Afternoon	$\downarrow^{n}$	$\uparrow^{n}$		-	-

Stricken gait problems to maintain upright posture and impaired balance are obvious motor symptoms in HD patients (Rüb et al., 2013). Contrary to humans, animal models except of non-human primates, are tetrapods, therefore they are more stable in motion.

Still, Walking, Hurdle and Pull back tests showed the motor impairment in TgHD minipigs. Worsening in Walking test was evident in TgHD boars, remarkable at the age of 6 - 7.9 years while it was not so obvious in TgHD sows. We suppose that this fact is caused by the body constitution of males and females. Sows are lower and wider while boars are higher, thus the center of gravity provides an advantage to females. Center of gravity is more rostral in boars what could make them more vulnerable to lose their balance on hind legs. Significant decline in walking was observed in TgHD sows at 4 - 5.9 years of age. We assume that the reason relates to lower Animal Body Mass Index (ABMI, calculated as a ratio among animal´s weight, height and length) of TgHD sows at 6 – 7 years compared to WTs (Ardan et al., unpublished data). Weight loss is a prominent feature of HD and it could facilitate the movement process of TgHD females. Similarly, worsening with age was observed in TgHD boars in Hurdle test, even though not significant. In sows, the lower score in Hurdle test was observed in younger (4-5.9Y) TgHD animals but improvement was detected in older (6-7.9Y) TgHD females. Again, we assume that the decreased weight of older TgHD females could help them to overcome the hurdle. Similar to HD patients, TgHD boars revealed disturbed balance and longer corrective response to unexpected shove. On the other hand, animals were able to learn from obtained experience and could predict that the shove situation could occur what was showed by increased ability to keep their stability when the test was repeated (data not shown). To our knowledge, these are the first impairments in motor phenotype with adult age onset described in HD large animal models.

Concerning fine motor skills, glossomotography proved an impairment of tongue protrusion in HD patients (Reilmann et al., 2010). Tongue tests showed that TgHD boars reached the treats from the holes of shallower depth. Moreover, the number of reached holes was significantly lower in comparison to WT males. A different situation was observed in TgHD sows. The number of reached holes, and their depth, was similar to WT controls. Similarly, no significant changes were detected in TgHD sows up to 40 months of age (Schuldenzucker et al., 2017). We suppose that this could be an effect of housing of TgHD and WT sows in shared cotes what could cause that WT dominate sow(s) had eaten more food and TgHD ones felt hungrier, therefore TgHD sows were more motivated to reach the treat. Moreover, this effect may be further supported by hyperphagia caused by attenuation of frontal lobe (cognitive and behavioral deterioration) commonly observed in HD patients (Trejo et al., 2004).

Similar phenomenon was observed in Skittle and Cover pan tests. These tests were assessed to investigate next distinctive feature of HD, cognitive decline (Dumas et al., 2013).

Age dependent diminution was observed in performance the cognitive tests in TgHD boars. TgHD sows had results similar to WT controls, thus showing more effort to perform the tests. Tests inquiring cognition were established in sheep, non-human primates and minipigs. Choice discrimination tests reflecting reversal learning were used in WT sheep (McBride et al., 2016) and TgHD minipigs (Schuldenzucker et al., 2017). No significant differences were observed neither in choice discrimination test nor in dominance test which was used for testing of dominant/aggressive behavior in TgHD sows up to 40 months of age (Schuldenzucker et al., 2017).

Balance beam and Seesaw tests mirror a response to stress stimuli and a recollection of memories. It represents tied connection between cognition and emotions (Marino and Colvin, 2015). Stress induced tests revealed a continuous decline in TgHD animals with age, significant in 6 - 7.9 year-old TgHD boars. All females obtained lower score in comparison to boars. These two tests required more courage to succeed in the task. Females and TgHD boars showed more fear to step on/pass the Balance beam/Seesaw. Thus, the impairment was a result of the abilities and characters and emotions of the individual animals.

Overall, TgHD animals spent shorter time performing the behavioral tests and achieved lower score for performed tasks (non-significant, data not shown), hence reflecting their reaction to stress – fear and consternation. Cognitive and Tongue tests showed decreased scores reached in the tests for TgHD boars which simultaneously spent shorter time by performing the tests (non-significant, data not shown). Tests showed that obtained experience caused that TgHD boars showed no interest to perform the task, because they realized that those were tasks in which they had minimal success. The reached test scores were lower than in WT controls (non-significant, data not shown). Contrarily, investigation time and achieved score were similar in TgHD and WT sows. TgHD sows showed more effort to perform these tests (non-significant, data not shown). Cognitive biases in pigs, similarly to humans, are influenced by mood and personality (Asher et al., 2016) and even if the emotions and mood are problematically investigated in pigs (Marino and Colvin, 2015), this study revealed the impact of pig´s emotions, personality and application of learning experiences on motor, cognitive and behavioral manifestation, furthermore connected to HD genotype.

Perspicuous sex related differences were observed in all test performed in this study. Even though both TgHD boars and TgHD sows had a reduced performance of the tests compared to WT, TgHD boars showed a significant decrease in performing Walking test, Balance test, Seesaw test and Skittles test at the age of 6 - 7.9 years, but sows did not. The boars demonstrated more courage to fulfill the tasks. The sows were generally fatter and

more hesitant by nature what presumably induced results achieved in the tests. Sex commonly modulates human behavior including many facets of human brain wide-spreading from ion channels to brain morphology (Cahill, 2014). The pattern of structural brain changes associated with huntingtin is strikingly different between men and women (Lee et al., 2017) what could explain observed differences in performing the tests among TgHD boars and sows.

Next, the automatic measurement for evaluation of the physical activity revealed non-significant diminution within the all day in TgHD boars of younger ages (2.6-4.5Y). But from the age of 4.6 years the physical activity was reduced only in the morning period while increased during the lunch time and in the afternoon. Significant accruement in physical activity was observed between younger and older TgHD boars what could be tied with the manifestation of the disease progression. Similarly, decreased morning activity and increased physical activity in later hours of the day occurred in HD patients. This feature is assigned to impaired circadian organization (Herzog-Krzywoszanska and Krzywoszanski, 2019; Kudo et al., 2011; Morton et al., 2005).

In conclusion, gradual progression of the disease was proved in TgHD minipigs. The outcomes correlate with the disease progression and can be applied for preclinical tests, particularly for ongoing longitudinal AAV5-miHTT preclinical testing in minipigs after they reach the age of phenotype manifestation. This approach was based on promising results from the short three months-study (Evers et al., 2018). Moreover, based on these and preliminary data of our current longitudinal experiment Food and Drug Administration as well as European Medicines Evaluation Agency approved this approach for phase I and II clinical trial. If here established methods and measures could prove postponing of phenotype development in our TgHD minipigs in ongoing longitudinal AAV5-miHTT experiments, it could together with the clinical data shorten the time for patients to receive the cure.

SUPPLEMENTAL FILES

Suppl. 1. Walking test. Video

Suppl. 2. Pull back test. Video

Suppl. 3. List of Animals in Longitudinal studies

MATERIALS AND METHODS

Animals

Transgenic minipigs (Sus scrofa domesticus, Linnaeus) with N-truncated human mutated huntingtin (Baxa et al., 2013) and their WT controls were used in this study. The individual animals were monitored by the tests during the 4 following years (2015 – 2018). 8 TgHD (4 males, 4 females) and 10 WT control (5 males, 5 females) animals in the age of 4 – 7.9 years were monitored in motor, cognitive and behavioral tests (Suppl. 3). Battery of behavioral tests was conducted 3 – 5 times each year. 6 TgHD minipigs and their 6 WT siblings in the age of 2.6 – 6.5 years were used for telemetry study (Suppl. 3). Physical activity was measured in six sessions (September 2015, December 2016, March 2017, September 2017, December 2017 and September 2018). All experiments were carried out according to the guidelines for the care and use of experimental animals and approved by the Resort Professional Commission of the CAS for Approval of Projects of Experiments on Animals (Approved protocol No. 53/2015).

Walking test

The changes in gait were observed by walking of the animal on the dry, straight floor. The gait was video-recorded in six-month interval. Scoring was as follows: 5 points for no visible gait problem and fluent walking, 4 points for slightly uneven weight bearing on one or more legs, 3 points for obvious deviation in weight bearing on one or more legs, with clear difficulties in walking, 2 points lowering of hind quarters close to the ground, placement of hind legs under the body, 1 point if the pig is unable to move 0 points if the animal refused to perform the test (Askeland et al., 2018).

Hurdle test

In the hurdle test (Fig. 6A) the animals were expected to pass the hurdle (height 15 cm, width 100 cm. Scoring was as follows: 5 points for passing across the hurdle without touching; 4 points for passing across the hurdle with touching of one leg; 3 points for passing across the hurdle with touching of two legs; 2 points for passing across the hurdle with touching of three legs; 1 point for passing across the hurdle with touching of 4 legs; 0 points if animal refused to perform the test (Askeland et al., 2018).

Pull back test

The animals were let to walk on dry, flat floor and unexpected shove was performed to the haunches area. The stability and reaction to sudden external force were evaluated.

Tongue test

Tongue test (Fig. 6B) was performed similarly as described previously (Schramke et al., 2016; Schuldenzucker et al., 2017). Shortly, a board containing 12 holes with stepwise increasing depth from 1 - 6.5 cm was used. Pigs were expected to pick up as many treats (biscuits) as possible from a board. The holes were marked from 1 (the shallowest one) to 12 (the deepest one). Two parameters were analyzed and the scoring was as follows: In the Tongue Number of reached treats test 1 point for each one hole with eaten treat, and in the Tongue Deepest hole test the score was the same as a mark of the deepest hole from which the treat was reached.

Skittles test

In the Skittles test (Fig. 6C) the animals were expected to flip as many skittles as possible. Scoring was as follows: 1 point for each one tumbled skittle (1-7 points) and 0 points if animal refused to perform the test.

Cover pan test

Cover pan (Fig. 6D) obtained a treats hidden under the 6 movable/sliding covers. Animals were expected to move the cover and reach the treat under it. Scoring was as follows: 1 point for each one moved cover (1-6 points) and 0 points if animal refused to perform the test.

Balance beam test

The balance beam (Fig. 6E) consists of 2.5 m long inclined plane, 3.0 m long beam and extended plane (1.15 x 1.3 m). The animal was expected to step up to an inclined plane, cross the beam, turn back in the extended part and return back down. Scoring was as follows: 5 points for passing across the whole beam, turning in the extended part and going back down; 4 points for passing across the whole beam, not turning in extended part, crawfishing back down; 3 points for stepping on (any part of the) beam; 2 points for stepping on inclined plane with all 4 legs; 1 point for stepping on inclined plane with 2 forelegs and 0 points if animal refused to perform the test (Askeland et al., 2018).

Seesaw test

During the seesaw test (Fig. 6F) the pig was expected to pass over the seesaw (3.0 m in length and 0.4 m in width. Scoring: 5 points for passing across the whole seesaw; 4 points for passing to the equilibrium position, crawfishing back down; 3 points for stepping onto and walking on the seesaw with all 4 legs (the equilibrium position is not reached); 2 points for stepping on the seesaw and crawfishing back; 1 point for stepping on the seesaw with only two fore legs; 0 points if animal refused to perform the test (Askeland et al., 2018).

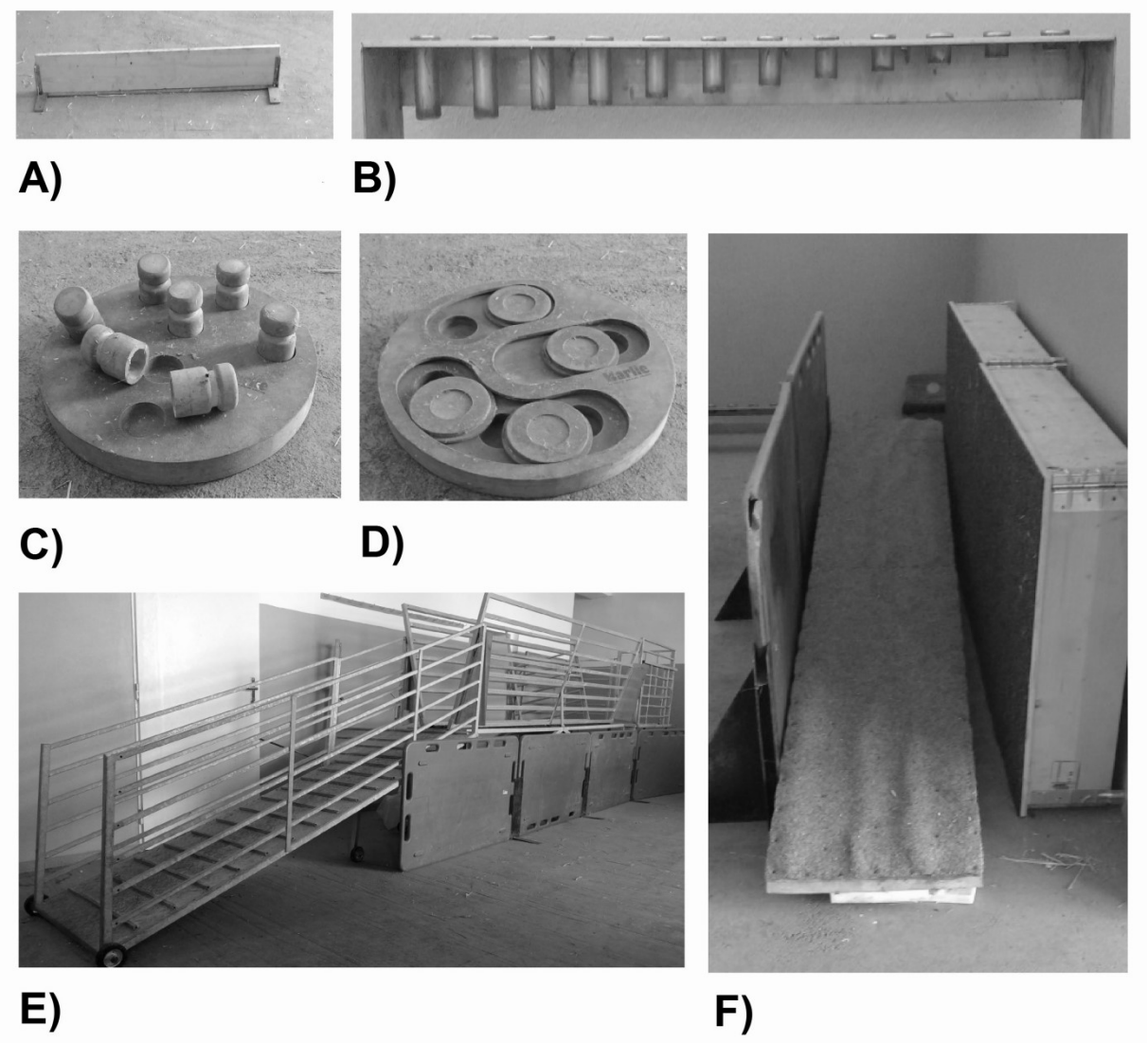

Fig. 6 Motor, cognitive and behavioral studies equipment. A) Hurdle. B) Tongue board. C) Skittles pan. D) Cover pan. E) Balance beam. F) Seesaw.

Telemetric monitoring of Physical activity

TgHD boars were monitored during one week in each session. Physical activity was evaluated in 3 different day intervals: Morning (2:30-4:30 AM, before morning feeding), Lunch (9:40-12:00 AM) and 3rd Afternoon (2:50-3:50 PM, before afternoon feeding). Telemetric system rodentPACK2 obtained from emka TECHNOLOGIES (France) was used in the experiments. Telemetric system consisted of small transmitters and central receivers. Every transmitter could acquire x, y, z and total acceleration. Data were sampled at frequency 100 Hz with resolution ± 2g. Minipig boars wore collars with transmitters during the experiments (Pokorny

et al., 2015). PC collected and stored data from receivers using iox2 software from emka TECHNOLOGIES. All events during the measurement sessions were recorded, e. g. time of feeding, cleaning, veterinary and technician intervention or other activities. The first session including no disturbing activities was used for the statistical analysis. The period of early morning (just before staff coming after night (before morning feed)) was analyzed. This period is hypothetically daily time with minimal external influences. Total acceleration (gravity acceleration [g]), computed by telemetric system and representing the physical activity of animal, was processed by our scripts for open-source tool SciLab. The total physical activity was sampled at 100 Hz and averaged over 10 min. Generated physical activity (mean from 10 min) from the TgHD and the WT boars were consequently averaged and used for statistical analysis.

Statistics

Evaluators of all of the tests were blinded for the genotype of the animals. All statistics were carried out in GraphPad Prism. Calculation of statistical significance was computed using Student's t-test or Mann-Whitney test. All figures show the mean results and error bars represent standard error of the mean (SEM). Significance was set to $p \leq 0.05$ (* $p \leq 0.05$, ** $p \leq 0.01$).

CONFLICT OF INTEREST

The authors have no conflict of interest to report.

FUNDING

The research leading to these results has received funding from the Norwegian Financial Mechanism 2009-2014 and the Ministry of Education, Youth and Sports under Project Contract number MSMT-28477/2014, COST LD15099, National Sustainability Programme, project number LO1609 (Czech Ministry of Education, Youth and Sports), and by institutional research support from Charles University in Prague PROGRES Q26/LF1/ 3.

AUTHOR CONTRIBUTION STATEMENT

MB, BL, and MS performed the behavioral studies. SJ, MP, JJ and JKl performed telemetry study. MB, BL, MS, SJ, MP and ZE designed the experiments and interpreted results. MB and ZE wrote the manuscript and SJ and JK revised it. All authors discussed the results and commented on the manuscript.

REFERENCES

Asher, L., Friel, M., Griffin, K. and Collins, L. M. (2016). Mood and personality interact to determine cognitive biases in pigs. *Biology letters* **12**,.

Askeland, G., Rodinova, M., Štufková, H., Dosoudilova, Z., Baxa, M., Smatlikova, P., Bohuslavova, B., Klempir, J., Nguyen, T. D., Kuśnierczyk, A., et al. (2018). A transgenic minipig model of Huntington's disease shows early signs of behavioral and molecular pathologies. *Disease Models & Mechanisms* **11**, dmm035949.

Baxa, M., Hruska-Plochan, M., Juhas, S., Vodicka, P., Pavlok, A., Juhasova, J., Miyanohara, A., Nejime, T., Klima, J., Macakova, M., et al. (2013). A Transgenic Minipig Model of Huntington's Disease. *Journal of Huntington's disease* **2**, 47–68.

Beighton, P. and Hayden, M. R. (1981). Huntington's chorea. *South African medical journal = Suid-Afrikaanse tydskrif vir geneeskunde* **59**, 250.

Beraldi, R., Chan, C.-H., Rogers, C. S., Kovács, A. D., Meyerholz, D. K., Trantzas, C., Lambertz, A. M., Darbro, B. W., Weber, K. L., White, K. A. M., et al. (2015). A novel porcine model of ataxia telangiectasia reproduces neurological features and motor deficits of human disease. *Human Molecular Genetics* **24**, 6473–6484.

Brandt, J., Strauss, M. E., Larus, J., Jensen, B., Folstein, S. E. and Folstein, M. F. (1984). Clinical correlates of dementia and disability in Huntington's disease. *Journal of clinical neuropsychology* **6**, 401–12.

Cahill, L. (2014). Fundamental sex difference in human brain architecture. *Proceedings of the National Academy of Sciences of the United States of America* **111**, 577–8.

Caron, N. S., Wright, G. E. and Hayden, M. R. (1993). *Huntington Disease*.

David, A. S., Jeste, D. V, Folstein, M. F. and Folstein, S. E. (1987). Voluntary movement dysfunction in Huntington's disease and tardive dyskinesia. *Acta neurologica Scandinavica* **75**, 130–9.

Dumas, E. M., van den Bogaard, S. J. A., Middelkoop, H. A. M. and Roos, R. A. C. (2013). A review of cognition in Huntington's disease. *Frontiers in bioscience (Scholar edition)* **5**, 1–18.

Eddy, C. M., Parkinson, E. G. and Rickards, H. E. (2016). Changes in mental state and behaviour in Huntington's disease. *The Lancet Psychiatry* **3**, 1079–1086.

Evers, M. M., Miniarikova, J., Juhas, S., Vallès, A., Bohuslavova, B., Juhasova, J., Skalnikova, H. K., Vodicka, P., Valekova, I., Brouwers, C., et al. (2018). AAV5-miHTT Gene Therapy Demonstrates Broad Distribution and Strong Human Mutant Huntingtin Lowering in a Huntington's Disease Minipig Model. *Molecular Therapy*.

Herzog-Krzywoszanska, R. and Krzywoszanski, L. (2019). Sleep Disorders in Huntington's Disease. *Frontiers in psychiatry* **10**, 221.

Herzog–Krzywoszanska, R. and Krzywoszanski, L. (2019). Sleep Disorders in Huntington's Disease. *Frontiers in Psychiatry* **10**, 221.

Howland, D. S. and Munoz-Sanjuan, I. (2014). Mind the gap: Models in multiple species needed for therapeutic development in Huntington's disease. *Movement Disorders* **29**, 1397–1403.

Jacobsen, J. C., Bawden, C. S., Rudiger, S. R., McLaughlan, C. J., Reid, S. J., Waldvogel, H. J., MacDonald, M. E., Gusella, J. F., Walker, S. K., Kelly, J. M., et al. (2010). An ovine transgenic Huntington's disease model. *Human Molecular Genetics* **19**, 1873–1882.

Kocerha, J., Liu, Y., Willoughby, D., Chidamparam, K., Benito, J., Nelson, K., Xu, Y., Chi, T., Engelhardt, H., Moran, S., et al. (2013). Longitudinal transcriptomic dysregulation in the peripheral blood of transgenic Huntington's disease monkeys. *BMC Neuroscience* **14**, 88.

Krizova, J., Stufkova, H., Rodinova, M., Macakova, M., Bohuslavova, B., Vidinska, D., Klima, J., Ellederova, Z., Pavlok, A., Howland, D. S., et al. (2017). Mitochondrial Metabolism in a Large-Animal Model of Huntington Disease: The Hunt for Biomarkers in the Spermatozoa of Presymptomatic Minipigs. *Neurodegenerative Diseases* **17**, 213–226.

Kudo, T., Schroeder, A., Loh, D. H., Kuljis, D., Jordan, M. C., Roos, K. P. and Colwell, C. S. (2011). Dysfunctions in circadian behavior and physiology in mouse models of Huntington's disease. *Experimental neurology* **228**, 80–90.

Lai, J.-S., Goodnight, S., Downing, N. R., Ready, R. E., Paulsen, J. S., Kratz, A. L., Stout, J. C., McCormack, M. K., Cella, D., Ross, C., et al. (2018). Evaluating cognition in individuals with Huntington disease: Neuro-QoL cognitive functioning measures. *Quality of Life Research* **27**, 811–822.

Lee, J. K., Ding, Y., Conrad, A. L., Cattaneo, E., Epping, E., Mathews, K., Gonzalez-Alegre, P., Cahill, L., Magnotta, V., Schlaggar, B. L., et al. (2017). Sex-specific effects of the Huntington gene on normal neurodevelopment. *Journal of Neuroscience Research* **95**, 398–408.

Macakova, M., Bohuslavova, B., Vochozkova, P., Pavlok, A., Sedlackova, M., Vidinska, D., Vochyanova, K., Liskova, I., Valekova, I., Baxa, M., et al. (2016). Mutated Huntingtin Causes Testicular Pathology in Transgenic Minipig Boars. *Neuro-degenerative diseases* **16**, 245–59.

Marino, L. and Colvin, C. M. (2015). *Thinking Pigs: A Comparative Review of Cognition, Emotion, and Personality in Sus domesticus*.

McBride, S. D., Perentos, N. and Morton, A. J. (2016). A mobile, high-throughput semi-automated system for testing cognition in large non-primate animal models of Huntington disease. *Journal of neuroscience methods* **265**, 25–33.

Morton, A. J. and Howland, D. S. (2013). Large Genetic Animal Models of Huntington's Disease. *Journal of Huntington's Disease* **2**, 3–19.

Morton, A. J., Wood, N. I., Hastings, M. H., Hurelbrink, C., Barker, R. A. and Maywood, E. S. (2005). Disintegration of the sleep-wake cycle and circadian timing in Huntington's disease. *The Journal of neuroscience : the official journal of the Society for Neuroscience* **25**, 157–63.

Nance, M. A. (1998). Huntington Disease: Clinical, Genetic, and Social Aspects. *Journal of Geriatric Psychiatry and Neurology* **11**, 61–70.

Pokorny, M., Juhas, S., Juhasova , J., Klima, J., Motlik, J., Klempir, J. and Havlik, J. (2015). Telemetry Physical Activity Monitoring in Minipig's Model of Huntington's Disease. *Cesk Slov Neurol N*. 78/111 (Supplementum 2), 39-42

Reilmann, R., Bohlen, S., Klopstock, T., Bender, A., Weindl, A., Saemann, P., Auer, D. P., Ringelstein, E. B. and Lange, H. W. (2010). Tongue force analysis assesses motor phenotype in premanifest and symptomatic Huntington's disease. *Movement disorders : official journal of the Movement Disorder Society* **25**, 2195–202.

Rodinova, M., Krizova, J., Stufkova, H., Bohuslavova, B., Askeland, G., Dosoudilova, Z., Juhas, S., Juhasova, J., Ellederova, Z., Zeman, J., et al. (2019). Skeletal muscle in an early manifest transgenic

minipig model of Huntington's disease revealed deterioration of mitochondrial bioenergetics and ultrastructure impairment. *Disease Models and Mechanisms* - in press.

Rüb, U., Hoche, F., Brunt, E. R., Heinsen, H., Seidel, K., Del Turco, D., Paulson, H. L., Bohl, J., von Gall, C., Vonsattel, J.-P., et al. (2013). Degeneration of the cerebellum in Huntington's disease (HD): possible relevance for the clinical picture and potential gateway to pathological mechanisms of the disease process. *Brain pathology (Zurich, Switzerland)* **23**, 165–77.

Schramke, S., Schuldenzucker, V., Schubert, R., Frank, F., Wirsig, M., Ott, S., Motlik, J., Fels, M., Kemper, N., Hölzner, E., et al. (2016). Behavioral phenotyping of minipigs transgenic for the Huntington gene. *Journal of Neuroscience Methods* **265**, 34–45.

Schuldenzucker, V., Schubert, R., Muratori, L. M., Freisfeld, F., Rieke, L., Matheis, T., Schramke, S., Motlik, J., Kemper, N., Radespiel, U., et al. (2017). Behavioral testing of minipigs transgenic for the Huntington gene-A three-year observational study. *PloS one* **12**, e0185970.

Smith, M. A., Brandt, J. and Shadmehr, R. (2000). Motor disorder in Huntington's disease begins as a dysfunction in error feedback control. *Nature* **403**, 544–549.

Trejo, A., Tarrats, R. M., Alonso, M. E., Boll, M.-C., Ochoa, A. and Velásquez, L. (2004). Assessment of the nutrition status of patients with Huntington's disease. *Nutrition* **20**, 192–196.

Uchida, M., Shimatsu, Y., Onoe, K., Matsuyama, N., Niki, R., Ikeda, J. E. and Imai, H. (2001). Production of transgenic miniature pigs by pronuclear microinjection. *Transgenic Research* **10**, 577–582.

Unified Huntington's Disease Rating Scale: reliability and consistency. Huntington Study Group. (1996). *Movement disorders : official journal of the Movement Disorder Society* **11**, 136–42.

Vidinská, D., Vochozková, P., Šmatlíková, P., Ardan, T., Klíma, J., Juhás, Š., Juhásová, J., Bohuslavová, B., Baxa, M., Valeková, I., et al. (2018). Gradual Phenotype Development in Huntington Disease Transgenic Minipig Model at 24 Months of Age. *Neuro-degenerative diseases* **18**, 107–119.

Vodička, P., Smetana, K., Dvořáková, B., Emerick, T., Xu, Y. Z., Ourednik, J., Ourednik, V. and Motlík, J. (2005). The Miniature Pig as an Animal Model in Biomedical Research. *Annals of the New York Academy of Sciences* **1049**, 161–171.

Vuong, K., Canning, C. G., Menant, J. C. and Loy, C. T. (2018). Gait, balance, and falls in Huntington disease. In *Handbook of clinical neurology*, pp. 251–260.

Yan, S., Tu, Z., Liu, Z., Fan, N., Yang, H., Yang, S., Yang, W., Zhao, Y., Ouyang, Z., Lai, C., et al. (2018). A Huntingtin Knockin Pig Model Recapitulates Features of Selective Neurodegeneration in Huntington's Disease. *Cell* **173**, 989-1002.e13.

Yang, S.-H., Cheng, P.-H., Banta, H., Piotrowska-Nitsche, K., Yang, J.-J., Cheng, E. C. H., Snyder, B., Larkin, K., Liu, J., Orkin, J., et al. (2008). Towards a transgenic model of Huntington's disease in a non-human primate. *Nature* **453**, 921–4.

Yang, D., Wang, C. E., Zhao, B., Li, W., Ouyang, Z., Liu, Z., Yang, H., Fan, P., O'Neill, A., Gu, W., et al. (2010). Expression of Huntington's disease protein results in apoptotic neurons in the brains of cloned transgenic pigs. *Human Molecular Genetics* **19**, 3983–3994.

Paper VII

Grunting in a Genetically Modified Minipig Animal Model for Huntington's Disease – a Pilot Experiments

Tykalova, T., Hlavnicka, J., Macakova, M., ***Baxa, M****., Cmejla, R., Motlik, J., Klempir, J., and Rusz, J. (2015).*

.

Ces a Slov Neurol a Neurochir. 2015;78/111(Suppl 2):61-65.

IF 0.209

.

Motivation of the study

Voice and speech malfunctions have been reported in many of patients with HD. Even if humans and pigs have perceptible different anatomy of the articulation organs, the same trends in pathophysiological processes can be assumed in both porcine grunting and human phonation. Therefore, the main aim of the study was to design recording of grunting from minipigs.

Summary

We performed the experiments with a cohort of 17 TgHD and 16 WT age-matched controls. The recorder was fixed under the animal's belly. The microphone was then fastened on the top of the pig's head, close to its ears.

Firstly, we investigated the ways how to stimulate grunting in the minipigs. We tested both positive and negative stimulation including feeding, sound stimulation, hindering in movement or unpleasant touch. Feedeing resulted in the best outcomes. We obtained satisfactory grunting from 73% of animals. We chosen only rapidly-repeated or single grunts for evaluation; high-frequency squeals were not included in analyses. Despite the fact that no significant difference was detected in number of grunts, TgHD pigs tended to grunt more often and accomplished rapidly repeated grunts.

My contribution

I participated on experimental design and conducted the experiments.

Grunting in a Genetically Modified Minipig Animal Model for Huntington's Disease – Pilot Experiments

Chrochtání u geneticky modifikovaného zvířecího modelu miniprasat pro Huntingtonovu chorobu – pilotní experimenty

Abstract

Huntington's disease (HD) is an autosomal-dominant neurodegenerative disorder characterized by the impairment of voluntary and involuntary movements, behavioral disorders and cognitive decline. Besides the main motor symptoms, voice and speech disorders have been documented in a large majority of patients with HD. The animal model of pigs is often used in preclinical studies. Although there are obvious differences in the anatomy of the articulation organs between pigs and humans, the same trends in pathophysiological mechanisms can be expected in both grunting and human phonation. The main aim of the study was therefore to design a suitable experiment that would allow for acquisition of a sufficiently long recording of grunting from as many pigs as possible. The second goal was to perform the final version of the experiment in all available pigs and to evaluate the amount and quality of the acquired recordings. The database consists of 17 HD transgenic minipigs and 16 healthy siblings. Tested variants of the experiment, performed on subgroup of four sows, were divided into four subgroups: (a) positive – feeding, (b) positive – sound stimulation, (c) negative – hindering in movement, (d) negative – unpleasant touch. The evaluation of the quality of the elicited recording was performed using audio software where pure pig grunting was selected and all acoustic artefacts deleted. The best results were reached using the experiment in which: (i) a recording device is put on the pig's body, (ii) the pig is left alone for few minutes in the pen in order to calm down, and (iii) a person enters the room and tries to offer the pig food while walking backwards. As a result, the pig follows the person and grunts. Sufficiently long (20 single grunts or more) and clear recordings were received from 24 out of 33 pigs (73%). The realisation of the experiment is therefore possible.

http://dx.doi.org/10.14735/amcsnn20152S61

The authors declare they have no potential conflicts of interest concerning drugs, products, or services used in the study.
Autoři deklarují, že v souvislosti s předmětem studie nemají žádné komerční zájmy.
The Editorial Board declares that the manuscript met the ICMJE "uniform requirements" for biomedical papers.
Redakční rada potvrzuje, že rukopis práce splnil ICMJE kritéria pro publikace zasílané do biomedicínských časopisů.

T. Tykalova[1], J. Hlavnicka[1], M. Macakova[2], M. Baxa[2], R. Cmejla[1], J. Motlik[2], J. Klempir[3,4], J. Rusz[1,3]

[1] Department of Circuit Theory, Faculty of Electrical Engineering, Czech Technical University in Prague, Czech Republic
[2] Institute of Animal Physiology and Genetics, AS CR, v.v.i., Libechov, Czech Republic
[3] Department of Neurology and Centre of Clinical Neuroscience, 1st Faculty of Medicine, Charles University in Prague, Czech Republic
[4] Institute of Anatomy, 1st Faculty of Medicine, Charles University in Prague, Czech Republic

✉ **Ing. Tereza Tykalova**
Department of Circuit Theory
Faculty of Electrical Engineering
Czech Technical University in Prague
Technická 2
166 27 Praha 6, Czech Republic
e-mail: tykalter@fel.cvut.cz

Accepted for review: 5. 10. 2015
Accepted for print: 23. 10. 2015

Key words

Huntington's disease – grunting – transgenic pigs – animal models – voice and speech disorders

Klíčová slova

Huntingtonova nemoc – chrochtání – transgenní model miniprasat – animální modely – poruchy hlasu a řeči

Souhrn

Huntingtonova nemoc (HN) je autozomálně dominantní neurodegenerativní onemocnění charakterizované poškozením volních a mimovolních pohybů, poruchami chování a zhoršením kognitivních funkcí. Společně s hlavními motorickými příznaky byly poruchy hlasu a řeči pozorovány u většiny pacientů s HN. Zvířecí prasečí model je často používán pro výzkum v preklinických studiích. I přes zjevné rozdíly v anatomii artikulačních orgánů mezi prasaty a lidmi lze očekávat stejné trendy u patofyziologických mechanizmů s ohledem na chrochtání i lidskou fonaci. Hlavním cílem této studie bylo proto navržení vhodného experimentu, který umožní získání dostatečně dlouhého záznamu chrochtání od co největšího počtu prasátek. Dalším cílem studie bylo zrealizovaní výsledné verze experimentu na celé databázi a vyhodnocení množství a kvality získaných nahrávek. Databáze použitá pro studii zahrnovala 17 HN transgenních miniprasátek a 16 zdravých sourozenců ze stejných vrhů. Testované varianty experimentu, provedené na části databáze zahrnující čtyři prasnice, byly rozděleni do čtyř podskupin: (a) pozitivní – krmení, (b) pozitivní – zvuková stimulace, (c) negativní – bránění v pohybu, (d) negativní – nepříjemné doteky. Hodnocení kvality získaných nahrávek bylo provedeno s pomocí audio softwaru, ve kterém bylo izolováno čisté prasečí chrochtání a všechny akustické artefakty vymazány. Nejlepších výsledků bylo dosaženo s použitím experimentu při kterém: (i) je záznamové zařízení upevněno na tělo prasátka, (ii) prasátko je ponecháno několik minut o samotě v místnosti, aby se uklidnilo a (iii) osoba vstoupí do místnosti a snaží se nabízet prasátku krmivo zatímco před ním couvá. V důsledku tohoto jednání prasátko následuje osobu s krmením, což je doprovázeno chrochtáním. Dostatečně dlouhé (20 chrochtnutí a více) a čisté nahrávky byly získány od 24 z 33 prasátek (73 %). Závěrem lze tedy říci, že experiment je proveditelný.

Introduction

Huntington's disease

Huntington's disease (HD) is an autosomal-dominant inherited neurodegenerative disorder caused by an expansion in the number of CAG repeats (36 repeats or more) on the short arm of chromosome 4p16.3 in the Huntingtone gene [1,2], which is characterized by uncoordinated body movements, psychological dysfunction and a reduction in cognitive decline resulting in dementia. The prevalence of HD is estimated to be about 4–8 subjects for 100,000 people [3] with the onset of the first symptoms typically occurring in the fourth decade of life. From a clinical perspective, HD is primarily manifested by involuntary movements termed as chorea, which may be accompanied by bradykinesia, motor impersistence, and deficits in movement planning, aiming, tracing, and termination [4,5]. Additionally, rigidity or/and dystonia may occur in some cases as HD progresses. Although the onset of symptoms and the rate of progression may vary, the prognosis implies relentless deterioration with significantly reduced life expectancy, as no treatment is currently available to stop disease progression [6].

Animal models of HD

Animal models are crucial in the development, evaluation and validation of new drugs and therapies for neurological disorders. A wide range of HD animal models have been generated to date including nonmammalian animals (Drosophila, C. elegans or zebrafish), rodents, sheep, pigs and non-human primates (for review see [7].) In general, each of these animal models shows some biochemical and neuronal features similar to HD in humans [7]. In particular, most effort has been put into research of mouse and rat HD models, as these mammals are relatively cheap to maintain and easy to breed. Although the rodents contributed significantly to the understanding of the molecular basis for behavioural and neuronal abnormalities [7–9], rodents and humans differ in many ways. For example, HD and other neurodegenerative diseases are age-dependent disorders, yet the lifespans of rodents and humans differ drastically, indicating that aging processes in different species are not identical [10]. In addition, the anatomy, physiology and function of the brain in large mammals are much more complex than those of rodents. From the clinical point of view, the rodents' small brain size also limits their utility for using non-invasive imaging methods such as magnetic resonance imaging which are commonly used in human patients [11]. These differences clearly indicate that the anatomy as well as physiological function of monkeys and pigs are much closer to humans than those of rodents, and also explain why large animal models would be better for mimicking the pathological features seen in human patients [10]. Using of transgenic minipigs is also more cost-effective and raises fewer ethical issues compared to primates.

Voice and speech disorders in human HD and pig animal model of HD

Voice and speech disorders, known as hyperkinetic dysarthria, are a common sign of HD, developing in more than 90% of HD patients in the course of the disease [12]. Typical signs of hyperkinetic dysarthria in HD include voice dysfunction, articulation deficits, irregular loudness variation and abnormalities in speech timing [12–16]. Interestingly, slight changes in voice and speech production have also been observed in persons with preclinical stages of HD [13,16]. Voice and speech disorders may thus have the potential to serve as a valuable biomarker of disease onset [13,16] and may help to determine the appropriate time for medical interventions in the preclinical trials focused on neuroprotective treatment.

Although there are obvious differences in the anatomy of articulation organs between pigs and humans, one might expected that similar trends of decreasing voice quality and articulatory undershooting will be observed in both grunting and human phonation due to the same HD-related pathophysiology mechanisms. For instance, if the imprecise articulation of vowels in human HD patients is characterized by centralization of formant frequencies [12], a similar trend can be expected in HD pig grunting since the articulatory organs (tongue, lips, soft palate, jaw, and pharynx cavity) in both models should have been influenced by the same motor disturbances such as chorea, rigidity or bradykinesia. Indeed, in a previous study [14] investigating phonatory dysfunction in 34 HD patients, a correlation was found between voice deficits and involuntary (rigidity, dystonia, and chorea) components of Unified HD Rating Scale.

Types of grunting in healthy pigs

The previous study [17] investigated the types of vocalization in a group of 67 large

Fig. 1. Fixation of recording device.

Fig. 2. Final design of the experiment with supportive devices.

white pigs and revealed three distinctive types of pig grunting: (a) *single grunts* – appear to be associated with investigatory behaviour or contact calls in group, (b) *single squeals* – may have similar function as single grunts but result from a higher level of arousal and (c) *rapidly repeated grunts* – appear to have either a greeting or threat function [17]. From acoustical point of view, squeals that are mainly expressed in situations of urgent threat or high stress are high-frequency calls while grunts are typically low-frequency calls [18]. Although there is no previous research focused on possible acoustic grunting changes due neurodegenerative disorders in animal pig models, it might be expected that low-frequency calls, i.e. rapidly repeated or single grunts, will be more suitable for acoustic analyses.

Recording experiment

In the previously published literature [17–22] focusing mainly on investigation of stress correlates or possibility to distinguish different emotional states, several types of experiments were used to obtain pig vocalization. It appears that the most popular experiment involved castration [18–20] or isolation of the subject from groupmates [21] or piglets from sows [18,20]. Another experiment applied positive stimulations such as nursing grunting or reunion with sows to provoke grunting [18,20,22]. However, most of these experiments are limited to sows and piglets or cannot be repeated frequently, which would limit their practical usage in the preclinical trials where determination of the appropriate time for medical interventions would be of interest.

The aims of the study

The main aim of the study was to design a suitable experiment that would allow acquisition of a sufficiently long recording of grunting from as many subjects as possible and, at the same time, would be applicable to pigs of different ages and genders with the possibility of repeating the experiment several times with the same subject. The second goal was to perform the final version of the experiment with all available pigs and to evaluate the amount and quality of the acquired recordings.

Methodology

Database of pigs

The database consists of 17 HD transgenic minipigs (4 male, 13 female) and 16 healthy siblings (1 male, 15 female). The animals were from the first, second and third generation. The mean age of HD transgenic minipigs group was 32.5 (SD 15.6, range 8–60) months while the mean age of healthy minipigs group was 23.7 (SD 16.3, range 8–60) months. No significant differences in age were found between the healthy and the transgenic group ($p = 0.12$). All animals were born and bred at the experimental farm of the Institute of Animal Physiology and Genetics in Libechov [23].

Recording device

Speech samples were recorded using 24bit 96kHz wave/MP3 recorder (Edirol R-09HR, Roland, Japanese) and a head-mounted condenser microphone (Beyerdynamic Opus 55, Heilbronn, Germany) which were previously successfully used by our group for the recording and subsequent analyses of voice and speech disorders in persons with HD [12,14]. Grunt signals were sampled at 48 kHz with 16bit resolution. The recording volume acquire was kept constant over the recording procedure in all pigs. The recorder was put into a small cloth case with lockable zippers and an adjustable fabric belt and fastened around the pig's body so that the recorder was situated under the pig's belly. The microphone was then fixed with sticking tape on the top of the pig's head close to its ears. In addition, the cable connecting microphone with recorder was fixed on the pig's back, so as not to become twisted between the pig's forelegs. As a result, the microphone was situated approximately 15 to 25 cm from the pig's snout based on its size. See Fig. 1 for details of recording device fixation.

Proposed versions of the experiment

In previously published literature, mainly experiments including piglets or nursing sows were used [18,20,22] for acquisition of pig vocalizations. However, reliance on the female gender and specific time periods would limit the practical usage of such experiments in the preclinical trials where determination of the appropriate time for medical interventions would be of interest. Moreover, experiments with a strongly negative context are also not feasible, as pigs might not be willing to collaborate if repeating of experiment is required. Therefore we decided to design and test other possible variants of experimental design. For testing purposes, a subgroup of 4 pigs including 2 healthy and 2 transgenic sows from the second generation was used. Tested va-

riants of the experiment were divided into four subgroups:

1. Positive – feeding:
- bowl with fodder brought into the room by well-known person,
- small titbit (10 raisins) hidden around the room or in a heap of straw,
- bowl with fodder hidden under a large perforated object.

2. Positive – sound stimulation:
- recorded sound of another pig's grunting playing from loudspeaker,
- recorded sound of barking dog playing from loudspeaker.

3. Negative:
- a known person will enter the room and stay motionlessly facing a wall for 5 min,
- the pig will be left alone in the room for 5 min while behind the door people will speak loudly,
- the pig will be left alone in the room for 5 min while behind the door another pig of the opposite sex or their piglets will be fetched up,
- a person will hinder the pig from strolling freely around the room using big plastic boards,
- the pig will be annoyed by a person (touching ears, scratching on head etc).

4. Another modification of experiment based on acquired experiences.

The final standardised version of the experiment was proposed based on results obtained from the tested variants and performed with all 33 available subjects.

Evaluation of acquired recordings

The evaluation of the amount and quality of elicited recording was performed using the acoustics software Praat [24]. The parts of recordings that included pure pig grunting with no acoustic artefacts (i.e., human speech, smacking or chewing of pigs, stamping of hoofs, tinkling of handle of bucket or other background noise) were separated. In addition, all parts of the recording that were too loud or too quiet with respect to setting of the recording acquire were also deleted. We selected only rapidly-repeated or single grunts; high-frequency squeals were not involved. To ensure the same experimental condition for all pigs, the gruntings were selected within first 5 min after the actual beginning of the experiment. For the purposes of further analyses, rapidly repeated grunts were recalculated and treated as single grunts; as a result, 30 „single grunts" per pig were selected if available. Subsequently, the type of presented grunting, the total number of grunts, and duration of recording procedure were calculated for each pig. Finally, the percentage of correctly recorded pigs was assigned.

Tab. 1. Breakdown by number and type of grunting.

Number of grunts	Transgenic pigs (n = 17)			Healthy control pigs (n = 16)		
	number of pigs	SG	SG + RRG	number of pigs	only SG	SG + RRG
0	2	–	–	3	–	–
1–20	0	–	–	4	4	0
21–40	4	2	2	6	4	2
41–80	8	2	6	1	0	1
>80	3	0	3	2	0	2

SG – single grunts, RRG – rapidly repeated grunts.

Statistics

As the Kolmogorov-Smirnov test for independent samples showed that the parameters were normally distributed, the two sample t-test was used to assess group differences. The Pearson coefficient was calculated to determine correlations between age and number of grunts. The level of significance was set at $p < 0.05$.

Results

Proposed versions of the experiment

The tested sows did not respond optimally for any of the proposed experiments mentioned in the methodology. In particular, they did not react at all to the person, who brought the bowl with fodder into the room. Searching for raisins hidden around the room resulted in continued smacking but no grunting. Although the pigs were very interested in the bowl with fodder hidden under a large perforated crate, the occasional grunting they performed was also accompanied by disturbing acoustic artefacts in the form of noise caused due to hitting into the box in an effort to lift it, which prevented the practical use of the recordings. Furthermore, the crate was quickly demolished by the pigs.

Positive sound stimulations in the form of another pig's grunting or a barking dog also resulted in the pig's reaction; however, the response was only in the form of adjustment of the head and ears in the direction of the sound. In addition, they were interested in sound stimulus only for a short period of time and when they heard the same recording for the third time, they do not react at all.

Negative stimulation turned to be slightly better with respect to grunting. In particular, pigs did not respond to the familiar person ignoring them or to the presence/occasional grunting of other pig or piglets behind the wooden door, i.e., they did not try to communicate with them. On the other hand, hindering pigs from strolling freely around the room using big plastic boards and annoying them with unpleasant touches indeed resulted in pigs grunting. Pigs were annoyed mainly by touches associated with slapping, scratching or squeezing under the neck and around ears. However, hindering with boards led mainly to single squeals, and single grunts were presented only occasionally. With respect to irritating touches, apart from the single squeals also single grunts relatively often occurred.

Design of final experiment

Due to the disappointing results of the originally proposed experiments, various modifications were subsequently tested. The best results were eventually reached using experiment where: (i) a recording device is put on the pig's body, (ii) the pig is left alone for a few minutes in the pen in order to calm down, and (iii) a person enters the room and tries to offer the pig fodder while walking backwards. As a result, the pig follows the person and grunts. Food is necessary to offer using the aids that pigs know from everyday life; in our case it was a metal bucket and a plastic scoop of angular shape (Fig. 2). To

increase the effectiveness of the experiment (the amount of obtained grunting), it is feasible to use supportive sounds, e. g., clinking of metal handle with the bucket. In addition, it is useful to perform the experiment with hungry pigs (omitting two feeding doses) and with a well-known figurant (a person from whom the pigs are accustomed to get food). Although the experiment worked successfully even without these supportive conditions, more time was demanded to obtain the required amount of grunting. The presented design of the experiment led mainly to rapidly repeated grunts or single grunts that are thought to be more suitable for acoustic analysis than squeals.

Evaluation of acquired recordings

Using the final version of the experiment, we were able to record grunting samples of appropriate quality and amount (at least 20 single grunts) from 24 out of 33 pigs (73%). The mean number of grunts in the HD transgenic group was 53.0 (SD 34.3, range 0–120) while the mean number of grunts in the healthy group was 33.5 (SD 41.3, range 0–155). Although there were found no significant difference in number of grunts between both groups ($p = 0.15$), the transgenic pigs tend to grunt more and also often performed rapidly repeated grunts. Interestingly, no correlation was revealed between age and number of grunts ($r = 0.002$, $p = 0.98$). Detailed results on the number and type of grunting are depicted in Tab. 1. Considering the duration of the experiment, the average time was 13.5 (SD 3.0, range 9–20) min with no differences between groups ($p = 0.77$).

Discussion

As a part of this study, a standardized version of the experiment based on manipulative offering of fodder to pigs was designed and resulted in a satisfactory amount of grunting in 73% of pigs while only five pigs (15%) remained entirely silent. These results are comparable with other studies, as some silent or motionless behaviours have also been previously reported [17,18,20]. For instance, the study by Tallet et al. [18] which surveys vocalization of 84 piglets from 34 litters using 11 different contexts of emission, reported that in some situations such as nursing only one or two piglets of a litter generally vocalise.

On the contrary, a study by Marchant et al. [17] achieved obviously better results, as they were capable to obtain vocalization from 66 out of 67 gilts using a standard human approach test. Unfortunately, we cannot agree with these findings since we have tried to replicate this kind of experiment in a subgroup of four pigs and did not record almost any vocalization at all. This discrepancy might be caused by the different level of pig socialization with humans, since we observed that our pigs were rather afraid than curious considering presence of an unfamiliar person. Indeed, the lower level of socialization might also be a reasonable explanation why our healthy pigs tend to produce fewer vocalizations than transgenic ones.

Conclusion

With positive motivation using food and appropriate visual and audio stimulations, it is possible to persuade pigs to grunt. Sufficiently long (20 single grunts) and clean recordings were received from 73% of pigs. Our experiment is designed to be applicable to both genders and various ages and thus might be successfully used for acquisition of pig grunting in future research focused on longitudinal investigation of possible disturbances in pigs' vocalization due to HD.

Acknowledgements

The study was supported by the Czech Science Foundation (GACR 102/12/2230), Czech Technical University in Prague (SGS 15/199/OHK3/3T/13) and Charles University in Prague (PRVOUK-P26/LF1/4). This work was also supported by ExAM CZ.1.05/2.1.00/03.0124.

References

1. Gusella JF, Wexler NS, Conneally PM, Naylor SL, Anderson MA, Tanzi RE et al. A polymorphic DNA marker genetically linked to Huntington's disease. Nature 1983; 306(5940): 234–238.
2. Kremer B, Goldberg P, Andrew SE, Theilmann J, Telenius H, Zeisler J et al. A worldwide study of the Huntington's disease mutation: the sensitivity and specificity of measuring CAG repeats. New Engl J Med 1994; 330(20): 1401–1406.
3. Harper PS. The epidemiology of Huntington's disease. Hum Genet 1992; 89(4): 365–376.
4. Berardelli A, Noth J, Thompson PD, Bollen EL, Curra A, Deuschl G et al. Pathophysiology of chorea and bradykinesia in Huntington's disease. Mov Disord 1999; 14(3): 398–403.
5. Paulsen JS. Cognitive impairment in Huntington's disease: diagnosis and treatment. Curr Neurol Neurosci Rep 2011; 11(5): 474–483. doi: 10.1007/s11910-011-0215-x.
6. Lee ST, Kim M. Aging and neurodegeneration. Molecular mechanisms of neuronal loss in Huntington's disease. Mech Ageing Dev 2006; 127(5): 432–435.
7. Zuccato C, Valenza M, Cattaneo E. Molecular mechanisms and potential therapeutical targets in Huntington's disease. Physiol Rev 2010; 90(3): 905–981. doi: 10.1152/physrev.00041.2009.
8. Davies SW, Turmaine M, Cozens BA, DiFiglia M, Sharp AH, Ross CA et al. Formation of neuronal intranuclear inclusions underlies the neurological dysfunction in mice transgenic for the HD mutation. Cell 1997; 90(3): 537–548.
9. Reddy PH, Williams M, Charles V, Garrett L, Pike-Buchanan L, Whetsell WO jr et al. Behavioural abnormalities and selective neuronal loss in HD transgenic mice expressing mutated full-length HD cDNA. Nat Genet 1998; 20(2): 198–202.
10. Li XJ, Li W. Beyond mice: genetically modifying larger animals to model human diseases. J Genet Genomics 2012; 39(6): 237–238. doi: 10.1016/j.jgg.2012.05.006.
11. Bendixen E, Danielsen M, Larsen K, Bendixen C. Advances in porcine genomics and proteomics-a toolbox for developing the pig as a model organism for molecular biomedical research. Brief Funct Genomics 2010; 9(3): 208–219. doi: 10.1093/bfgp/elq004.
12. Rusz J, Klempir J, Tykalova T, Baborová E, Cmejla R, Ruzicka E et al. Characteristics and occurrence of speech impairment in Huntington's disease: possible influence of antipsychotic medication. J Neural Trans 2014; 121(12): 655–664. doi: 10.1007/s00702-014-1229-8.
13. Vogel AP, Shirbin C, Andrew J, Churchyard AJ, Stout JC. Speech acoustic markers of early stage and prodromal Huntington's disease: a marker of disease onset? Neuropsychologia 2012; 50(14): 3273–3278. doi: 10.1016/j.neuropsychologia.2012.09.011.
14. Rusz J, Klempir J, Baborova E, Tykalova T, Majerova V, Cmejla R et al. Objective acoustic quantification of phonatory dysfunction in Huntington's disease. PLoS One 2013; 8(6): e65881. doi: 10.1371/journal.pone.0065881.
15. Skodda S, Schlegel U, Hoffman R, Saft C. Impaired motor speech performance in Huntington's disease. J Neural Transm 2014; 121(4): 399–407. doi: 10.1007/s00702-013-1115-9.
16. Rusz J, Saft C, Schlegel U, Hoffman R, Skodda S. Phonatory dysfunction as a preclinical symptom of Huntington's disease. PLoS One 2014; 9(11): e113412. doi: 10.1371/journal.pone.0113412.
17. Marchant JN, Whittaker X, Brooma DM. Vocalisations of the adult female domestic pig during a standard human approach test and their relationships with behavioural and heart rate measure. Appl Anim Behav Sci 2001; 72(1): 23–39.
18. Tallet C, Linhart P, Policht R, Hammerschmidt K, Simecek P, Kratinova P et al. Encoding of situations in the vocal repertoire of piglets (Sus scrofa): a comparison of discrete and graded classifications. PLoS One 2013; 8(8): e71841. doi: 10.1371/journal.pone.0071841.
19. Cordeiro AF, Naas IA, Medeiros BB, Maia PD, Pereira EM. Energy expenditure in vocalizations of pigs under stress. Engenharia Agricola 2013; 33: 896–901.
20. Tallet C, Spinka M, Maruscakova I, Simecek P. Human perception of vocalizations of domestic piglets and modulation by experience with domestic pigs (Sus scrofa). J Comp Psychol 2010; 124(1): 81–91. doi: 10.1037/a0017354.
21. Schrader L, Todt D. Vocal quality is correlated with levels of stress hormones in domestic pigs. Ethology 1998; 104(10): 859–876.
22. Schon PC, Puppe B, Gromyko T, Manteuffel G. Common features and individual differences in nurse grunting of domestic pigs (Sus scrofa): a multi-parametric analysis. Behaviour 1999; 136: 49–66.
23. Baxa M, Hruska-Plochan M, Juhas S, Vodicka P, Pavlok A, Juhasova J et al. A transgenic minipig model of Huntington's disease. J Huntingtons Dis 2013; 2(1): 47–68. doi: 10.3233/JHD-130001.
24. Boersma P, Weenink D. PRAAT, a system for doing phonetics by computer. Glot Int 2001; 5(9–10): 341–345.

DISCUSSION

Large animals respresent an important biomedical models since they may provide a powerful backgroung for testing the therapeutic interventions.

Generation of germline transgenic large animals with human mutant huntingtin gene

We generated TgHD minipig by lentiviral transduction of HIV1 vectors encoding the N-terminal (1-548 aminoacids) part of human HTT gene which contained repetitive sequence of 145 glutamines under the control of the human HD promoter. Vectors were microinjected into porcine zygotes in syngamy and one TgHD founder saw was born after embryotransfer. Genomic analyses revealed that one copy of the construct was inserted into chromosome 1 and an in-frame deletion of the expanded polyQ tract from original 145 to consequent 124 glutamines was found. The TgHD animals were not mosaics, since the expression of mutant Htt was confirmed in all tissues tested across several generations [51]. Both female and male transmissions of the HD transgene were proved in 6 generations of TgHD minipigs with an almost equal number of transgenic and WT piglets in each litter. Hence, the lentiviral construct and its integration had no influence on survival or normal development through multiple generations. Long insert jumping library whole-genome sequencing revealed no direct disruption any annotated gene neither no further breakpoint or integration complexity or other genomic rearrangement caused by the transgene integration [53]. Even if the first attempts of heterozygote TgHD matings did not result in homozygous progeny [51], currently we dispose with several F1 homozygous TgHD minipigs, both males and females (unpublished).

Lentiviral transduction was also used for generation of HD non-human primates (*Macaca mulatta*) and HD sheep (*Ovis aries*). In contrast to our strategy, HD monkeys were created by lentiviral transduction of MII arrested oocytes followed by intracytoplasmic sperm injection [48], [49], [54]. The first HD monkey model encoded for exon 1 of huntingtin gene (HD exon 1 monkey) and showed very high neotanal mortality. Only one from five HD exon 1 monkey lived longer than one month [49], [55], [56]. Moreover, this one animal had incorporated a single copy of HTT transgene with 29Qs instead of transducted 84Qs. Thus, multiple copies of very short N-terminal part of human HTT with long polyQ sequence could cause an early death in monkeys since the second HD monkey model that encoded for exon 1–10 of the human HTT with 73Qs (HD exon 1-10 monkey) [48] reached adult age [55], [57], [58]. Similar to our approach, HD transgenic sheep were created by pronuclear

microinjection of lentiviral vectors. A proportion of the numbers of transgenic animals and microinjected zygotes transferred to surrogate females were 1.5% in HD sheep and 3.5% in TgHD minipigs. By contrast to our model, HD sheep carried a full length human HTT gene with a sequence of 73 CAG repeats. Five of six transgenic lambs had transgene integrated at a various but single genomic locus however in multiple copies. Therefore, one of the founders was chosen for breeding to next generations (OVT73 = Kiwi line) and further analyses [41].

Except for ours, next two HD pig models were generated by different approaches for transgenesis. The first germline transgenic HD pigs were created by somatic cell nuclear transfer technology. These pigs encoded for the first 208 aminoacids of human huntingtin gene with a tract of 105 glutamines [47]. Similar to the HD exon1 monkeys, transgenic piglets appeared normal at birth but four of five died within a month. The fifth one founder was viable [47] but did not survive to produce the progeny [52]. Embryos encoded for 208 amino acids of human HTT with 160Qs failed to develop [47].

Secondly, very prospective approach using CRISPR/Cas9 was applied and resulted in HD knock-in (HD KI) pigs expressing human exon 1 with a large 150 CAG repeat [52].

The studies indicated that different approaches to transgenesis can result in large animal models of various spieces and transgene pattern. Each one of the approaches has its pros and cons and needs to be considered in designing of the experimental study. The length of transgene in viral vectors is limited, what was a reason why N-truncated HD models were created. Next, lentiviral strategy is highly random and may result in incorporation of multi copies of transgene into various loci in the genome. Thus, the founders and offspring can differ in manifesting symptoms because the expression levels of the transgene can be influenced by the localization in the genome and by the transgene copy numbers. On the other hand, SCNT leads to non-chimeric animals in the first generation what is not a certainty with application of lentiviral technique. The rates of transgenesis and viability of offspring in pig were higher with lentiviral delivery than with a cloning strategy [47], [59], [60]. Moreover, SCNT in combination with CRISPR/Cas9 enables specific genetic modifications of the endogenous genes.

In the end, several different HD large animal models were generated in various species diverging in the lengths of human huntingtin gene and its polyQ repetition, in localization of incorporated transgene to the genome and in copy number of inserted constructs. Moreover, HD KI pig model expressed exon 1 of mutant human Htt at the endogenous levels while transgenic models expressed two alleles of endogenous huntingtin plus mutant Htt

form. A consequence of different strategies chosen for generation of HD models is different phenotype manifestations (see below).

Sperm and testicular degeneration

Although HD is distinguished mainly by neurodegeneration, the expression of mutant Htt leads to selective cellular dysfunction and degeneration not only in central nervous system but also in peripheral tissues [61]. The first pathological phenotype observed in TgHD minipigs was dysfunction of spermatozoa and degeneration of testicular tissue. This may be not so surprising when we consider very similar gene expression patterns in brain and testis [62].

We observed the decreased sperm number, motility and progressivity as well as reduced ability to penetrate the oocytes with intact zona pellucida in 13-month-old boars [51]. These parameters worsened with age in both F1 and F2 generations [51], [53]. Decreased concentration of semen and/or the changes in sperm motility may be related to notable reduction in phosphodiesters/γATP ratio in testis of 24-month-old TgHD minipigs [63] because phosphodiesters peak consists mainly of glycerophosphocholine [64] and there was observed a positive correlation between the glycerophosphocholine concentration and sperm motility [64], [65]. Next, we revealed deformed nuclei with incomplete chromatin, absence of residual bodies and alterations in acrosome in TgHD spermatozoa. We detected changes mainly in the mid-part of the tail manifesting by multipled axonemes often associated with disorganized mitochondrial sheaths [53].

We demonstrated age-deteriorated changes in seminiferous epithelium of 24- and 36-month-old TgHD boars. Sertoli cells and cells of spermatogenic lineage showed proceeded apoptosis exhibiting by increased density and vacuolation of cytoplasm, dilatation of endoplasmatic reticulum, swollen mitochondria and structural alterations of nuclei [53]. Previous data discerned apoptosis which manifested by diffuse cytoplasmic vacuolization, condensed nuclei and electron dense cytoplasm in spermatids [66] and also by disruption of seminiferous tubules by large vacuoles [67] in mice HD models. Testicular degeneration was perceived also in postmortem samples from HD patients [34]. Moreover, we proved significantly impaired spermatogenesis in 36-month-old TgHD boars [53].

To exclude the impact of fertility-related hormones on testicular degeneration, we examined the plasma levels of luteinizing hormone, inhibin-α and testosterone. We found

no significant difference between TgHD and control boars [53], correspondingly with observations in HD patients [68].

We detected comparable expression levels of mtHtt in TgHD testis and central nervous system tissues of 16-month-old animals [51]. Moreover, we revealed genotype specific fragmentation of huntigtin protein with some fragments enriched or particularly expressed only in TgHD tissues. The presence of these fragments was largely demonstrable in 24-, 36- and 48-month-old testes [53], [69], but they were also detected in brain tissue [70]. As we showed later, the mtHtt fragmentation in brain was age-dependent and fragments accumulated gradually in TgHD minipigs up to 48 months [Ardan et al., 2019; submitted]. These data may elucidate the earlier pathological changes occuring in testis.

Localization of mtHtt to midpiece of spermatozoa [53], [63], colocalization of mtHtt with mitochondrion [69] and alterations in mitochondrial sheaths [53] indicated potential process of changes in mitochondrial metabolism. Analyses of 14 to 47-month-old spermatozoa revealed proportionate age-dependent reduction of complex II subunit succinate dehydrogenase A (SDHA) and aconitase 2 contents in TgHD boars [69]. The lower contents of SDHA and succinate dehydrogenase B (SDHB) subunits were observed in striatal neurons of HD individuals [71]. The decrease in succinate dehydrogenase (SDH) may signify an early response to oxidative stress [69].

Little is known about reproductive features in large HD animal models. In contrary with our findings, no significant difference in sperm viability was proved in HD macaque model [62]. Data describing semen and testicular parameters in ovine and next porcine models of HD were not published up to date.

Alterations in mitochondrial metabolism

Studies in HD patients and HD rodent models pointed out relation of alterations in mitochondrial metabolism and HD pathology [72]–[74]. Deterioration of energy metabolism was showed in the caudate, putamen and cortex of presymptomatic HD carriers [75], [76]. These observations were supported by the localization of mtHtt to brain mitochondria [77]–[80] which was age-dependent in HD mouse model [77] and corresponded with the disease progression.

Disturbances of mitochondrial complex II were observed in the striatum [28], [29], [81] and peripheral tissues [82] of HD patients. We did not prove changes neither in mitochondrial electron transport activities nor in activities of pyruvatedehydrogenase, citrate synthase and cytochrome c oxidase in TgHD brains up to 48 months of age [83].

However, decreased activity of SDH in TgHD spermatozoa [69] and muscle tissue [84] could imply that amendments in mitochondria bioenergetics appeared in these tissues prior to modifications in brain, probably due to higher energy demands of sperms and muscles. In HD monkey model, transcription analysis revealed longitudinal (age 5 to 39 months) significant dysregulation of NDUFA5 gene which is a part of mitochondrial respiratory chain [48].

Data indicated that mitochondrial functions may be inhibited by induced oxidative stress [27]. 8-hydroxydeoxyguanosine, a marker of an oxidized DNA, was showed to be remarkable elevated in the mtDNA of caudate [28] the same as in mtDNA of parietal cortex of HD patients. Likewise, increased 8-OHdG level was detected in HD mouse brains [25], [85]. Even if we observed a tendency towards higher levels of 8-oxoG, comparable levels of malondialdehyde did not confirm an oxidative stress in TgHD brains up to 48 months of age. Furthermore, we did not detect a difference in levels of 5-hydroxycytosine (other oxidized base lesion). We suggested that increased 8-oxoG levels were related to analtered repair activity [83].

It was showed that elevated damage of nuclear DNA is antecedent to impaired mitochondrial activity in peripheral blood mononuclear cells from HD patients [82]. We did not observe differences in nuclear DNA damage in TgHD brain tissues. However, we detected decreased levels of mitochondrial DNA damage in basal ganglia [83]. Similarly, diminished mtDNA damage was showed in HD subjects [82]. Next, we found brain region dependent changes in mtDNA copy number where we detected reduced mtDNA levels in frontal cortex and increased levels in basal ganglia [83]. Thus, it seems that mtHtt expression variously influences different brain regions. The decrease in mtDNA copy number was observed also in brains of HD patients [86], thorough individual brain regions were not compared.

Brain pathology

We confirmed comparable mtHtt expression in different brain regions including cortex, caudate nucleus and putamen of TgHD minipig [51]. Similarly, mtHtt protein was expressed at equivalent levels from various parts of brains of HD sheep [87]. No brain region specific difference in mtHtt expression was observed either in HD monkey models [55]. Conversely, dissimilar expression of mtHtt was found in cortex, striatum and cerebellum of HD KI pigs [52].

Evidence of a presence of fragmented mtHtt was showed in the pre-symptomatic HD gene carriers [19]. Fragments of mtHtt caused cellular toxicity, induced apoptosis [88], [89] and their nuclear localization corresponded to the progression of the disease [90]–[92].

We detected tissue specific accumulation of mtHtt fragments in brains of 24-month-old TgHD animals [70]. We also showed severe mtHtt fragmentation in 48-month-old TgHD brains. However, we demonstrated less fragmentation and presence of smears in Western blot which possibly indicated a presence of oligomeric structures in 60-70-month-old TgHD putamen samples [Ardan et al., 2019; submitted]. We supposed that fragments started to form oligomeric structures which are precursors of aggregates. Similar age-dependent aggregation process was described in R6/2 and knock-in HD mice [93]. Oligomeric mtHtt was found in the brains of exon 1 HD monkeys which died few days after the birth [49]. The presence of mtHtt fragments was shown in brains of HD KI pigs [52]. Neuronal intranuclear inclusions of mtHtt were proved in sheep [87], knock-in pig [52] and in monkey [57] models of HD. We did not confirm presence of mtHtt in nuclear fractions of brain tissues. Howeever, the presence of mtHtt was evident in testicular nuclear fraction, hence implicated that testicular degeneration preceded degeneration of the brain [70].

A hallmark of HD pathology is a presence of mtHtt aggregates in brain. Aggregate formation was observed in mice [94] the same as in large HD animal models. Small mtHtt aggregates were found in neurites and bodies of neuronal cells in brains of HD KI pigs up to 5 months of age [52]. Neuropil aggregates were detected in cortex of 18-month old HD sheep [87]. HD monkey models resulted in genotype specific formation of aggregates when more abundant aggregates were detected in HD exon 1 monkey with 29Qs than in HD exon 1-10 with 73 Qs monkey in the same age of 5 years [55]. Even if a repetition of 29 glutamines in huntingtin gene does not cause HD in humans, based on a normal wild-type rhesus macaque length of 10–11 polyQ repeats in huntingtin gene, HD exon 1 monkey was expected to develop HD phenotype [48]. We observed inclusions in neuronal axons in TgHD cortex at the age of 60-70 months [Ardan et al., 2019; submitted].

Striatum is the most stricken brain region in HD with extensive loss of the medium-sized spiny neurons [95] which selectively express DARPP-32, an integrator of neurotransmission. We revealed age-related decrease in numbers of DARPP-32 positive cells in caudate nucleus and putamen of 16 to 70-month-old TgHD pigs [51], [70] [Ardan et al., 2019; submitted]. Downregulation of DARPP-32 expression was observed in various HD rodent models before the manifestation of clinical symptoms [96], [97]. Loss of neuronal cells was confirmed in striatum of both HD KI pig [52] and HD monkey [55] models, but not in HD sheep [87] even if Jacobsen et al. [80] reported reduction of DARPP-32 expression in striatum of a single 7-month-old transgenic lamb.

Ionized calcium-binding adapter molecule 1 (Iba-1) immunostaining showed microglial activation in brains of 24-, 48- to 60-70-month-old TgHD pigs [70], [Ardan et al., 2019; submitted] what was in consistence with elevated levels of IL-8 and IL-1β in TgHD microglial secretome [98]. Similarly, abundance of of IL-8 and IL-1β linked to increased microglia activation was observed in premanifest HD patients [99]. Several studies pointed on elevated levels of specific cytokines occurring up to a decade prior to the onset of clinical phenotype [100], [101]. Reactive astrogliosis with typical upregulation of gliar fibrillary acidic protein (GFAP) belongs to early pathological event in HD KI mice and increase in both GFAP and Iba-1 levels was observed in HD KI pigs brains [52], [102]–[104]. We detected elevated GFAP levels in brains of 60-70-month-old TgHD animals [Ardan et al., 2019; submitted]. No difference of GFAP immuno-reactivity was discerned in 6-, 18- and 36-month-old HD sheep [87].

Moreover, we demonstrated age-dependent increase of demyelination from 24 months of age [70], [Ardan et al., 2019; submitted]. Reduced myelination was observed also in various mice models prior to neurodegeneration [104]–[106]. Likewise, demyelination was showed in brains of HD KI pigs [52]. Our results were in compliance with a finding that activated microglia cause demyelination of white matter [107].

Numerous MRI studies have pictured specific regional atrophy in the brain that occurred earlier than clinical symptoms were manifested in HD gene carrriers [24], [108]–[113]. Our MRI data showed expansion of lateral ventricles in 6-7-year-old brains of three assessed TgHD animals [70]. Enlarged lateral ventricles and reduced size of striatum were observed in HD KI pigs [52] at 5 months and in HD exon 1 monkey at 24 months of age while there was not obvious atrophy in HD exon1-10 monkeys at 4 years [55] and HD sheep at 5 years [114].

The studies suggested that the distinct structure of mtHtt inserts and lengths of polyQ sequence determine the nature of the brain neuropathology. For example, formation of mtHtt aggregates and proceeding apoptosis was confirmed in transgenic piglets with N-truncated 208 aminoacids mtHTT (Yang 2010). Our TgHD minipigs with N-truncated 548aa mtHTT demonstrated slow, progressive loss of medium size spiny neurons, reduced demyelinaton, activated microglia and reactive astrogliosis with the presence of the first axonal inclusions at the age of 60-70 months [51], [70], [Ardan et al., 2019; submitted]. HD monkey model with HD exon 1 showed the aggregation, decreased number of neuronal cells and enlarged lateral ventricles at 2 years, whereas HD showed exon1-10 formation of mtHtt aggregates, a loss of neuronal cells in striatum but no brain atrophy at the age of 5 years [49], [56], [57].

HD sheep that expressed full length mtHtt no brain neurodegeneration except of neuropil aggregates was observed up to 5 years of age [87]. However, HD KI pigs that encoded for full length mutant huntingtin demonstrated the most severe neurological phenotype with the nuclear aggregates, neuronal loss, activated microglia, elevated GFAP level, reduced myelination and increased volume of ventricles at 5 months [52]. More robust brain degeneration in KI pigs could be caused by the specific expression of solely two endogenous alleles of huntingtin (one wild type + one mutant) while all of the other HD large animal models expressed two endogenous plus one transgenic allele of huntingtin. The mtHtt location and its copy number in genome could also affect the brain pathology. Not neglected should be the number of CAG in polyQ stretch in mtHTT which is the highest from all large HD models generated up to date.

Clinical symptoms manifestation

HD gene carriers had analogous growth trajectory to their controls within the childhood [115]. Various studies presented weight loss in HD patients despite of adequate or even increased caloric intake [116], [117]. The longer polyQ repetition the more acute loss of the weight was observed [118]. We calculated ABMI which reflected individual parameters of the animals (weight, height, length). ABMI trajectory was similar in TgHD and control minipigs up to 4 years of age when ABMI started to lessen. The ABMI decrease was evident in 6-7-year-old TgHD sows and slight non-significant decrease was observed also in 6-7-year-old TgHD boars (Ardan, 2019). Likewise, there was no difference in weight of HD and control monkeys up to 2 years of age (4 years is considered as a young adulhood in rhesuses) [56]. The body weights of F0 and F1 HD KI pigs were comparable up to 5 months, then gradual loss of weight was observed up to 30 months [52]. Slowly reduced ABMI in TgHD minipigs corresponded with mild brain neurodegeneration and late clinical symptoms onset in this model of HD. The number of 150 CAG in polyQ tract of HD KI pigs was in consistence with continual proportion of polyQ length and weight loss. Even if TgHD minipig encoded for 124Qs in mtHtt, this sequence is a mix of CAG/CAA triplets which was used to provide stable polyQ stretch. The stability of CAG/CAA tract was demonstrated among several generations of the TgHD progeny where the number of glutamines was still the same in different tissues [51]. Therefore, the slow decrease in AMBI may be an effect of CAG/CAA mix in polyQ sequence in TgHD minipigs.

The most characteristic feature of HD is motor deficits. The most notable symptom is chorea, but many patients confront inadequate walking balance [7], [8] or tongue persistence

protrusion [9]. We observed gait and fine motor task impairment as well as altered reactions to unexpected balance disruption in 6-7.9-year-old TgHD boars. Obversely, significant gait decline was showed in 4-5.9-year-old TgHD sows while it was not so obvious in older females [Baxa et al., 2019; submitted]. This contrast could be a result of various body constitution and/or different ABMI between boars and sows. Abnormal walking pattern and respiratory problems were demonstrated in both F0 and F1 HD KI pigs [52]. Transgenic pigs that expressed N-terminal 208aa mtHtt died posnataly and severe chorea phenotype was observed in some of them before death. Both different survival periods and phenotype manifestations were supposed to be an effect of different mtHtt expression levels among the animals [47]. Comparably, HD monkeys that expressed exon 1 died soon after the birth while they indicated chorea, dystonia and difficulties in swallowing and breathing [49]. Special case was HD monkey expressing an exon 1 with 29Qs that exhibited facial chorea and dystonia at the age of 18 several episodes of seisures in 24 months [55]. HD monkeys that encoded for exon 1-10 of mtHTT developed dystonia at 2 years of age and difficulties with a fine motor tasks were observed at 3 years [55]. No apparent motor symptoms were seen in HD sheep [114], [119], [120].

HD patients experience cognitive dysfunctions, too. We revealed age-dependent decline in cognitive performance of 6-7.9-year-old TgHD boars. Cognitive deterioration was observed in 8-month-old HD exon 1 monkey and got worse with aging [55], [56] while the first clear cognitive changes were showed in 36-month-old HD exon 1-10 monkeys [55]. Even if a several tests for monitoring of cognitive skills in HD sheep were established [121]–[123], no changes were observed till the age of 5 years.

A stressful environment may cause the performance of activities more difficult for persons with HD. We showed gradual age-dependent decline in stress-induced execution in TgHD animals, remarkable in 6-7.9-year-old TgHD boars. HD carriers have to face many stresfull situations and it was proved that chronic stress leads to anxiety [124]. Even if the anxiety is a direct effect of stress or only a reaction to stressful situations, a high prevalence of anxiety was shown in both pre-symptomatic and symptomatic HD patients [125]. Similarly, HD monkeys displayed increased stress induced anxiety [58].

Disorganized day-night activity pattern was described in HD patients [15]. Abnormalities in circadian rhytm were also illustrated in mouse [15] and sheep [114] models of HD. We revealed incrased physical activity in the afternoon in TgHD boars older than 4.5 years [Baxa et al., 2019; submitted].

Previous studies revealed involuntary vocalization interrupting the speech melody. Phnonatory dysfunction positively correlated with degree of disease severity [10]. We assesed the grunting of TgHD minipigs [126] and demonstrated altered vocalization in trasnegenic animals [Tykalova et al., unpublished].

Similar to brain neurodegeneration, the severity, frequency and onset of clinical symptoms is related to the content of mtHTT gene, its expression level and to the polyQ repeat length in various HD large animal models. N-truncated mtHtt pig and monkey models indicated involuntary movements and died postnatally, except of one HD monkey which expressed mtHtt with 29 glutamines [47], [49]. This one HD monkey exhibited seizures in the age of 2 years and presented more acute development of dystonia and cognitive failures than HD exon 1-10 monkeys. Considering also the fact that seizure is common in juvenile rather than in an adult form of HD [127], [128], HD exon 1 monkey simulated juvenile HD while the others HD monkeys recapitulated slow progression of the disease [55]. Full-length mtHtt ovine model showed no clinical symptoms except for disruption of sleep-wake activity up to the 5 years of age and therefore it indicated long pre-manifest stage [114], [119]. Conversely, HD KI pigs that expressed full-length endogenous huntingtin with 150Qs developed walking abnormalities in youg age [52]. Even though, our TgHD pigs have expressed N-truncated mtHTT with 124 glutamines, we observed relatively mild and slowly progressive manifestation of clinical symptoms. We have sustained this by the single copy of transgene in porcine genome and stable CAG/CAA repetition.

In conclusion, no single HD animal model imitated the human disease phenotype in a satisfactory manner. However, a lot can be yielded from all of the HD animal models since they can be involved in designs for pre-clinical testing, especially for gene therapies. Potentialities of using the monitoring and therapeutic equipments (e.g. MRI, PET, EEG) that are applied in human conditions together with long lifespan made large animal valuable models for predicting biodistribution, safety and efficacy of potential therapeutic treatments.

CONCLUSIONS

We have generated transgenic minipig with N-terminal part of human mutant huntingtin gene carrying 124 glutamines in polyQ repetition. One copy of transgene inserted into chromosome 1 did not disrupt any coding sequence in porcine genome. We confirmed expression of mutant huntingtin protein in the brain as well as in peripheral tissues. Both female and male transmissions of the HD transgene were proved and development of animals was normal through multiple generations.

The summary of phenotypic manifestation in TgHD minipig is illustrated in Figure 1.

We revealed continuos age-related accumulation of mtHTT fragments until the age of 4 years. Oligomeric forms rather than fragmented mtHtt were observed in TgHD brains older than 5 years. Moreover, we detected mtHtt inclusions in the neuronal axons. We demonstrated progressive brain degeneration since age-dependent neuronal loss, activated microglia, reactive astrogliosis and demyelination were confirmed. Neurodegenerative changes correlated to gradual alterations of mtHtt forms.

We showed that spermatozoa cells and testis may serve as biomarkers for monitoring of the disease progression in pre-clinical stage of the disease. Sperm and testicular degeneration caused by expression of mtHtt was observed about 4 years prior to the manifestation of the first clinical symptoms.

We developed new tests for monitoring the vocalization, cognitive and stress-induced performances in TgHD minipigs. We observed age- and sex-related gait impairment as well as decline in cognitive functions and deterioration in stress-induced functioning. Physical activity was increased in the afternoon. Changes in clinical phenotype were significant in 6-7.9-year-old animals thus exhibiting slow, progressive clinical phenotype in TgHD minipigs. Remarkable changes in behavioral, motor and cognitive functions were observed roughly two years after occurrence of significant changes in brain.

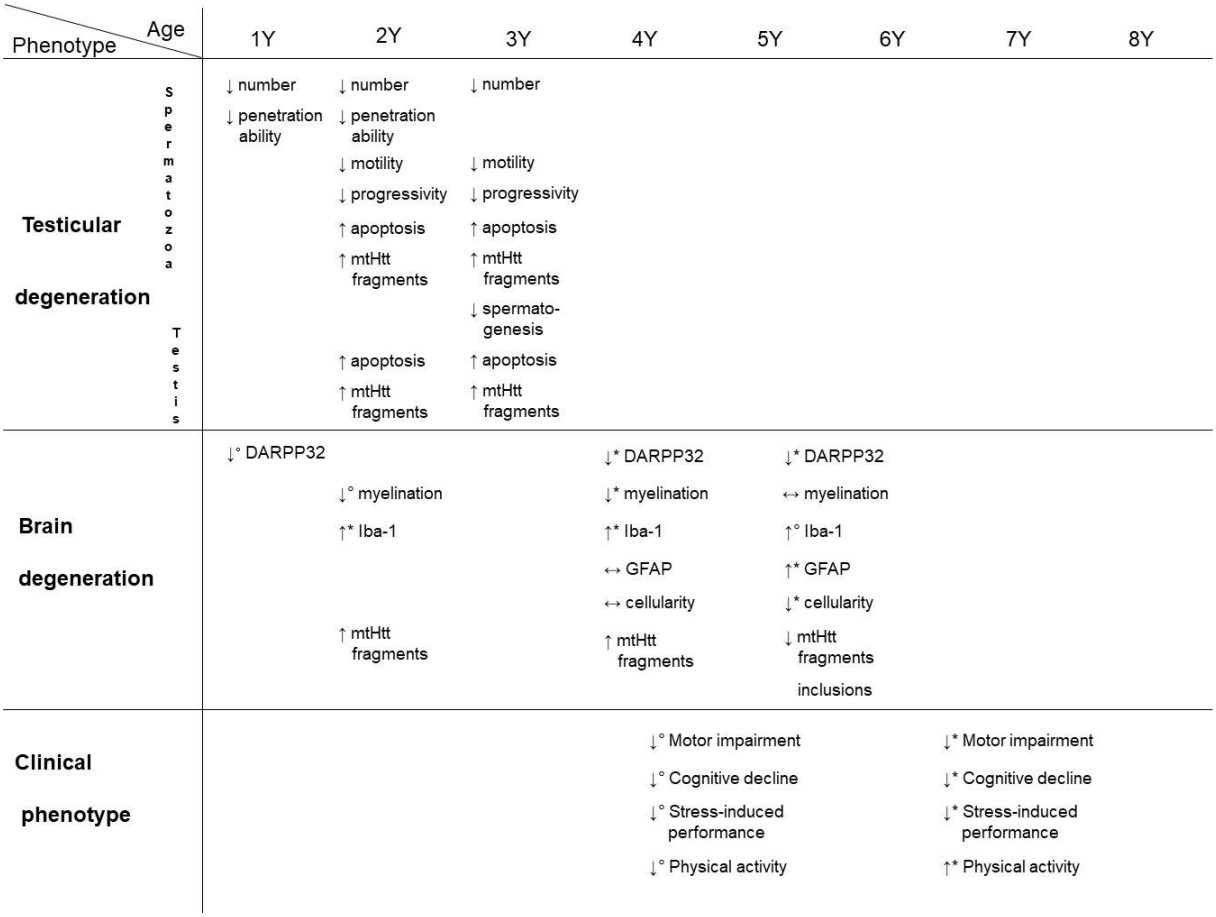

Fig.1 HD-like phenotype manifestation in TgHD minipigs. TgHD animals were compared to their sex- and age- matched controls. The impairment (↓), the improvement (↑) or the similarity (↔) in investigated parameters is illustrated. * = significant results, ° = non-significant results. Decreased fertility parameters, proceeding apoptosis and presence of mtHtt fragments were revealed in TgHD spermatozoa and testis. Testicular and sperm degeneration was detected about 2 years earlier than significant changes in TgHD brains and about 4 years prior to the first clinical symptoms. Age-dependent neuronal loss, reduced myelination, activation of microglia and reactive astrogliosis as well as increasing mtHTT fragmentation up to the age of 4 years (Y) were showed in TgHD brains. Furhermore, mtHtt inclusions were identified in the neuronal axons of 5-6-year old TgHD animals. Brain degeneration was obvious about 2 years prior to the first remarkable clinical phenotype.

FUTURE PROSPECTS

Gene-lowering therapy using miRNA approach showed encouraging results in TgHD minipigs in the short three months survey [129] which followed up to longitudinal miRNA gene-lowering investigation. Considering the results obtained in Evers´s study and preliminary data from our ongoing research, both Food and Drug Administration and European Medicines Evaluation Agency approved this approach for phase I and II clinical trial. We believe that the complete data from our ongoing longitudinal study could support the clinical trials and thus accelerate the receiving of the cure by the patients.

Next item which should be considered is the expression of two copies of endogenous huntingtin gene as well as extra copies of mutant HTT transgene in all of the large animal models of HD, excluding HD KI pigs. Over-expression of total huntingtin had an impact on phenotype manifestation in HD mice models [33], [130] and may be expected in large animals, too. Therefore, knock-in models were developed. HD KI pig encoding for human exon 1 huntingtin with 150Qs had very rapid onset of clinical symptoms and high mortality up to 10 months of age. Another one HD knock-in pig with prolonged endogenous porcine huntingtin up to 85 glutamines (HD KI-85Qs) was generated at Exemplar Genetics (Sioux City, IA; unpublished). Currently, we have established a colony of F1 generation of HD KI-85Qs pigs. We will use information gained by this study to proceed with characterization of this new promissing HD minipig model.

REFERNECES

[1] C. Zuccato, M. Valenza, and E. Cattaneo, "Molecular Mechanisms and Potential Therapeutical Targets in Huntington' s Disease," *Physiol Rev*, vol. 90, no. 3, pp. 905–981, 2010.

[2] J. M. Gil and A. C. Rego, "Mechanisms of neurodegeneration in Huntington's disease," *European Journal of Neuroscience*, vol. 27, no. 11. pp. 2803–2820, 2008.

[3] M. E. MacDonald *et al.*, "A novel gene containing a trinucleotide repeat that is expanded and unstable on Huntington's disease chromosomes," *Cell*, vol. 72, no. 6, pp. 971–983, 1993.

[4] R. R. Brinkman, M. M. Mezei, J. Theilmann, E. Almqvist, and M. R. Hayden, "The likelihood of being affected with huntington disease by a particular age, for a specific CAG size," *Am. J. Hum. Genet.*, vol. 60, no. 5, pp. 1202–1210, 1997.

[5] J.-M. Genetic Modifiers of Huntington's Disease (GeM-HD) Consortium *et al.*, "Identification of Genetic Factors that Modify Clinical Onset of Huntington's Disease.," *Cell*, vol. 162, no. 3, pp. 516–26, Jul. 2015.

[6] J. F. Gusella, M. E. MacDonald, and J. M. Lee, "Genetic modifiers of Huntington's disease," *Movement Disorders*, vol. 29, no. 11. pp. 1359–1365, 2014.

[7] N. S. Caron, G. E. Wright, and M. R. Hayden, *Huntington Disease*. 1993.

[8] K. Vuong, C. G. Canning, J. C. Menant, and C. T. Loy, "Gait, balance, and falls in Huntington disease," in *Handbook of clinical neurology*, vol. 159, 2018, pp. 251–260.

[9] R. Reilmann *et al.*, "Tongue force analysis assesses motor phenotype in premanifest and symptomatic Huntington's disease," *Mov. Disord.*, vol. 25, no. 13, pp. 2195–2202, Oct. 2010.

[10] J. Rusz *et al.*, "Objective Acoustic Quantification of Phonatory Dysfunction in Huntington's Disease," *PLoS One*, vol. 8, no. 6, 2013.

[11] J. Rusz *et al.*, "Characteristics and occurrence of speech impairment in Huntington's disease: possible influence of antipsychotic medication," *J. Neural Transm.*, vol. 121, no. 12, pp. 1529–1539, 2014.

[12] J. Brandt, M. E. Strauss, J. Larus, B. Jensen, S. E. Folstein, and M. F. Folstein, "Clinical correlates of dementia and disability in Huntington's disease.," *J. Clin. Neuropsychol.*, vol. 6, no. 4, pp. 401–12, Nov. 1984.

[13] J. S. Lai *et al.*, "Evaluating cognition in individuals with Huntington disease: Neuro-QoL cognitive functioning measures," *Qual. Life Res.*, vol. 27, no. 3, pp. 811–822, Mar. 2018.

[14] C. M. Eddy, E. G. Parkinson, and H. E. Rickards, "Changes in mental state and behaviour in Huntington's disease," *The Lancet Psychiatry*, vol. 3, no. 11, pp. 1079–1086, Nov. 2016.

[15] J. A. Morton, N. I. Wood, M. H. Hastings, C. Hurelbrink, R. A. Barker, and E. S. Maywood, "Disintegration of the sleep-wake cycle and circadian timing in

Huntington's disease," *J. Neurosci.*, vol. 25, no. 1, pp. 157–163, 2005.

[16] M. DiFiglia *et al.*, "Aggregation of huntingtin in neuronal intranuclear inclusions and dystrophic neurites in brain," *Science (80-.).*, vol. 277, no. 5334, pp. 1990–1993, 1997.

[17] G. Hoffner, S. Souès, and P. Djian, "Aggregation of expanded huntingtin in the brains of patients with Huntington disease.," *Prion*, vol. 1, no. 1, pp. 26–31, 2007.

[18] P. Lajoie and E. L. Snapp, "Formation and Toxicity of Soluble Polyglutamine Oligomers in Living Cells," *PLoS One*, vol. 5, no. 12, p. e15245, Dec. 2010.

[19] L. M. Mende-Mueller, T. Toneff, S. R. Hwang, M. F. Chesselet, and V. Y. H. Hook, "Tissue-specific proteolysis of huntingtin (htt) in human brain: Evidence of enhanced levels of N- and C-terminal htt fragments in Huntington's disease striatum," *J. Neurosci.*, vol. 21, no. 6, pp. 1830–1837, 2001.

[20] C. L. Wellington *et al.*, "Caspase cleavage of mutant huntingtin precedes neurodegeneration in Huntington's disease," *J. Neurosci.*, vol. 22, no. 18, pp. 7862–7872, 2002.

[21] T. Toneff *et al.*, "Comparison of huntingtin proteolytic fragments in human lymphoblast cell lines and human brain," *J. Neurochem.*, vol. 82, no. 1, pp. 84–92, 2002.

[22] M. F. Peters *et al.*, "Nuclear targeting of mutant huntingtin increases toxicity," *Mol. Cell. Neurosci.*, vol. 14, no. 2, pp. 121–128, 1999.

[23] G. Bartzokis *et al.*, "Myelin breakdown and iron changes in Huntington's disease: Pathogenesis and treatment implications," *Neurochem. Res.*, vol. 32, no. 10, pp. 1655–1664, Sep. 2007.

[24] J. S. Paulsen *et al.*, "Striatal and white matter predictors of estimated diagnosis for Huntington disease," *Brain Res. Bull.*, vol. 82, no. 3–4, pp. 201–207, 2010.

[25] M. B. Bogdanov, O. A. Andreassen, A. Dedeoglu, R. J. Ferrante, and M. F. Beal, "Increased oxidative damage to DNA in a transgenic mouse model of Huntington's disease," *J. Neurochem.*, vol. 79, no. 6, pp. 1246–1249, 2001.

[26] H. Gemba, S. ichi Kyuhou, R. ichi Matsuzaki, and Y. Amino, "Oxidative damage to mitochondrial DNA in Huntington's disease parietal cortex," *Neurosci. Lett.*, vol. 272, no. 1, pp. 53–56, 1999.

[27] S. Hands, M. U. Sajjad, M. J. Newton, and A. Wyttenbach, "In vitro and in vivo aggregation of a fragment of huntingtin protein directly causes free radical production," *J. Biol. Chem.*, vol. 286, no. 52, pp. 44512–44520, 2011.

[28] S. E. Browne *et al.*, "Oxidative damage and metabolic dysfunction in huntington's disease: Selective vulnerability of the basal ganglia," *Ann. Neurol.*, vol. 41, no. 5, pp. 646–653, 1997.

[29] M. Gu, M. T. Gash, V. M. Mann, F. Javoy-Agid, J. M. Cooper, and A. H. V. Schapira, "Mitochondrial defect in Huntington's disease caudate nucleus," *Ann. Neurol.*, vol. 39, no. 3, pp. 385–389, 1996.

[30] M. Mielcarek and M. Isalan, “A shared mechanism of muscle wasting in cancer and Huntington’s disease,” *Clin. Transl. Med.*, vol. 4, no. 1, 2015.

[31] R. R. Ribchester *et al.*, “Progressive abnormalities in skeletal muscle and neuromuscular junctions of transgenic mice expressing the Huntington’s disease mutation,” *Eur. J. Neurosci.*, vol. 20, no. 11, pp. 3092–3114, 2004.

[32] L. Djoussé, B. Knowlton, L. A. Cupples, K. Marder, I. Shoulson, and R. H. Myers, “Weight loss in early stage of Huntington’s disease,” *Neurology*, vol. 59, no. 9, pp. 1325–1330, 2002.

[33] J. M. Van Raamsdonk *et al.*, “Body weight is modulated by levels of full-length Huntingtin,” *Hum. Mol. Genet.*, vol. 15, no. 9, pp. 1513–1523, 2006.

[34] J. M. Van Raamsdonk *et al.*, “Testicular degeneration in Huntington disease,” *Neurobiol. Dis.*, vol. 26, no. 3, pp. 512–520, 2007.

[35] P. Harjes and E. E. Wanker, “The hunt for huntingtin function: Interaction partners tell many different stories,” *Trends in Biochemical Sciences*, vol. 28, no. 8. pp. 425–433, 2003.

[36] Huntington Study Group, “A randomized, placebo-controlled trial of coenzyme Q10 and remacemide in Huntington’s disease,” *Neurology*, vol. 57, no. 3, pp. 397–404, Aug. 2001.

[37] A. McGarry *et al.*, “A randomized, double-blind, placebo-controlled trial of coenzyme Q10 in Huntington disease,” *Neurology*, vol. 88, no. 2, pp. 152–159, Jan. 2017.

[38] S. M. Hersch *et al.*, “The CREST-E study of creatine for Huntington disease,” *Neurology*, vol. 89, no. 6, pp. 594–601, Aug. 2017.

[39] I. E. Holm, A. K. O. Alstrup, and Y. Luo, “Genetically modified pig models for neurodegenerative disorders,” *Journal of Pathology*, vol. 238, no. 2. pp. 267–287, 2016.

[40] D. S. Howland and I. Munoz-Sanjuan, “Mind the gap: Models in multiple species needed for therapeutic development in Huntington’s disease,” *Mov. Disord.*, vol. 29, no. 11, pp. 1397–1403, Sep. 2014.

[41] J. A. Morton and D. S. Howland, “Large genetic animal models of huntington’s disease,” *J. Huntingtons. Dis.*, vol. 2, no. 1, pp. 3–19, 2013.

[42] P. Vodicka *et al.*, “The miniature pig as an animal model in biomedical research.,” *Ann. N. Y. Acad. Sci.*, vol. 1049, no. 1, pp. 161–71, May 2005.

[43] N. Matsuyama *et al.*, “Identification and characterization of the miniature pig Huntington’s disease gene homolog: Evidence for conservation and polymorphism in the CAG triplet repeat,” *Genomics*, vol. 69, no. 1, pp. 72–85, 2000.

[44] C. Galli *et al.*, “Somatic Cell Nuclear Transfer and Transgenesis in Large Animals: Current and Future Insights,” *Reprod. Domest. Anim.*, 2012.

[45] A. Hofmann *et al.*, “Efficient transgenesis in farm animals by lentiviral vectors,” *EMBO Rep.*, 2003.

[46] C. R. Long, M. E. Westhusin, and M. C. Golding, “Reshaping the transcriptional frontier: Epigenetics and somatic cell nuclear transfer,” *Mol. Reprod. Dev.*, vol. 81, no. 2, pp. 183–193, 2014.

[47] D. Yang *et al.*, “Expression of Huntington’s disease protein results in apoptotic neurons in the brains of cloned transgenic pigs,” *Hum. Mol. Genet.*, vol. 19, no. 20, pp. 3983–3994, 2010.

[48] J. Kocerha *et al.*, “Longitudinal transcriptomic dysregulation in the peripheral blood of transgenic Huntington’s disease monkeys,” *BMC Neurosci.*, vol. 14, no. 88, pp. 1–10, 2013.

[49] S. H. Yang *et al.*, “Towards a transgenic model of Huntington’s disease in a non-human primate,” *Nature*, vol. 453, no. 7197, pp. 921–924, 2008.

[50] J. C. Jacobsen *et al.*, “An ovine transgenic Huntington’s disease model,” *Hum. Mol. Genet.*, vol. 19, no. 10, pp. 1873–1882, May 2010.

[51] M. Baxa *et al.*, “A transgenic minipig model of huntington’s disease,” *J. Huntingtons. Dis.*, vol. 2, no. 1, pp. 47–68, 2013.

[52] S. Yan *et al.*, “A Huntingtin Knockin Pig Model Recapitulates Features of Selective Neurodegeneration in Huntington’s Disease,” *Cell*, vol. 173, no. 4, pp. 989-1002.e13, 2018.

[53] M. Macakova *et al.*, “Mutated Huntingtin Causes Testicular Pathology in Transgenic Minipig Boars.,” *Neurodegener. Dis.*, vol. 16, no. 3–4, pp. 245–59, 2016.

[54] A. W. S. Chan and S. H. Yang, “Generation of transgenic monkeys with human inherited genetic disease,” *Methods*, vol. 49, no. 1, pp. 78–84, 2009.

[55] A. W. S. Chan *et al.*, “Progressive cognitive deficit, motor impairment and striatal pathology in a transgenic huntington disease monkey model from infancy to adulthood,” *PLoS One*, vol. 10, no. 5, pp. 1–16, 2015.

[56] A. W. S. Chan *et al.*, “A two years longitudinal study of a transgenic Huntington disease monkey,” *BMC Neurosci.*, vol. 15, no. 36, pp. 1–11, 2014.

[57] B. R. Snyder and A. W. S. Chan, “Progress in developing transgenic monkey model for Huntington’s disease,” *Journal of Neural Transmission*, vol. 125, no. 3. pp. 401–417, 2018.

[58] J. Raper, S. Bosinger, Z. Johnson, G. Tharp, S. P. Moran, and A. W. S. Chan, “Increased irritability, anxiety, and immune reactivity in transgenic Huntington’s disease monkeys,” *Brain. Behav. Immun.*, vol. 58, pp. 181–190, 2016.

[59] I. A. Polejaeva *et al.*, “Cloned pigs produced by nuclear transfer from adult somatic cells,” *Nature*, vol. 407, no. 6800, pp. 86–90, 2000.

[60] C. Chiang *et al.*, “Complex reorganization and predominant non-homologous repair following chromosomal breakage in karyotypically balanced germline rearrangements and transgenic integration,” *Nat. Genet.*, vol. 44, no. 4, pp. 390–397, 2012.

[61] P. G. Bhide *et al.*, “Expression of normal and mutant huntingtin in the developing

brain," *J. Neurosci.*, vol. 16, no. 17, pp. 5523–5535, 1996.

[62] S. P. Moran, T. Chi, M. S. Prucha, Y. Agca, and A. W. S. Chan, "Cryotolerance of sperm from transgenic rhesus macaques (Macaca mulatta)," *J. Am. Assoc. Lab. Anim. Sci.*, vol. 55, no. 5, pp. 520–524, 2016.

[63] M. Jozefovicova *et al.*, "31P MR spectroscopy of the testes and im munohistochemical analysis of sperm of transgenic boars carried N-terminal part of human mutated huntingtin," *Ces. a Slov. Neurol. a Neurochir.*, vol. 78, pp. 2528–2533, 2015.

[64] J. van der Grond *et al.*, "The progression of spermatogenesis in the developing rat testis followed by 31P MR spectroscopy," *Magn. Reson. Med.*, vol. 23, no. 2, pp. 264–274, 1992.

[65] B. T. Hinton and B. P. Setchell, "Concentrations of glycerophosphocholine, phosphocholine and free inorganic phosphate in the luminal fluid of the rat testis and epididymis.," *J. Reprod. Fertil.*, vol. 58, no. 2, pp. 401–406, 1980.

[66] B. R. Leavitt *et al.*, "Wild-type Huntingtin reduces the cellular toxicity of mutant Huntingtin in vivo," *Am. J. Hum. Genet.*, vol. 68, no. 2, pp. 313–324, 2001.

[67] J. M. Van Raamsdonk *et al.*, "Loss of wild-type huntingtin influences motor dysfunction and survival in the YAC128 mouse model of Huntington disease," *Hum. Mol. Genet.*, vol. 14, no. 10, pp. 1379–1392, 2005.

[68] N. Saleh *et al.*, "Neuroendocrine disturbances in Huntington's disease," *PLoS One*, vol. 4, no. 3, 2009.

[69] J. Krizova *et al.*, "Mitochondrial Metabolism in a Large-Animal Model of Huntington Disease: The Hunt for Biomarkers in the Spermatozoa of Presymptomatic Minipigs," *Neurodegener. Dis.*, vol. 17, no. 4–5, pp. 213–226, 2017.

[70] D. Vidinská *et al.*, "Gradual Phenotype Development in Huntington Disease Transgenic Minipig Model at 24 Months of Age," *Neurodegener. Dis.*, vol. 18, no. 2–3, pp. 107–119, Jun. 2018.

[71] A. Benchoua *et al.*, "Involvement of mitochondrial complex II defects in neuronal death produced by N-terminus fragment of mutated huntingtin," *Mol. Biol. Cell*, vol. 17, no. 4, pp. 1652–1663, 2006.

[72] J. M. A. Oliveira, "Nature and cause of mitochondrial dysfunction in Huntington's disease: Focusing on huntingtin and the striatum," *Journal of Neurochemistry*, vol. 114, no. 1. pp. 1–12, 2010.

[73] J. M. A. Oliveira, "Mitochondrial bioenergetics and dynamics in Huntington's disease: Tripartite synapses and selective striatal degeneration," *Journal of Bioenergetics and Biomembranes*, vol. 42, no. 3. pp. 227–234, 2010.

[74] M. Damiano, L. Galvan, N. Déglon, and E. Brouillet, "Mitochondria in Huntington's disease," *Biochimica et Biophysica Acta - Molecular Basis of Disease*, vol. 1802, no. 1. pp. 52–61, Jan-2010.

[75] A. Feigin *et al.*, "Metabolic network abnormalities in early Huntington's disease: An [18F]FDG PET study," *J. Nucl. Med.*, vol. 42, no. 11, pp. 1591–1595, 2001.

[76] A. Ciarmiello *et al.*, “Brain white-matter volume loss and glucose hypometabolism precede the clinical symptoms of Huntington’s disease,” *J. Nucl. Med.*, vol. 47, no. 2, pp. 215–222, 2006.

[77] A. L. Orr *et al.*, “N-terminal mutant huntingtin associates with mitochondria and impairs mitochondrial trafficking,” *J. Neurosci.*, vol. 28, no. 11, pp. 2783–2792, 2008.

[78] E. Petrasch-Parwez *et al.*, “Cellular and subcellular localization of huntington aggregates in the brain of a rat transgenic for Huntington disease,” *J. Comp. Neurol.*, vol. 501, no. 5, pp. 716–730, 2007.

[79] A. V. Panov *et al.*, “Early mitochondrial calcium defects in Huntington’s disease are a direct effect of polyglutamines,” *Nat. Neurosci.*, vol. 5, no. 8, pp. 731–736, 2002.

[80] Y. S. Choo, G. V. W. Johnson, M. MacDonald, P. J. Detloff, and M. Lesort, “Mutant huntingtin directly increases susceptibility of mitochondria to the calcium-induced permeability transition and cytochrome c release,” *Hum. Mol. Genet.*, vol. 13, no. 14, pp. 1407–1420, 2004.

[81] W. L. Stahl and P. D. Swanson, “Biochemical abnormalities in Huntington’s chorea brains,” *Neurology*, vol. 24, no. 9, pp. 813–819, 1974.

[82] G. Askeland *et al.*, “Increased nuclear DNA damage precedes mitochondrial dysfunction in peripheral blood mononuclear cells from Huntington’s disease patients,” *Sci. Rep.*, vol. 8, no. 1, pp. 1–9, 2018.

[83] G. Askeland *et al.*, “A transgenic minipig model of Huntington’s disease shows early signs of behavioral and molecular pathologies,” *DMM Dis. Model. Mech.*, vol. 11, no. 10, p. dmm035949, Oct. 2018.

[84] M. Rodinova *et al.*, “Deterioration of mitochondrial bioenergetics and ultrastructure impairment in skeletal muscle of a transgenic minipig model in the early stages of Huntington’s disease,” *Dis. Model. Mech.*, vol. 12, no. 7, p. dmm038737, 2019.

[85] S. J. Tabrizi *et al.*, “Mitochondrial dysfunction and free radical damage in the Huntington R6/2 transgenic mouse,” *Ann. Neurol.*, vol. 47, no. 1, pp. 80–86, 2000.

[86] A. Siddiqui *et al.*, “Mitochondrial DNA damage Is associated with reduced mitochondrial bioenergetics in Huntington’s disease,” *Free Radic. Biol. Med.*, vol. 53, no. 7, pp. 1478–1488, 2012.

[87] S. J. Reid *et al.*, “Further molecular characterisation of the OVT73 transgenic sheep model of huntington’s disease identifies cortical aggregates,” *J. Huntingtons. Dis.*, vol. 2, no. 3, pp. 279–295, 2013.

[88] A. S. Hackam *et al.*, “The influence of huntingtin protein size on nuclear localization and cellular toxicity,” *J. Cell Biol.*, vol. 141, no. 5, pp. 1097–1105, 1998.

[89] D. Martindale *et al.*, “Length of huntingtin and its polyglutamine tract influences localization and frequency of intracellular aggregates,” *Nat. Genet.*, vol. 18, no. 2, pp. 150–154, 1998.

[90] F. Saudou, S. Finkbeiner, D. Devys, and M. E. Greenberg, “Huntingtin acts in the nucleus to induce apoptosis but death does not correlate with the formation of

intranuclear inclusions," *Cell*, vol. 95, no. 1, pp. 55–66, 1998.

[91] J. Velier *et al.*, "Wild-type and mutant huntingtins function in vesicle trafficking in the secretory and endocytic pathways," *Exp. Neurol.*, vol. 152, no. 1, pp. 34–40, 1998.

[92] M. DiFiglia *et al.*, "Huntingtin is a cytoplasmic protein associated with vesicles in human and rat brain neurons," *Neuron*, vol. 14, no. 5, pp. 1075–1081, 1995.

[93] K. Sathasivam *et al.*, "Identical oligomeric and fibrillar structures captured from the brains of R6/2 and knock-in mouse models of Huntington's disease," *Hum. Mol. Genet.*, vol. 19, no. 1, pp. 65–78, Jan. 2010.

[94] A. H. P. Jansen *et al.*, "Frequency of nuclear mutant huntingtin inclusion formation in neurons and glia is cell-type-specific," *Glia*, vol. 65, no. 1, pp. 50–61, Jan. 2017.

[95] J. P. Vonsattel, R. H. Myers, T. J. Stevens, R. J. Ferrante, E. D. Bird, and E. P. Richardson, "Neuropathological classification of huntington's disease," *J. Neuropathol. Exp. Neurol.*, vol. 44, no. 6, pp. 559–577, 1985.

[96] M. Y. Heng, S. J. Tallaksen-Greene, P. J. Detloff, and R. L. Albin, "Longitudinal evaluation of the Hdh(CAG)150 knock-in murine model of Huntington's disease," *J. Neurosci.*, vol. 27, no. 34, pp. 8989–8998, Aug. 2007.

[97] B. Woodman *et al.*, "The Hdh(Q150/Q150) knock-in mouse model of HD and the R6/2 exon 1 model develop comparable and widespread molecular phenotypes.," *Brain Res. Bull.*, vol. 72, no. 2–3, pp. 83–97, Apr. 2007.

[98] I. Valekova *et al.*, "Revelation of the IFNα, IL-10, IL-8 and IL-1β as promising biomarkers reflecting immuno-pathological mechanisms in porcine Huntington's disease model," *J. Neuroimmunol.*, vol. 293, pp. 71–81, Apr. 2016.

[99] M. Politis *et al.*, "Increased central microglial activation associated with peripheral cytokine levels in premanifest Huntington's disease gene carriers," *Neurobiol. Dis.*, vol. 83, pp. 115–121, Nov. 2015.

[100] K. H. Chang, Y. R. Wu, Y. C. Chen, and C. M. Chen, "Plasma inflammatory biomarkers for Huntington's disease patients and mouse model," *Brain. Behav. Immun.*, vol. 44, pp. 121–127, 2015.

[101] M. Björkqvist *et al.*, "A novel pathogenic pathway of immune activation detectable before clinical onset in Huntington's disease," *J. Exp. Med.*, vol. 205, no. 8, pp. 1869–1877, 2008.

[102] S. Palfi *et al.*, "Expression of mutated huntingtin fragment in the putamen is sufficient to produce abnormal movement in non-human primates," *Mol. Ther.*, vol. 15, no. 8, pp. 1444–1451, 2007.

[103] Z. X. Yu, S. H. Li, J. Evans, A. Pillarisetti, H. Li, and X. J. Li, "Mutant huntingtin causes context-dependent neurodegeneration in mice with Huntington's disease," *J. Neurosci.*, vol. 23, no. 6, pp. 2193–2202, 2003.

[104] H. Li, S. H. Li, Z. X. Yu, P. Shelbourne, and X. J. Li, "Huntingtin aggregate-associated axonal degeneration is an early pathological event in Huntington's disease mice.," *J. Neurosci.*, vol. 21, no. 21, pp. 8473–81, Nov. 2001.

[105] L. Menalled and D. Brunner, “Animal models of Huntington’s disease for translation to the clinic: Best practices,” *Mov. Disord.*, vol. 29, no. 11, pp. 1375–1390, 2014.

[106] R. T. Yi Teo *et al.*, “Structural and molecular myelination deficits occur prior to neuronal loss in the YAC128 and BACHD models of Huntington disease,” *Hum. Mol. Genet.*, vol. 25, no. 13, pp. 2621–2632, Apr. 2016.

[107] L. Peferoen, M. Kipp, P. van der Valk, J. M. van Noort, and S. Amor, “Oligodendrocyte-microglia cross-talk in the central nervous system,” *Immunology*, vol. 141, no. 3. pp. 302–313, Mar-2014.

[108] K. M. Biglan *et al.*, “Refining the diagnosis of huntington disease: The PREDICT-HD study,” *Front. Aging Neurosci.*, vol. 5, no. APR, p. 12, 2013.

[109] S. J. Tabrizi *et al.*, “Biological and clinical changes in premanifest and early stage Huntington’s disease in the TRACK-HD study: The 12-month longitudinal analysis,” *Lancet Neurol.*, vol. 10, no. 1, pp. 31–42, 2011.

[110] S. J. Tabrizi *et al.*, “Predictors of phenotypic progression and disease onset in premanifest and early-stage Huntington’s disease in the TRACK-HD study: Analysis of 36-month observational data,” *Lancet Neurol.*, vol. 12, no. 7, pp. 637–649, 2013.

[111] N. Z. Hobbs *et al.*, “The progression of regional atrophy in premanifest and early Huntington’s disease: A longitudinal voxel-based morphometry study,” *J. Neurol. Neurosurg. Psychiatry*, vol. 81, no. 7, pp. 756–763, 2010.

[112] E. H. Aylward *et al.*, “Striatal volume contributes to the prediction of onset of Huntington disease in incident cases,” *Biol. Psychiatry*, vol. 71, no. 9, pp. 822–828, 2012.

[113] E. H. Aylward *et al.*, “Longitudinal change in regional brain volumes in prodromal Huntington disease,” *J. Neurol. Neurosurg. Psychiatry*, vol. 82, no. 4, pp. 405–410, 2011.

[114] J. A. Morton *et al.*, “Early and progressive circadian abnormalities in Huntington’s disease sheep are unmasked by social environment,” *Hum. Mol. Genet.*, vol. 23, no. 13, pp. 3375–3383, 2014.

[115] J. K. Lee *et al.*, “Measures of growth in children at risk for Huntington disease,” *Neurology*, vol. 79, no. 7, pp. 668–674, 2012.

[116] N. A. Aziz *et al.*, “Systemic energy homeostasis in Huntington’s disease patients,” *J. Neurol. Neurosurg. Psychiatry*, vol. 81, no. 11, pp. 1233–1237, 2010.

[117] F. Mochel *et al.*, “Early energy deficit in Huntingdon disease: Identification of a plasma biomarker traceable during disease progression,” *PLoS One*, vol. 2, no. 7, 2007.

[118] N. A. Aziz, M. A. Van Der Marck, H. Pijl, M. G. M. Olde Rikkert, B. R. Bloem, and R. A. C. Roos, “Weight loss in neurodegenerative disorders,” *J. Neurol.*, vol. 255, no. 12, pp. 1872–1880, 2008.

[119] R. R. Handley *et al.*, “Metabolic disruption identified in the Huntington’s disease transgenic sheep model,” *Sci. Rep.*, vol. 6, no. February, pp. 1–11, 2016.

[120] D. J. Skene *et al.*, "Metabolic profiling of presymptomatic Huntington's disease sheep reveals novel biomarkers," *Sci. Rep.*, vol. 7, no. February, pp. 1–16, 2017.

[121] D. Glynn, E. A. Skillings, and A. J. Morton, "A comparison of discrimination learning in touchscreen and 2-choice swim tank using an allelic series of Huntington's disease mice," *J. Neurosci. Methods*, vol. 265, pp. 56–71, 2016.

[122] S. D. McBride, N. Perentos, and A. J. Morton, "A mobile, high-throughput semi-automated system for testing cognition in large non-primate animal models of Huntington disease," *J. Neurosci. Methods*, vol. 265, pp. 25–33, 2016.

[123] J. C. Stout, Y. Glikmann-Johnston, and S. C. Andrews, "Cognitive assessment strategies in Huntington's disease research," *J. Neurosci. Methods*, vol. 265, pp. 19–24, 2016.

[124] S. Khan and R. Alam, "Chronic Stress Leads to Anxiety and Depression," *Ann. Psychiatry Ment. Heal.*, vol. 5, pp. 14–17, 2017.

[125] M. Dale and E. van Duijn, "Anxiety in Huntington's disease," *J. Neuropsychiatry Clin. Neurosci.*, vol. 27, no. 4, pp. 262–271, 2015.

[126] T. Tykalova *et al.*, "Grunting in a genetically modified minipig animal model for Huntington's disease - Pilot experiments," *Ces. a Slov. Neurol. a Neurochir.*, vol. 78, pp. 2S61-2S65, 2015.

[127] L. J. Cloud *et al.*, "Seizures in juvenile Huntington's disease: Frequency and characterization in a multicenter cohort," *Mov. Disord.*, vol. 27, no. 14, pp. 1797–1800, 2012.

[128] N. Geevasinga, F. H. Richards, K. J. Jones, and M. M. Ryan, "Juvenile Huntington disease," *J. Paediatr. Child Health*, vol. 42, no. 9, pp. 552–554, 2006.

[129] M. M. Evers *et al.*, "AAV5-miHTT Gene Therapy Demonstrates Broad Distribution and Strong Human Mutant Huntingtin Lowering in a Huntington's Disease Minipig Model," *Mol. Ther.*, vol. 26, no. 9, pp. 2163–2177, 2018.

[130] M. A. Pouladi *et al.*, "Marked differences in neurochemistry and aggregates despite similar behavioural and neuropathological features of Huntington disease in the full-length BACHD and YAC128 mice," *Hum. Mol. Genet.*, vol. 21, no. 10, pp. 2219–2232, 2012.